UNIVERSITY OF
LIVERPOOL

ANALYTICAL ASPECTS OF METAL SEMICONDUCTOR BARRIERS BASED ON ORGANIC SEMICONDUCTORS

Thesis submitted in accordance with the requirements of the
University of Liverpool for the degree of Doctor in Philosophy

By

MALINA MAHADAVAN

JUNE 2008

ACKNOWLEDGEMENTS

I would like to express my sincere appreciation and gratitude to Professor W. Eccleston for his encouragement, guidance and invaluable time spent sharing his vast knowledge of solid-state electronics with me.

I also want to express my gratitude to PolyApply for providing financial support under Framework 6. Many thanks to Giles Lloyd from Merck Chemicals Ltd for providing us with various organic materials and to Soeren Steudel from IMEC (Leuven) for kindly sending us the experimental data for vertical diodes based on vacuum-deposited pentacene.

I would like to thank all members of the Molecular Electronic Group (MEG) particularly Dr. Sedghi, Dr. Donaghy and Robert Myers for the useful discussions. I would also like to thank Paul Aden and Eleanor Watters for their friendship and for making my time as a student a pleasant and enjoyable one. Special thanks to Mr. Kevin Molloy for his technical knowledge and willingness to always provide assistance.

Finally, I wish to extend my sincere appreciation and gratitude to my parents for their love, support and encouragement. I would also like to express my heartfelt thanks to Rajesh for his love, encouragement, understanding and support throughout my research. Special thanks to my sister and brother in law for their guidance, advice and support.

ABSTRACT

Over recent years, research into organic semiconductors has intensified considerably due to the increasing commercial viability of inexpensive, flexible, large area electronic applications. In particular, the introduction of a new generation of small molecule based organic semiconductors has increased the possibility of achieving high field effect mobilities. So far pentacene seems to be the most promising candidate since it yields field effect mobilities that are comparable to that of hydrogenated amorphous silicon (a-Si:H). Recently, a mobility larger than 1.2 $cm^2V^{-1}s^{-1}$ and an on/off ratio greater than 10^8 was reported for a thin film transistor (TFT) made with triisopropylsilyl pentacene (TIPS-pentacene) as the active material. The solution processability of TIPS-pentacene is advantageous since solution-processed organic TFTs are needed to pave the way for low cost manufacturing approaches such as inkjet printing and roll-to-roll processing. One of the main potential applications for organic materials is in low cost radio frequency identification (RFID) tags operating at a frequency of 13.56MHz. The high frequency operation of RFID tags will be most demanding on the rectifying component of the circuit which can be based either on a TFT or a rectifying diode.

This thesis is primarily concerned with analysing metal semiconductor barriers made with a variety of organic semiconductors such as highly regioregular poly(3-hexylthiophene) (P3HT), polytriarylamine (PTAA) (S1105) and vacuum-deposited pentacene. The work includes a review of the various charge transport models proposed along with a discussion on the Meyer Neldel Rule (MNR) which is a commonly occurring phenomenon in organic semiconductors. A simple analytical model that demonstrates the empirical relationship between mobility and carrier density is also developed. This general dependency is formally known as the Universal Mobility Law (UML).

The electrical characteristics of Schottky junctions made between aluminium and various organic solids are investigated. Both P3HT and PTAA are highly disordered semiconductors whilst pentacene is a small molecule organic semiconductor akin to polycrystalline inorganic solids. The analysis of the pentacene vertical diode is thus extensively based on the model developed by Eccleston.

The Al-PTAA Schottky diode is found to not only yield a high rectification ratio but also an extremely low off current which suggests that the device is most suitable for low current

circuit operations. In contrast, diodes based on P3HT and pentacene demonstrate much weaker rectifying properties. Nevertheless, in these diodes, the non-saturation of the reverse currents allows the dopant densities of the materials to be determined.

The new current density expression developed for organic based Schottky diodes allows the characteristic temperature of the exponential distribution of intrinsic carriers (T_0) and states (T_c) to be determined directly from the forward current density voltage characteristic. The Meyer Neldel energy representing the exponential density of states (DOS) is then obtained using the value of T_c. In general, the MN energy estimated from the exponential current regime of the diodes range between 30 meV and 35 meV.

Special attention is given to the saturation current region of the diodes as relatively high currents are needed to satisfy the demands of RFID related circuits. The saturation current of the as-synthesised P3HT diode was found to obey Ohm's law over the entire applied voltage range. In contrast, the PTAA and pentacene diodes demonstrate a transition from ohmic to space charge limited (SCL) conduction with increasing applied bias. The saturation current regime of these diodes is modelled using the new SCL current expression developed for disordered materials. The intrinsic value of T_c determined for both diodes suggests the absence of dopant states at higher energies. The effects of changing the back metal/organic interface and further with doping with 2,3-dichloro-5,6-dicyano-1,4-benzoquinone (DDQ) on the saturation region of Al-PTAA Schottky diodes are also studied.

Finally, the temperature variation of the current density voltage characteristics of as-synthesised P3HT and PTAA Schottky diodes are analysed. Below room temperature, the distinct fall in the forward exponential slope leads to much larger ideality factors η. This is attributed to the non-ideal behaviour of the Schottky barrier interface with decreasing temperature. The anomalous rise in η is attributed to a number of possibilities including the presence of extrinsic trapping states, carriers taking alternative routes to other potential barriers and the lack of validity of the flat quasi Fermi level approximation. Modelling the saturation current region of the PTAA diode with the new SCL current expression yields a self-consistent value of T_c at relatively high temperatures. The steep decline in the Meyer Neldel energy observed at lower temperatures is mainly attributed to the formation of a potential barrier at the back metal/organic interface.

CONTENTS

CHAPTER 1

INTRODUCTION

This chapter provides a brief introduction to the subject of organic semiconductors and devices. The organisation of the thesis together with the experimental techniques used is also presented here.

1.1 INTRODUCTION TO ORGANIC SEMICONDUCTORS AND DEVICES

Organic semiconductors have been studied extensively since the discovery of the first semiconducting material, polyacetylene some 30 years ago [1, 2]. There has been continued interest in these materials as they show great promise for the realisation of inexpensive, flexible, large area electronic applications. So far major advances have been achieved in areas such as high-*K* dielectrics [3, 4], small molecule organic semiconductors [5, 6], surface treatments [7] and organic film morphology and molecular ordering [8-10].

Research into organic materials is largely motivated by their potential application in active matrix liquid crystal display (AMLCD) and low cost radio frequency identification (RFID) tags. For commercialisation, RFID tags will have to operate at a frequency of 13.56 MHz thus creating a need for high mobility organic semiconductors [11]. This demand has led to the introduction of a new generation of small molecule based semiconductors such as pentacene [12, 13], N, N'-diphenyl-N,N'-bis(1-naphthyl)-1,1'-biphenyl-4,4'-diamine (α-NPD) [14] and *para*-sexiphenyl (6P) [15]. Unfortunately, these materials are normally deposited via vacuum evaporation and in order to achieve low fabrication costs, solution processability becomes a critical issue. Solution-processed organic thin film transistors (OTFTs) are needed to pave the way for low cost manufacturing approaches such as inkjet printing and roll-to-roll processing. More recently, a mobility larger than 1.2 $cm^2V^{-1}s^{-1}$ and an on/off ratio greater than 10^8 was reported for a TFT made with solution-processed triisopropylsilyl pentacene (TIPS-pentacene) as the active material [5]. Despite being visibly non-uniform, solution-cast TIPS-pentacene films are said to have improved molecular ordering and consequently yield improved TFT characteristics as compared to spin or dip coating [16].

The high frequency operation of RFID tags will be most demanding on the rectifying component of the circuit which can be based either on a TFT or a rectifying diode. Although TFTs are easier to integrate, limitations on the minimum channel length increases the need for high field effect mobilities. However, it must also be considered that carrier mobility extracted from the space charge limited current (SCLC) of diodes is generally lower than the field effect mobility of OTFTs due to the higher carrier density achieved in the channel of the transistors compared with diodes. This thesis is mainly concerned with studying the electrical characteristic of rectifying diodes made with a variety of organic semiconductors namely poly(3-hexylthiophene) (P3HT), polytriarylamine (PTAA) (S1105) and vacuum-deposited pentacene [17]. PTAA is a proprietary material purchased from Merck Chemicals Ltd (previously Avecia).

A simple analytical model is developed which demonstrates the universal dependence of mobility on carrier density in organic materials. The model approximates the band tail of a Gaussian distribution using an exponential function as it is believed to provide considerable insight into charge transport in organic solids by allowing conventional device physics to be employed. More interestingly, the model proves the Universal Mobility Law (UML) without taking into account the hopping mechanism which is believed to govern charge transport in disordered materials.

The UML is of particular importance since it forms the basis for the quantitative modelling of all organic devices. It enables material dependent parameters like the characteristic temperature of the exponential distribution of states T_c and its corresponding Meyer Neldel (MN) energy to be extracted from the electrical characteristic of the diodes. The Meyer Neldel energy is a commonly observed phenomenon in organic semiconductors. *Table 1.1* lists the Meyer Neldel energy obtained from the measurement and subsequent modelling of devices such as Schottky diodes, metal-insulator-semiconductor (MIS) diodes and thin film transistors made with a variety of organic semiconductors.

Special attention is also given to the saturation region of the diodes as high currents are needed to satisfy the demand of RFID related circuits. For instance, the saturation current in the as-synthesised P3HT diode was found to obey an ohmic relationship. This is believed to be related to the presence of large quantities of residual dopant from the synthesis process. The P3HT diode also exhibits a much weaker rectifying behaviour compared to the much purer polytriarylamine. In contrast, the saturation region of the PTAA and vacuum-deposited pentacene Schottky diodes show a transition from ohmic to space charge limited conduction at higher applied fields. Even though P3HT and PTAA show almost comparable forward currents, space charge effects are observed in the latter because there are insufficient dopant ions to compensate the increasing density of holes in the neutral region of the organic film. In addition, the extremely low off currents obtained for the Al-PTAA Schottky diode makes it ideal for low current circuit operations. The effects of changing the back metal/organic interface and further with doping with 2,3-dichloro-5,6-dicyano-1,4-benzoquinone (DDQ) on the saturation current region of Al-PTAA Schottky diodes are also studied.

Analysis of the vacuum-deposited pentacene vertical diode is extensively based on the model developed by Eccleston for polycrystalline inorganic semiconductors [19]. The molecular structure of small molecule organic semiconductors is rather complex but for convenience, it is assumed to consist of arrays of small molecules displaying crystalline-like behaviour and boundary regions which are highly amorphous. Conduction through the pentacene diode is

believed to be dominated by the disordered grain boundaries thus allowing the *J-V* characteristic to be analysed in terms of the model developed for disordered solids.

Organic Solid	*Measurement*	*T (K)*	*T_c (K)*	*m*	*Meyer Neldel energy (meV)*
P3HT	Schottky diode (exponential)	300	390	0.3	34
	Schottky diode (dopants)	300	840	1.8	70
	TFT	300	410	0.37	34
	MIS diode (Debye length)		423	0.41	35
PTAA	Schottky diode (exponential)	300	384	0.28	33
	Schottky diode (saturation)	300	468	0.56	40
	Schottky diode (dopants)	300	840	1.8	70
	TFT	300	381	0.27	32
vacuum-deposited pentacene	Schottky diode (exponential)	300	347	0.16	30
	Schottky diode (saturation)	300	375	0.25	32
	TFT	300	365	0.22	31

Table 1.1: Characteristic temperature of the exponential DOS (T_c), exponent of the UML (m) and the Meyer Neldel energy for highly regioregular P3HT, PTAA and vacuum-deposited pentacene measured from a range of devices. The result also includes work done by other members of the group [18].

The temperature variation of the current density voltage characteristics of as-synthesised P3HT and polytriarylamine Schottky diodes is also studied. The forward exponential currents of the diodes are analysed using both the conventional and newly developed current density expression for organic Schottky diodes. In addition, the saturation current region of the PTAA diode is also modelled using the newly developed SCL current equation to confirm the self-consistency of T_c with varying temperature.

1.2 THESIS ORGANISATION

A brief summary of the chapters in this thesis is as follows:

Chapter 2 explores the numerous charge transport models proposed so far to describe conduction in disordered organic semiconductors. A general agreement regarding the charge transport mechanism is yet to be reached reflecting the difficulty of the problem of hopping mobility in these materials. The possible origin and consequence of the Meyer Neldel Rule (MNR) in organic solids is also briefly discussed. The Meyer Neldel energy is believed to be closely related to the thermally activated behaviour of charge carriers. Since disordered materials are characterised by a distribution of localised states, the exact nature of the states needed to maintain charge neutrality is discussed. Ignoring amphoteric states, the localised states lying in the top and bottom half of the energy gap are categorised as either donor-like or acceptor-like. A simple yet comprehensive analytical model is also developed to demonstrate the charge carrier density dependence of mobility commonly observed in disordered semiconductors. Through a simple comparison with crystalline solids, the empirical relationship between mobility and carrier density, formally known as the Universal Mobility Law (UML) is established.

Chapter 3 focuses mainly on the electrical characterisation of Schottky diodes made with as-synthesised and doped poly(3-hexylthiophene) (P3HT). It begins with the fundamental theory of operation of organic based metal semiconductor diodes. Thermionic emission and diffusion theory which are considered to be the two main conduction mechanisms governing carrier transport across Schottky barriers are also discussed. A simple current density expression which enables the characteristic temperature of the intrinsic energetic distribution of carriers and states to be determined directly from the current voltage characteristic of diodes is presented. In addition, the conduction mechanism in an undoped P3HT film is established experimentally by measuring the deviation along the voltage axis for each of the measured current levels. To explore the effects of doping on electrical conduction, 2,3-dichloro-5,6-dicyano-1,4-benzoquinone (DDQ) is incorporated into P3HT by percentage in weight.

Chapter 4 reviews the original space charge limited current (SCLC) theory developed for crystalline solids where carrier motion is generally described by a single mobility term. A new space charge limited current expression incorporating the Universal Mobility Law (UML) is developed to reflect the carrier density dependence of mobility in disordered semiconductors. The electrical characterisation of polytriarylamine (PTAA), a proprietary

material purchased from Merck Chemicals Ltd is studied in detail. A value for the intrinsic T_c and consequently T_0 is determined by modelling the saturation current regime of the PTAA diode with the new SCLC equation. In addition, changes in the saturation current level as a result of varying the back metal/organic interface and further with doped PTAA films are also explored. The experimental current density voltage characteristic for a vacuum-deposited pentacene vertical diode is also presented. Analysis of current flow through this diode is based extensively on the analytical model developed by Eccleston for polycrystalline inorganic materials.

Chapter 5 is primarily concerned with the temperature variation of the current density voltage characteristics of as-synthesised P3HT and PTAA Schottky diodes. The variation of dopant density and hence the free hole density in P3HT with temperature is studied from the reverse *J-V* characteristics. The idea of a self-consistent value of T_c with varying temperature is explored through the quantitative modelling of the exponential current region of both the diodes and also the forward saturation current region of the PTAA Schottky diode. In addition, the activation energy of P3HT and PTAA is extracted experimentally from the Arrhenius plot of the reverse current density at relatively high temperatures.

Chapter 6 summarises the work undertaken as well as the findings of the experiments presented in this thesis. Recommendations for future work are also included in this chapter.

1.3 EXPERIMENTAL TECHNIQUES

The highly regioregular poly(3-hexylthiophene) (P3HT) and 2,3-dichloro-5,6-dicyano-1,4-benzoquinone (DDQ) used in this work was purchased from Aldrich Chemical Co while polytriarylamine (PTAA) is a proprietary organic semiconductor obtained from Merck Chemicals Ltd (previously Avecia). The various metal electrodes used in the fabrication of the organic Schottky diodes were thermally evaporated under a vacuum pressure of ~ 10^{-3} Torr. The DC characterisation of the devices was performed using a PC controlled Hewlett Packard 4145B parameter analyser.

The variable temperature measurement of the P3HT and PTAA Schottky diodes was performed at 10^{-1} Torr vacuum and a liquid nitrogen cryostat was used to cool the samples down. The diodes were fabricated on polyethylene terephthalate (PET) flexible substrates instead of glass to reduce the margin of error between the measured and the actual sample temperature. The DC characterisation was carried out using a PC controlled Keithley 615 Electrometer and 230 Voltmeter.

Fabrication and the subsequent electrical characterisation of the vacuum-deposited pentacene vertical diode were carried out by Steudel *et. al* based at IMEC (Leuven) [17]. The experimental data was recently provided to us for further analysis. The Au layer was sputtered onto a Si wafer with 100nm of thermally grown SiO_2 layer and patterned via a lift-off process. The pristine Au electrode was later UV-ozone cleaned for 5 mins to increase the metal work function in order to make a good ohmic contact with the semiconductor. The pentacene purchased from Fluka was purified by gradient sublimation at 100 mTorr under forming gas (96% N_2, 4% H_2). The pentacene layer was then deposited onto the modified Au coated substrate at a temperature of 20°C with a deposition rate of ~ 3 $Å s^{-1}$ under ultra-high vacuum of ~ 4 x 10^{-9} Torr. Following the pentacene deposition, a 140 nm thick layer of Al was evaporated. Electrical characterisation of the diode was performed with an Agilent 4156C parameter analyser.

1.4 CONTRIBUTIONS

The following contributions are made in this thesis:

- In disordered organic semiconductors characterised by a wide distribution of localised states, the energy states lying in the top half of the energy gap must be acceptor-like whilst the bottom half must be donor-like in consistent with the experiments. For convenience, the possibility of having amphoteric states is ignored.

- A model demonstrating the universal dependency of mobility on carrier density is presented. The empirical relationship commonly known as the Universal Mobility Law (UML) is established by approximating the density of states in disordered materials by an exponential function and subsequently comparing it to crystalline solids where the conduction/valence band is treated as having an abrupt edge.

- From the *J-V* characteristic of the Al-poly(3-hexylthiophene) (P3HT) Schottky diode, the characteristic temperature of the intrinsic distribution of carriers T_0 is determined. The value of T_0 is estimated to be ~ 1301K. The intrinsic DOS which also follows an exponential function is represented by the constant T_c equal to ~ 390K. This corresponds to a Meyer Neldel (MN) energy of ~ 34 meV.

- The non-ideal behaviour observed in the forward *J-V* characteristic of the Al-P3HT Schottky diode yields a T_c and a MN energy of ~ 580K and 50 meV respectively. The fairly large value of T_c suggests the presence of both intrinsic and extrinsic trap states at lower energies.

- A good linear fit is obtained for the experimental plot of $ln\ J_R$ against $V^{0.25}$ thus allowing the dopant density in as-synthesised P3HT to be calculated. Also, the ratio of the space charge region width to the Debye length is estimated to be ~ 8 suggesting that the abrupt depletion approximation may still apply.

- A slope of nearly 1 was calculated from the double logarithmic plot of J against V_{bulk} indicating that as-synthesised P3HT exhibits ohmic behaviour. This is attributed to the presence of residual dopant ions from the synthesis process which helps to maintain charge neutrality in the neutral region of the diode.

- A new space charge limited current (SCLC) expression incorporating the Universal Mobility Law (UML) is developed for disordered organic semiconductors.

- Modelling the saturation current regime of a modified Au-polytriarylamine (PTAA)-Al diode with the newly developed SCLC equation yields a magnitude of T_c equal to ~ 468K and a MN energy of 40 meV. This reflects the absence of dopant states at higher energies and is consistent with the notion that PTAA is a much purer organic semiconductor compared to P3HT.

- The forward saturation current of PTAA Schottky diodes is found to be affected by the nature of the back metal/organic interface and further by doping with DDQ.

- The analytical modelling involving a UV-O_3 modified Au/pentacene/Al vertical diode gives a value of T_c equal to ~ 347 – 375K and a MN energy of between 30 meV and 32 meV in close agreement with TFT results based on the same material. It is suggested that small molecule organic semiconductor may be described by a MN energy close to ~ 30 meV whilst crystalline and disordered semiconductors are represented by an energy of 26 meV and 33 – 40 meV respectively.

- A nearly constant dopant density of ~ 10^{16} cm^{-3} is obtained from the reverse *J-V* characteristics of the Al-P3HT Schottky diode in the temperature range of between 240K and 290K. This result suggests that extrinsic carriers contributed by the dopants will continue to dominate conduction at relatively high temperatures. This phenomenon referred to as 'carrier inversion' was first observed in crystalline semiconductors *e.g.* silicon.

- Modelling the forward saturation current region of the Al-PTAA diode with the newly developed SCL current expression yields a constant Meyer Neldel energy of ~ 31 meV in the temperature range of between 248K and 295K. Below 248K, however, there is a steep decline in MN energy with decreasing temperature. The erroneous results obtained at lower temperatures are believed to be associated with the formation of a potential barrier at the modified Au/PTAA interface.

- The Arrhenius plot of reverse current density at relatively high temperatures yields an activation energy E_a of ~ 0.17 eV and ~ 0.2 eV for P3HT and PTAA respectively.

A similar value of E_a is obtained for P3HT from the Arrhenius plot of conductivity determined from the forward *J-V* characteristics.

1.5 REFERENCES

[1] H. Shirakawa, E. J. Louis, A. G. MacDiarmid, C. K. Chiang and A. J. Heeger, *J. Chem. Soc. Chem. Commun.* **16**, 578, 1977.

[2] A. J. Heeger, *Synth. Met.* **125**, 23, 2002.

[3] C. D. Dimitrakopoulos, S. Purushothaman, J. Kymissis, A. Callegari and J. M. Shaw, *Science* **283**, 822, 1999.

[4] L. A. Majewski, R. Schroeder and M. Grell, *Adv. Mater.* **17**, 192, 2005.

[5] S. K. Park, C. –C. Kuo, J. E. Anthony and T. N. Jackson, *IEDM Tech. Dig.* 113, 2005.

[6] S. K. Park, T. N. Jackson, J. E. Anthony and D. A. Mourey, *Appl. Phys. Lett.* **91**, 063514, 2007.

[7] S. C. Lim, S. H. Kim, J. H. Lee, M. K. Kim, D. J. Kim and T. Zyung, *Synth. Met.* **148**, 75, 2005.

[8] H. Sirringhaus, P.J. Brown, R.H. Friend, M. M. Nielse, K. Bechgaard, B.M. W. Langeveld-Voss, A. J. H. Spiering, A. J. Janssen, E. W. Meijer, P. Herwig and D. M. De Leeuw, *Nature* **401**, 685, 1999.

[9] D. H. Kim, Y.D. Park, Y. Jang, H. Yang, Y.H. Kim, J. I. Han, D. G. Moon, S. Park, T. Chang, M. Joo, C. Y. Ryu and K. Cho, *Adv. Funct. Mater.* **15**, 77, 2005.

[10] D. J. Gundlach, Y. –Y. Lin, T. N. Jackson, S. F. Nelson and D. G. Schlom, *IEEE Electron Device Lett.* **18**, 87, 1997.

[11] K. Finkenzeller, *"RFID Handbook"* Vol. 1, Wiley, New York, 2002.

[12] S. F. Nelson, Y. –Y. Lin, D. J. Gundlach and T. N. Jackson, *Appl. Phys. Lett.* **72**, 1854, 1998.

[13] C. D. Dimitrakopoulos and P. R. L. Malenfant, *Adv. Mater.* **14**, 99, 2002.

[14] A. Fleissner, H. Schmid, C. Melzer and H. V. Seggern, *Appl. Phys. Lett.* **91**, 242103, 2007.

[15] D. J. Gundlach, Y. –Y. Lin, T. N. Jackson and D. G. Schlom, *Appl. Phys. Lett.* **71**, 3853, 1997.

[16] S. K. Park, J. E. Anthony and T. N. Jackson, *IEEE Electron Device Lett.* **28**, 877, 2007.

[17] S. Steudel, K. Myny, V. Arkhipov, C. Steibel, S. De Vusser, J. Genoe and P. Heremans, *Nature Mater.* **4**, 597, 2005.

[18] N. Sedghi, D. Donaghy, M. Raja and W. Eccleston *(private communication)*.

[19] W. Eccleston, *IEEE Trans. Electron Devices* **53**, 474, 2006.

CHAPTER 2

CHARGE TRANSPORT IN DISORDERED ORGANIC SEMICONDUCTORS

The various charge transport models proposed for organic materials are reviewed. This includes the polaron model, the Gaussian disorder model, the multiple trapping and release (MTR) model and the variable range hopping (VRH) model. The Meyer Neldel rule (MNR) which is a commonly occurring phenomenon in organic solids is also explored. In organic solids, it is important to understand the nature of the distribution of localised states. Hence, the combination of acceptor-like and donor-like states consistent with experiments is discussed in detail. A simple analytical model which demonstrates the empirical relationship between the so-called effective mobility and carrier density, formally known as the Universal Mobility Law (UML) is also presented.

2.1 INTRODUCTION

In general, advances in the field of organic electronics are stimulated by the development of organic semiconductors made using new chemical formulations. Since their discovery, organic semiconductors have been considered as rather promising materials as they provide the opportunity to produce low cost, large area electronic circuits. Over recent years, the understanding of disordered organic materials in terms of their physical, chemical and electronic properties has gained significant ground. But having said that, there are still critical areas in which a general agreement is yet to be reached namely the charge transport mechanism in disordered organic semiconductors.

A simple yet accurate analytical model is fundamental to the design of integrated circuits based on organic materials. This chapter opens by reviewing the various analytical models proposed so far to describe conduction in disordered materials. It is believed that localisation in disordered materials is dominated either by strong electron-phonon coupling which leads to the so-called polaron based model or by inherent energetic and spatially induced disorder. Various disorder models based on either a Gaussian or an exponential DOS are discussed.

The chapter then progresses to review the so-called Meyer Neldel rule (MNR) which was first observed in inorganic polycrystalline materials. The thermally activated behaviour observed in a wide variety of disordered organic materials has been found to obey the MN rule. Even though it is a commonly occurring phenomenon in organic solids, the microscopic origin of the MNR still remains unknown. In the following section, the nature of the localised states in disordered semiconductors is discussed. Ignoring amphoteric states, the localised states lying in top and bottom half of the energy gap are classified as either donor-like or acceptor-like. The combination of states, however, must be such that only a low gate voltage is needed to reach minimum channel current in consistent with experiments.

Finally, a model is developed to illustrate the carrier concentration dependence of mobility observed in disordered materials. The model compares a disordered material to a crystalline solid where carrier motion is traditionally described by a single mobility term. The model proves the empirical relationship between mobility and carrier concentration in disordered materials, formally known as the Universal Mobility law (UML). It becomes increasingly evident in subsequent chapters that the UML forms the basis of our analytical model.

2.2 CHARGE TRANSPORT MODELS

Over recent years, the main focus has been on developing analytical models to explain charge transport in structurally disordered organic semiconductors. Although these models might differ in their analytical approach, it is generally agreed that carrier motion in organic materials is governed by thermally assisted tunnelling between localised states. In view of the spatial and energetic disorder, the density of states (DOS) in disordered materials is assumed to follow a Gaussian distribution [1]. But in some models, the Gaussian is often approximated by an exponential function. There is still no general agreement, however, on whether the Gaussian or the exponential approximation provides a more exact description of the conduction mechanism. A range of charge transport models used to describe organic materials are discussed which includes the Poole Frenkel model, the polaron based model, the Gaussian disorder model, the variable range hopping (VRH) model and the multiple trapping and release model (MTR).

2.2.1 THE POLARON MODEL

Polaronic motion is often mentioned in conjunction with charge transport in disordered materials due to their strong electron-phonon coupling. This coupling is associated with the tendency of conjugated molecules to alter their geometry upon charging. In this model, the origin of localisation in conjugated polymers is explained via the formation of polarons.

Polaronic effects are observable in any polarisable material, where the Coulomb field of an individual charge carrier first polarises its surrounding lattice and subsequently couples itself to it. The charge with its accompanying deformation acts like a quasi-particle and is called a polaron; a term introduced by the famous physicist Landau. Since the charge carrier entrains the lattice deformation it induces, the polaron is said to be 'self trapped'.

A description of polaron transport can be provided for both crystalline and disordered semiconductors. However, polaron mobilities in disordered materials are often orders of magnitude lower than in their crystalline counterpart since the physical properties of a polaron can differ greatly depending on the strength of its electron-phonon coupling [2, 3]. Large polarons with spatially extended wave functions are formed when long range electron-lattice interactions dominate. Due to their long range crystallinity, conventional semiconductors like silicon only experience a weak electron-phonon coupling thus allowing their carriers to exhibit Drude-like conduction. In the Drude model, the charge carriers in a

semiconductor are considered to be practically free, interacting with the lattice only through momentum altering collisions.

In contrast, when the lattice deformation compares with inter-atomic distances as it is in the case of disordered materials, the polaron is termed as 'small'. In other words, small polarons are formed when self-trapped carriers are severely localised at a single site by sufficiently strong short range electron-lattice interactions. In disordered materials, the spatial extent of the coupling is generally restricted by the large number of structural defects. The theory of small polaron transport was first developed by Yamashita and Kurosawa [4] and Holstein [5]. Holstein describes the polaronic motion using a Hamiltonian consisting of an electron term given by the overlap integral J, a lattice term corresponding to the sum of harmonic oscillators vibrating at a unique frequency ω_0 and finally, an electron-phonon coupling term quantified by the so-called polaron binding energy, E_b. The polaron binding energy is determined from the sum of the increase in kinetic energy of the self-trapped carrier as it resists the contraction of its wave function, the fall in potential energy as a result of its coupling to the lattice deformation and the strain energy associated with creating the potential well that binds the charge carrier [2].

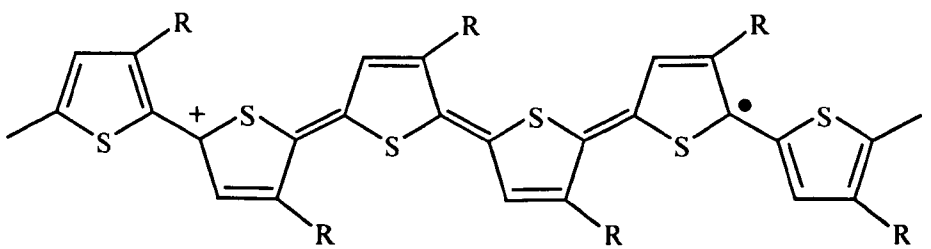

Figure 2.2.1: Schematic representation of the change in geometry of a poly(3-alkylthiophene) chain due to the formation of a positively charged polaron.

Polaron motion is believed to take place via a succession of random jumps between adjacent sites. Recently, Emin introduced the coincidence concept where carrier hopping is said to occur between localised states which are momentarily equal in energy [6]. Such energy coincidences are achieved via thermal deformations of the lattice. Based on the lifetime of the coincidence, he classified the hopping events into adiabatic and non-adiabatic transitions [7]. In an adiabatic transition, the lifetime of the coincidence is much larger than the carrier transit time thus leading to a hopping probability which is essentially unity. In contrast, if the carrier transit time is longer and the carrier fails to continuously follow the lattice deformations, the process is termed as non-adiabatic.

In the high temperature limit, the polaronic transport is viewed as a phonon-assisted hopping motion and the mobility of an adiabatic small polaron is given by

$$\mu = \frac{\omega_0 q \delta}{2\pi kT} \exp - \left(\frac{E_b}{kT} \right) \qquad 2.2.1$$

where q is the electronic charge, δ is the average intermolecular distance, ω_0 is the lattice frequency, k is the Boltzmann constant, T is the absolute temperature and E_b is the polaron binding energy. *Equation 2.2.1* predicts a thermally activated behaviour for mobility in agreement with the fact that polaronic transport occurs via thermally induced lattice deformations. It should be noted, however, that deviation from the thermally activated law is observed at low temperatures.

2.2.2 MILLER ABRAHAM HOPPING RATE

Although there is a controversy regarding the treatment of the DOS in disordered organic semiconductors, it is widely accepted that transport in these materials proceed by hopping of charge carriers between strongly localised energy states. The first sight of hopping conduction or otherwise known as impurity conduction was in lightly doped inorganic semiconductors at very low temperatures. At both low temperatures and impurity concentrations, transport is dominated by carriers hopping between shallow impurity states. The hopping conduction mechanism was first suggested by Conwell [8] and Mott [9]. Later, Miller and Abraham proposed a hopping model based on a single-phonon jump rate description [10].

The Miller Abraham formalism has since become increasingly important in the modelling of charge transport in disordered organic materials. Disorder in organic materials is believed to be caused by fluctuations in the lattice polarisation energy and/or the distribution in the conjugation lengths of individual polymer chains. The hopping rate of carriers from occupied localised state i to empty localised state j is dependent on the distance R_{ij} between the states i and j and the energy barrier, $E_j - E_i$ and is given by

$$\nu_{ij} = \nu_0 \exp - \left(2\alpha R_{ij}\right) \begin{cases} \exp - \left(\dfrac{E_j - E_i}{kT} \right) & \text{if } E_j > E_i \\ 1 & \text{if } E_j < E_i \end{cases} \qquad 2.2.2$$

where ν_0 is the attempt-to-hop frequency and α is the reciprocal of the localisation length which is assumed to be equal for all states. The term $\exp\left(-2\alpha R_{ij}\right)$ from *equation 2.2.2* takes

account of the tunnelling probability between isoenergetic sites whilst the second exponential term represents the Boltzmann factor for hops upward in energy. For organic materials, *equation 2.2.2* is still valid in the high temperature limit. In inorganic semiconductors, however, 'carrier inversion' occurs whereby charge carriers move from the dopant states into the conduction/valence band edge, where a substantially higher number of energy levels exist. Hence hopping transport vanishes leaving band-like transport to dominate at higher temperatures.

This model neglects multiphonon processes which has been argued to control transport if charge carriers in organic materials are localised polarons [11, 12]. The omission of this process could ultimately lead to the wrong temperature dependence of mobility. In the past, those favouring the disorder based transport models concluded that electron-phonon coupling is sufficiently weak thus making polaronic effects negligible [1]. Recently, Bleibaum *et al.* proposed a hopping model similar to this but with a prefactor which depends on the electron-phonon coupling strength, the phonon density of states and other properties of organic materials [13].

2.2.3 POOLE FRENKEL CONDUCTION

Charge transport in disordered organic materials has long been reported to exhibit Poole Frenkel-like electric field dependence [14]. The earliest of such reports was based on experiments by Gill [15]. According to the Poole Frenkel law, the hopping mobility, μ can simply be expressed as

$$\mu \propto \exp\left(\gamma\sqrt{F}\right) \qquad 2.2.3$$

where F is the applied field and γ is the so-called material dependent Poole Frenkel constant which typically decreases with increasing temperature.

The Poole Frenkel-like behaviour in organic materials is thought to originate from the energetic or positional disorder of localised states such that the constant, γ is generally determined by the width of the density of states or the extent of the positional disorder characterised by the hopping distance. However, the absence of a high density of charged coulombic centres and hopping distances which are approximately the order of an interatomic distance in disordered organic materials are both counter intuitive to the typical Poole Frenkel-like behaviour.

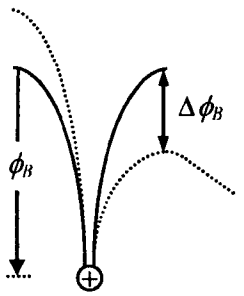

Figure 2.2.2: A schematic representation of Poole Frenkel conduction involving a positively charged ion. The solid line represents the potential energy experienced by an electron without an external field whilst the dotted line is in the presence of a field. The external field lowers the height of the potential barrier by an amount $\Delta\phi_B$.

In the original model, charge carriers once released by the ionisation of atoms are said to experience the coloumbic potential of the newly formed ions. The application of an external field will then modify this potential in such a way as to increase the transfer rate between localised states as shown in *figure 2.2.2*. Due to this strong coulomb interaction, the hopping distances for carriers are much larger, more than ten times the interatomic distance. In disordered materials, however, it will be demonstrated in *section 2.4* that charge neutrality can only be achieved if states in the bottom half of the energy gap are donor-like and in the top half are acceptor-like. Hence removing an electron from an acceptor-like state in an n-type material for example will return the state to its neutral condition. The absence of a coulombic force between the free charge carrier and the neutral state will result in significantly smaller hopping distances in disordered organic solids thus casting doubts over the possibility of a Poole Frenkel-like conduction mechanism. A more accurate description of charge transport in organic solids is thus thought to be provided by the variable range hopping mechanism.

2.2.4 GAUSSIAN DISORDER MODEL

From his Monte Carlo simulation study, Bässler developed a hopping model for conduction in disordered organic materials along with proposing a Gaussian shape for the description of their density of states [1]. It is believed that the random energetic distribution of localised states in disordered systems is best represented by a Gaussian DOS.

The Gaussian density of states is given by

$$g(E) = \frac{N_t}{\sigma\sqrt{2\pi}} \exp - \left(\frac{E^2}{2\sigma^2} \right) \qquad 2.2.4$$

where σ is the width of the Gaussian, E is the energy of the localised states and N_t is the total concentration of localised states.

In his model, Bässler claims that the Fermi Dirac statistics is irrelevant as charge carriers are said to hop in an almost empty DOS. It appears that restricting the model to a sufficiently low concentration of charge carriers forms the basis of this assumption. This severely limits the validity of the model to small carrier concentrations.

Like most hopping based models, the hopping rate follows the Miller Abraham formalism. The electron-phonon coupling is assumed to be sufficiently weak such that polaronic effects can be neglected. Bässler cites two forms of disorder in his model; the first being the energetic disorder which he refers to as diagonal disorder and the other the so-called off-diagonal disorder which is associated with variation in energy site distances. In this model, he studies mainly the temperature and field dependence of carrier mobility. The temperature dependence of drift mobility is given by

$$\mu(T) \propto \exp\left(\frac{1}{T^2} \right) \qquad 2.2.5$$

It can be seen clearly that *equation 2.2.5* predicts a non-Arrhenius temperature dependence for mobility. This dependence was favoured over the conventional form as it gave more realistic values for the prefactor μ_0. But since this model was proposed, there has been accumulating amount of experimental evidence showing thermally activated behaviour for carrier mobility in various disordered organic materials [16-18]. More recently, Coehoorn *et al.* demonstrated that this phenomenon can be easily explained by considering charge carrier concentration dependence of mobility in Gaussian disorder models [19]. In this paper, he showed that at low carrier concentrations, $\ln(\mu)$ varied approximately linearly with $1/T^2$ but as the carrier concentration increased, a linear function of $1/T$ is obtained. This finding also meant that the need for a polaronic based transport model becomes less obvious as temperature dependence of disordered materials can be fully understood using simple disorder models.

In addition, Bässler also demonstrated a field dependence of carrier mobility reminiscent of Poole Frenkel behaviour at high electric fields.

$$\mu(F) \propto \exp(F)^{1/2} \qquad 2.2.6$$

Here F is the applied electric field.

In the low field regime, he showed that carrier mobility drops with increasing field due to enhanced off-diagonal disorder. With increased disorder, the low field is said to promote new charge transfer routes which include short hops opposite to the field direction as poor wave function overlap between isoenergetic sites hinders carrier motion in the field direction. The probability of hopping transitions in the opposite direction increases at lower fields thus giving rise to enhanced drift mobility values. The Poole Frenkel-like behaviour is restored at higher fields as the lowering of energy barriers between localised states by the field effect dominates. More recently, Baranovskii reviewed this phenomenon and dismissed it as a misinterpretation of the TOF experimental data caused by neglecting the diffusive nature of charge transport at low fields [20].

Much earlier, Poole Frenkel-like carrier mobility dependence had already been demonstrated through experiments by Gill [15] and later by others [21-23]. However, as highlighted by Garstein and Conwell [24], a spatially correlated potential for charge carriers is needed to explain the Poole Frenkel behaviour in the low field region. Dunlap *et al.* [25, 26] developed a theoretical model based on charge-dipole interactions to explain this phenomenon but its applicability is rather doubtful as most conjugated polymers do not have a permanent dipole moment [22]. In order to elucidate this field dependence, Yu *et al.* proposed an alternative mechanism based on thermal fluctuations in the molecular geometry that modify the energy levels of the localised states [27, 28].

The main drawback of Bässler's model is that it is extensively based on computer simulations thereby restricting the expressions to only numerical solutions. Later, Baranovskii *et al.* proposed the first semi-analytical model for the description of hopping transport in a Gaussian DOS [29, 30]. His model relies heavily on the concept of transport energy which again comes with the penalty that it is valid only under low fields and for small charge densities. This concept of a transport energy was first introduced for a purely exponential DOS [31]. In addition, his model also makes use of percolation theory. By including the percolation criterion, $B_c \approx 2.7$ in the final expression for drift mobility, the model demands the existence of an infinite percolation path across localised states with

energies lower than the transport energy. In this model, the variable range hopping (VRH) theory is used to illustrate the dependence of carrier mobility on concentration of localised states. The variable range nature of the hopping process is reflected by taking into account the energy dependence of the hopping distance, *R*.

For systems with a Gaussian DOS, the concentration dependence of drift mobility is explained using the generalised form given as

$$\mu \alpha \exp\left[-C\left(N\alpha^3\right)^{-p}\right] \qquad 2.2.7$$

where N is the concentration of localised states, α is the localisation length and both p and C are reported to be temperature dependent parameters. This is in contrast to previous claims of *equation 2.2.7* being universal to all disordered organic materials with values of C and p equal to 2 and 1/3, respectively [32, 33]. By recognising the temperature dependence of p and C, Baranovskii showed that consistent estimates of α can be obtained directly from the drift mobility experimental data of doped polymer matrixes for example NIPK/PVK [33] and TNF/PVK [15].

2.2.5 VARIABLE RANGE HOPPING (VRH) MODEL

Variable range hopping (VRH) occurs only in systems where the energy variation between subsequent states is large compared to the thermal energy kT. The concept of VRH was first introduced by Mott [34] in 1968 for a system with a constant density of states (DOS). He presented an analytical expression for the temperature dependence of conductivity when the Fermi level was located in the region of the hopping states. The Mott formula states that

$$\sigma \sim \exp\left[-\left(T_1/T\right)^{1/4}\right] \qquad 2.2.8$$

where σ is the conductivity, T is the absolute temperature and $T_1 = 128/9\pi a^3 N_F k$ where N_F is the density of states at the Fermi level and a is the size of the localised states. In such a system, he argued that hopping over far distances and hopping to higher energies are equally probable as the density of states is assumed to be homogeneously distributed around the Fermi level.

This is quite different to the case of disordered organic semiconductors where the DOS is commonly approximated by an exponential function. In an exponential distribution of states,

the characteristic hop is an activated jump since there are more states available at higher energies. So a carrier may either hop over a small distance with a high activation energy or hop over a large distance with a low activation energy. This makes the temperature dependence of carrier transport strongly dependent on the density of localised states.

In two- and three-dimensional systems, the most comprehensive methods for calculating hopping conductivity are said to be based on percolation theory [35]. Historically, the percolation approach for VRH system in an exponential density of states was first suggested by Grunewald and Thomas [36]. Much later, Vissenberg and Matters [37] presented a modified approach to explain the temperature and gate voltage dependence of field effect mobility observed in organic transistors made by Brown *et al.* [16]. By then, both these dependencies had already been explained by Horowitz *et al.* using the multiple trapping and release (MTR) model [38]. The MTR model will be elaborated further in the subsequent section.

The model presented by Vissenberg and Matters studies the influence of temperature and the occupational probability of states on the conductivity of systems having an exponential DOS. With the aid of percolation theory, they developed an analytical expression for conductivity.

Their model mainly focuses on transport properties at low carrier densities and low temperatures. Only under both these conditions will carrier transport be determined by the tail of the DOS. The density of states in disordered material, *g(E)* is given by

$$g(E)=\frac{N_t}{kT_0}\exp\left(\frac{E}{kT_0}\right) \qquad \left(-\infty<E\leq 0\right) \qquad 2.2.9$$

where N_t is the number of states per unit volume, k is the Boltzmann constant and T_0 is a parameter which describes the width of the exponential distribution.

In determining the charge carrier density, the Fermi Dirac distribution is used to describe the falling occupancy of the localised states with increasing energy. The Maxwell Boltzmann approximation is not favoured as most of the hopping is believed to take place between tail states close to the Fermi level, E_F. It is in the energy range close to E_F that the Maxwell Boltzmann statistic deviates from the Fermi Dirac distribution but only by a factor of 2. The approximation generally works better at energies more than $3kT$ above the Fermi level. In the past, when the Fermi Dirac statistics is replaced with the Maxwell Boltzmann approximation, the conductivity has been reported as being simply proportional to the carrier

concentration [36, 39]. This is thought to be an artefact caused by neglecting the exact carrier occupancy of localised states.

The charge carrier density of the system is thus given by

$$\delta N_t \approx \exp\left(\frac{E_F}{kT_0}\right)\Gamma\left(1-T/T_0\right)\Gamma\left(1+T/T_0\right) \qquad 2.2.10$$

where δ is the fraction of states occupied, E_F is the energy of the Fermi level and $\Gamma(z)=\int_0^\infty dy \exp(-y)y^{z-1}$. *Equation 2.2.10* breaks down at temperatures $T > T_0$ as transport is no longer dominated by hopping between tail states.

As mentioned earlier, the overall conductivity of the system is determined using percolation theory. At low applied voltages, the system is viewed as a resistor network having the conductance

$$G_{ij} = G_0 \exp(-s_{ij}) \qquad 2.2.11$$

where G_{ij} is the conductance between sites i and j and G_0 is the prefactor.

The exponent term in *equation 2.2.11* is given by

$$s_{ij} = 2\alpha R_{ij} + \frac{|E_i - E_F| + |E_j - E_F| + |E_i - E_j|}{2kT} \qquad 2.2.12$$

where α is the effective overlap of electronic wave functions, R_{ij} is the distance between sites i and j and E_i and E_j correspond to the energy of sites i and j respectively. The first term in *equation 2.2.12* describes the tunnelling process between the two sites whilst the second term takes account of the activation energy required for a hop upward in energy as well as the occupancy of sites i and j.

The conductivity of a percolation based system [40, 41] is given as

$$\sigma = \sigma_0 \exp(-s_c) \qquad 2.2.13$$

where σ_0 is the prefactor and s_c is the exponent of the critical percolation conductance $G_c = G_0 \exp(-s_c)$.

According to the theory, after ignoring hopping between sites with decreasing s_{ij}, the conductivity decreases sharply at a critical value s_c. This value defines the onset of percolation; when the first infinite cluster is formed. This is deemed as the most crucial step for transport through a macroscopic disordered system. The isolated clusters are expected to increase in size with increasing s_{ij}. At s_c, the clusters are connected to their neighbouring sites by a critical number of bonds given by B_c. For three dimensional disordered systems, the percolation criterion, B_c is ~ 2.8.

In this model, the percolation criterion is analytically expressed as

$$B_c \approx \pi \left(\frac{T_0}{2\alpha T}\right)^3 N_t \exp\left(\frac{E_F + s_c kT}{kT_0}\right) \qquad 2.2.14$$

In developing *equation 2.2.14*, the positions of the energy sites are taken to be randomly distributed and a large fraction of carrier hopping is assumed to occur between tail states $(-E_F >> kT_0)$. Furthermore, the maximum energy hop is assumed to be large $(s_c kT >> kT_0)$.

Finally combining *equations 2.2.10*, *2.2.13* and *2.2.14* yields an expression for conductivity of the system:

$$\sigma(\delta,T) = \sigma_0 \left(\frac{\pi N_t \delta (T_0/T)^3}{(2\alpha)^3 B_c \Gamma\left(1 - T/T_0\right)\Gamma\left(1 + T/T_0\right)} \right)^{\frac{T_0}{T}} \qquad 2.2.15$$

Equation 2.2.15 shows that conductivity is strongly dependent on carrier concentration. In fact, conductivity varies as a function of $(\delta N_t)^{T_0/T}$. This is similar to the result obtained from our model. However, we have not used percolation theory which is essential to the derivation of an analytical expression for conductivity in this model. In contrast we have simply applied conventional device physics to an exponential DOS, an approximation increasingly associated with disordered organic materials. A full description of our model is presented in *section 2.5.*

In addition, *equation 2.2.15* demonstrates that the conductivity shows a thermally activated behaviour $\sigma \sim \exp -[E_a/kT]$ with activation energy, E_a which is weakly dependent on temperature. This activated behaviour of charge carrier transport is directly related to the exponential rise in DOS. In an exponential DOS, carriers are more likely to hop upwards in

energy as there are more states available at higher energies. This is why, in the past, hopping in exponential DOS is often described as activation from the Fermi energy to a specific transport level [31, 43].

2.2.6 MULTIPLE TRAPPING AND RELEASE (MTR) MODEL

Hydrogenated amorphous silicon (a-Si:H) is one of the most widely known disordered inorganic material to demonstrate a transport mechanism different to that of single crystalline materials. Carrier mobility in a-Si:H film is at least a few orders of magnitude lower than its crystalline counterpart. The MTR model was first introduced by Le Comber and Spear to account for the low carrier mobility in this amorphous material [43]. Charge transport in this material is limited by a distribution of localised trap states located within its energy gap. In this model, a narrow band is associated with a high concentration of trap states. The traps could either be deep traps, located in the centre of the gap, or shallow traps located close to the conduction or valence band. Much later, Monroe adapted the model for systems having an exponential DOS to account for hopping transitions over states energetically deeper than a critical energy level called the transport energy. The model was found to closely resemble the MTR process with the transport energy playing the role of the band edge.

More recently, Horowitz *et al.* [38, 44] successfully applied the MTR model to describe transport in sexithiophene (6T) and dihexylsexithiophene (DH6T) based TFTs. Using the MTR model, Horowitz demonstrated that charge transport in organic materials is dependent on temperature, the energy level of the trap states and the applied gate voltage. The MTR model assumes an exponential distribution of trap states. Charge carriers hop easily between localised states at energies above a critical energy known as the transport energy, E_T. At low energies, however, the carriers are immobilised in localised states which act like traps due to the decreasing DOS. The injected and thermal charge carriers will interact with these lower lying trap states as they transit through the organic material. According to the model, the charge carriers will first be trapped into the localised states with a probability close to unity and subsequently released via a thermally activated process as illustrated in *figure 2.2.3*. Since the release mechanism is thermally activated, the carrier mobility is strongly dependent on temperature.

The trap-controlled drift mobility, μ_D is given by

$$\mu_D = \mu_0 \alpha \exp - \left(\frac{E_a}{kT} \right) \qquad 2.2.16$$

where μ_0 is the carrier mobility at the transport energy, α is the ratio between the effective density of states at the transport level and the density of traps and E_a is the energy of the trap state. Similar to the VRH model, *equation 2.2.16* predicts an Arrhenius-like temperature dependence for carrier mobility.

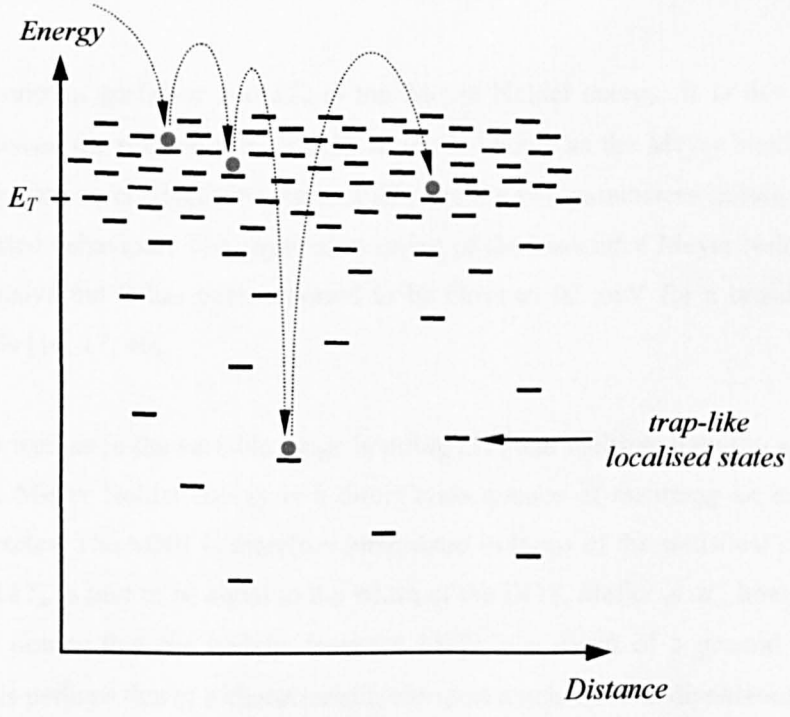

Figure 2.2.3: Schematic representation of the multiple trapping and release (MTR) model where carriers are momentarily immobilised in deep trap-like localised states before being thermally released to states at or above the transport energy E_T. The filled circles represent both thermal and injected charge carriers.

2.3 MEYER NELDEL RULE (MNR)

The thermally activated behaviour of a wide variety of physical, chemical and biological processes has been found to obey the so-called Meyer Neldel rule (MNR). This rule was first observed by Meyer and Neldel in inorganic polycrystalline materials [45]. Although it has since become a commonly occurring phenomenon, the microscopic origin of the MNR is nowhere closer to being fully understood. Numerous theories have been proposed to explain the occurrence of this rule in inorganic and organic semiconductors.

According to the MNR, any property say, Y which has been observed to obey the thermally activated law is given by

$$Y = Y_0 \exp -\left(\frac{E_a}{kT}\right) \qquad 2.3.1$$

where E_a is the activation energy and Y_0 is the prefactor which increases exponentially with E_a according to the following relationship:

$$Y_0 = Y_{00} \exp\left(\frac{E_a}{kT_m}\right) \qquad 2.3.2$$

Here Y_{00} is a constant prefactor and kT_m is the Meyer Neldel energy. It is this empirical relationship between the prefactor, Y_0 and E_a which is known as the Meyer Neldel rule. In organic semiconductors, conductivity and mobility are the two parameters known to exhibit thermally activated behaviour. The physical meaning of the associated Meyer Neldel energy still remains elusive but it has been reported to be close to 40 meV for a broad range of organic materials [16, 17, 46].

In our model as well as in the variable range hopping [37] and multiple trapping and release model [38], the Meyer Neldel energy is a direct consequence of assuming an exponential distribution of states. The MNR is therefore interpreted in terms of the statistical shift of the Fermi level and kT_m is said to be equal to the width of the DOS. Meijer *et al.*, however, have expressed their doubts that the widely observed MNR is a result of a general DOS and suggests that it is perhaps due to a characteristic transport mechanism in disordered materials [17]. This notion of the MNR being related to the charge transport mechanism has been shared by Yelon *et al.* in the past [47, 48]. He explained the MNR using a multiphonon process to describe carrier hopping in inorganic amorphous semiconductors. He said that the MNR stems from a phonon activated process where the energy of the process itself is significantly larger than a typical excitation. The much larger activation energy obtained in experiments suggests the involvement of multiple phonons. As the activation energy rises, more phonons are required and additional conduction paths will be created for charge transfer.

The extension of this theory to organic semiconductors depends on whether or not it is justified to use multiphonon process to describe hopping of carriers between localised states. Most disorder based transport models choose to ignore polaronic effects as energetic disorder is believed to be the dominant source of charge localisation in organic materials. Also, unlike inorganic semiconductors, the activation energy obtained for most disordered

materials is of the order of a phonon energy which is certainly in contrary to the belief of transport being a multiphonon process. But Emin argues that albeit the activation energy is comparable to the phonon energy, the transport should still be regarded as a multiphonon process [11, 12].

There is still no general agreement if the MNR is a result of a common DOS or if it is directly related to the polaronic nature of charge carriers in disordered materials. Nevertheless, the ubiquitous value of the Meyer Neldel energy suggests that it must have a common origin in all disordered materials.

2.4 ACCEPTOR-LIKE AND DONOR-LIKE STATES

The main characteristic features of disordered organic semiconductors are their narrow Gaussian distribution of localised states and a Fermi level, E_F which lies in the band-tail of the Gaussian function. In contrast, crystalline semiconductors like silicon have virtually no energy levels lying within the energy gap close to the Fermi level. All the electronic states are delocalised forming wide energy bands known as the conduction and valence band for electrons and holes respectively. It is only in an n-type or p-type doped semiconductor that a dopant level exists within the energy gap close to the conduction or valence band edge.

Since it is only in disordered materials that the Fermi level lies in a distribution of localised states, it becomes increasingly important to understand the nature of these energy states. There are three types of states namely acceptor-like, donor-like and amphoteric. An acceptor-like state is one that exists only in a negative or neutral condition, a donor-like state only in a positive or neutral condition and finally an amphoteric state that can exist in any of the three conditions. Ignoring amphoteric states, different combinations of states are considered for the simple case of a discrete energy level lying in the top and bottom half of the energy gap as in *figure 2.4.1*. The movement of the Fermi level, E_F through such a broad range of energy is only hypothetical and should not be taken to reflect what happens in practice as it will require the application of an infinitely large electric field. In general small changes in the Fermi level are sufficient to yield substantial changes in carrier concentration.

Suppose that both the energy levels are donor-like, the system will be highly positively charged when E_F coincides with the hole transport level, E_{ht} as empty donor-like states are positive. Here the hole transport level is akin to the valence band in conventional semiconductors. As mentioned earlier, changes in the net charge of the system are studied by virtually moving the Fermi level through the energy gap. As the Fermi level moves higher in

energy away from E_{ht}, an increasing proportion of the lower donor-like level becomes filled with charge carriers. The carrier occupancy of the discrete level increases according to the Fermi Dirac statistics and the system experiences a drop in positive charge similar to the distribution function as illustrated in *figure 2.4.1*. The net positive charge of the system will continue to fall as E_F moves through the next donor-like level located in the top half of the gap. It will vanish to zero when E_F coincides with the electron transport level, E_{et}. The electron transport level resembles the conduction band. Only when both the donor-like energy levels are completely filled will the system attain charge neutrality. At the mid gap and energies close to it, there is no visible change in charge due to the absence of any discrete energy levels. The net positive charge of the system suggests that a very high gate voltage will be needed to achieve minimum channel current.

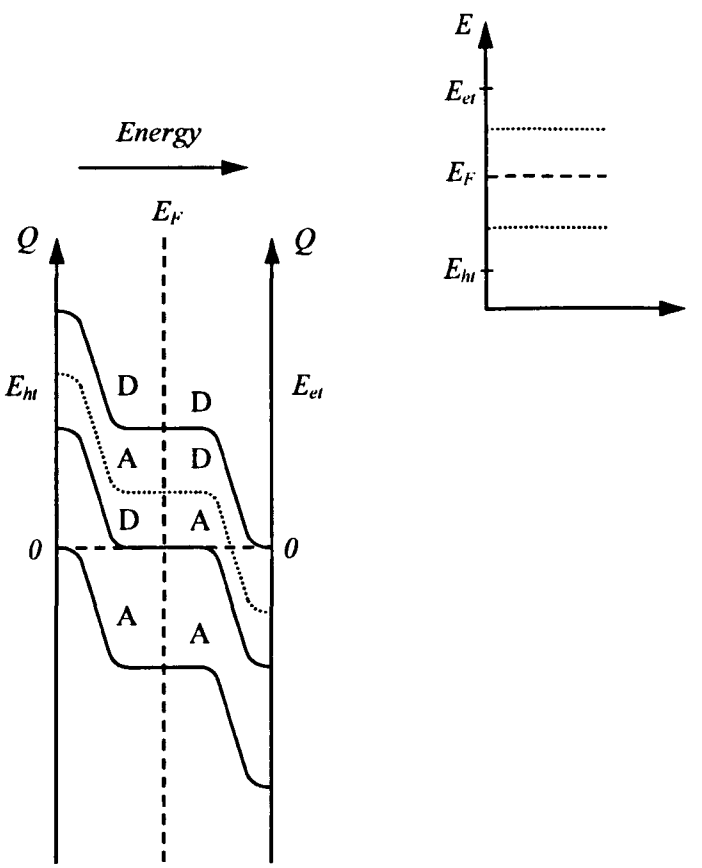

Figure 2.4.1: Charge distribution with energy for different combinations of donor-like (D) and acceptor-like (A) levels as E_F is hypothetically moved through the energy gap of the semiconductor. The A/D curve corresponds to the lower energy level having a smaller density of states than the higher donor-like level. Inset illustrates the relative position of the discrete energy levels (dotted line) in the top and bottom half of the gap. E_{ht} and E_{et} are the hole and electron transport levels respectively.

Another possibility will be for the lower energy level to be donor-like and the higher energy level to be acceptor-like. With an unoccupied donor-like energy level, the system starts out being positively charged but quickly gains charge neutrality as E_F approaches mid gap. This corresponds to the ideal situation where both the donor-like and acceptor-like level exists in their respective neutral condition. Such a situation is consistent with experiment as it suggests that only a small gate bias is required to swing the transistor into operation. Once the Fermi level moves further in energy, the acceptor-like level will also be filled resulting in the system having a net negative charge. This means that the condition for charge neutrality is only satisfied when the Fermi level lies at or close to the centre of the energy gap.

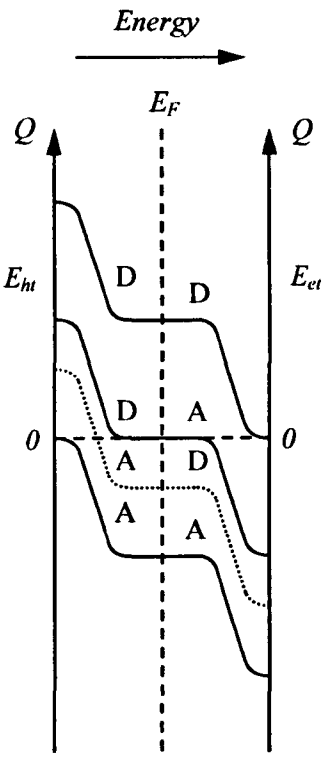

Figure 2.4.2: Distribution of charge when the discrete level in the top half of the energy gap has a smaller density of states than its lower energy counterpart. Asymmetry in the density of states only affects the A/D configuration (dotted line) causing it to shift downwards along the charge axis.

If the donor-like and acceptor-like levels are swapped around, the distribution in net charge will be exactly the same provided that both the energy levels are symmetrical. Unfortunately, in practice, the energy levels almost always differ in terms of their density of states. This discrepancy will cause the acceptor-like/donor-like curve to be shifted along the charge axis but will have no effect on the other combination of states. If the density of states of the donor-like level is larger, the curve will be shifted higher along the charge axis as in *figure*

2.4.1. This is associated with the system having a net positive charge when the Fermi level reaches the centre of the gap. Conversely, if the acceptor-like level in the bottom half of the gap dominates, the shift will be towards more negative charge as in *figure 2.4.2.* Hence the system will always lack charge neutrality thereby requiring the application of a large gate voltage.

Finally, if the two hypothetical energy levels are acceptor-like, the system will retain its charge neutrality as long as the levels remain empty. As the Fermi levels moves progressively through higher energies, a larger fraction of the energy levels become filled resulting in a net negative charge. The system will become highly negatively charged when E_F equals the electron transport level. Similar to the donor-like/donor-like case, a large gate voltage of the opposite polarity will be needed to negate the effects of the negatively charged energy levels.

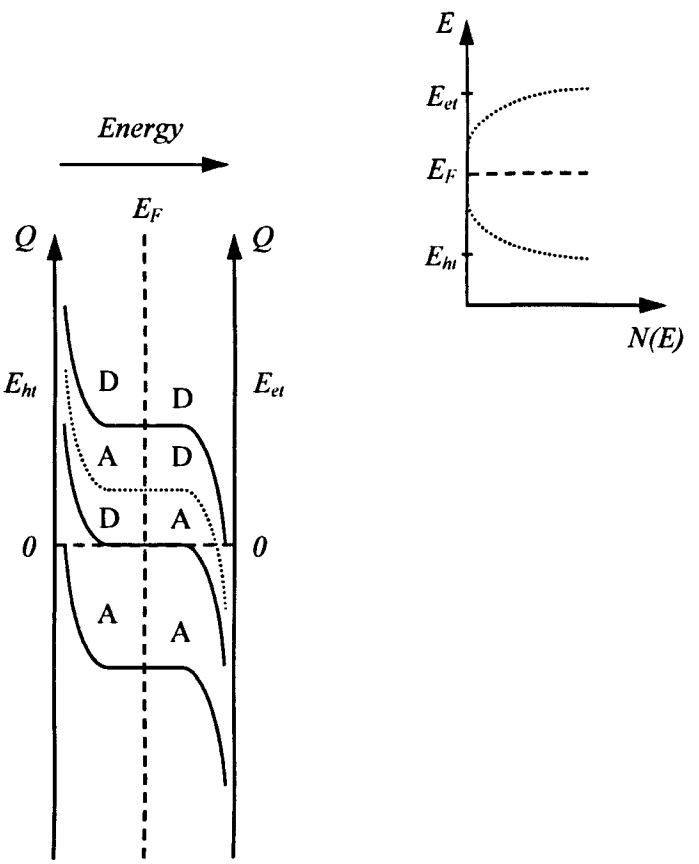

Figure 2.4.3: Variation in charge with energy for a disordered organic semiconductor characterised by an exponential distribution of localised states. The A/D curve (dotted line) shown corresponds to the hole distribution having a much smaller density of localised states compared to the electron energy distribution. The inset is a schematic representation of the exponential density of states, N(E) generally assumed in organic solids.

Variation in charge distribution with shifts in the Fermi level is relatively simple to understand for the case of discrete energy levels. However, the distribution of localised states in disordered organic materials is often represented by an exponential function. So in organic semiconductors, the top and bottom half of the energy gap will each have an exponentially rising DOS for electrons and holes respectively as shown in *figure 2.4.3*. Now the combined effect of an exponential distribution of localised states and the falling carrier occupancy governed by the Fermi Dirac distribution function must be taken into account. The result is an exponential energy distribution of charge carriers. Since the charge distribution of any system is clearly governed by the carrier occupancy of the localised states, the net charge will also be exponentially distributed as in *figure 2.4.3*. Again for the acceptor-like/donor-like configuration, the asymmetrical DOS for holes and electrons will lead to a visible shift along the charge axis. Due to the exponential nature of the DOS, the net charge of the system will continue to increase/decrease as it approaches the hole and electron transport level, only reaching a fixed value at infinity.

Regardless of the distribution of energy states, donor-like states in the bottom half of the energy gap and acceptor-like states in the top half is the only combination in close agreement with experimental observations. Only under such circumstances will a small gate voltage be sufficient to achieve minimum channel current in a transistor.

2.5 CHARGE CARRIER DENSITY DEPENDENCE OF HOPPING MOBILITY IN AN EXPONENTIAL DENSITY OF STATES (DOS)

The numerous analytical models developed to describe charge transport in disordered organic materials reflect the sheer complexity of the problem of hopping mobilities. A general agreement is still yet to be reached on whether a Gaussian or an exponential function provides a more accurate description of the distribution of states in the region of operation of a variety of devices.

In our model, we simply use the variable range hopping (VRH) theory together with an exponential density of states as an approximation to the Gaussian function. An exponential density of states is used in the analytical model since the band tail of a Gaussian function, for any particular energy range, is quite accurately an exponential as shown in *figure 2.5.1*. The Fermi level is also widely believed to lie in the band tail of a Gaussian distribution suggesting that hopping transitions at energies within the band tail are likely to dominate conduction. The exponential approximation of the DOS does provide considerable insight into charge transport in disordered materials by allowing conventional device physics to be

employed. The exponential dependence of localised states with increasing energy, E in disordered organic solids is given by

$$N(E) = \frac{N_0}{kT_c} \exp\left(\frac{E}{kT_c}\right) \qquad 2.5.1$$

where N_0 represents the number of states per unit volume at energy $E = 0$, E is the energy of localised states, k is the Boltzmann constant and T_c is the characteristic temperature of the exponential function. The term kT_c in *equation 2.5.1* corresponds to the so-called Meyer Neldel energy. *Equation 2.5.1* is similar to the approximation given by Vissenberg and Matters [41] and is thus limited to low carrier concentrations and temperatures in order for charge transport to be dominated by the band tail of the DOS. At high temperatures, the exponential DOS will dominate over the Fermi Dirac statistics suggesting an infinitely increasing carrier concentration.

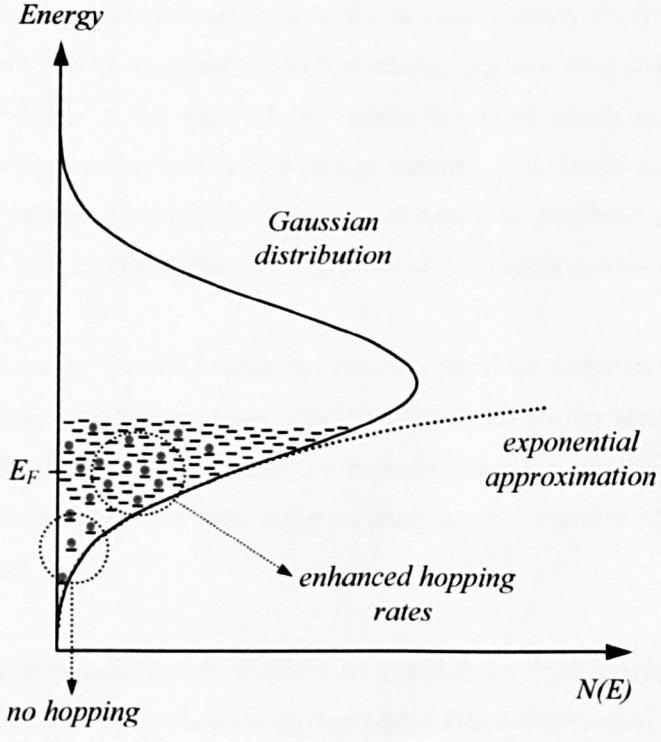

Figure 2.5.1: Schematic representation of the energy range in which a Gaussian DOS can be quite accurately approximated by an exponential function. At low energies, the occupancy is assumed to be unity with no hopping events taking place but hopping rates are enhanced at energies close to the Fermi level.

In an exponential distribution of states, the transport of carriers are said to be governed by hopping *i.e.* thermally activated tunnelling between states. According to the concept of

Variable Range Hopping (VRH), carriers may either hop over a small distance with a high activation energy or hop over a long distance with a low activation energy. It appears, however, that an analytical model which well describes the experimental results can be developed without having to consider the exact mechanism by which carriers move in an exponential distribution of localised states.

Classically, the motion of charge carriers in ordered inorganic semiconductors is described through drift and diffusion by a single mobility term, μ_c. According to the drift current equation,

$$J = \mu_c q N_c \exp -\left(\frac{E_c}{kT}\right)\exp\left(\frac{E_F}{kT}\right)F \qquad 2.5.2$$

Here J is the drift current density, N_c corresponds to the effective density of states in the conduction band, E_c is the energy of the conduction band, E_F is the Fermi level and F is the applied field. Despite the parabolic variations in the density of states of crystalline materials, a unique mobility can still be assigned to the free charge carriers. This is made possible by the high density of states at the edge of the conduction band which is large enough to accommodate all thermal and even injected charge carriers. The charge carriers residing in what appear to be an abrupt band edge will have a constant effective mass and hence behave as if they have a constant mobility. This is the prerequisite for using *equation 2.5.2.*

Over the years, the carrier mobility term has become the most important figure of merit quoted in all semiconductor devices. Hence tradition has it that carrier motion in disordered organic materials should also be described by a single classical mobility term albeit the carriers are now distributed over a wide range of energies and therefore should experience different hopping rates.

In our model, we have chosen to only consider an exponential DOS together with a falling carrier occupancy with energy as dictated by the Fermi Dirac distribution function, *f(E)* to determine the carrier concentration of the system. The Fermi Dirac statistics, in general, describes the probability of occupation of carriers in energy states under thermal equilibrium conditions. In reality, this distribution is applied even under steady state conditions as charge carriers are assumed to reach thermodynamic equilibrium. This assumption allows for a Fermi level, E_F to be defined.

The Fermi Dirac distribution function is given by

$$f(E) = \frac{1}{1 + \exp\left(\frac{E - E_F}{kT}\right)} \qquad 2.5.3$$

where E_F is the Fermi level of the semiconductor.

For most practical purposes, the Fermi Dirac function is replaced by the Maxwell Boltzmann approximation. In conventional semiconductors, this approximation is used only when the Fermi level, E_F is several kT away from the conduction or valence band edge. Fortunately, inorganic semiconductors which are often either p or n type doped will satisfy this condition. The Maxwell Boltzmann approximation is defined as

$$f(E) = \begin{cases} \exp -\left(\frac{E - E_F}{kT}\right) & \text{if } E > E_F \\ 1 & \text{if } E \leq E_F \end{cases} \qquad 2.5.4$$

where E is the energy of the localised states.

In disordered semiconductors which have a continuous distribution of trap states, one might wonder how the use of the Maxwell Boltzmann statistics is justified. As mentioned earlier, transport in disordered semiconductors occurs via hopping of charge carriers. Charge carriers will only be able to hop into a neighbouring site if the site is empty. Otherwise, repulsive Coulombic interaction between similarly charged carriers will make the particular hop energetically unfavourable. Below the Fermi level, only a small fraction of localised states remain empty and the states are located further apart which renders charge carriers in this energy range practically immobile. Hence, it is fair to assume that the occupancy, which is the fraction of states occupied, is close to unity. By doing so, hopping transitions in the lowest energy range are simply neglected. As for states above E_F, the occupancy starts off being half full but then falls rapidly with increase in energy. This sharp drop in carrier occupancy above the Fermi level is a direct consequence of the exponential function.

Besides this, *equation 2.5.1* also states that the density of states is much larger at higher energies implying that the probability of carrier hopping rises appreciably as the localised states become less far apart. The combined effect of decreasing carrier occupancy and increasing energy states leads to the charge transport being dominated by hopping events close to the Fermi level. Above the Fermi level, the use of the Maxwell Boltzmann approximation in place of the Fermi Dirac statistic will only lead to a maximum error of a

factor of 2. This small margin of error is also thought to be partially offset by ignoring the small number of hopping transitions that occur below the Fermi level.

Since only hopping events taking place above the Fermi level are considered to contribute to conduction, charge carrier density, n in disordered organic materials is given by *(Appendix B)*

$$n = \int_{E_F}^{\infty} N(E) f(E) dE$$

$$n = \frac{N_0 T_0}{T_c} \exp\left(\frac{E_F}{kT_c}\right) \qquad 2.5.5$$

where $\frac{1}{T_0} = \frac{1}{T} - \frac{1}{T_c}$.

From recent experiments, it was found that $T_c > T$ which makes it possible to have a closed form solution that has carrier density decreasing with energy. The relationship between T_o and T_c obtained in deriving *equation 2.5.5* provides valuable information regarding the transport mechanism in disordered semiconductors. The term T_0 is believed to represent the energy distribution of charge carriers which also follows an exponential function. This equation gives a simple yet comprehensive relationship between carrier distribution, energetic disorder and thermal effects in disordered materials. Further study of the equation gives us reason to believe that energetic disorder is in fact directly proportional to $1/T_c$ which in the special case of crystalline semiconductors is equal to zero. When that happens, the energetic distribution of carriers is simply characterised by the lattice temperature.

The carrier concentration dependence on the characteristic temperature of the exponential DOS, T_c in *equation 2.5.5* seems to be counter intuitive and is still not yet fully understood. The expression itself, however, is not disputed as it has already been confirmed by experiments [49]. One possible explanation for this phenomenon is thought to be associated with the fact that E_F lies in the band tail of the Gaussian distribution. This means that the distribution of states must be relatively small at energies below E_F but is strongly exponential beyond E_F. Hence altering the position of E_F by reducing the measurement temperature for instance will induce a change in carrier concentration and lead to carriers being crammed into a marginally smaller energy range. The distribution of carriers across the whole energy range will, however, remain essentially the same. So the charge carrier distribution continues to match that of the DOS and is characterised, as expected, by exactly

the same parameter, kT_c. Conversely, a distinct value of kT_c is obtained when the energetic position of the Fermi level is varied by artificially doping the intrinsic material.

Having determined the carrier concentration of the system, a drift current equation similar to *equation 2.5.2* can be obtained for disordered materials

$$J = \mu_{eff}\, q \frac{N_0 T_0}{T_c} \exp\left(\frac{E_F}{kT_c}\right) F \qquad 2.5.6$$

Here μ_{eff} is the so-called effective mobility needed to yield the correct units for J. μ_{eff} resembles the classical mobility term defined in conventional semiconductors. The relevance of the term μ_{eff} in disordered materials can be better understood by making a direct comparison with crystalline semiconductors for which the equation was originally developed. In the absence of current flow, an ordered semiconductor with a conduction band is contacted with a disordered organic material as in *figure 2.5.2*. Band bending due to a possible work function difference between the two materials and the likely presence of trapped charges are ignored in this case. Hence, under thermal equilibrium, the carrier flux from the disordered to the ordered semiconductor must be equal to the flux in the opposite direction. Also, a single energy level much like the conduction band in ordered materials must be capable of representing current in the disordered semiconductor. For simplicity, this energy level is termed the effective transport energy and is equal in energy to E_c. If an effective transport energy should exist, it must apply to all current levels including the zero current case.

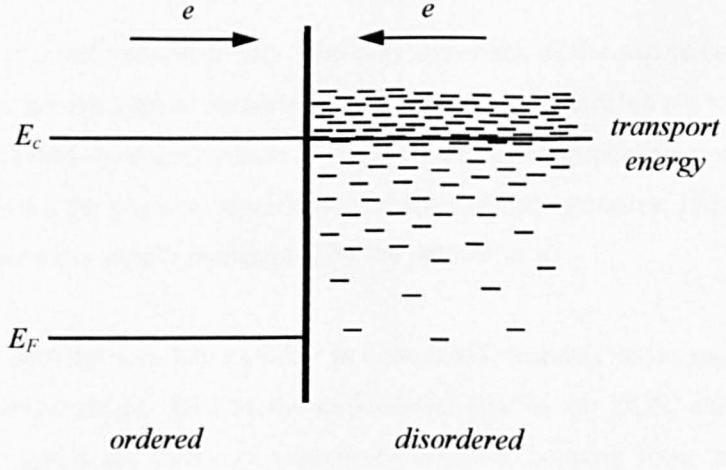

Figure 2.5.2: Schematic energy diagram of an ordered semiconductor in direct contact with a disordered semiconductor. Band bending due to possible work function differences and presence of trapped charges are neglected. Under thermal equilibrium, the electron flux in both materials must be equal and opposite in direction.

Suppose the charge density, n in disordered semiconductors is to be represented like its ordered counterpart by a single energy level E_c having an effective density N_c, the expression will then have the following form.

$$n = N_c \exp\left(\frac{E_F}{kT}\right)\exp-\left(\frac{E_c}{kT}\right) \qquad 2.5.7$$

Equation 2.5.5 can be rearranged to give

$$\exp\left(\frac{E_F}{kT}\right) = \left[n\frac{T_c}{N_0 T_0}\right]^{\frac{T_c}{T}} \qquad 2.5.8$$

With the aid of *equations 2.5.7* and *2.5.8*, the experimentally determined effective mobility μ_{eff} in disordered organic semiconductors is given by

$$\mu_{eff} = \mu_c N_c \exp-\left(\frac{E_c}{kT}\right)\left[\frac{T_c}{N_0 T_0}\right]^{\frac{T_c}{T}} n^{\left(\frac{Tc}{T}\right)-1} \qquad 2.5.9$$

Equation 2.5.9 can be further simplified to

$$\mu_{eff} = \mu_0 n^{\left(\frac{Tc}{T}\right)-1} \qquad 2.5.10$$

where $\mu_0 = \mu_c N_c \exp-\left(\frac{E_c}{kT}\right)\left[\frac{T_c}{N_0 T_0}\right]^{\frac{T_c}{T}}$ and is known as the mobility prefactor. The value of μ_0 can be determined experimentally. The only drawback of the expression for μ_0 is that most of the terms are not typical parameters of disordered materials but are rather a result of representing the exponential distribution of states by a single transport energy. This makes it harder to understand the physical significance of the mobility prefactor. Hence, in practice, the mobility prefactor is simply represented by the parameter K.

Equation 2.5.10 demonstrates that mobility in disordered materials varies superlinearly with charge carrier concentration. Due to the exponential rise in the DOS, charge carriers at different energy levels are likely to experience different hopping rates; hence the term effective mobility. Charge carriers residing at higher energy levels will have higher mobilities as there are more unoccupied energy states which are less far apart. This empirical relationship between effective mobility and carrier concentration is commonly known as the Universal Mobility law (UML). This concept of a Universal Mobility Law (UML) was first

introduced by Brown *et. al* from measurements made on field effect transistors (FETs) doped with poly(β'-dodecyloxy- α, α',- α', α"terthienyl) (polyDOT$_3$) [16]. It should be noted that the exponent in *equation 2.5.10* shows a dependence on the characteristic temperature of the DOS T_c [50].

Although conduction in disordered organic materials differs greatly from that of conventional semiconductors, it is still possible to describe carrier motion by an effective mobility which is conceptually similar to the classical mobility term but shows a strong dependence on carrier concentration. The most common observation of this dependence is the field effect hole mobility in FETs which is at least an order of magnitude larger than the hole mobility in light emitting diodes (LEDs) based on the same disordered organic material.

2.6 CONCLUSIONS

This chapter discusses in detail the various charge transport models proposed to describe conduction in disordered organic materials. It is generally agreed that carrier motion in disordered materials occurs via thermally assisted tunnelling (*i.e.* hopping) between localised states. Charge transport is also reported to exhibit thermally activated behaviour which means that carrier mobility will fall with decreasing temperature.

The transport models reviewed here are based on either the polaronic or disorder phenomenon. Those who advocate the polaron based model believe that localisation in organic materials is dominated by their strong electron-phonon coupling. Up until now the polaron model was amongst the few models that promoted the idea of an Arrhenius-like temperature dependence for carrier mobility. But recently, Coehoorn *et al.* showed that taking into account the carrier concentration dependence of mobility in Gaussian disorder models can explain both the $1/T^2$ and $1/T$ dependence observed in organic materials. This finding means that the need for a polaronic based transport model becomes less obvious as temperature effects in disordered materials can now be fully understood even with a Gaussian disorder model. Furthermore, polaron binding energies are much smaller than the Gaussian disorder width which suggests that disorder effects must dominate. The occurrence of Poole Frenkel-like conduction in organic semiconductors is rather doubtful since hopping distances reported for these materials are significantly smaller than that suggested by the model.

The energetic distribution of states in organic materials is widely believed to follow a Gaussian distribution. Some disorder models, however, have chosen to approximate the DOS by an exponential function since the band tail of a Gaussian is quite accurately an exponential. The exponential approximation is also supported by the belief that the Fermi level lies in the band tail of the Gaussian function. Both the Gaussian disorder models developed by Bässler and later by Baranovskii are valid only in the small carrier concentration limit. Their models, however, fail to take into account the possible dependence of mobility on carrier concentration. In contrast, the model developed by Vissenberg and Matters using the VRH concept and the multiple trapping and release (MTR) model both utilize an exponentially rising DOS. Like them, we believe that an exponential DOS provides considerable insight into the charge transport mechanism of disordered materials. The VRH model is said to be valid only at low carrier concentrations and temperatures in order for transport to be dominated by the band tail of the DOS. This model also derives the widely

observed empirical relationship between conductivity and carrier density using percolation theory. Both models predict an Arrhenius-like temperature dependence for carrier mobility.

The occurrence of the Meyer Neldel rule in disordered organic materials is also discussed. Many theories have been proposed in an attempt to elucidate the origin of this rule. For models using an exponential DOS, the statistical shift of the Fermi level in the DOS seems to be the most likely explanation. In the past, however, the MNR has been related to the hopping of charge carriers via a multiphonon process. Yelon *et al.* said that the MNR stems from a phonon activated process where the energy of the process itself is significantly larger than a typical excitation. The applicability of this theory to organic materials, however, hinges on whether or not it is justified to describe hopping events using the multiphonon process. The smaller polaron binding energy compared to the Gaussian disorder width suggests that energetic disorder is likely to dominate over polaronic effects. A Meyer Neldel energy close to 40 meV is reported for a wide variety of organic materials.

The nature of localised states lying in the bottom and top half of the energy gap is discussed briefly. The three types of localised states are acceptor-like, donor-like and amphoteric. Having ignored amphoteric states, the only configuration consistent with experiments was determined to be donor-like states in the bottom half of the energy gap and acceptor-like states in the top half. Only under such conditions will a small gate voltage be sufficient to reach minimum channel current in a transistor.

In crystalline semiconductors, carrier motion is traditionally described by a unique mobility term. Extending this practice to disordered organic materials seems inappropriate since charge carriers at different energies experience different hopping rates. By comparing a crystalline semiconductor in direct contact with a disordered one, we demonstrate that it is possible to describe carrier motion using a single transport level akin to the conduction/valence band edge. In doing so, an effective mobility term which is strongly dependent on carrier concentration is obtained for disordered materials. The effective mobility also shows a dependence on the characteristic temperature of the exponential DOS T_c through the exponent term. Unlike the VRH based model, we successfully demonstrate the Universal Mobility Law (UML) which relates mobility to carrier density without using the percolation approach. The UML is considered as an important electrical property of disordered organic materials since in poly(3-hexylthiophene) (P3HT), the carrier density dependence of mobility dominates even at acceptor concentrations as low as 10^{16} cm^{-3}.

2.7 REFERENCES

[1] H. Bässler, *Phys. Stat. Solidi B* **175**, 15, 1993.

[2] D. Emin, *Phys. Rev. B* **48**, 13691, 1993.

[3] T. Holstein, *Ann. Phys.* **281**, 706, 2000.

[4] J. Yamashita and T. Kurosawa, *J. Phys. Chem. Solids* **5**, 34, 1958.

[5] T. Holstein, *Ann. Phys.* **8**, 343, 1959.

[6] D. Emin, "Basic Issue of Electric Transport in Insulating Polymers", *Handbook of Conducting Polymers*, Ed. T. A. Skotheim, Marcel Dekker, New York, 1985.

[7] D. Emin and T. Holstein, *Ann. Phys.* **53**, 439, 1969.

[8] E. M. Conwell, *Phys. Rev.* **103**, 51, 1956.

[9] N.F. Mott, *Can. J. Phys.* **34**, 1356, 1956.

[10] A. Miller and E. Abraham, *Phys. Rev.* **120**, 745, 1960.

[11] D. Emin, *Phys. Rev. Lett.* **32**, 303, 1974.

[12] D. Emin, *Adv. Phys.* **24**, 305, 1975.

[13] O. Bleibaum, H. Böttger and V. V. Bryksin, *Phys. Rev. B* **66**, 104203, 2002.

[14] J. Frenkel, *Phys. Rev.* **54**, 647, 1938.

[15] W.D. Gill, *J. Appl. Phys.* **43**, 5033, 1972.

[16] A.R. Brown, C. P. Jarrett, D. M. de Leeuw and M. Matters, *Synth. Met.* **88**, 37, 1997.

[17] E. J. Meijer, M. Matters, P.T. Herwig, D. M. de Leeuw and T. M. Klapwijk, *App. Phys. Lett.* **76**, 3433, 2000.

[18] E. J. Meijer, D. B. A. Rep, D. M. de Leeuw, M. Matters, P. T. Herwig and T.M. Klapwijk, *Synth. Met.* **121**, 1351, 2001.

[19] R. Coehoorn, W. F. Pasveer, P.A. Bobbert and M. A. J. Michels, *Phys. Rev. B* **72**, 155206, 2005.

[20] S. D. Baranovskii, O. Rubel and P. Thomas, *J. Non-Cryst. Solids* **352**, 1644, 2006.

[21] P.M. Borsenberger, *J. Appl. Phys.* **68**, 6263, 1990.

[22] P.W.M. Blom, M.J.M. de Jong and M.G. Van Munster, *Phys. Rev. B* **55**, 656, 1997.

[23] H.C.F. Martens, P.W.M. Blom and H.F.M. Schoo, *Phys. Rev. B* **61**, 7489, 2000.

[24] Y.N. Gartstein and E.M. Conwell, *Chem. Phys. Lett.* **245**, 351, 1995.

[25] D.H. Dunlap, P.E. Parris, and V.M. Kenkre, *Phys. Rev. Lett.* **77**, 542, 1996.

[26] S.V. Novikov, D.H. Dunlap, V.M. Kenkre, P.E. Parris and A.V. Vannikov, *Phys. Rev. Lett.* **81**, 4472, 1998.

[27] Z.G. Yu, D.L. Smith, A. Saxena, R.L. Martin and A.R. Bishop, *Phys. Rev. Lett.* **84**, 721, 2000.

[28] Z.G. Yu, D.L. Smith, A. Saxena, R.L. Martin and A.R. Bishop, *Phys. Rev. B* **63**, 85202, 2001.

[29] S. D. Baranovskii, H. Cordes, F. Hensel and G. Leising, *Phys. Rev. B* **62**, 7934, 2000.

[30] O. Rubel, S.D. Baranovskii, P. Thomas and S. Yamasaki, *Phys. Rev. B* **69**, 014206, 2004.

[31] D. Monroe, *Phys. Rev. Lett.* **54**, 146, 1985.

[32] A. Nemeth-Buhin, C. Junasz, V. I. Arkhipov and H. Bässler, *Philos. Mag. Lett.* **74**, 295, 1996.

[33] S. J. S. Lemus and J. Hirsc, *Philos. Mag. A* **53**, 25, 1986.

[34] N. F. Mott and E. A. Davis, *"Electronic Processes in Non-Crystalline Materials"*, 2nd Ed., Oxford University Press, London, 1979.

[35] B.I. Shklovskii and A.L. Efros, *"Electronic Properties of Doped Semiconductors"*, Springer, Heidelberg, 1984.

[36] M. Grunewald and P. Thomas, *Phys. Stat. Solidi B* **94**, 125, 1979.

[37] M. C. J. M. Vissenberg and M. Matters, *Phys. Rev. B* **57**, 12964, 1998.

[38] G. Horowitz, R. Hajlaoui and P. Delannoy, *J. Phys. III France* **5**, 355, 1995.

[39] F. R. Shapiro and D. Adler, *J. Non-Cryst. Solids* **74**, 189, 1985.

[40] M. Sahimi, *"Applications of Percolation Theory"*, Taylor & Francis, London, 1994.

[41] V. Ambegaokar, B. I. Halperin and J. S. Langer, *Phys. Rev. B* **4**, 2612, 1971.

[42] S. D. Baranovskii, T. Faber, F. Hensel and P. Thomas, *J. Phys.: Condensed Matter* **9**, 2699, 1997.

[43] P. G. Le Comber and W. E. Spear, *Phys. Rev. Lett.* **25**, 509, 1970.

[44] G. Horowitz, *J. Mater. Chem.* **9**, 2021, 1999.

[45] W. Meyer and H. Neldel, *Z. Tech. Phys.* (Leipzig) **18**, 588, 1937.

[46] J. C. Wang and Y. F. Chen, *Appl. Phys. Lett.* **73**, 948, 1998.

[47] A. Yelon and B. Movaghar, *Phys. Rev. Lett.* **65**, 618, 1990.

[48] A. Yelon, B. Movaghar and H. M. Branz, *Phys. Rev. B* **46**, 12244, 1992.

[49] N. Sedghi, D. Donaghy, M. Raja, S. Badriya, S. J. Higgins and W. Eccleston, *J. Non-Cryst. Solids* **352**, 1641, 2006.

[50] Y. Roichman, Y. Preezant and N. Tessler, *Phys. Stat. Solidi A* **201**, 1246, 2004.

CHAPTER 3

ELECTRICAL CHARACTERISATION OF POLY(3-HEXYLTHIOPHENE) SCHOTTKY DIODES

This chapter looks at the properties and operation of metal semiconductor barriers. The charge transport mechanism across the Schottky barrier along with the image force lowering effect is discussed. A brief introduction to the properties of poly(3-alkylthiophenes) (P3ATs) is also included. As-synthesised and doped P3HT Schottky diodes are characterised and the characteristic temperature corresponding to the exponential distribution of intrinsic states and carriers is determined from the current density voltage measurements. In addition, a method for determining the conduction mechanism in the neutral region of the P3HT diode is also presented.

3.1 INTRODUCTION

The behaviour of metal/semiconductor interface is extremely crucial to the performance of organic semiconductor devices. The interface formed between a metal and an organic semiconductor can be classified as either ohmic, low resistance or rectifying. An ohmic contact is generally regarded as one that provides equal access to both electrons and holes. This simple definition, however, does not lend itself well to disordered organic semiconductors. Here metals such as gold which is widely reported to make an ohmic contact with poly(3-hexylthiophene) promotes the passage of holes but not electrons, at least not in equal proportions [1, 2]. In a low resistance contact, there will either be a small barrier or no barrier at all for a single type of charge carrier. Ohmic and low resistance contacts are, however, often assumed to be the same [3]. Schottky barriers which are perhaps the most common form of rectifying contacts owe their rectifying property to the formation of a large potential barrier at the metal/semiconductor interface. The height of the resulting potential barrier may be easily altered by the application of an external voltage.

A Schottky diode has a sandwich structure consisting of two metal electrodes on either side of an organic semiconductor. One of the electrodes will be a metal of a low work function like aluminium or titanium as it forms a Schottky barrier with most p-type organic semiconductors. Meanwhile the other electrode will usually be gold as it is one of few metals known to make an ohmic contact with organic semiconductors. Given that it is possible to apply relatively large voltages across Schottky diodes without causing any performance degradation, these devices allow a much wider energetic distribution of localised states to be studied. In both MOS capacitors and TFTs, the field effect only permits charge transport across lower lying energy states to be analysed.

This chapter is primarily concerned with the electrical characterisation of Schottky diodes made with poly(3-hexylthiophene) (P3HT). First a basic understanding of the operation of metal semiconductor diodes and the two main charge transport models: diffusion theory and thermionic emission is presented. These models were originally developed for Schottky barriers involving inorganic semiconductors but have since been extended to describe conduction in organic based Schottky diodes. The chapter then progresses to review the Schottky effect which is known to dominate the barrier height $q\phi_B$ under reverse bias conditions. The properties of poly(3-alkylthiophenes) and the fabrication procedure of Schottky diodes made with poly(3-hexylthiophene) are also presented. The electrical conduction in an as-synthesised P3HT Schottky diode is discussed based on its current density voltage measurement. In this discussion a simple model which allows the

determination of the intrinsic values of T_0 and T_c is presented. The experimental result of a P3HT Schottky diode doped with 2,3-dichloro-5,6-dicyano-1,4-benzoquinone (DDQ) is also reviewed. It has already been established that dopants like DDQ significantly improve the conductivity of disordered organic materials [4, 5].

3.2 METAL SEMICONDUCTOR DIODES

A potential barrier or otherwise also known as a Schottky barrier is formed when a metal of an appropriate work function is brought into contact with a semiconductor. The potential barrier mainly results from the difference in work function between the metal and the semiconductor [6]. But in some instances the barrier may also be affected by the presence of trapped charges at the interface.

Since a majority of disordered organic materials are intrinsically p-type, *figure 3.2.1* shows the energy diagram of a low work function metal in contact with a p-type semiconductor. To clearly illustrate the shape of the potential barrier envisaged in disordered semiconductors, the localised states are distributed in a succession of energy levels with the absence of any off-diagonal disorder. But in practice, the localised states will be randomly distributed making it harder to distinguish the potential barrier lying close to the metal-semiconductor interface. It is also believed that the random energetic distribution will have an effect on charge transport across the Schottky barrier as it provides alternative charge transfer routes leading to other potential barriers.

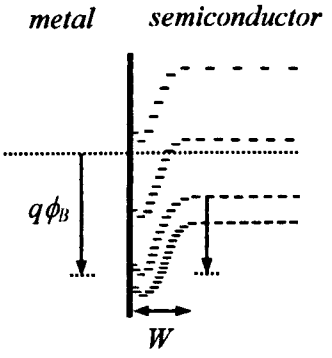

Figure 3.2.1: Simplified energy diagram for a metal/p-type disordered organic semiconductor at quasi thermal equilibrium without any applied voltage. $q\phi_B$ represents the barrier height, V_{bi} the built in potential of the semiconductor and W the width of the space charge region.

A flat quasi Fermi level is defined for the majority charge carriers which are holes in the case of a p-type semiconductor. The quasi Fermi level E_F is essentially a hypothetical energy level defined to validate the Fermi Dirac distribution function in a system which is no longer in true thermal equilibrium [7]. Often individual quasi Fermi levels are defined for holes and electrons in a single semiconductor. The energy difference between both the Fermi levels

will prompt electrons to be injected from the metal into the semiconductor. The electron transfer will cease once the quasi Fermi level has aligned itself with that of the metal as in *figure 3.2.1* indicating that the system has finally reached thermodynamic equilibrium. A potential barrier which is not truly parabolic forms within the semiconductor. The barrier has a non-parabolic shape due to the attractive electrostatic force experienced by carriers in the semiconductor towards the metal from their image charge. The potential barrier is associated with a space charge region consisting of uncompensated acceptor ions occupying a layer of thickness *W*. The assumption that the semiconductor is homogeneous leads to a uniform distribution of acceptor ions. The resulting potential barrier qV_{bi} will impede the movement of holes across the metal semiconductor interface.

The rectifying properties of a Schottky barrier can be studied simply through the application of an external voltage. When a negative voltage is applied on the p-type semiconductor, the potential barrier is enhanced giving rise to a much wider space charge region as in *figure 3.2.2*. The higher potential barrier makes it harder for holes to flow across the interface. The current is thus mainly associated with the flow of holes from the metal.

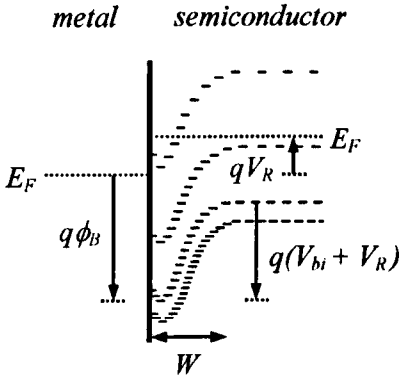

Figure 3.2.2: Energy diagram for a metal/p-type semiconductor under reverse bias. The semiconductor is assumed to be in quasi thermal equilibrium even in the presence of current flow thus giving rise to a flat quasi Fermi level E_F. V_R corresponds to the negative voltage applied on the semiconductor with respect to the metal.

When the polarity of the applied voltage is reversed, the potential barrier to the movement of holes is significantly reduced. Even holes located at much higher energy states will now be able to cross into the metal. The space charge region adjacent to the interface shrinks as a higher concentration of holes compensates an increasing number of acceptor ions. *Figure 3.2.3* shows the energy diagram of a Schottky barrier under such conditions. The observed exponential rise in current is believed to be associated with the exponential distribution of

holes. The strong rise in current ceases when a higher fraction of the applied voltage starts to fall across the neutral region. The saturation current level is thus said to be limited by the resistivity of the neutral region. More recently, it was found that the interface formed between the semiconductor and the so-called ohmic contact may also affect the saturation current.

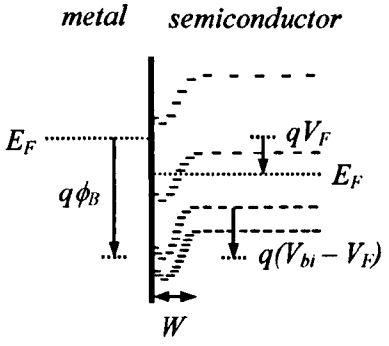

Figure 3.2.3: Energy diagram for a metal/p-type disordered semiconductor at forward bias. V_F is the positive voltage applied on the semiconductor with respect to the metal.

3.3 TRANSPORT MECHANISMS IN SCHOTTKY DIODES

Charge transport across Schottky barriers made with disordered organic materials is often described using models which were originally developed for inorganic semiconductors. The models detail the different mechanisms by which majority charge carriers overcome the potential barrier formed at the metal semiconductor interface. The two most common transport mechanisms are diffusion and thermionic emission. Quantum mechanical tunnelling also occurs but it is limited to heavily doped materials where the potential barrier is extremely thin. The thin potential barrier will allow charge carriers to easily tunnel through.

Diffusion theory was first introduced by Wagner (1931) and later by Schottky and Spenke (1939). According to this theory, the current is limited by a combination of drift and diffusion within the space charge region adjacent to the metal. Much later, Bethe (1942) proposed the thermionic emission model which has since proven to accurately describe transport in high mobility semiconductors e.g. silicon. In this model, the current is said to be controlled by the emission of carriers from the semiconductor over the top of the barrier into the metal.

The key distinction between these two models is the position at which the quasi Fermi level of the semiconductor equilibrates with the metal Fermi level when a bias is applied across the Schottky barrier as shown in *figure 3.3.1*. In the diffusion model, the quasi Fermi level is believed to coincide with the metal Fermi level at the interface thus allowing equilibrium to be reached within the semiconductor. This means that carriers at the top of the barrier are in equilibrium with their metal counterparts and do not change with applied bias. Closer to the interface, the gradient of the quasi Fermi level will drive the carriers into the metal. The current is therefore said to be limited by the transport of majority carriers across the space charge region.

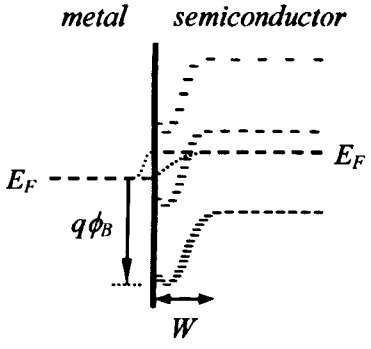

Figure 3.3.1: Simplified energy diagram of a metal/p-type disordered semiconductor showing the equilibration of the quasi Fermi level with the metal Fermi level according to diffusion theory (square dotted line) and the thermionic emission theory (dotted line). $q\phi_B$ is the barrier height whilst W is the width of the space charge region.

In the thermionic emission model, however, the quasi Fermi level does not coincide with the metal Fermi level at the interface. Instead it is assumed to remain flat throughout the space charge region much like a p-n junction and reaches equilibrium only in the metal. Gossick highlighted that carriers emitted from the semiconductor are in fact not in thermal equilibrium with their metal counterparts as they possess more energy [8]. To illustrate the difference in Fermi levels, he regarded the carriers emitted from the semiconductor different from the intrinsic carriers of the metal and crudely termed them as 'hot' carriers. But as these 'hot' carriers move through the metal, they will lose their energy through collisions and the quasi Fermi level will eventually fall to that of the metal. The current is thus controlled by the concentration of charge carriers having sufficient energy to overcome the barrier. According to Bethe, this model applies only if the mean free path of the carriers is greater than the distance over which the barrier falls by an amount kT from its maximum value [9]. In other words, the thermionic emission model is valid only in materials with high carrier mobilities.

For both models, the forward current density follows the general relationship [10],

$$J = J_0 \exp\left[\left(\frac{qV}{\eta kT}\right) - 1\right] \qquad 3.3.1$$

where q is the electronic charge, V is the applied voltage, η is the ideality factor, k is the Boltzmann constant and T is the absolute temperature. J_0 corresponds to the saturation current density and it varies depending on which mechanism controls current flow.

In the diffusion theory, the saturation current density, J_{D0} for a conventional p-type semiconductor is given by

$$J_{D0} = qN_V \mu F_{\max} \exp -\left(\frac{q\phi_B}{kT}\right) \qquad 3.3.2$$

where N_V is the effective density of states in the valence band, μ is the carrier mobility, ϕ_B is the barrier height and F_{max} is the maximum field strength in the space charge layer, ignoring image force lowering of the barrier.

For the thermionic emission model, the saturation current density, J_{TE0} is given as [10]

$$J_{TE0} = A^* T^2 \exp -\left(\frac{q\phi_B}{kT}\right) \qquad 3.3.3$$

where A^* is the Richardson constant.

Equation 3.3.1 tells us that both models predict an exponential rise in current with increasing applied voltage. The strong rise in current must be associated with an exponential energetic distribution of charge carriers. Only *equation 3.3.1* will be used in the modelling of the current density voltage characteristics of Schottky diodes made with disordered organic semiconductors. The current in these diodes will eventually deviate from *equation 3.3.1* as a higher fraction of the applied voltage starts to falls across the neutral region. The saturation current is believed to be either ohmic or space charge limited depending on the amount of dopant present in the intrinsic material. Higher dopant concentrations are thought to help compensate the build up of charge carriers in the neutral region.

3.4 THE SCHOTTKY EFFECT

The barrier height $q\phi_B$ of a Schottky diode is strongly dependent on the electric field in the space charge region. The barrier height is thus affected by the image force lowering effect and the application of an external electric field [10]. The image force lowering effect in a p-type semiconductor arises from the attractive force experienced by a hole from its negative image charge lying equidistance from the metal semiconductor interface as illustrated in *figure 3.4.1*. The image force experienced by a hole located at an arbitrary distance x from the interface is given by

$$F = -\frac{q^2}{4\pi\varepsilon_0\varepsilon_\infty(2x)^2} = -\frac{q^2}{16\pi\varepsilon_0\varepsilon_\infty x^2} \qquad 3.4.1$$

where q is the electronic charge, ε_0 is the permittivity of free space, ε_∞ is the high frequency permittivity of the semiconductor and $2x$ is the distance between the hole and its image charge. The high frequency permittivity is used in *equation 3.4.1* as charge carriers close to the interface are expected to approach the metal with thermal velocity. This consequently gives the semiconductor insufficient time to become fully polarised by the electric field. But even in silicon, the transit time of the charge carriers has been reported to marginally exceed the high frequency limit [11]. Hence in practice the static permittivity is generally used in place of the high frequency permittivity.

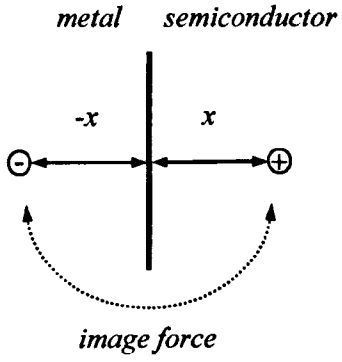

Figure 3.4.1: Image force effect between a hole in the p-type semiconductor and its image negative charge lying equidistance from the metal semiconductor interface.

The potential energy of holes as a result of the image force is given by

$$E(x) = -\frac{q^2}{16\pi\varepsilon_0\varepsilon_\infty}\int_\infty^x \frac{1}{x^2}dx = \frac{q^2}{16\pi\varepsilon_0\varepsilon_\infty x} \qquad 3.4.2$$

Equation 3.4.2 shows that the potential energy of holes decreases with distance ultimately reaching zero at infinity.

As mentioned earlier, the barrier height is also modified by the presence of an external field in the space charge region of the semiconductor. The potential energy of the holes due to the external field is given by

$$E(x) = qxF \qquad 3.4.3$$

where F corresponds to the applied field. In contrast the external field causes the potential energy of holes to increase linearly with distance.

The combined potential energy of holes as a function of distance is thus given by

$$E(x) = \frac{q^2}{16\pi\varepsilon_0\varepsilon_\infty x} + qxF \qquad 3.4.4$$

The maximum potential energy occurs at a distance x_m from the metal semiconductor interface thus resulting in the barrier height being reduced by an amount $\Delta\phi_B$ as illustrated in *figure 3.4.2*. The distance x_m corresponds to the position in semiconductor where the field due to the image force is equal and opposite to that of the applied field.

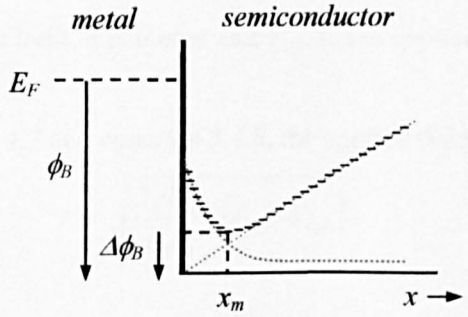

Figure 3.4.2: The barrier lowering effect on localised states in a p-type disordered semiconductor due to the combined effect of the external field (dotted line) and image force (square dotted line). The barrier is lowered by $\Delta\phi_B$ at a distance x_m.

The expression for x_m is given by

$$x_m = \sqrt{\frac{q}{16\pi\varepsilon_0\varepsilon_\infty F}} \qquad 3.4.5$$

The magnitude of the barrier lowering $\Delta\phi_B$ is thus given by

$$\Delta\phi_B = x_m F + \frac{q}{16\pi\varepsilon_0\varepsilon_\infty x_m} = 2x_m F \qquad 3.4.6$$

Since the image force lowering effect is only significant close to the metal semiconductor interface, the electric field is approximated as being equal to its maximum value.

The electric field in the space charge region is generally determined by the distribution of acceptor ions. According to Poisson's equation, the variation in potential with distance for a uniform distribution of acceptor ions is given by

$$\frac{d^2V}{dx^2} = \frac{qN_A}{\varepsilon_0\varepsilon_s} \qquad 3.4.7$$

where q is the electronic charge, N_A is the acceptor ion concentration and ε_s is the static dielectric constant of the semiconductor.

Integrating *equation 3.4.7* from the semiconductor surface to the edge of the space charge region yields an expression for the depletion width W.

$$W = \sqrt{\frac{2\varepsilon_0\varepsilon_s}{qN_A}\left(V_{bi} - V_{app}\right)} \qquad 3.4.8$$

Here V_{bi} corresponds to the built in potential and V_{app} to the applied voltage.

With the aid of *equation 3.4.7* and *equation 3.4.8*, the applied field is expressed as

$$F = \sqrt{\frac{2qN_A}{\varepsilon_0\varepsilon_s}\left(V_{bi} - V_{app}\right)} \qquad 3.4.9$$

Having developed expressions for the applied field and x_m, the barrier lowering $\Delta\phi_B$ from *equation 3.4.6* can now be redefined as

$$\Delta\phi_B = 2\left[\frac{q}{16\pi\varepsilon_0\varepsilon_\infty}\right]^{1/2}\left[\frac{2qN_A}{\varepsilon_0\varepsilon_s}\left(V_{bi} - V_{app}\right)\right]^{1/4} = \left[\frac{q^3 N_A}{8\pi^2\varepsilon_0^{\,3}\varepsilon_s\varepsilon_\infty^{\,2}}\left(V_{bi} - V_{app}\right)\right]^{1/4} \qquad 3.4.10$$

Equation 3.4.10 shows the barrier lowering to be a function of the applied voltage. In the reverse direction, the increasing depletion width causes the barrier height to reduce and shift closer to the metal semiconductor interface as in *figure 3.4.3* [10]. Meanwhile, in the forward

direction, the significantly smaller space charge region causes the top of the barrier to move away from the semiconductor surface. Due to the strong dependence on the external field, the Schottky effect is more dominant in the reverse direction. In the absence of the Schottky effect, the reverse current is expected to saturate with increasing applied voltage. In forward bias, current is dominated by holes from much higher energy states crossing into the metal.

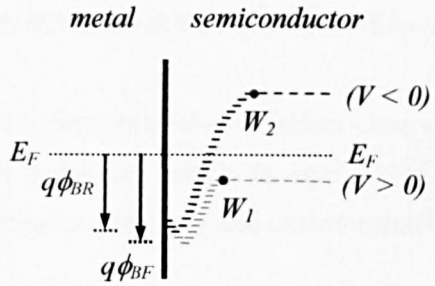

Figure 3.4.3: Energy diagram illustrating the Schottky effect for a metal/p-type organic semiconductor under different biasing conditions for a single energy level. The barrier heights under forward and reverse bias are $q\phi_{BF}$ and $q\phi_{BR}$ respectively. W_1 and W_2 denote the width of the space charge region under both biasing conditions.

Taking into account the image force lowering of the barrier, the reverse current density is given by [12]

$$J_R = J_0 \exp\left[\frac{q}{kT}\left(\frac{q^3 N_A\left(V_{app} - V_{bi} - {kT_c}/{q}\right)}{8\pi^2 \varepsilon_0^{\,3} \varepsilon_s \varepsilon_\infty^{\,2}}\right)^{1/4}\right] \qquad 3.4.11$$

where J_0 is a constant, k is the Boltzmann constant and T_c is the characteristic temperature of the exponential distribution of localised states.

Equation 3.4.11 predicts that the reverse current density will vary as a function of $\left(V_{app} - V_{bi} - {kT_c}/{q}\right)^{1/4}$. The term ${kT_c}/{q}$ is included in the above expression to account for the gradual increase in carrier concentration at the edge of the space charge region. The carrier concentration increases to its intrinsic value over a short distance known as the effective Debye length L_{De}. Interestingly, the effective Debye length in organic semiconductors shows a dependence on the characteristic temperature T_c of the exponential DOS and not the absolute temperature as it is in the case of crystalline semiconductors. The influence of the distribution of localised states is expected as charge carriers obey Pauli Exclusion Principle

and thus fill up states at lower energy levels with increasing concentrations. In practice, the space charge region is assumed to have an abrupt edge. The validity of the abrupt depletion edge approximation in disordered organic semiconductors will be elaborated later in this chapter. The Schottky theory also assumes the metal to have a uniform density of states whilst takes no account of the nature of charge transport in the semiconductor material.

3.5 PROPERTIES OF POLY(3-ALKYLTHIOPHENES) (P3ATs)

Polythiophenes are perhaps the most extensively studied class of conjugated polymers in recent decades due to their solubility which is atypical of polyconjugated systems, polycrystalline structure, electrical conductivity and environmental and thermal stability.

Poly(3-alkylthiophene) was first chemically synthesised in 1985 by incorporating an alkyl side chain into the β-position of the thiophene ring [13, 14]. P3ATs with alkyl groups longer than butyl (R = C_4H_9) are readily soluble in common organic solvents. The most commonly used P3ATs are synthesised with either a hexyl (R = C_6H_{13}), octyl (R = C_8H_{17}) or dedocyl (R = $C_{10}H_{21}$) side chain. The length of the alkyl side chain has been reported to have a significant effect on the physical properties of the material with longer alkyl substituents enhancing the interlayer structural ordering but at the expense of the melting point and thermal stability [15].

Since 3-alkylthiophene monomers are neither centrosymmetric nor possess a symmetry axis, three types of diad regioisomers are formed upon the coupling of two 3-alkylthiophene rings namely the head-to-tail coupling (HT), head-to-head coupling (HH) and the tail-to-tail coupling (TT) [16]. This unfortunately leads to the coexistence of four spectroscopically distinct triads structures: HT-HT, TT-HT, HT-HH and TT-HH in a non-regioregular poly(3-alkylthiophene) as shown in *figure 3.5.1*.

The highly undesirable head-to-head (HH) coupling experiences steric repulsion between both the alkyl side chains and the lone pairs of the adjacent sulphur atoms. Regiorandom P3ATs with the unfavourable HH couplings are thus unable to access planar configuration as a result of the odd placement of the solubilising alkyl substituents. This leads to the loss of conjugation and the consequent inhibition of the intrachain charge mobility [17]. In contrast regioregular, head-to-tail (HT) P3ATs readily adopts a low energy planar conformation leading to highly conjugated polymers and enhanced two-dimensional conductivity. Regioregular P3ATs also exhibit a smaller energy gap (1.7 eV) which is 0.4 eV lower compared to regiorandom P3ATs (2.1 eV) [17].

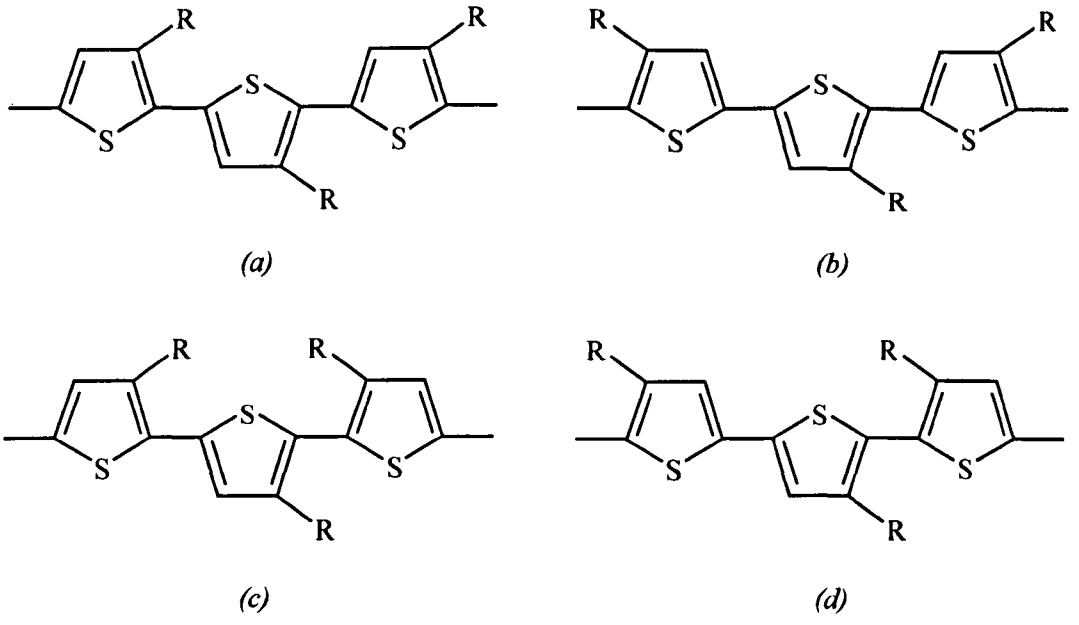

Figure 3.5.1: Possible triad regioisomer structures in a non-regioregular poly(3-alkylthiophene) (a) HT-HT coupling (b) TT-HT coupling (c) HT-HH coupling and (d) TT-HH coupling.

The extent of the molecular orbital overlap determines the energy requirements of charge carrier moving along the conjugated polymer chain. Hence it is extremely crucial for poly(3-alkylthiophene) to contain regioregular structures that provide maximum intramolecular orbital overlap and efficient interchain π packing. Generally regioregular P3HT with a high content of head-to-tail (HT) coupling (> 98%) are used in the fabrication of organic based devices.

3.6 FABRICATION OF POLY(3-HEXYLTHIOPHENE) (P3HT) SCHOTTKY DIODES

Since the organic semiconductors used are intrinsically p-type, only metals with low work functions such as aluminium and titanium will form a Schottky barrier with these materials. The structure of a Schottky diode made with poly(3-hexylthiophene) as the active semiconductor is shown in *figure 3.6.1*.

The Schottky metal of choice is evaporated onto a pre-cleaned glass substrate. For a diode made with as-synthesised P3HT, 5 mg of the material is weighed and dissolved in approximately 5 ml of xylene. Xylene is favoured since its relatively high boiling point (138°C) causes it to evaporate much slower than solvents such as chloroform [18]. The increased drying time is thought to lead to the formation of films with increased crystallinity particularly for poly(3-hexylthiophene) where efficient interchain π stacking is crucial for charge transport. The solutions are generally heated to enhance the solubility of the organic material.

Once the material has completely dissolved, it is solution-cast onto the metal coated substrate under non-vacuum conditions. Solution-cast films are known to lack uniformity due to their increased thickness. Nevertheless, the largely thicker cast film is still preferred as it eliminates the possibility of short-circuiting during probing. The sample is left to dry in a vacuum environment overnight. The final fabrication step involves the shadow mask evaporation of gold dots which are 1mm in diameter.

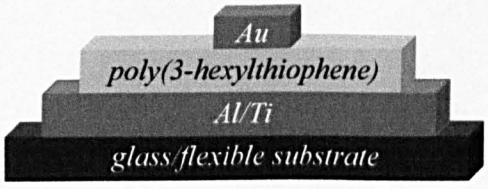

Figure 3.6.1: Schematic diagram of a poly(3-hexylthiophene) (P3HT) Schottky diode fabricated on glass/flexible substrate. The Schottky contact is typically either aluminium or titanium whilst gold serves as the ohmic contact.

Occasionally the Schottky diodes are fabricated on polyethylene terephthalate (PET) flexible substrates instead of glass slides particularly for the purpose of temperature related measurements. In such instances, both the Schottky and ohmic contacts are shadow mask

evaporated to form 2 mm wide strips. Diodes are only created at the crossing point between the Au and Al strips which help reduce the likelihood of short-circuiting during probing as solution-cast films on flexible substrates often have smaller thicknesses.

The DC characterisation of the Schottky diodes was performed in air using a Hewlett Packard 4145B semiconductor parameter analyser. The measurements were taken at a step size of 50 mV.

3.7 ELECTRICAL CONDUCTION IN POLY(3-HEXYLTHIOPHENE) (P3HT)

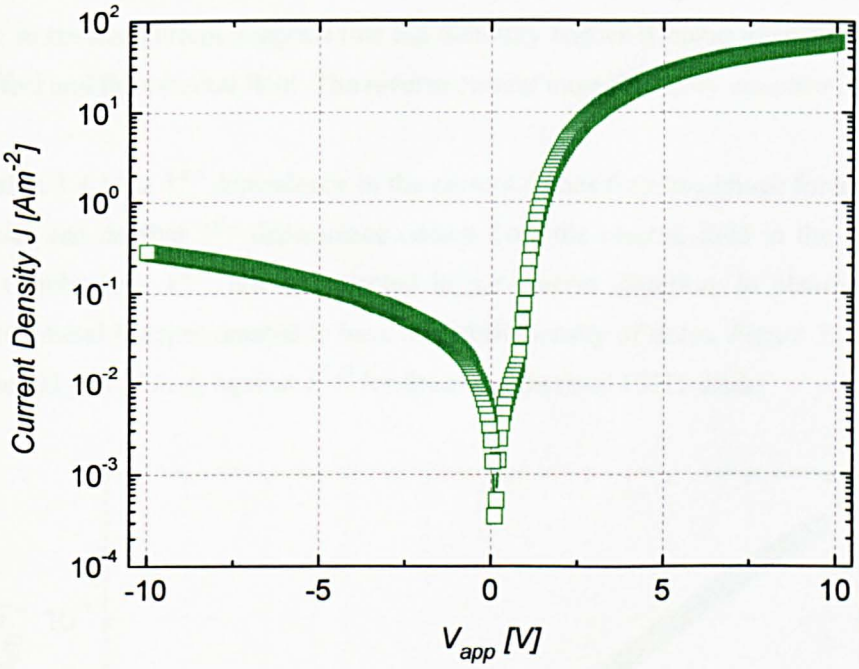

Figure 3.7.1: Current density voltage characteristic of Al-P3HT-Au Schottky diode. The voltage was applied on the top gold electrode. The diode exhibits non-ideal behaviour in the forward direction. The measurements were taken at a step voltage of 50 mV.

Figure 3.7.1 shows the semi-logarithmic current density voltage characteristic for a metal semiconductor diode made with highly regioregular, as-synthesised poly(3-hexylthiophene) (P3HT). The P3HT diode only gives a rectification ratio of ~ 10^3. Poly(3-akylthiophene) is one of the earliest organic semiconductors to be used in the field of organic electronics and it is intrinsically p-type. The diode characteristics obtained for organic semiconductors differ in a number of ways to their inorganic counterparts owing to the dispersive nature of charge transport in these materials. Unlike silicon where charge carriers are governed by band-like transport, the carriers in organic materials are distributed across a wide range of energies in self-localised energy states. This ultimately limits the so-called effective carrier mobility in disordered materials.

Focusing on the reverse characteristic of the diode, the current does not appear to saturate with increasing applied voltage. When the top gold contact of the diode is negatively biased, the space charge region adjacent to the metal extends and the distribution of localised states in the neutral region of the p-type semiconductor shifts upwards in energy with increasing voltage. As a result the barrier to the movement of holes increases and current is dominated

by the flow of holes from the metal. Assuming that there is no barrier at the gold contact, almost all the applied voltage falls across the space charge region. The small yet steady increase in reverse current suggests that the Schottky barrier is being lowered by the image force effect and the external field. The reverse current must thus obey *equation 3.4.11*.

In *equation 3.4.11*, a $V^{0.5}$ dependence in the current comes from the image force lowering of the barrier and another $V^{0.5}$ dependence comes from the electric field in the space charge region. Combined a $V^{0.25}$ law is expected in the reverse direction. In obtaining *equation 3.4.11*, the metal is approximated to have a uniform density of states. *Figure 3.7.2* shows the experimental plot of $ln\ J_R$ against $V^{0.25}$ for the as-synthesised P3HT diode.

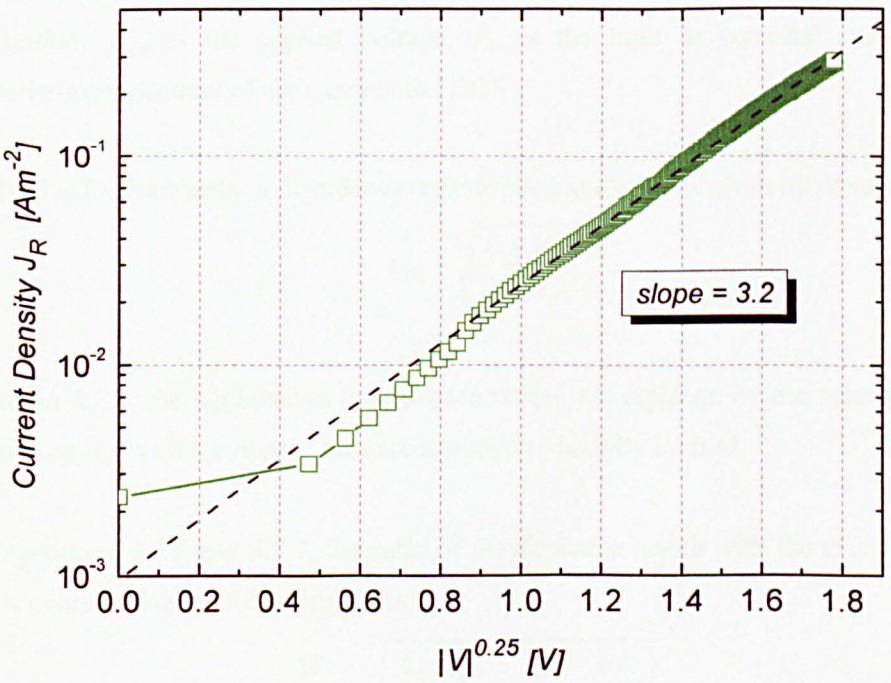

Figure 3.7.2: J_R against $|V|^{0.25}$ for the Al-P3HT-Au Schottky diode. The straight line indicates a fit to equation 3.4.11. The dopant density calculated from the slope is ~ 1.73 x 10^{16} cm^{-3}.

In *figure 3.7.2*, the straight line fit at applied voltages above 1V indicates a good agreement with the Schottky theory. The fact that the ¼ power law is accurately obeyed suggests that the assumption of an abrupt depletion edge holds true even in disordered materials. The terms V_{bi} and kT_c/q in *equation 3.4.11* are responsible for the non-linearity observed at very low applied voltages.

The validity of the abrupt depletion edge approximation in disordered organic semiconductors can be established by determining the ratio of the depletion width W with the effective Debye length L_{De} [10]. The effective Debye length is an important material dependent parameter. Here it corresponds to the distance over which the hole concentration increases close to its intrinsic value and the semiconductor becomes effectively neutral.

Traditionally the width of the space charge region is given by

$$W = \sqrt{\frac{2\varepsilon_0\varepsilon_s}{qN_A}\left(V_{app} - V_{bi} - \frac{kT_c}{q}\right)} \qquad 3.7.1$$

where ε_s is the static dielectric constant of the semiconductor, N_A is the acceptor ion concentration, V_{app} is the applied voltage, V_{bi} is the built in potential and T_c is the characteristic temperature of the exponential DOS.

The effective Debye length in disordered organic semiconductor is given by *(Appendix C)*

$$L_{De} = \sqrt{\frac{\varepsilon_0\varepsilon_s kT_c}{q^2 N_A}} \qquad 3.7.2$$

In *equation 3.7.2*, the equilibrium hole concentration p is replaced by the concentration of acceptor ions N_A as all the dopant ions are assumed to be fully ionised.

Using *equations 3.7.1* and *3.7.2*, the ratio of the depletion width with the effective Debye length is expressed in the following form:

$$\frac{W}{L_{De}} = \sqrt{\frac{2q}{kT_c}\left(V_{app} - V_{bi} - \frac{kT_c}{q}\right)} \qquad 3.7.3$$

At voltages above 1V where the ¼ power law is obeyed, the terms V_{bi} and kT_c/q can be neglected. As will be discussed later, the intrinsic characteristic temperature T_c of the as-synthesised P3HT diode is equal to ~ 390K. This gives a value of ~ 8 for the ratio of W/L_{De} at an applied voltage of 1V. This means that the width of the space charge region is at least 8 times larger than the effective Debye length. So despite the gradual rise in hole concentration, the abrupt depletion edge approximation is still applicable in disordered organic semiconductors.

The acceptor ion concentration N_A can be determined easily from the slope of the $ln\ J_R$ against $V^{0.25}$ plot with the aid of *equation 3.4.11*. This method involves assuming a uniform doping profile of acceptor ions in the space charge region of the semiconductor. In diodes, the carrier concentration in the semiconductor is generally assumed to be equal to the dopant concentration. Shallow dopant states in conventional semiconductors are almost entirely ionised due to the interplay of the high density of states at the valence/conduction band edge and the Fermi Dirac statistics. The charge carriers are consequently almost entirely free and are approximately equal to N_A. For easy reference, we have termed this phenomenon as 'carrier inversion' and the same is assumed to occur in disordered materials. The carriers from the dopant atoms are believed to occupy lower energy states. From *figure 3.7.2*, the value of N_A and hence the hole concentration p was calculated to be approximately equal to $1.73\times10^{16}\ cm^{-3}$.

In Schottky diodes, the dopant concentration is crucial for determining the bulk mobility of charge carriers. Although carrier mobility is probably the most important figure of merit for crystalline semiconductor devices, its relevance in disordered materials is still under much debate. In band transport, carriers move in a set of delocalised energy levels with similar mobilities. With hopping transport, however, the motion of charge carriers between localised states is strongly dependent on both the hopping distance as well as the energetic distribution of states. In a p-type material for instance, the probability of carrier hopping becomes increasingly higher at lower energies. Hence motion in disordered organic materials can only be described in terms of an effective mobility due to their strong dependence on carrier concentration. The magnitude of the effective bulk mobility can be determined from the forward *J-V* characteristic of a diode.

In the forward direction, the current is seen to rise exponentially at low applied voltages. The forward *J-V* characteristic of an as-synthesised P3HT diode made with a bottom aluminium contact is generally non-ideal. It has a small 'kink' that separates two distinct exponential current regions. In the past, the 'kink' has been associated with the existence of an interfacial layer and/or trapping in the region adjacent to the metal [12]. More recent studies suggest that the lower exponential current regime might actually provide valuable information regarding the energetic distribution of localised states at lower energies.

The application of a positive voltage on the gold electrode significantly lowers the potential barrier for holes. The sharp rise in current is associated with the exponential decline in carrier occupancy given by the Maxwell Boltzmann approximation of the Fermi Dirac

statistics. If like conventional semiconductors there is only a single energy barrier at the interface which all carriers must overcome, then all the charge carriers will have to reach this particular energy level first before crossing into the metal. Fortunately, the same applies even in the case of an exponential density of states since the charge carriers are also exponentially distributed and hence will each see the same potential barrier as illustrated in *figure 3.7.3*. This idea, however, ignores the possibility of carriers taking alternative routes leading to other potential barriers. But the close agreement obtained between the analytical model and experimental results suggest that this might be a reasonable approximation.

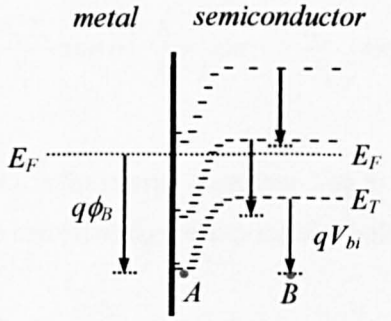

Figure 3.7.3: In the model involving an exponential density of states, each of the exponentially distributed holes in the p-type semiconductor is thought to see the same potential barrier qV_{bi}. The localised states are distributed in a succession of energy levels without the presence of any off-diagonal disorder to clearly illustrate the shape of the potential barrier envisaged in disordered semiconductors.

Transport across Schottky barriers is determined, in general, by the density of charge carriers occupying energy states above the top of the barrier close to metal semiconductor interface. In a material with an exponential DOS, the larger T_c value compared to T suggests that the carrier distribution must be controlled by the energy of the quasi Fermi level E_F while the exponential rise in current suggests there must be almost no bending of the Fermi level. So a flat quasi Fermi level is defined and carriers are assumed to obey the Maxwell Boltzmann statistics since deviation from the equilibrium carrier concentration is negligible.

So far the only evidence that supports the existence of a flat quasi Fermi level comes from the experimental results of Schottky diodes made with crystalline silicon. In such diodes, the ideality factor η calculated from the exponential current regime has a value close to unity [19]. This implies that carriers crossing into the metal must come from only an energy kT within the conduction/valence band edge. Hence the quasi Fermi level can be considered to be almost flat as deviation from equilibrium conditions must be small.

The total charge carrier concentration contributing to current flow in the forward direction of the diode is given by

$$\int N(E)f(E)\,dE = \int \frac{N_0}{kT_c}\exp-\left(\frac{E_F - E}{kT}\right)\exp-\left(\frac{E}{kT_c}\right)dE \qquad 3.7.4$$

where N_0 is the number of states per unit volume and E is the energy of the localised states.

Then, integrating from the top of the barrier to infinity yields the resulting current density *(Appendix D)* [20]

$$J\,\alpha\,\frac{N_0 T_0}{T_c}\exp-\left(\frac{E_F}{kT}\right)\exp-\left(\frac{E_B}{kT_0}\right)\exp\left(\frac{qV_{app}}{kT_0}\right) \qquad 3.7.5$$

where E_F is the Fermi level, E_B is the energy corresponding to the top of the barrier and T_0 is the characteristic temperature representing the exponential hole distribution.

Equation 3.7.5 can be simplified to

$$J\,\alpha\exp\left(\frac{qV_{app}}{kT_0}\right) \qquad 3.7.6$$

This method of determining the current density takes no account of the charge transport mechanism across the Schottky barrier. In the past, diffusion has been reported to be the dominant barrier transport mechanism in disordered materials due to the relatively short mean free path of carriers [21]. Charge transport is therefore believed to be affected by the absence of an electric field at the top of the Schottky barrier. The combination of low carrier mobility and zero electric field suggests that there might be an element of diffusion driving the carriers across the barrier. The width of the barrier peak is, however, very small and diffusive transport is traditionally caused by the existence of a concentration gradient. Hence it is extremely doubtful that the small barrier width will allow the formation of a concentration gradient large enough to drive an exponential current. Inadequacy in the theory raises questions over the role of diffusion mechanism in charge transport across Schottky barriers.

In our model we simply assume a flat quasi Fermi level across the space charge region even in the presence of current flow. By doing so, all the charge carriers in the semiconductor are assumed to have reached quasi thermal equilibrium. Hence the hole concentration at point *A* in the semiconductor as shown in *figure 3.7.3* is equal to the concentration at point *B*. With

increasing positive voltage, the potential barrier at the interface is effectively lowered. Higher energy states in the neutral region of the semiconductor shift downwards in energy by an amount qV_{app} thus allowing an increasing number of holes to cross into the metal. The increasing density of holes arriving at the top of the barrier is expected to favour higher energy states over lower ones. This causes the holes to accelerate up the potential hill adjacent to the metal. Since there are doubts over the role of diffusion in controlling current flow across the Schottky barrier, no account is taken of the conduction mechanism in the analysis. Only the exponential distribution of localised states and the falling carrier occupancy are used in *equation 3.7.4* since the current is generally determined by the energetic distribution of charge carriers above the top of the barrier.

In deriving *equation 3.7.5*, the energy corresponding to top of the barrier of a single level E_B is used as the lower integration limit. As discussed earlier, each of the exponentially distributed charge carriers will see the same potential barrier. If the semiconductor is assumed to be n-type, at low energies, the fewer number of localised states located further apart will limit the electron hopping transitions to almost zero. But with increase in energy, the hopping probability of the electrons will rise sharply due to the combined effect of the exponential DOS and the Fermi Dirac statistic. Hence there must be a minimum energy level located somewhere above the Fermi level beyond which electrons are able to hop into empty states with relative ease. This minimum energy level is called the transport energy E_T and E_B corresponds to the energy of its barrier peak. The use of a transport energy, however, restricts the model to only small carrier concentrations. In inorganic semiconductors the minimum energy level corresponds to the conduction band edge.

It should also be noted that the exponential term in *equation 3.7.6* has the denominator kT_0. In the previous chapter, when the charge carriers were integrated from the Fermi level to infinity, the denominator was determined as kT_c. The two very different results suggest that the denominator is strictly dependent on the lower integration limit. The earlier kT_c result was attributed to the fact that the Fermi level lies in the band tail of the distribution where there is a slow rise in the density of states. If this is true, then the transport energy must lie in the region of the DOS which is strongly exponential. The combined effect of a strongly exponential DOS and the exponential decline in carrier occupancy given by the Maxwell Boltzmann statistics leads to an exponential distribution of charge carriers characterised by a new constant T_0.

The exponential part of the forward characteristic was found to accurately obey *equation 3.7.6* with the slope giving the value of T_0. Experimentally T_0 was found to be ~ 1301K. It

should be noted that this value corresponds to the characteristic temperature of the intrinsic carriers as dopant states are too high in energy to contribute to conduction. This value of T_0 predicts that the carriers contributing to current must come from within about $4kT$ of the transport energy; almost 4 times the energy width determined for crystalline semiconductors. This is believed to be a direct consequence of the energetic disorder inherent in organic materials. But despite the energetic disorder, carriers are still expected to come from only energies close to the transport energy or else there will be almost no possibility of an exponential rise in current with applied voltage.

In conventional semiconductors the current density expression has the form:

$$J \alpha \exp\left(\frac{qV_{app}}{\eta kT}\right) \qquad 3.7.7$$

where η corresponds to the ideality factor and T is the absolute temperature.

Comparing *equations 3.7.6* and *3.7.7* gives

$$T_0 = \eta T \qquad 3.7.8$$

As mentioned earlier, η is very close to unity in silicon based Schottky diodes. This reflects the almost ideal Schottky barrier formed at the metal/silicon interface. The interface is therefore almost free of any extrinsic trap states and carriers contributing to current flow come from within an energy kT of the conduction/valence band edge. In disordered organic materials, however, the ideality factor lies in the range of between 3 and 5 [12, 22]. Assuming that trapping in extrinsic states is negligible, the significantly larger value of η is believed to be a direct consequence of the exponential distribution of states in organic materials. This assumption allows the best possible determination of T_0 and hence T_c. *Equation 3.7.8* gives an ideality factor of ~ 4.3 for the as-synthesised P3HT diode.

The relationship between the constant T_0 and the characteristic temperature of the exponential DOS T_c is given by

$$\frac{1}{T_0} = \frac{1}{T} - \frac{1}{T_c} \qquad 3.7.9$$

Equation 3.7.9 gives a value of ~ 390K for the intrinsic T_c. This corresponds to an intrinsic Meyer Neldel energy of ~ 34 meV which is in close agreement with the Meyer Neldel energy obtained from MOS capacitors and TFTs made with the same material [23, 24]. The

value of T_c is expected to remain constant for a particular organic material with no dependence on ambient temperature.

In the previous chapter, it was shown that mobility in disordered materials is strongly dependent on their carrier concentration. The exponent term m in the empirical relationship is closely related to T_c and is given by

$$m = \frac{T_c}{T} - 1 \qquad 3.7.10$$

From *equation 3.7.10*, m is estimated to be approximately 0.3. This value of m corresponds in particular to the dependence of the effective mobility on the intrinsic carrier concentration of the material. A much larger value of m is obtained when charge carriers from dopants states are involved in current transport [25].

Another important feature of the forward *J-V* characteristic is the visibly stronger exponential rise in current at extremely low applied voltages. The lower exponential current regime is believed to be associated with the presence of extrinsic trap states. Native oxide layers are known to form on Al surfaces upon exposure to ambient environment. Using *equation 3.7.6*, a value of ~ 621K is obtained for T_0. This corresponds to a T_c value of ~ 580K and a Meyer Neldel energy of ~ 50 meV. Coincidentally, a Meyer Neldel energy almost twice its intrinsic value (~ 70 meV) is obtained when as-synthesised P3HT is intentionally doped with varying amounts of 2,3-dichloro-5,6-dicyano-1,4-benzoquinone (DDQ) [25]. This leads us to believe that the introduction of additional extrinsic states either by the incorporation of dopants of any variety or the formation of a non-ideal barrier gives a significantly larger T_c value. The value of m associated with the lower exponential current region is approximately equal to 0.93. The dependence of mobility on carrier concentration is clearly enhanced by the presence of additional trap states. In a p-type material, the exponential current regime at very low applied voltages corresponds to states located much lower in energy. Since there is a higher concentration of states at lower energies, a larger effective mobility and hence a stronger rise in current is to be expected.

Although the model developed is mainly concerned with current flow from the organic semiconductor into the metal, it must be noted that in forward bias, a much smaller injection current also flows from the metal. A detailed study of current flow across metal-organic interfaces has been carried out by Scott and Malliaras [26]. Using the Langevin theory in conjunction with the concept of image potential at a metal interface and the principle of detailed balance, they derived the surface recombination velocity and effective Richardson

constant describing charge injection at the interface between an organic semiconductor and a metal.

With increasing positive bias on the gold contact, a higher fraction of the applied voltage V_{app} starts to fall across the neutral region as shown in *figure 3.7.4.* The smaller fraction falling across the barrier and the space charge region eventually leads to a deviation from *equation 3.7.6.* The current across the barrier is believed to saturate as it becomes limited by the resistivity of the neutral region. In a more recent study, the nature of the back metal/organic interface was also found to affect the forward saturation current.

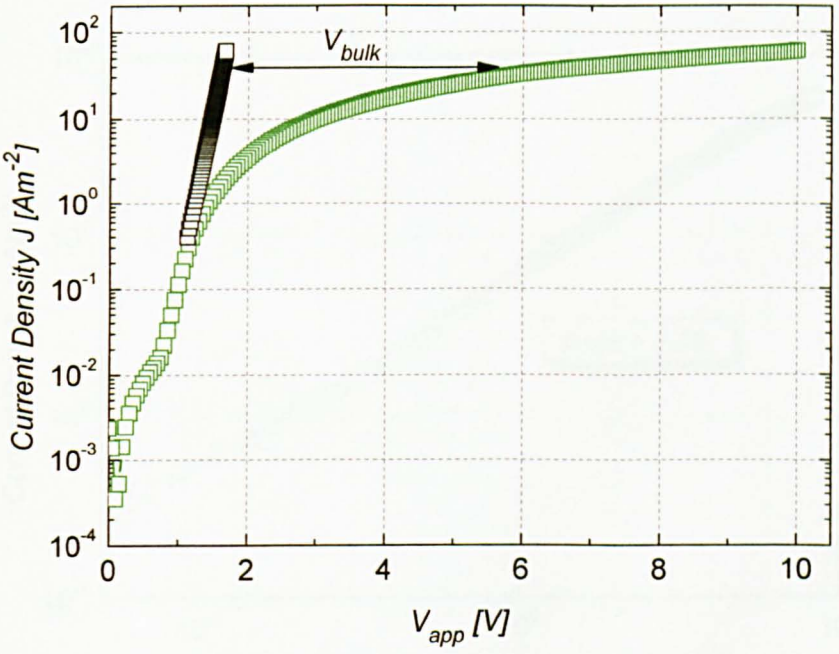

Figure 3.7.4: Forward J-V characteristic for Al-P3HT-Au Schottky diode. At high applied voltages, a higher fraction of the potential falls across the neutral region leading to a deviation from equation 3.7.6. The potential drop across the neutral region V_{bulk} is obtained by measuring the deviation along the voltage axis for each of the measured current levels.

The nature of the neutral region can be determined experimentally by plotting a double logarithmic plot of current density against voltage drop across the neutral region V_{bulk}. The bulk voltage is obtained by excluding the potential drop across the barrier and the space charge region from the applied voltage for each of the measured current levels as shown in *figure 3.7.4.* A diode with an ohmic neutral region should, ideally, have a slope of unity. The slope of the J against V_{bulk} plot in *figure 3.7.5* was calculated to be ~ 1.09. This proves that

the as-synthesised P3HT exhibits ohmic behaviour. In addition this also validates the assumption that no potential is dropped across the Au electrode.

Despite the high carrier density in the forward direction, the material is able to remain electrically neutral due to the presence of a high concentration of oppositely charged dopant ions. The charge on the carriers occupying the neutral region is compensated for by the dopant ions as illustrated in *figure 3.7.6*. Hence there are no space charge effects and provided that there is no potential drop across the gold contact the neutral region will exhibit ohmic behaviour.

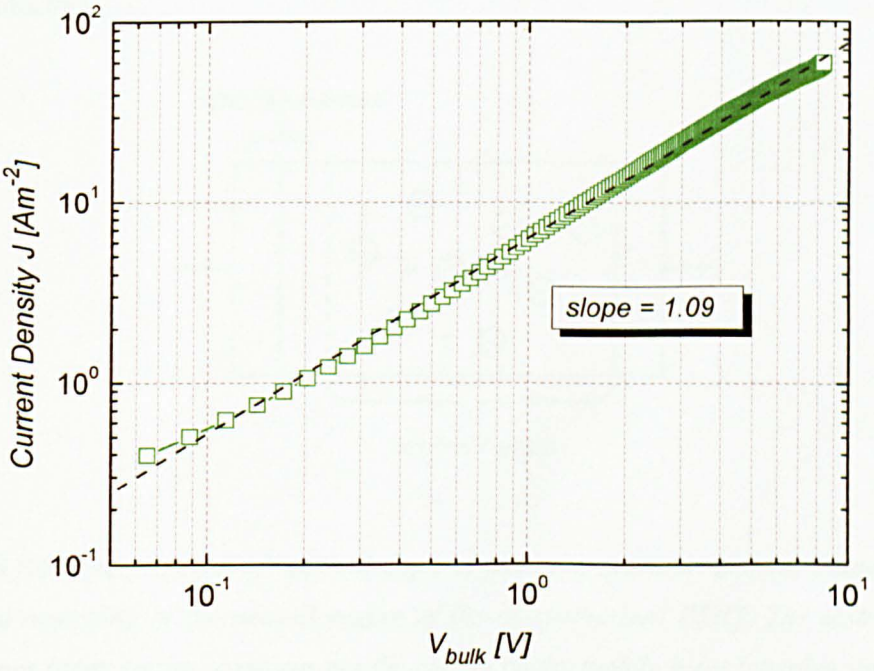

Figure 3.7.5: Current density against V_{bullk} for Al-P3HT-Au Schottky diode. The slope is calculated to be ~ 1.09 indicating that the neutral region of the diode is ohmic. The ohmic nature of P3HT is attributed to the presence of residual dopants from the synthesis process.

As tradition would have it, a value for the so-called effective hole mobility μ_{eff} may be calculated from the saturation regime as current is limited purely by the resistivity of the neutral region. The intrinsic hole concentration p is assumed to be equal to the dopant concentration N_A obtained from the reverse diode characteristic and is used in the bulk mobility calculations.

The effective bulk mobility for holes is given by

$$\mu_{eff} = \frac{J x_p}{q N_A V_{bulk}} \qquad 3.7.11$$

where J is the current density, x_p is the polymer film thickness, q is the electronic charge and V_{bulk} is the voltage drop across the neutral region.

Equation 3.7.11 estimates the effective hole bulk mobility of as-synthesised P3HT to be ~ 2.7×10^{-5} cm^2 V^{-1} s^{-1} assuming a film thickness of 1μm. This mobility value is very low compared to those generally obtained for crystalline and even amorphous inorganic semiconductors.

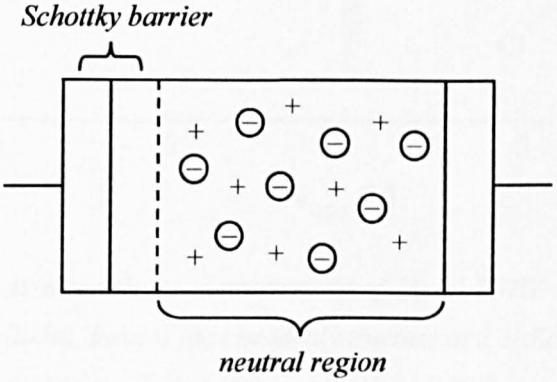

Figure 3.7.6: The presence of residual dopants from the synthesis process helps maintain electrical neutrality in the neutral region of the as-synthesised P3HT. The distribution of dopant ions (open circles) compensates the charge on the mobile holes (positive sign).

Previous work on Schottky diodes has demonstrated that the effective bulk mobility of an as-synthesised P3HT diode also fits on the universal mobility curve [25]. The universal mobility curve is a general plot of conductivity against carrier density obtained by doping the as-synthesised P3HT with various concentrations of DDQ. This result confirms the presence of residual dopants in the as-synthesised material. The identity of the residual dopant, however, still remains unknown. But more importantly, this result suggests that the physical mechanism by which the residual dopant increases the mobility must be the same as DDQ. Both types of dopant are thought to contribute additional charge carriers which fill up lower energy states thereby leading to a strong enhancement of effective bulk mobility dependence on hole concentration.

3.7.1 ELECTRICAL CONDUCTION IN DOPED POLY(3-HEXYLTHIOPHENE) (P3HT)

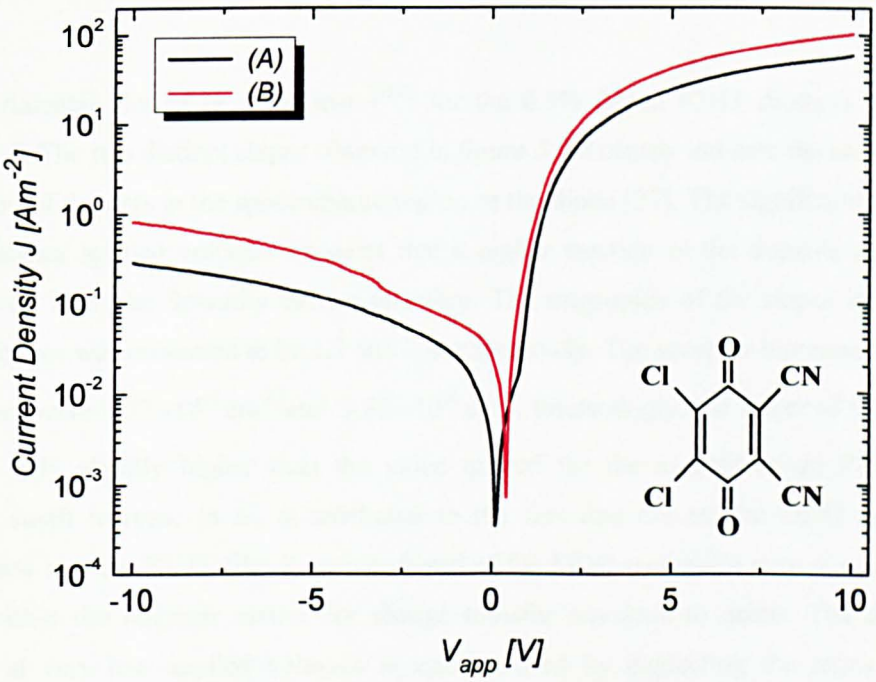

Figure 3.7.7: Current density voltage characteristic of (A) Al-P3HT-Au and (B)0.5% doped Al-P3HT-Au Schottky diodes. Inset is the chemical structure of 2,3-dichloro-5,6-dicyano-1,4-benzoquinone (DDQ) used in the doping of as-synthesised P3HT.

Figure 3.7.7 shows the current density voltage characteristic for metal semiconductor diodes made with as-synthesised P3HT and 0.5% doped P3HT. The P3HT material is intentionally doped with 2,3-dichloro-5,6-dicyano-1,4-benzoquinone (DDQ) to improve its conductivity. DDQ is said to act as an oxidising agent thus causing the simultaneous transfer of electrons and the formation of mobile holes along the polymer backbone. Upon gaining electrons, the DDQ molecules will become negatively charged ions. DDQ has previously been used as a dopant in polymers such as poly$(DOT)_3$ where it was demonstrated to have significantly enhanced the conductivity and hence the field effect mobility of charge carriers [4].

The current through the 0.5% doped P3HT diode is, in general, higher than the undoped P3HT. DDQ is believed to contribute additional free charge carriers which are expected to obey Pauli Exclusion Principle and rapidly fill up lower lying energy states. In the reverse direction, the current increases gradually with applied voltage suggesting that like the as-synthesised P3HT diode, it may obey the following equation:

$$J_R = J_0 \exp\left[\frac{q}{kT}\left(\frac{q^3 N_A\left(V_{app} - V_{bi} - {kT_c}/{q}\right)}{8\pi^2 \varepsilon_0{}^3 \varepsilon_s \varepsilon_\infty{}^2}\right)^{1/4}\right] \qquad 3.7.12$$

The experimental plot of $ln\ J_R$ against $V^{0.25}$ for the 0.5% doped P3HT diode is shown in *figure 3.7.8*. The two distinct slopes observed in *figure 3.7.8* clearly indicate the non-uniform distribution of dopants in the space charge region of the diode [27]. The significantly steeper slope at higher applied voltages suggests that a higher fraction of the dopants must exist further away from the Schottky barrier interface. The magnitude of the slopes at low and higher voltages was estimated to be 1.7 and 3.8 respectively. The acceptor ion concentrations N_A obtained were $1.37\times10^{15}\,cm^{-3}$ and $3.57\times10^{16}\,cm^{-3}$. Interestingly, the larger of the two N_A values is only slightly higher than the value quoted for the as-synthesised P3HT. The relatively small increase in N_A is attributed to the fact that not all the DDQ molecules incorporated into the P3HT film is active. Some of the DDQ molecules may not be ideally located within the polymer matrix for charge transfer reactions to occur. The deviation observed at very low applied voltages is again caused by neglecting the terms V_{bi} and ${kT_c}/{q}$ in *equation 3.7.12*.

In the forward direction, the current increases exponentially at low voltages much like the as-synthesised P3HT diode. However, the non-ideal behaviour associated with extrinsic trap states seems to have vanished with doping. We know that doping contributes additional free charge carriers which occupy successively lower energy states. In addition, from the as-synthesised P3HT diode, it can be concluded that the energy range containing the extrinsic states is relatively narrow. Hence it is believed that the increased hole concentration leads to a larger fraction of extrinsic states being occupied which consequently limits the probability of carrier hopping taking place via these energy states. Meanwhile the wider energetic distribution of intrinsic states is left to dominate conduction even at extremely low applied voltages. From a study involving poly(3-methylthiophene) (P3MT) Schottky diodes, it was reported that the loss of the kink leads to the appearance of a voltage offset as seen in *figure 3.7.7*. It was suggested that the voltage offset is associated with a permanent polarisation within the interfacial layer [22].

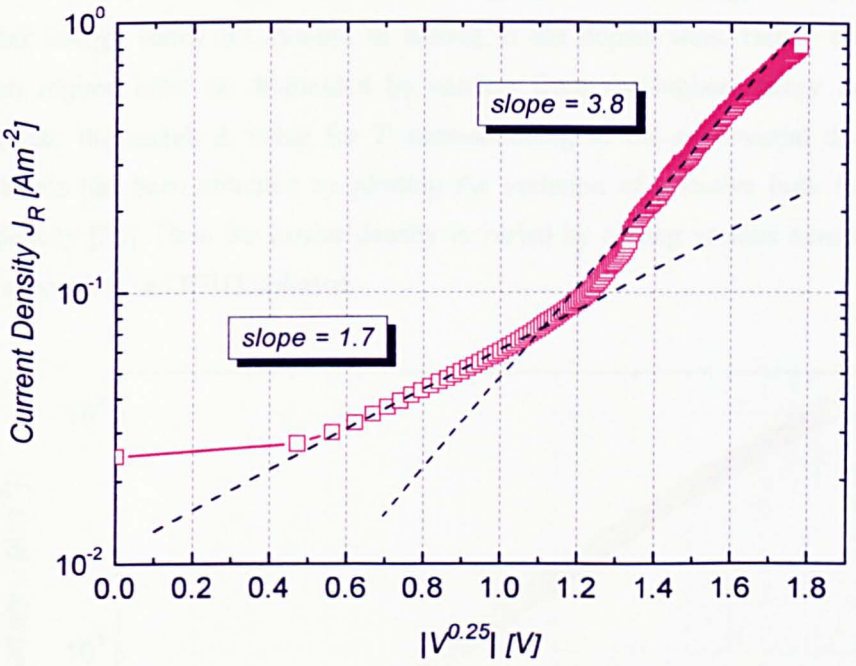

Figure 3.7.8: Reverse current density against $V^{0.25}$ for the 0.5% doped Al-P3HT-Au Schottky diode. Different slopes are obtained at low and high applied voltages corresponding to dopant densities N_A of 1.37 x 10^{16} cm^{-3} and 3.57 x 10^{16} cm^{-3} respectively. The two values of N_A suggests that the dopants are non-uniformly distributed within the space charge region of the diode.

The value of T_0 determined from the exponential region of the forward characteristic is ~ 1239K. Again this corresponds to the energetic distribution of intrinsic charge carriers as the extrinsic states introduced by the DDQ molecules are located much higher in energy and hence will not be involved in conduction at low applied voltages. The ideality factor η calculated for the 0.5% doped P3HT diode is ~ 4.1. The presence of trap states predicted by the significantly large value of η is related to the exponential distribution of intrinsic energy states. The characteristic temperature T_c representing the exponential distribution is equal to ~ 396K and the corresponding Meyer Neldel energy is 34 meV. The exponent m in the universal law relating mobility and carrier concentration is equal to ~ 0.31. Clearly, all the parameters are in close agreement with the values obtained earlier for the as-synthesised P3HT diode.

With increasing positive voltage on the Au electrode, the current across the Schottky barrier starts to saturate as a higher fraction of the applied voltage is dropped across the neutral

region. The potential barrier at the interface is effectively lowered as higher energy states in the neutral region are shifted downwards in energy by an amount qV_{app}. In doped materials, the higher energy states are thought to belong to the dopant ions. Hence current in the saturation regime must be dominated by carriers from the higher energy dopant states crossing into the metal. A value for T_c corresponding to the exponential distribution of dopant levels has been obtained by plotting the variation of effective bulk mobility with carrier density [25]. Here the carrier density is varied by adding various amounts of DDQ into the as-synthesised P3HT solution.

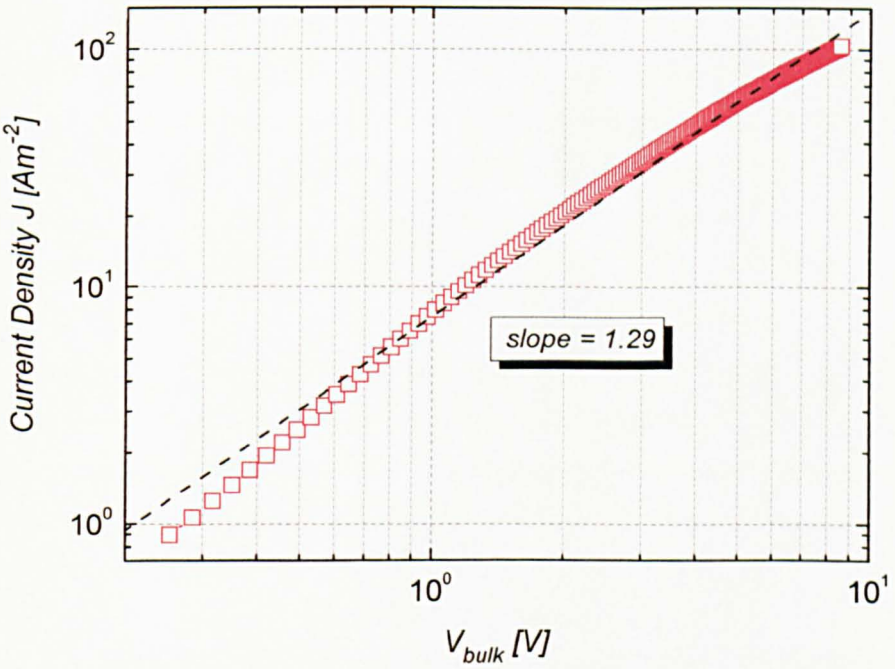

Figure 3.7.9: J against V_{bulk} for the 0.5% doped Al-P3HT-Au diode. The slope obtained from the plot is ~ 1.29. A diode with an ohmic neutral region should, ideally, have a slope of 1. The lack of agreement with the theoretical value could be due to the formation of a potential barrier at the doped P3HT/Au interface.

It has already been shown experimentally that the neutral region of as-synthesised P3HT exhibits ohmic behaviour. *Figure 3.7.9* shows a similar double logarithmic plot of J against V_{bulk} for the 0.5% doped P3HT Schottky diode. A diode with an ohmic neutral region will typically have a slope of 1. The doped P3HT diode, however, gives a slope of ~ 1.29. It is believed that the addition of the DDQ molecules to P3HT might have an effect on the potential barrier formed at the semiconductor/gold interface. This method of determining the electrical behaviour of the neutral region assumes that no potential is dropped across the Au electrode. If the gold however fails to make an ohmic contact with the organic

semiconductor, the assumption no longer holds true and the potential falling across the contact must be determined and consequently deducted from the bulk voltage. It is impossible to determine the potential drop across the Au electrode from the simple current density voltage measurement. A method that would allow the potential distribution across the entire diode structure to be mapped for different applied voltages needs to be developed.

3.8 CONCLUSIONS

The main characteristic feature of disordered organic semiconductors is their random distribution of localised states commonly described by either a Gaussian or an exponential function. The density of states (DOS) in organic materials must be studied if the electronic properties of the material are to be fully understood. Schottky diodes are ideal for this purpose as large voltages may be applied across the organic semiconductor thus allowing a wider energetic distribution of localised states to be analysed.

A Schottky diode was fabricated with aluminium, a low work function metal and as-synthesised poly(3-hexylthiophene) (P3HT). The P3HT was solution-cast onto the Schottky metal prior to the evaporation of the Au electrode. Gold is commonly reported to make an ohmic contact with P3HT. The Al-P3HT-Au diode gave a rectification ratio of only ~ 10^3 and exhibits non-ideal behaviour in the forward direction. This non-ideality is attributed to the presence of extrinsic trap states in the semiconductor.

A straight line fit was obtained for the experimental plot of $ln\ J_R$ against $V^{0.25}$ indicating that the diode obeys the ¼ power law quite accurately at voltages above 1V. This theory assumes a uniform density of states in the metal and an abrupt depletion edge in the semiconductor. The validity of the abrupt approximation was confirmed by determining the ratio of the depletion width W and the effective Debye length L_{De}. The ratio of W/L_{De} for the as-synthesised P3HT diode was calculated to be ~ 8 for an applied voltage of 1V. The abrupt depletion approximation may therefore still be applicable in Schottky diodes based on organic semiconductors. The linear fit also suggests that the dopant ions are uniformly distributed in the space charge region of the semiconductor. The acceptor ion concentration N_A and hence the hole concentration p for the as-synthesised P3HT was calculated to be ~ $1.73\times10^{16}\ cm^{-3}$. The rather high dopant density calculated for the as-synthesised P3HT is attributed to the presence of residual dopants from the synthesis process.

In the forward direction, a rapid rise in current was observed at low applied voltages. The exponential rise in current is associated with the exponential decline in carrier occupancy given by the Maxwell Boltzmann approximation of the Fermi Dirac statistic. The Maxwell Boltzmann statistics may be used to describe carrier occupancy since a flat quasi Fermi level is assumed in the semiconductor even in the presence of current flow. Like conventional semiconductors, each carrier in the disordered material is said to see the same potential barrier since the exponential density of states (DOS) leads to a similar exponential energetic

distribution of carriers. Good agreement was obtained between the analytical model and experiments despite ignoring the possibility that carriers might take alternative routes leading to other potential barriers.

The slope of the exponential part of the forward characteristic yields the magnitude of T_0, the characteristic temperature representing the exponential energetic distribution of carriers. The value of T_0 for the Al-P3HT diode was estimated to be ~ 1301K. This corresponds to the intrinsic carriers since dopants states are too high in energy to contribute to the conduction process. The value of T_0 also suggests that the carriers supporting the current originate from a much wider energy range, close to $4kT$ from the transport energy compared to only kT in inorganic semiconductors. The ideality factor η determined for the as-synthesised P3HT diode was ~ 4.3. Assuming that trapping in extrinsic states is negligible, the significantly larger value of η is believed to be associated with the exponential distribution of localised states characteristic of disordered organic materials. The constant T_c representing the intrinsic exponential DOS was found to be ~ 390K and the corresponding Meyer Neldel energy was ~ 34 meV.

At extremely low applied voltages, a much stronger exponential rise in current was observed. The magnitude of T_0 was estimated to be ~ 621K. The corresponding values for T_c and MN energy were approximately ~ 580K and 50 meV respectively. The slightly higher Meyer Neldel energy suggests the existence of extrinsic trap states at lower energies. These states must lie within a narrow energy range since it dominates only at very low applied voltages.

The forward current starts to saturate as a higher fraction of the applied voltage falls across the neutral region. A good linear fit was obtained from the double logarithmic plot of J against V_{bulk} and the slope was estimated to be ~ 1.09. This suggests that as-synthesised P3HT exhibits ohmic behaviour. The slope of almost 1 also implies that there is no potential drop across the Au electrode. From the saturation regime, the value of the effective hole bulk mobility for the as-synthesised P3HT was determined to be ~ 2.7×10^{-5} cm^2 V^{-1} s^{-1}. The effective mobility term is conceptually similar to the classical mobility term in conventional semiconductors except that the former shows a strong dependence on carrier density.

To improve the conductivity and hence the effective bulk mobility of the as-synthesised P3HT, the material is deliberately doped with 0.5% of 2,3-dichloro-5,6-dicyano-1,4-benzoquinone (DDQ) by weight. DDQ is thought to contribute additional free charge carriers which obey Pauli Exclusion Principle and rapidly fill up lower lying energy states. In

general, the current through the doped P3HT Schottky diode is higher than its as-synthesised P3HT counterpart. Two distinct slopes were obtained from the plot of $ln\ J_R$ against $V^{0.25}$ suggesting that the dopant ions are not uniformly distributed across the space charge region. Since the slope is steeper at higher reverse voltages, a higher fraction of the dopants is believed to exist further away from the Schottky barrier interface. The dopant densities were calculated to be ~ $1.37\times10^{15}\,cm^{-3}$ and $3.57\times10^{16}\,cm^{-3}$ at low and high applied voltages respectively. The relatively small increase in dopant density compared to the as-synthesised P3HT is attributed to the fact that not all the DDQ molecules added to the P3HT solution is active.

The values of T_0 and T_c measured for the 0.5% doped P3HT Schottky diode were almost the same as those obtained for the as-synthesised P3HT diode. This suggests that the dopant states introduced by DDQ must lie at higher energies and hence only participate in conduction at higher applied voltages. The experimental plot of J against V_{bulk} gave a slope of ~ 1.29. Ideally, the slope should be unity if the neutral region of the diode is ohmic. The significantly larger slope value obtained is believed to result from the formation of a potential barrier at the Au/organic interface since as-synthesised P3HT has been found to obey Ohm's law.

3.9 REFERENCES

[1] H. Tomozawa, D. Braun, S. Phillips, A. J. Heeger and H. Kroemer, *Synth. Met.* **22**, 63, 1987.

[2] H. Tomozawa, D. Braun, S. D. Phillips, R. Worland, A. J. Heeger and H. Kroemer, *Synth. Met.* **28**, 687, 1989.

[3] H. K. Henisch, "*Semiconductor Contacts*", Oxford Science Series, 1984.

[4] C. P. Jarrett, R. H. Friend, A. R. Brown and D. M. de Leeuw, *J. Appl. Phys.* **77**, 6289, 1995.

[5] M. Raja, G. C. R. Lloyd, N. Sedghi, W. Eccleston, R. Di Lucrezia and S. J. Higgins, *J. Appl. Phys.* **92**, 1441, 2002.

[6] W. Schottky, R. Strömer and F. Waibel, *Hochfrequenztechnik* **37**, 162-165, 1931.

[7] E. H. Rhoderick, *J. Phys. D: Appl. Phys.* **3**, 1153, 1970.

[8] B. R. Gossick, *Solid State Electron.* **6**, 445, 1963.

[9] E. H. Rhoderick, *J. Phys. D: Appl. Phys.* **5**, 1920, 1972.

[10] S. M. Sze, "*Physics of Semiconductor Devices*", J. Wiley and Sons, 1981.

[11] S. M. Sze, C.R. Crowell and D. Kahn, *J. Appl. Phys.* **35**, 2534, 1964.

[12] I. Musa and W. Eccleston, *Jpn. J. Appl. Phys.* **37**, 4288, 1998.

[13] K. Y. Jen, R. Obodi and R. L. Elsenbaumer, *Polym. Mater. Sci. Eng.* **53**, 79, 1985.

[14] R. L. Elsenbaumer, K. Y. Jen and R. Obodi, *Synth. Met.* **15**, 169, 1986.

[15] X. Qiao, X. Wang and Z. Mo, *Synth. Met.* **118**, 89, 2001.

[16] R. D. McCullough, *Adv. Mater.* **10**, 93, 1998.

[17] William Kemp, "*NMR in Chemistry*", Macmillan, 1986.

[18] J. F. Chang, B. Sun, D. W. Breiby, M. N. Nielsen, T. I. Sölling, M. Giles, I. McCulloch and H. Sirringhaus, *Chem. Mater.* **16**, 4772, 2004.

[19] M. P. Lepselte and S. M. Sze, *IEEE Transactions on Electron Devices* **15**, 434, 1968.

[20] W. Eccleston *(private communication)*.

[21] C. R. Wronski, D. E. Carlson and R. E. Daniel, *Appl. Phys. Lett.* **29**, 602, 1976.

[22] H. L. Gomez, G. W. Jones and D. M. Taylor, *Synth. Met.* **85**, 1351, 1997.

[23] D. Donaghy and W. Eccleston *(private communication)*.

[24] N. Sedghi, D. Donaghy, M. Raja, S. Badriya, S. J. Higgins and W. Eccleston, *J. Non-Cryst. Solids* **352**, 1641, 2006.

[25] M. Raja, N. Sedghi, S. Badriya, S. J. Higgins, G. C. R. Lloyd and W. Eccleston, *ESSDERC Proc.*, 253-256, 2005.

[26] J. C. Scott and G. G. Malliaras, *Chem. Phys. Lett.* **299**, 115, 1999.

[27] M. Raja, *PhD Thesis*, University of Liverpool, 2004.

CHAPTER 4

SPACE CHARGE LIMITED CURRENTS IN ORGANIC SEMICONDUCTORS

This chapter reviews the conventional space charge limited current (SCLC) theory introduced for inorganic semiconductors. Following that, the new SCL current expression developed for disordered semiconductor which incorporates the Universal Mobility Law (UML) is presented. The saturation current region of Schottky diodes is particularly important since high currents are needed for their application in RFID related circuits. The electrical characteristics of diodes based on polytriarylamine (PTAA) and vacuum-deposited pentacene are presented. The effects of varying the back metal/organic interface and further with doped PTAA films on the saturation current are also studied.

4.1 INTRODUCTION

One of the main reasons for research into organic semiconductors is their potential application in low cost radio frequency identification (RFID) tags. To be commercially viable, RFID tags would have to operate at a frequency of 13.56 MHz thus creating a need for high mobility organic semiconductors [1]. The high frequency operation of RFID tags is most demanding on the rectifying component of the circuit which would be based either on a thin film transistor (TFT) or a rectifying diode. Thin film transistors are, in general, easier to integrate but limitations on the minimum channel length significantly increases the demand for large carrier mobilities. Hence, to achieve high frequency operation, it is fundamentally important to first understand the device physics of organic rectifying diodes. The saturation region of Schottky diodes is studied in detail as high currents are required to satisfy the demand of RFID related circuits.

The chapter opens by reviewing the original theory of space charge limited currents (SCLC) developed for crystalline semiconductors. This theory, however, is deemed inappropriate for use in disordered organic semiconductors due to the distinct nature of charge transport in these materials. We oppose the description of carrier motion in disordered materials by a single classical mobility term as carriers are distributed across a wide range of energies and should thus experience different hopping rates. Hence a new space charge limited current expression incorporating the Universal Mobility Law (UML) is developed.

The chapter also discusses the electrical characterisation of polytriarylamine (PTAA) (S1105), a high purity organic semiconductor purchased from Merck Chemicals Ltd. The current in the saturation region demonstrates space charge effects which is associated with the low doping density of the material. Modelling the saturation region with the new SCLC equation allows a value for T_c and consequently T_0 to be determined. Interestingly, the values correspond to the intrinsic distribution of localised states and carriers respectively thus suggesting the absence of dopant states at higher energies. In addition, the effect of the back metal/organic interface and doping with DDQ on the saturation currents are also studied. The barriers formed at metal/organic interfaces are influenced by the deposition of self-assembled monolayers (SAMs) and the formation of interface dipoles.

The demand for high mobility organic semiconductors has led to the introduction of a new generation of small molecule based materials such as pentacene, N, N'-diphenyl-N,N'-bis(1-naphthyl)-1,1'-biphenyl-4,4'-diamine (α-NPD) and *para*-sexiphenyl (6P) [2, 3]. Amongst them, pentacene is the most promising candidate since it exhibits a field effect hole mobility

which is comparable to the electron field effect mobility of hydrogenated amorphous silicon (a-Si:H). Recently, a mobility greater than 1.2 $cm^2V^{-1}s^{-1}$ was reported for a solution processed TFT made with triisopropylsilyl pentacene (TIPS-pentacene) as the active material [4].

In this chapter, the experimental *J-V* curve for a vacuum-deposited pentacene vertical diode kindly provided to us by Steudel *et al.* based in IMEC is discussed in detail [5]. Analysis of current transport in this material is extensively based on the model developed by Eccleston for polycrystalline inorganic semiconductors [6]. The structure of pentacene is assumed to consist of arrays of small molecules that display crystalline-like behaviour and also boundary regions which are highly amorphous. Charge transport, however, is believed to be dominated by the disordered grain boundaries and the self-consistent values obtained for T_c and T_0 suggests that the experimental measurement lends itself rather well to the analytical model. Like PTAA, the current through the vacuum-deposited pentacene diode becomes space charge limited at higher applied voltages.

4.2 THEORY OF SPACE CHARGE LIMITED CURRENTS (SCLC)

The onset of space charge limited currents (SCLC) in semiconductors and insulators signify the significant departure from Ohm's law. It occurs when the injected carrier concentration in a semiconductor or insulator exceeds or becomes comparable to the thermal free carriers. Space charge effects are commonly observed in semiconductors having low carrier mobilities or a high density of trap states. The build up of charge carriers in a semiconductor leads to a non-linear variation of the electric field F. This consequently results in a sharp rise in voltage and a strong dependence of current upon the applied voltage.

The theory of one-carrier space charge limited currents is based on two simplifying assumptions; (1) the anode/cathode has an infinite reservoir of charge carriers available for injection and (2) diffusion currents are ignored as it is deemed important only in regions neighbouring the injecting contact. Both these assumptions suggest that the properties of the injecting contact may be ignored.

Hence, provided that there is no voltage drop across the injecting contact, the current at low applied voltages will start off being ohmic. By increasing further the applied voltage, a space charge region will form within the semiconductor which screens the contact from the electric field. The current subsequently becomes limited by the space charge region and deviates from Ohm's law. However if a potential barrier forms at the semiconductor/metal interface, the current flow will then most likely be dominated by the characteristics of the contact. The effect of metal/organic interfaces will be discussed in more detail later in the chapter.

The theory of space charge limited currents (SCLC) was first introduced by Rose [7] and subsequently studied extensively by Lampert and Mark [8, 9].

4.2.1 TRAP FREE MATERIAL WITH HIGH CONDUCTIVITY

A highly conductive material refers to one that has a high intrinsic free carrier concentration and high carrier mobility like a metal or a heavily doped semiconductor. The thermally generated free carriers are uniformly distributed throughout the material. In the presence of an external field, charge carriers will be injected from the anode/cathode into the material thus producing a space charge region. The width of the resulting space charge region is said to be inversely proportional to the conductivity of the material [9]. For a highly conductive material, the space charge region is limited to the region close to the injecting contact. This means the concentration of injected carriers is negligible compared to the thermal free carrier

concentration. Hence the position of the Fermi level remains essentially the same and current is controlled by the drift mechanism given by

$$J = n_f q \mu F \qquad 4.2.1$$

where J is the current density, q is the electronic charge, n_f is the intrinsic electron concentration, μ is the mobility of the free electrons and F is the external electric field.

Equation 4.2.1 shows that the current and voltage in highly conductive materials follow an ohmic relationship.

4.2.2 THE IDEAL INSULATOR

An ideal insulator is assumed to be free of traps and has negligible thermally generated free carriers. In such a material, only the injected carriers contribute to the space charge and consequently the current as the concentration of thermal free carriers is insignificant. The concentration of injected carriers is maximum near the injecting contact and decreases non-linearly with distance. As stated earlier, diffusion currents are ignored as it is only significant in the vicinity of the contact. The gradual change in free carrier concentration in the space charge region of the ideal insulator limits the magnitude of the diffusion current [9].

The current is thus dominated by the drift component and is given by

$$J = q n_f \mu F \qquad 4.2.2$$

where n_f is the free electron concentration and F is the electric field.

Here the free electron concentration is no longer uniformly distributed throughout the material and is given by Poisson's equation as

$$\frac{dF(x)}{dx} = -\frac{q n_f}{\varepsilon_0 \varepsilon} \qquad 4.2.3$$

where ε_0 is the permittivity of free space and ε is the relative dielectric constant of the material.

Rearranging *equation 4.2.3* gives

$$n_f = -\frac{\varepsilon_0 \varepsilon}{q}\left(\frac{dF(x)}{dx}\right) \qquad 4.2.4$$

Then substituting *equation 4.2.4* into *equation 4.2.1* gives

$$J = -\varepsilon_0 \varepsilon \mu F \left(\frac{dF(x)}{dx} \right) \qquad 4.2.5$$

Integrating the electric field F across the whole length of the material gives

$$\int_0^x J\,dx = -\varepsilon_0 \varepsilon \mu \int_F^0 F\,dF(x)$$

$$J = \frac{\varepsilon_0 \varepsilon \mu}{2x} F(x)^2 \qquad 4.2.6$$

where x is the distance between the contacts.

Substituting $F = -dV/dx$ into *equation 4.2.6* and integrating gives

$$J = \left(\frac{9}{8} \right) \varepsilon_0 \varepsilon \mu \left(\frac{V_{app}^{\ 2}}{x^3} \right) \qquad 4.2.7$$

where V_{app} is applied voltage.

Equation 4.2.7 is widely known as the trap free square law or Mott-Gurney law for ideal insulators under steady state conditions [10]. The equation states that the current is proportional to V_{app} squared. So a plot of *log* J against *log* V_{app} should, ideally, give a slope of 2.

With the aid of *equations 4.2.4* and *4.2.6*, the variation of free electron concentration n_f with distance x is given by

$$n_f = \left(\frac{\varepsilon_0 \varepsilon J}{2q^2 \mu} \right)^{\frac{1}{2}} x^{-\frac{1}{2}} \qquad 4.2.8$$

Equation 4.2.8 predicts that the free electron concentration will fall rapidly with increasing distance from the injecting contact. The non-uniform spatial distribution of electrons results in a non-linearly varying electric field as shown in *figure 4.2.1.*

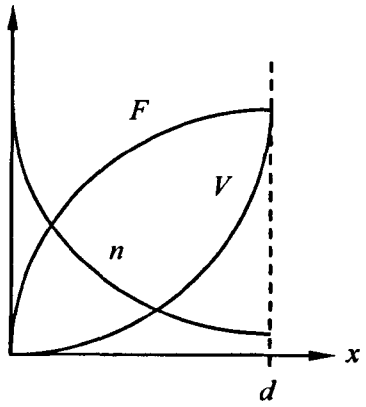

Figure 4.2.1: Variation of electric field, voltage and free electron concentration with distance in an ideal insulator with no traps. x is the distance measured with respect to the cathode while d corresponds to the distance between the electrodes.

4.2.3 THE IDEAL INSULATOR WITH THERMAL FREE CARRIERS

With the application of an external field, an ideal insulator is likely to have thermally generated carriers of concentration n_0. Initially when the injected free carrier concentration n_f is less than the thermal free carriers, the current will be ohmic. But once the concentration of injected carriers exceeds n_0, a space charge region forms and the current is said to obey *equation 4.2.7*. The uncompensated space charge is equal to the difference between the injected free carriers n_f and the thermal free carriers n_o.

The Poisson's equation is thus given as

$$n_f(x) - n_0 = \frac{\varepsilon_0 \varepsilon}{q}\left(\frac{dF(x)}{dx}\right) \qquad 4.2.9$$

The free carrier concentration will be highest at the injecting contact and approaches zero with increasing distance x. For any current density J, a plane $x = x_l$ exists within the material where the injected free carrier concentration is equal to the concentration of the thermal free carriers as illustrated in *figure 4.2.2*. At distances below x_l, the concentration of thermal free carriers is negligible and can therefore be ignored. The free carrier concentration in *equation 4.2.9* is then approximated as being equal to the injected carrier concentration n_f. At $x_l < x < d$, the concentration of thermal free carriers n_0 dominates causing space charge effects to be ignored and Ohm's law to control current flow.

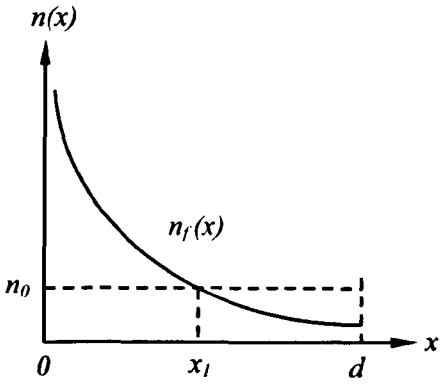

Figure 4.2.2: Spatial variation of the injected free carriers (solid line) in an insulator with thermally generated free carriers n_0. x_1 represents the position beyond which n_0 is significantly larger than the injected free carrier concentration n_f while d is the distance to the anode.

The current in the ideal insulator is thus neither purely ohmic nor space charge limited. A relationship between current and potential at low and high applied voltages can be determined using the regional approximation method [9]. The distance x_1 as a function of the current density J is given by

$$x_1 = \frac{\varepsilon_0 \varepsilon J}{2q^2 n_0^2 \mu} \qquad 4.2.10$$

The position of the plane $x = x_1$ is strongly dependent on the applied voltage. It moves further away from the injecting contact with increasing bias.

At low applied voltages, only a small current flows and the space charge region is narrow *i.e.* $x_1 << d$. The total free carrier concentration is equal to n_0 and the current obeys Ohm's law. Increasing the applied voltage further causes the space charge region to extend and at a particular voltage, the plane $x = x_1$ coincides with the opposite electrode *i.e.* $x_1 = d$. At even higher applied voltages, the concentration of injected free carriers significantly exceeds n_0 and the latter is neglected. Consequently, the current becomes purely space charge limited and is said to obey *equation 4.2.7.*

The crossover voltage V_x between the ohmic and space charge region is determined by equating *equations 4.2.2* and *4.2.7.*

$$V_x = \frac{8}{9}\frac{q n_0 d^2}{\varepsilon_0 \varepsilon} \qquad 4.2.11$$

Here d corresponds to the distance between the contacts.

4.2.4 THE INSULATOR WITH A SINGLE SET OF SHALLOW TRAPS

An insulator may have a single set of traps of density N_t at an arbitrary energy level E_t located much higher than the Fermi level E_F. At thermal equilibrium, a fraction of the trap states is occupied by charge carriers and since the states are shallow, the carrier occupancy is given by the Maxwell Boltzmann statistics. The concentration of trapped carriers is thus given as

$$n_t = N_t \exp -\left(\frac{E_t - E_F}{kT}\right) \qquad 4.2.12$$

For a p-type material, the trap states are located below the Fermi level and will be given by $(E_F - E_t)$.

In an insulator with traps, the space charge is given by the difference between the injected free and trapped carrier density $n_f + n_t$ and the density of thermally generated free and trapped carriers $n_0 + n_{t0}$. Consequently, Poisson's equation is defined as

$$\left(n_f - n_0\right) + \left(n_t - n_{t0}\right) = \frac{\varepsilon_0 \varepsilon}{q}\left(\frac{dF(x)}{dx}\right) \qquad 4.2.13$$

The regional approximation method is again used to determine the current voltage relationship. At low applied voltages, the insulator may be divided into four distinct regions as shown in *figure 4.2.3*. Initially, the insulator will be dominated by the region $x_3 < x < d$. But with further increase in voltage, the planes corresponding to x_3, x_2 and x_1 will progressively extend and coincide with distance d starting with x_3.

When $x_3 << d$, the trap states will have a negligible effect as it is located well above the Fermi level. This allows the thermally generated carriers to dominate *i.e.* $n_0 > n_f - n_0$ and $n_{t0} > n_t - n_{t0}$. Hence the space charge region will be negligible and Ohm's law may be applied. At higher applied voltages, however, the region $x_2 < x < x_3$ becomes dominant. Here n_0 and n_{t0} are significantly smaller than n_f and n_t respectively. The carriers contributing to the space charge region is thus given by $(n_f + n_t)$.

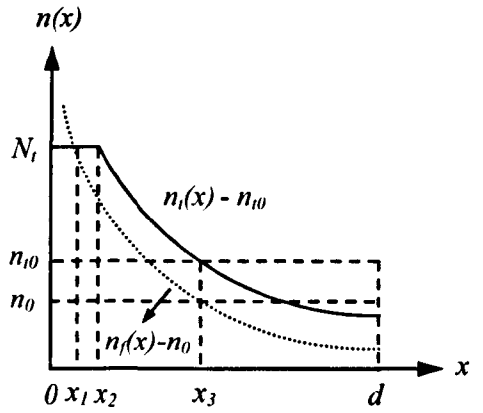

Figure 4.2.3: Schematic illustration of free and trapped carriers in an insulator with shallow traps of density N_t against distance from the injecting contact. x_1, x_2 and x_3 correspond to arbitrary positions along the length of the insulator.

The ratio of free injected carrier concentration to the total injected carrier concentration is given by the factor θ.

$$\theta = \frac{n_f}{n_f + n_t} \qquad 4.2.14$$

A value for θ may be calculated provided that the Fermi level is a few kT below the trap level.

$$\theta = \frac{1}{1 + \frac{N_t}{N_c}\exp\left(\frac{E_c - E_t}{kT}\right)} \approx \frac{N_t}{N_c}\exp -\left(\frac{E_c - E_t}{kT}\right) \qquad 4.2.15$$

Here N_c and E_c are the effective density of states and energy of the conduction band edge respectively. *Equation 4.2.15* shows that θ is independent of the position of the Fermi level or the applied voltage but is strongly dependent on the absolute temperature T.

In this trap controlled region, the current is space charge limited mainly by the injected carriers and is given by

$$\rho = n_f + n_t = \frac{n_f}{\theta} \qquad 4.2.16$$

where ρ is the total density of injected carriers.

Substituting *equation 4.2.16* into Poisson's equation and following the same stages as in the case of an ideal insulator gives the following expression for current density J in the trap controlled region.

$$J = \frac{9}{8}\mu\theta\varepsilon_0\varepsilon\frac{V_{app}^{\ 2}}{x^3} \qquad 4.2.17$$

At even higher applied voltages, the region $x_1 < x < x_2$ will dominate through the insulator. The trap states become virtually full as the Fermi level moves through the trap level and the trapped carriers n_t becomes approximately equal to N_t. The movement of the Fermi level is no longer restricted by trapping beyond this point and there is sharp rise in free carrier concentration and hence current with increasing applied voltage. In addition, the factor θ is no longer constant as the free carrier density increases at a much higher rate compared to n_t. This is called the trap filled limit (TFL) region. An exact solution does not exist for this region due to the visibly rapid rise in current with voltage. But there are suggestions that the steep slope might be related to the ratio of the trap density and the density of states at the conduction band edge [10].

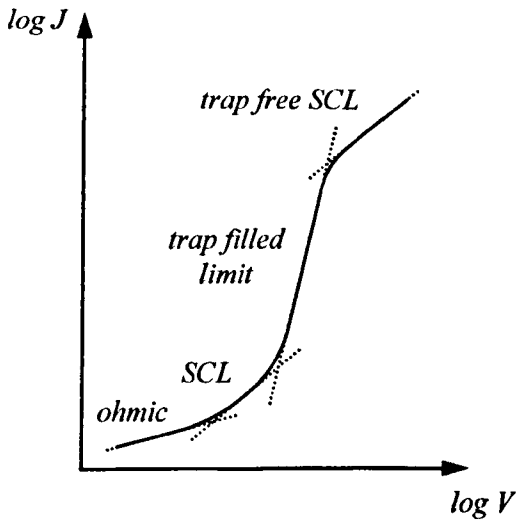

Figure 4.2.4: Schematic representation of the space charge limited current voltage characteristic for each of the four distinct regions described in the insulator. The sharp rise in current observed in the trap filled limit region is caused by the filling of the trap states by charge carriers.

In the region $x_0 < x < x_1$, the traps are practically full and N_t is much smaller than the free carrier concentration as shown in *figure 4.2.3*. The trapped carrier concentration is simply neglected and $\theta \approx 1$. Current is therefore space charge limited by free carriers similar to the case of a trap free insulator and is almost independent of temperature as $\theta \approx 1$. This called the trap free region since conduction mainly occurs in the conduction band away from the trap level. *Figure 4.2.4* shows the current voltage characteristic corresponding to all the four regions.

4.3 SPACE CHARGE LIMITED CURRENTS (SCLC) INCORPORATING THE UNIVERSAL MOBILITY LAW (UML)

The conventional space charge limited current (SCLC) given by the Mott-Gurney law was developed for inorganic semiconductors with a constant carrier mobility [10]. The description of carrier motion in these materials by a unique mobility term is made possible by the high density of states at the conduction/valence band edge. In an n-type inorganic semiconductor for example, carriers mainly occupy the lowest energy levels of the parabolic shaped conduction band and hence possess the same effective mass. Consequently the carriers behave as if they have the same mobility.

In disordered organic materials, however, the density of states is distributed across a wide range of energies. For small carrier concentrations, the distribution of localised states can be described quite accurately by an exponential function. Charge transport in disordered semiconductors with an exponential DOS has been linked to the Variable Range Hopping (VRH) mechanism [11]. According to the VRH model, the motion of carriers between localised states is strongly dependent on hopping distance and the energetic distribution of states. A significant increase in hopping transitions is expected as the localised states become less far apart thus resulting in a mobility that is largely dependent on carrier density. This makes the concept of carrier mobility in organic materials a poor one. The empirical relationship between the effective mobility and carrier density in disordered semiconductors is given by

$$\mu_{eff} = \mu_0 n^{\left(\frac{Tc}{T}\right)-1} \qquad 4.3.1$$

where μ_0 is the mobility prefactor, n is the carrier density and T_c is the characteristic temperature of the exponential density of states.

Equation 4.3.1 closely resembles the Universal Mobility Law (UML) first described by Brown *et al.* [12]. Hence it may also be expressed in the following form assuming $m = {}^{T_c}/_{T} - 1$

$$\mu = Kn^m \qquad 4.3.2$$

Here K is an arbitrary constant having the units of mobility and m is a material and temperature dependent exponent. *Equation 4.3.2* is, in general, valid for small carrier concentrations and for $T_c > T$. Since carriers in disordered semiconductors do not possess a constant mobility, the conventional Mott-Gurney law for space charge limited currents no longer seems appropriate for use in these materials. A more generalised expression which takes account of the carrier density dependence of mobility is required. In the past, a modified SCL current expression has been developed for the case of an exponential distribution of trap states in a crystalline semiconductor [13].

As stated above, carriers in disordered materials are not confined within a well defined edge but instead are distributed in energy. So although *equation 4.3.2* is derived under the assumption that all states are physically equivalent, carriers occupying the localised states at various energy levels will behave differently. The carrier occupancy of the localised states is governed by the position of the Fermi level E_F and in organic materials, the Fermi level is believed to lie in the band tail of the Gaussian distribution.

At energies below the Fermi level, there are fewer localised states which are located further apart and only a small fraction of these states are empty. Hence carriers at lower lying energy states are rendered as being practically immobile and the lower energy states are likened to trap states with a probability of occupancy close to unity. At energies much higher than the Fermi level, however, the significantly larger density of scarcely populated states allows charge carriers to hop between adjacent sites with relative ease. This condition allows a simple yet key distinction to be made between carriers located above and below the Fermi level. In the simplified picture, carriers below the Fermi level are regarded as trapped while those at much higher energies are considered to be free carriers which are able to contribute to current transport when an external field is applied.

This definition of free and trapped charge carriers is slightly different to the one used in inorganic semiconductors. The shallow traps often referred to in inorganic solids correspond to extrinsic energy levels located several kT away from the conduction band edge. In organic materials, however, the localised states containing both the trapped and free charge carriers

belong to the intrinsic exponential density of states. Hence a factor θ can also be defined in the case of disordered organic semiconductors. It represents the ratio of injected free carrier density at higher energy states to the total injected carrier density and is given by *(Appendix E)*

$$\theta = \frac{n_f}{n_f + n_t} = \frac{T}{T_c} \qquad 4.3.3$$

where T_c is the characteristic temperature representing the exponential distribution of localised states. *Equation 4.3.3* predicts that the factor θ defined for organic semiconductors is also temperature dependent. The magnitude of θ is, however, restricted to being less than 1 as the Universal Mobility Law given by *equation 4.3.1* is only valid for $T_c > T$ and small carrier densities. This means that the model will breakdown even before the density of free carriers becomes exceedingly larger than the concentration of trapped carriers.

At low temperatures, θ will be close to 0 indicating that the concentration of free carriers is significantly less than the trapped carrier density of the material. But with increasing temperature, an increasing number of charge carriers will possess sufficient energy to occupy higher energy states thus leading to a substantial increase in the free carrier density. Consequently, θ will approach 1 as T approaches T_c.

Poisson's equation is thus given by

$$\frac{dF(x)}{dx} = -\frac{q(n_f + n_t)}{\varepsilon_0 \varepsilon_s} = -\frac{qn_f}{\varepsilon_0 \varepsilon_s \theta} \qquad 4.3.4$$

where ε_0 is the permittivity of free space and ε_s is the static dielectric constant of the semiconductor.

Ignoring diffusion currents, the current density J in disordered materials will be controlled purely by the drift mechanism and is thus given by

$$J = n_f q \mu F \qquad 4.3.5$$

where n_f is the injected free electron concentration, q is the electronic charge, μ is the effective carrier mobility and F is the externally applied electric field.

Substituting for the effective mobility μ using *equation 4.3.2* gives

$$J = KqFn_f^{m+1} \qquad 4.3.6$$

The constant K is assumed to be independent of carrier concentration. An expression for the free carrier concentration n_f is obtained using *equation 4.3.6* and is substituted into *equation 4.3.4* to give

$$\frac{dF(x)}{dx} = -\frac{q}{\varepsilon_0 \varepsilon_s \theta}\left(\frac{J}{KqF}\right)^{\frac{1}{m+1}} \qquad 4.3.7$$

Integrating *equation 4.3.7* across the device thickness gives

$$F = \left(\frac{q}{\varepsilon_0 \varepsilon_s \theta}\left(\frac{m+2}{m+1}\right)\right)^{\frac{m+1}{m+2}}\left(\frac{J}{Kq}\right)^{\frac{1}{m+2}} x^{\frac{m+1}{m+2}} \qquad 4.3.8$$

where x corresponds to the thickness of the organic film. *Figure 4.3.5* shows the spatial and temperature dependence of the external electric field F. In disordered organic materials, the so-called effective mobility shows thermally activated behaviour as a result of the exponential rise in the DOS. In an exponential DOS, carriers are more likely to hop to higher energies where there are more empty states. Since traditionally mobility is closely related to the electric field, the temperature dependence is extended by means of the m term which is present throughout *equation 4.3.8*.

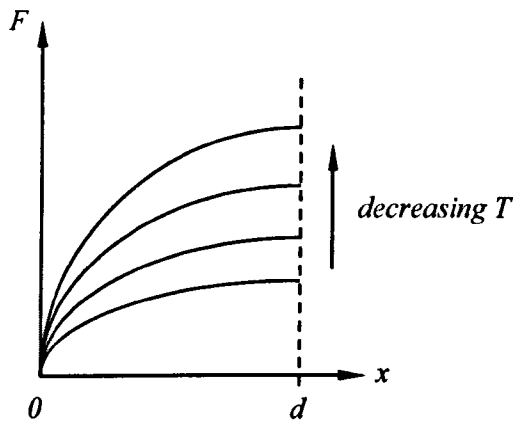

Figure 4.3.5: Schematic representation of the electric field as a function of temperature with distance across the disordered organic material from the injecting contact. The presence of the m term in the exponent for x leads to an enhancement of the electric field with decreasing T. Here d corresponds to the thickness of the organic film.

Substituting $F = -dV/dx$ into *equation 4.3.8* and integrating between V_{app} and 0 yields

$$V_{app} = \left(\frac{J}{Kq}\right)^{\frac{1}{m+2}} \left(\frac{q(m+2)}{\varepsilon_0 \varepsilon_s \theta (m+1)}\right)^{\frac{m+1}{m+2}} x^{\frac{2m+3}{m+2}} \frac{m+2}{2m+3} \qquad 4.3.9$$

where V_{app} is the applied voltage.

The generalised space charge limited current in disordered organic materials with an exponential density of states and consequently a carrier density dependent effective mobility is given by [7]

$$J = \frac{K}{q^m} \left(\frac{\varepsilon_0 \varepsilon_s \theta (m+1)}{m+2}\right)^{m+1} \left(\frac{2m+3}{m+2}\right)^{m+2} \frac{V_{app}{}^{m+2}}{x^{2m+3}} \qquad 4.3.10$$

Equation 4.3.10 demonstrates that the SCL currents in disordered materials have a modified voltage and material thickness dependence. Because of the m term, both the applied voltage and thickness x have a temperature dependence associated with it. On a double logarithmic scale, the current density continues to vary linearly with applied voltage but with a slope that is larger than 2. A value for m and T_c can be determined from the resulting slope. J also shows a stronger dependence on the thickness x. It should be noted that for a semiconductor with a constant mobility *i.e.* $m = 0$, the Mott-Gurney law given as $J = \left(9/8\right)\varepsilon_0 \varepsilon \mu \left(V_{app}{}^2/x^3\right)$ is retained.

4.4 FABRICATION OF POLYTRIARYLAMINE (PTAA) SCHOTTKY DIODES

In recent years, much purer organic materials with almost no residual doping has been synthesised by Merck Chemicals Ltd (previously Avecia). One of the proprietary organic materials supplied by Merck used in the fabrication of Schottky diodes is polytriarylamine (PTAA) (S1105). PTAA is a highly disordered organic semiconductor; it is more structurally disordered than even P3HT. However, PTAA is believed to contain far less quantities of residual dopant albeit not much is known about its synthesis process.

In PTAA diodes, the gold electrode is evaporated first since it has to be pre-treated with pentafluorobenzenethiol (PFBT) in order for the metal to make a good ohmic contact with the semiconductor. The self-assembled monolayer formed by pentafluorobenzenethiol on the gold electrode has been reported to act as an electron acceptor [14]. It increases the metal

work function by almost 1 eV thus significantly reducing the potential barrier seen by holes which are the majority charge carriers. The PFBT solution is prepared by dissolving 0.6 ml of PFBT in 450 ml of propanol. The gold coated glass substrate is immersed in the PFBT solution for approximately 10 minutes followed by propanol for a further 10 - 15 seconds to wash away any excess PFBT molecules.

The PTAA solution is prepared by dissolving approximately 30 mg of the material in 5 ml of xylene or dichlorobenzene (DCB). The solution is heated to enhance the solubility of the organic material. Care must be taken to avoid highly concentrated PTAA solutions as it causes the solution-cast film to peel off from the metal substrate upon drying. Similar to the P3HT based diode, the sample is left to dry in vacuum overnight prior to the shadow mask evaporation of the aluminium dots. *Figure 4.4.1* shows a schematic diagram of a PTAA Schottky diode.

The electrical characterisation of the Schottky diodes was performed in air using a HP4145B semiconductor parameter analyser. The measurements were taken at a step size of 50 mV.

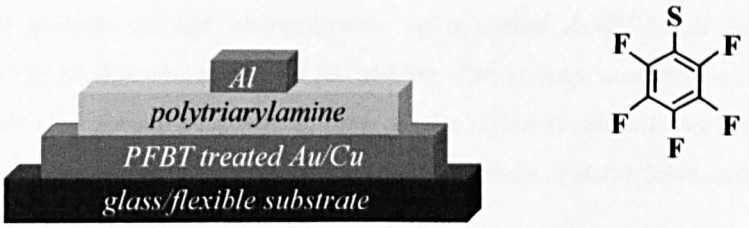

Figure 4.4.1: Structure of a polytriarylamine (PTAA) Schottky diode. The gold contact is treated in a PFBT solution to facilitate the formation of an ohmic contact to PTAA. Inset is the chemical structure of pentafluorobenzenethiol (PFBT).

4.5 ELECTRICAL CONDUCTION IN POLYTRIARYLAMINE (PTAA)

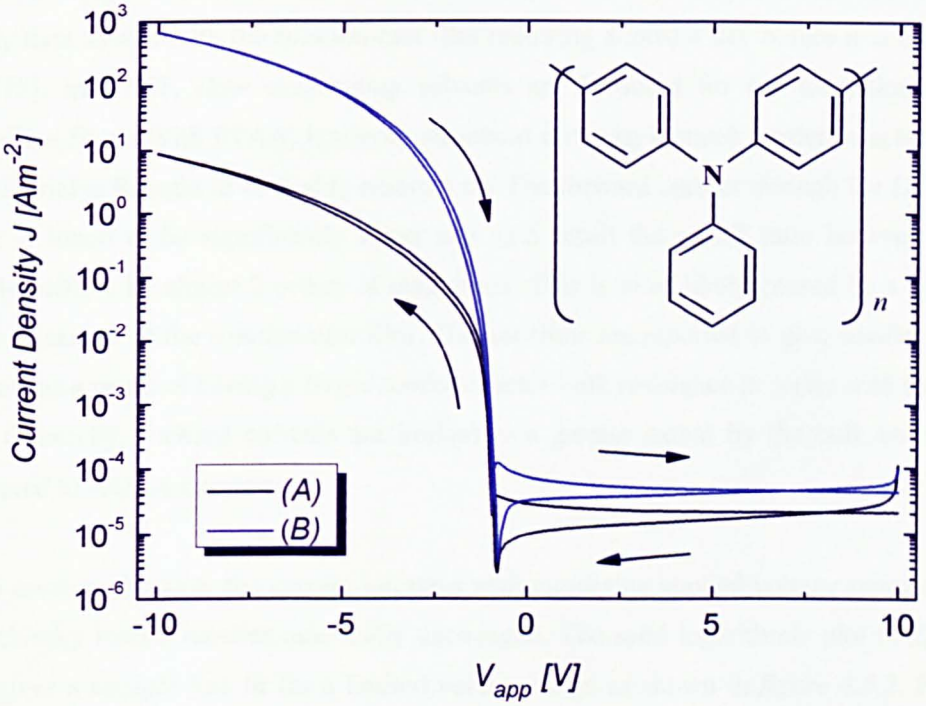

Figure 4.5.1: Current density voltage characteristic of modified Au-PTAA-Al Schottky diodes processed from (A) dichlorobenzene and (B) xylene. The voltage was applied on the top aluminium electrode. The forward current in both diodes differ by almost two orders of magnitude. Inset is a schematic illustration of the chemical structure of polytriarylamine.

Figure 4.5.1 shows the current density voltage characteristic for metal semiconductor diodes made with polytriarylamine (PTAA) dissolved in xylene and dichlorobenzene (DCB). Polytriarylamine is a highly amorphous p-type organic semiconductor and is readily soluble in most common organic solvents. The gold electrode is pre-treated with pentafluorobenzenethiol to help it make a good ohmic contact with PTAA. The *J-V* measurements were performed by sweeping the applied voltage on the aluminium top contact from 10V to -10V and back at steps of 50 mV.

The extremely low off currents produced by the PTAA Schottky diodes leads to remarkably high rectification ratios. The rectification ratio for the xylene and DCB based PTAA diodes are approximately 10^{8} and 10^{6} respectively. These ratios are significantly larger compared to the value quoted for the as-synthesised P3HT Schottky diode. The much higher off currents observed in P3HT is consistent with the belief that the material contains large amounts of residual dopant. It must be said that the relatively low off currents observed in PTAA diodes is highly desirable for ultra low current circuit operations.

The effect of dissolving the organic semiconductor polytrarylamine in two different solvents is shown in *figure 4.5.1.* The solvent dichlorobenzene has been reported to evaporate more slowly than xylene with the solution-cast film requiring almost a day before it is completely dry [15]. In P3HT, slow evaporating solvents are favoured for the formation of more crystalline films. With PTAA, however, structural ordering is much harder to achieve since the material is thought to be highly amorphous. The forward current through the DCB based diode is found to be significantly lower and as a result the on-off ratio between the two samples differs by almost 2 orders of magnitude. This is most likely caused by a difference in the thickness of the solution-cast film. Thicker films are reported to give smaller forward currents as a result of having a larger semiconductor bulk resistance in series with the barrier [16]. Generally, forward currents are limited to a greater extent by the bulk conductance compared to reverse currents.

In the reverse direction, the current saturates with increasing applied voltage suggesting that the Schottky barrier remains essentially unchanged. The semi logarithmic plot of J_R against $V^{0.25}$ gives a straight line fit for a limited voltage range as shown in *figure 4.5.2.* From the plot, the dopant density is estimated to be ~ 10^{13} cm^{-3}. This gives a depletion region and an effective Debye length that exceeds the thickness of the organic film. The thickness of solution-cast films is assumed, in general, to be approximately 1μm. This anomaly suggests that the diode does not obey the ¼ power law given by the simplified Schottky theory. The lack of agreement with theory makes it impossible to calculate the dopant density in polytriarylamine. And since the dopant density N_A is unknown, the effective bulk mobility of holes in the material also cannot be established.

For high purity materials such as PTAA, a much wider depletion region is expected to form at the Schottky barrier interface since the width of the depletion region is inversely proportional to the amount of dopant density present in the material. In other words, the space charge region in purer materials will extend further for small increments in applied voltages thus making it more likely for the space charge region to reach the back of the film. Once the space charge region hits the back of the film, the reverse current is expected to rise more sharply with applied voltage as the semiconductor starts to resemble an insulator. The current will vary as a function of $V^{0.5}$ instead of $V^{0.25}$ since an effectively larger applied field contributes to the lowering of the Schottky barrier.

The reverse current density is thus given by *(Appendix F)*

$$J_R = J_0 \exp\left[\frac{q}{kT}\left(\frac{q(V_R - V_{bi})}{4\pi\varepsilon_0\varepsilon_s x_p}\right)^{1/2}\right] \qquad 4.5.1$$

where J_0 is a constant, k is the Boltzmann constant, ε_0 is the permittivity of free space, ε_s is the static dielectric constant and x_p is the organic film thickness.

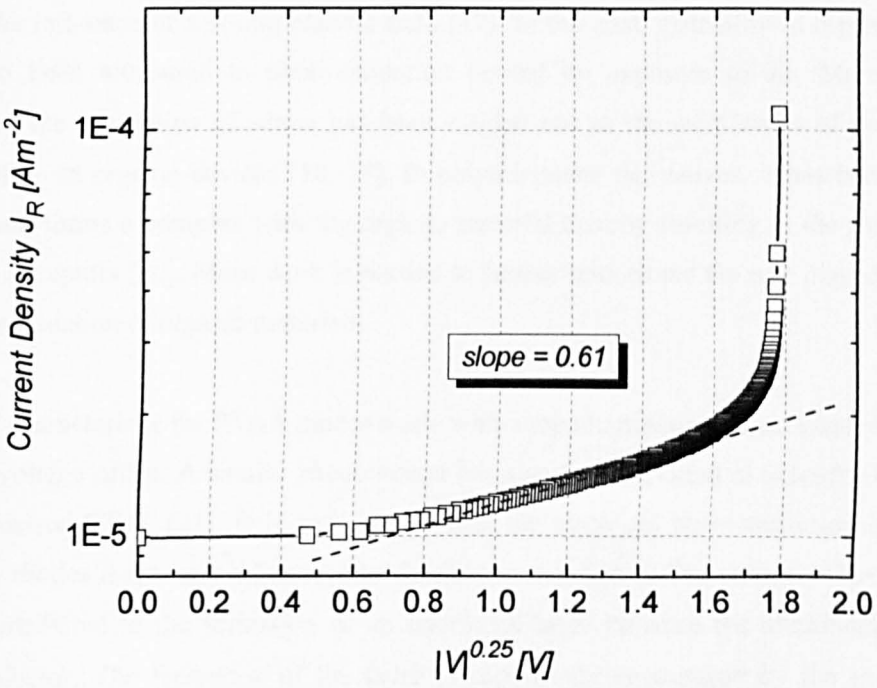

Figure 4.5.2: Reverse current density against $|V|^{0.25}$ for the treated Au-PTAA-Al Schottky diode processed from dichlorobenzene. The dopant density calculated from the slope is ~ 10^{13} cm^{-3}. This gives a depletion width that exceeds the thickness of the film which suggests that the diode does not obey the ¼ power law.

However, this cannot be true in the case of PTAA Schottky diodes since the reverse current stays almost constant with increasing applied voltage. Besides, intuitively, it is quite unlikely for the depletion region in PTAA Schottky diodes to reach the back of the film for the given voltage range as the organic film is solution-cast.

The saturation of the reverse current in PTAA diodes can therefore only be explained by the presence of trap states in the organic material which subsequently leads to the pinning of the quasi Fermi level. So instead of an expanding space charge region, the increasing negative

voltage applied on the semiconductor forces holes to be released from the trap states. This will limit the barrier lowering effect and as a result the current across the barrier stays almost constant. The assumption of a flat quasi Fermi level means that the trap states could lie anywhere along the length of the organic film. The pinning effect surprisingly disappears once the applied voltage is reversed.

A visibly large anticlockwise hysteresis is obtained in the reverse direction when the voltage sweep is reversed. Hysteresis which is a common manifestation of instability in organic based devices is often associated with the drifting of mobile ions within the organic film under the influence of a strong electric field [17]. In the past, instability in organic devices has also been attributed to photo-oxidation caused by exposure to air. More recently, however, the adsorption of ozone has been singled out as the main cause of performance degradation in organic devices [18, 19]. In polythiophene derivatives, it has been reported that ozone forms a complex with the organic material thereby resulting in the formation of shallow acceptors [20]. More work is needed to further understand the role played by ozone in the degradation of organic materials.

The *J-V* characteristic for PTAA diodes made with a top aluminium contact generally exhibit a small voltage offset. A similar phenomenon has also been reported in Schottky barriers to as-synthesised P3HT [21]. It is well known that the electrical characterisation of organic Schottky diodes is strongly influenced by fabrication conditions. The voltage offset observed here is attributed to the formation of an interfacial layer between the aluminium and the semiconductor. The formation of the layer is supposedly encouraged by the presence of residual atmospheric contaminants during metal deposition under insufficiently low pressures [22]. The voltage offset is said to be related to a permanent polarisation within the interfacial layer.

When a negative voltage is applied on the Al electrode, the Schottky barrier impeding the movement of holes from PTAA is significantly lowered. Consequently an exponential rise in current is observed with applied voltage. Provided that $T_c > T$, the exponential nature of the current is attributed to the exponential fall in carrier occupancy given by the Maxwell Boltzmann statistics. Using the simple analytical model presented in the previous chapter, the current across the barrier in the forward direction is given by

$$J \alpha \exp\left(\frac{qV_{app}}{kT_0}\right) \qquad 4.5.2$$

where T_0 represents the characteristic temperature of the exponential energetic distribution of holes.

A value for T_0 can be obtained by applying *equation 4.5.2* directly to the slope of the forward characteristic. From *figure 4.5.3*, T_0 is estimated to be approximately 481K. This value of T_0 is substantially smaller compared to the value quoted for the as-synthesised P3HT Schottky diode. The magnitude of T_0 corresponding to the intrinsic distribution of carriers is generally believed to lie in the region of between 800K and 1300K. Neglecting trapping in extrinsic states, current in the exponential part of the characteristic is believed to be supported by the intrinsic carriers as dopant states are located too high in energy and hence will only support current at higher applied voltages. However, the smaller value of T_0 obtained suggests the presence of an anomalous distribution of extrinsic states. These states are probably caused by the formation of a non-ideal barrier at the metal semiconductor interface. The extrinsic states must lie at lower energies since they influence the current across the Schottky barrier at low applied voltages.

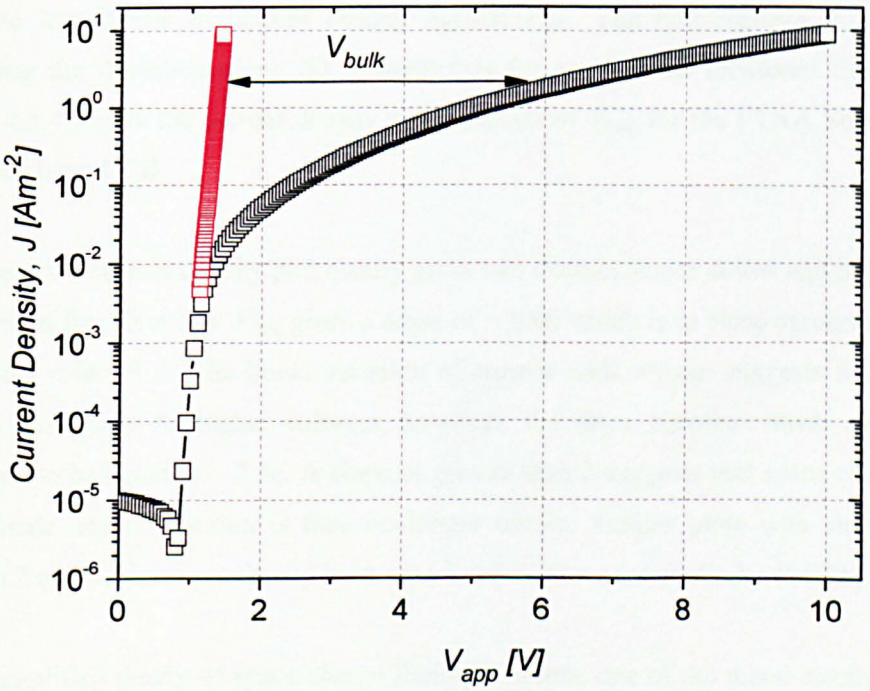

Figure 4.5.3: Forward J-V characteristic for a treated Au-PTAA-Al Schottky diode processed from dichlorobenzene. At higher applied voltages, only a small fraction of the potential falls across the barrier and the space charge region thus resulting in a strong deviation from equation 4.5.2.

The corresponding value of T_c describing the combined distribution of intrinsic and extrinsic states may be obtained using the following relationship.

$$\frac{1}{T_0} = \frac{1}{T} - \frac{1}{T_c} \qquad 4.5.3$$

Equation 4.5.3 gives a value of ~ 799K for T_c and a Meyer Neldel energy of ~ 69 meV. Coincidentally this larger T_c value is consistent with the results obtained when extrinsic dopant states are present [23]. Higher T_c values are generally associated with the introduction of extrinsic states into the intrinsic DOS of the organic material. A value of m equal to ~ 1.66 is obtained.

With further increase in applied voltage, a higher fraction of the potential is dropped across the neutral region which leads to a substantial deviation from *equation 4.5.2*. The potential across the barrier and the space charge region is thus relatively small. Assuming that the gold contact is ohmic, the saturation current will be limited purely by the resistivity of the neutral region. The current transport mechanism in the neutral region can be determined by plotting a double logarithmic of current density against V_{bulk}. The bulk voltage is obtained by measuring the deviation along the voltage axis for each of the measured current levels. *Figure 4.5.4* shows the current density as a function of V_{bulk} for the PTAA Schottky diode processed from DCB.

The saturation current density plot clearly gives two distinct slopes at low and high voltages. The straight line fit at low V_{bulk} gives a slope of ~ 0.98 which is in close agreement with the theoretical value of 1. The linear variation of current with voltage suggests that the diode obeys Ohm's law. At higher voltages, however, the slope becomes much steeper. It is calculated to be equal to ~ 2.56. A slope of greater than 2 suggests that space charge effects predominate and conduction is thus no longer ohmic. Similar plots with slopes ranging between 2 and 2.5 have previously been reported for other organic diodes [24-26]

In the simplified theory of space charge limited currents, one of the metal electrodes has to make an ohmic contact with the organic semiconductor in order for there to be an infinite supply of charge carriers. In the case of the PTAA Schottky diode, the Au electrode is assumed to be ohmic upon treatment with the contact solution pentafluorobenzenethiol (PFBT). It has been reported that the surface active thiol group can easily attach itself onto the metal electrode via the formation of a dative bond between the sulphur atom of the thiol group and the metal [14]. The self-assembled monolayer of PFBT deposited on the Au

surface is believed to act as an electron acceptor. The PFBT solution is said to increase the work function of the Au electrode by greater than 1 eV [27].

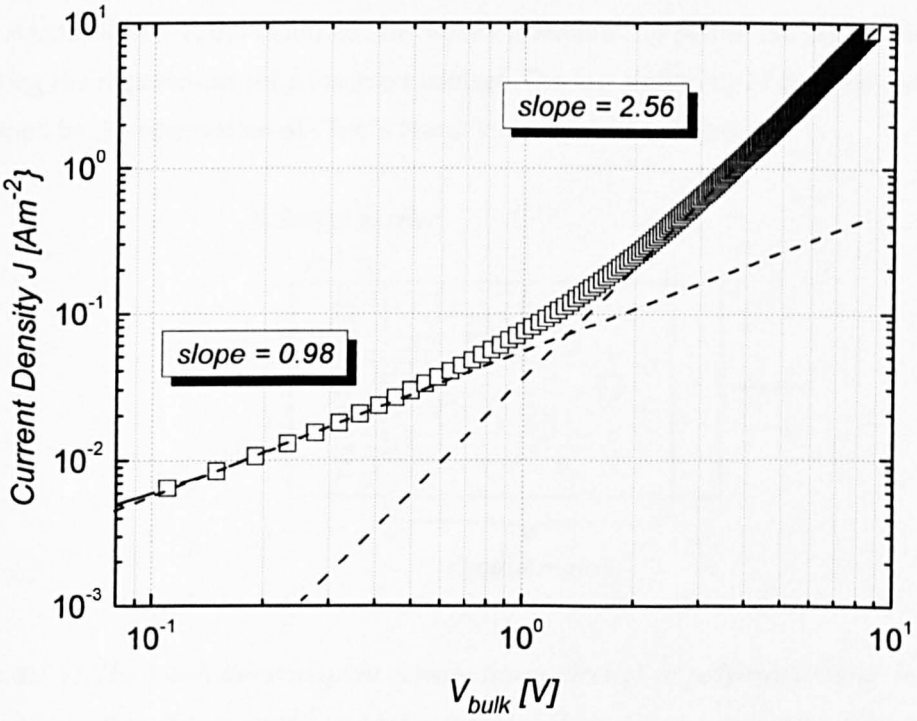

Figure 4.5.4: Current density against V_{bulk} for modified Au-PTAA-Al diode. Two distinct slopes are obtained at low and high voltages which are estimated to be 0.98 and 2.56 respectively. This suggests that the conduction changes from ohmic to space charge limited with increasing applied field.

At higher voltages, space charge effects seem to dominate conduction in PTAA diodes even though both PTAA and as-synthesised P3HT show almost comparable forward current levels. In *chapter 3*, it was demonstrated that the neutral region of an as-synthesised P3HT diode shows ohmic behaviour even at high applied voltages. This difference in bulk conduction between the two materials can be explained by the higher dopant density observed in as-synthesised P3HT. In PTAA, the dopant density is thought to be much lower and consequently, there are insufficient dopant ions to compensate the increasing density of holes in the neutral region of the organic film as illustrated in *figure 4.5.5*. The build up of majority carriers produces a non-linearly varying electric field which leads to a change in conduction from ohmic to space charge limited.

The analysis of space charge limited currents in the neutral region of a Schottky diode does not conform to the boundary conditions outlined in the classical treatment of SCL currents.

Traditionally, SCL currents are discussed within the framework of an insulator sandwiched between two metal electrodes of low resistivity. In a Schottky diode, however, the neutral region is sandwiched between a metal electrode and a space charge region as shown in *figure 4.5.5*. As stated above, the modified Au contact is assumed to permit the flow of holes thus satisfying the requirement for a reservoir contact. The low resistivity of the gold electrode is confirmed by the observation of Ohm's law at lower applied voltages.

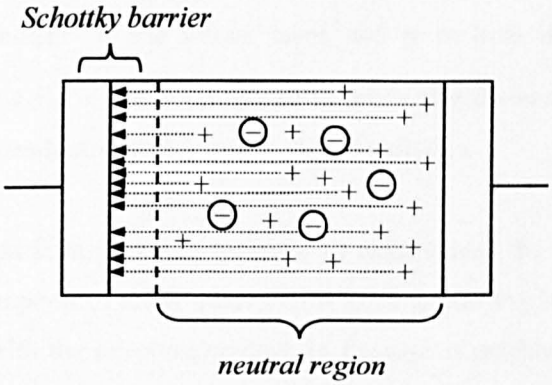

Figure 4.5.5: The much lower dopant density (open circles) in polytriarylamine leads to a high concentration of uncompensated holes (positive sign). Current transport at high applied voltages is therefore dominated by space charge effects.

On the opposite end, however, a space charge region neighbours the semiconductor bulk instead of a metal electrode. Fortunately, in forward bias, the width of the space charge region adjacent to the Al contact is significantly reduced by the lowering of the effective barrier height with increasing applied bias. The space charge region, however, does not possess an abrupt edge as illustrated in *figure 4.5.5*. In practice, the region extends further into the bulk by an effective Debye length L_{De}. The effective Debye length corresponds to the distance over which the low hole density increases to its intrinsic concentration. The abrupt depletion edge approximation is one of the simplifying assumptions used in the basic Schottky theory for analysing reverse *J-V* characteristics. Due to the exponential DOS, the Debye length in disordered organic materials is believed to be supported by a potential $\left(kT_c/q\right)$ of ~ 40 meV instead of the traditional 26 meV.

The analysis of carrier distribution and hence transport in semiconductors under steady state conditions is strongly dependent on the position of the quasi Fermi level. Provided that it is possible to assume a flat quasi Fermi level, all carriers in the organic semiconductor must be in quasi thermal equilibrium. *Figure 4.5.6* shows the energy diagram of a Schottky diode

with a so-called ohmic back contact. Again the localised states are represented in a succession of energy levels to clearly illustrate the energy variation envisaged in PTAA. In general, current transport in semiconductors occurs through a combination of drift and diffusion and can be expressed as *(Appendix G)*

$$J \propto p\frac{d\xi}{dx} \qquad 4.5.4$$

where $d\xi/dx$ is the gradient of the Fermi level and p is hole density in a p-type semiconductor. *Equation 4.5.4* is extremely useful in predicting the energy variation of the quasi Fermi level in semiconductors under steady state conditions.

In *figure 4.5.6*, a common Fermi level is assumed to exist across the entire length of the semiconductor. The assumption of a flat quasi Fermi level is best explained by means of a regional model starting with the injecting contact. In the region neighbouring the modified Au contact, the density of holes increases to infinity as it approaches the contact thus resulting in a steep concentration gradient. Hence, the diffusion component of the current predominates in the vicinity of the contact and according to *equation 4.5.4*, a high carrier density will only require a small gradient in the Fermi level to maintain current flow. Thus a constant Fermi level may be defined close to the metal electrode. In the simplified SCL current theory, the diffusion component of the current is ignored since it is deemed important only in the region adjacent to the contact.

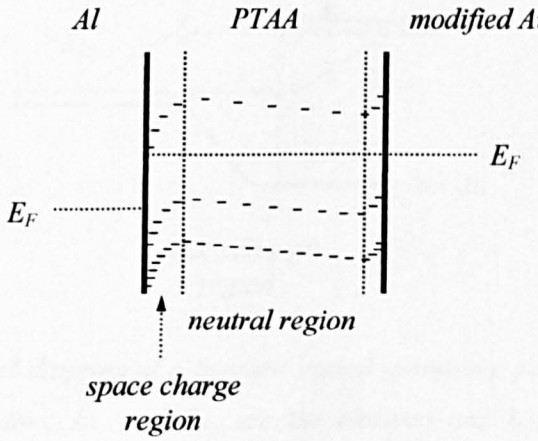

Figure 4.5.6: Simplified energy diagram for a modified Au-PTAA-Al Schottky diode under forward bias. A flat quasi Fermi level is assumed across the semiconductor including the space charge region. This means that all carriers are in thermal equilibrium and the Fermi Dirac statistics may be used to describe the carrier distribution.

At high applied voltages, the neutral region is controlled by space charge effects due to the build up of charge carriers. Again, a high concentration of holes suggests that the quasi Fermi level will remain unchanged throughout the semiconductor bulk. In the narrow space charge region adjacent to the Schottky barrier, however, the density of holes is expected to decrease drastically. Under such circumstances, *equation 4.5.4* predicts that a visible change in the Fermi level is required to maintain current flow. However, *figure 4.5.6* depicts a flat quasi Fermi level even through the space charge region. To elucidate this issue, similarities are drawn with the space charge region of a p-n junction diode [28]. In a p-n junction, the electron density in the n-type side of the junction is very high while in the p-type side, electrons are the minority carriers. Nevertheless, the requirement for current continuity dictates that the current on either side of the junction must be equal. So the electron quasi Fermi level will most likely have a very steep gradient in the p-type side and a rather small one in the n-type side as depicted in *figure 4.5.7*. Assuming that no recombination process takes place in the space charge region, every electron leaving the n-type material will move through the space charge region and reach the other end of the junction. This allows for a flat quasi Fermi level to be defined. In other words, the boundary condition on either sides of the p-n junction dictates that the Fermi level in the space charge region has a negligible gradient. The increase in electron density with distance across the space charge region is reflected by the bending of the conduction band edge E_c.

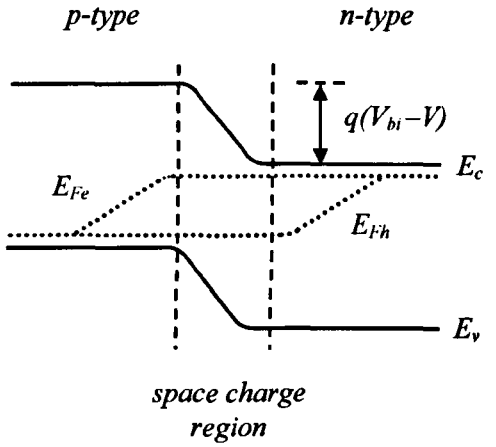

Figure 4.5.7: Energy level diagram of a forward biased symmetric p-n junction made with conventional semiconductors. E_{Fe} and E_{Fh} are the electron and hole quasi Fermi level respectively. Both the quasi Fermi levels are assumed to remain flat throughout the space charge region.

Based on the same concept, a flat quasi Fermi level is also assumed in the space charge region of Schottky diodes. Like p-n junctions, the decreasing hole density with approaching distance of the Schottky barrier is represented by the bending of the localised states away from the Fermi level as in *figure 4.5.6.* In the Debye length at the edge of the space charge region, the large hole concentration gradient will result in a flat quasi Fermi level.

Hence a common quasi Fermi level may be assumed across the entire film thickness. This assumption works better in disordered semiconductors compared to crystalline solids. In the latter, carriers gain additional kinetic energy from traversing through the material and interacting with the potential well of a large number of atoms in the crystal lattice. This phenomenon limits the validity of a flat quasi Fermi level and consequently the accuracy of the Fermi Dirac statistics. In contrast, disordered organic semiconductors are characterised by carriers hopping between localised energy states and the site spacing which controls the carrier hopping distance is commonly reported to lie between 1-2 nm [11, 29]. The substantially smaller distance travelled means that carriers in disordered materials are unlikely to get 'hot' and the notion of a flat quasi Fermi level is preserved.

In this model, the potential drop across the space charge region is assumed to be sufficient to get holes exiting the neutral region across the barrier and hence support the SCL current. The analysis of SCL currents in diodes is therefore assumed to be unaffected by the different boundary conditions. Another important factor to consider is the possible dependence of the SCL current on the width of the neutral region. Following the regional model approach, the organic film is divided into two regions; the space charge region and the neutral region. In forward bias, the lowering of the effective barrier height leads to a substantial reduction in the width of the space charge region. So, the increasing width of the neutral region will have to be taken into account in the analytical treatment of the SCL current provided the space charge region continues to shrink appreciably in the saturation current regime. But to simplify the analysis, we assume that the width of the neutral region stays almost constant. Although a stronger voltage dependence is expected for SCL currents, it is still not comparable to the exponential rise in current seen across the Schottky barrier before it is limited by the series resistance of the semiconductor bulk. Hence, the relatively small increment in saturation current observed suggests that the change in the space charge region width is negligible and can therefore be ignored. Consequently the rise in SCL current will only affected by the increase in potential drop across the neutral region.

For disordered materials with a carrier density dependent mobility, the space charge limited current is given by

$$J = \frac{K}{q^m}\left(\frac{\varepsilon_0\varepsilon_s\theta(m+1)}{m+2}\right)^{m+1}\left(\frac{2m+3}{m+2}\right)^{m+2}\frac{V_{app}{}^{m+2}}{x^{2m+3}} \qquad 4.5.5$$

According to *equation 4.5.5*, the slope of a double logarithmic plot of current density against voltage will be equal to $m + 2$. Hence, the value of m for the PTAA Schottky diode is ~ 0.56.

A value for T_c can be found using the following relationship:

$$m = \frac{T_c}{T} - 1 \qquad 4.5.6$$

From *equation 4.5.6*, T_c is estimated to be ~ 468K which gives a Meyer Neldel energy of ~ 40meV. Interestingly, this value of T_c corresponds to the intrinsic exponential distribution of states. This suggests that the higher energy states responsible for current flow in the saturation regime of the diode are almost free of dopant states thus allowing the determination of the intrinsic value of T_c. The absence of additional dopant states also proves that polytriarylamine is a much purer organic semiconductor than its predecessor, as-synthesised P3HT. In P3HT diodes, the effective bulk mobility obtained from the saturation regime of the forward characteristic obeys the universal mobility relationship. As mentioned in *chapter 3*, the universal mobility plot yields a Meyer Neldel energy almost double its intrinsic value.

The characteristic temperature for the distribution of intrinsic carriers T_0 is approximately equal to 836K. The values of T_c and T_0 calculated for the PTAA Schottky diode are consistent with those obtained from TFTs made with the same material [30].

In this newly developed SCLC model, we have only considered the carrier density dependence of the effective mobility. In the model developed by Pasveer *et al.*, however, the occurrence of SCL currents in light emitting diodes (PLEDs) made with poly[4'-(3,7-dimethyloctyloxy)-1,1'-biphenylene-2,5-vinylene](NRS-PPV) and poly(2-methoxy-5-(3',7'-dimethyloctyloxy)-*p*-phenylene vinylene) (OC_1C_{10}-PPV) is analysed by taking into account the carrier density, temperature and also field dependence of mobility in a Gaussian shaped density of states [31]. The model accurately predicts the experimentally observed SCLC density voltage relationship up to applied voltages of around 50V.

4.5.1 EFFECT OF THE BACK METAL/ORGANIC INTERFACE

Figure 4.5.8 shows the current density voltage characteristic for polytriarylamine (PTAA) Schottky diodes made with two different back metal contacts; Au and Cu and with and without surface treatment with pentafluorobenzenethiol (PFBT). Aluminium is used as the Schottky metal in all the devices. The *J-V* curves clearly demonstrate that the forward current and hence the rectification ratio of the diodes depend strongly on the choice of the back metal contact. Current flow at high applied voltages is therefore limited by the properties of the back metal/organic interface. Previously, the forward current was thought to saturate as a result of the series resistance associated with the semiconductor bulk.

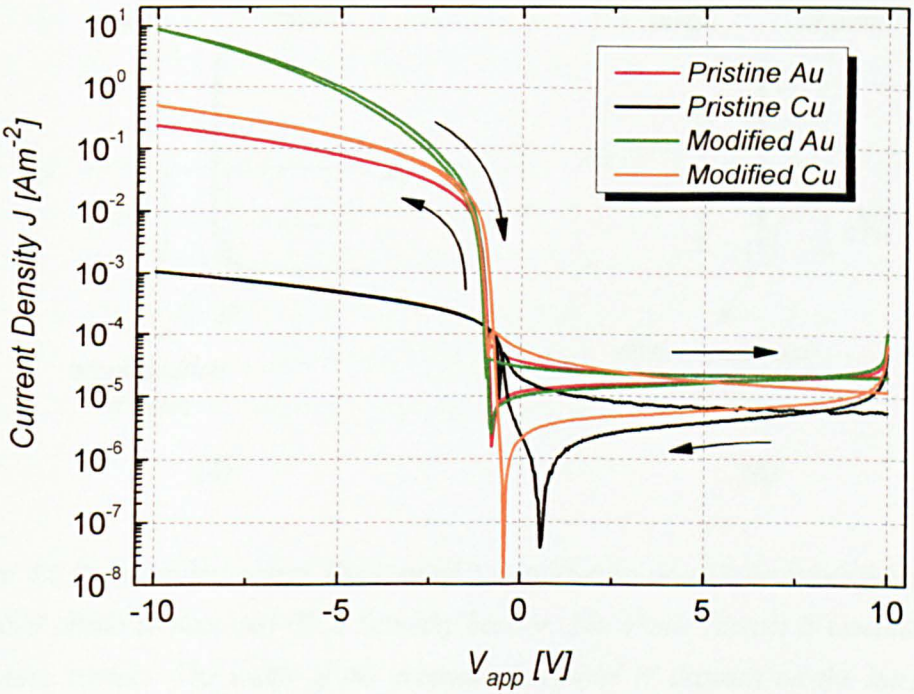

Figure 4.5.8: Current density voltage characteristics of Al-PTAA Schottky diodes with pristine and modified Au and Cu electrodes. The voltage was applied on the top aluminium electrode. The lower saturation currents are associated with the formation of a barrier at the back metal/organic interface.

The theoretical work function of gold is larger than that of copper. Pristine Au is generally quoted as having a work function of ~ 5.1 eV whilst copper is about 4.7 eV. In practice the work function of metals could differ significantly from their theoretical value as it is sensitive to the deposition method used and also on the chemical nature of the resulting

metal/organic interface. PTAA like most other organic semiconductors is intrinsically p-type and therefore requires a high work function metal to make good ohmic contact with it.

Ideally, an ohmic contact is characterised by the absence of a potential barrier and an infinite recombination-generation rate [28]. The former ensures that carrier transport in either direction is strictly proportional to the field at any point without the complications relating to space charge effects. Meanwhile, the infinite recombination-generation rate also helps prevent space charge formation since carriers are being supplied and removed by the metal contact exactly at the rate required by transport in the semiconductor. So the Fermi level in the metal and semiconductor line up and there is no bending of energy states in the semiconductor side of the interface.

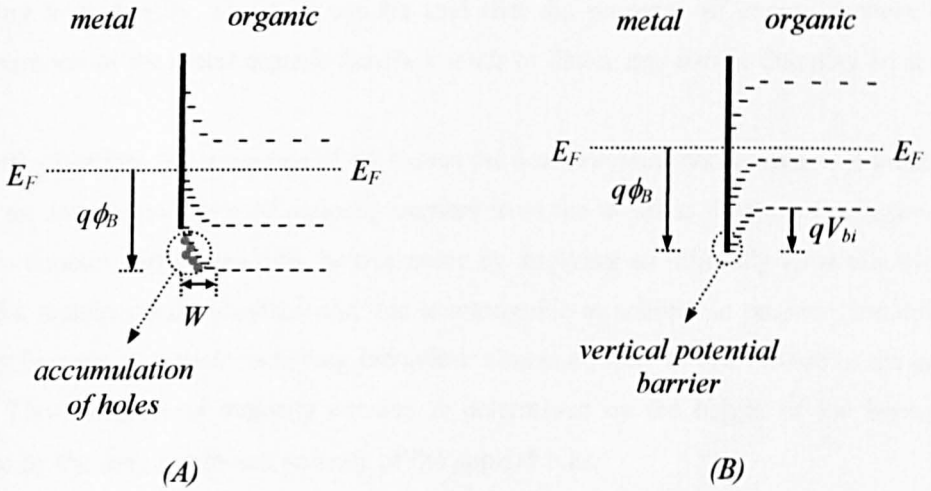

Figure 4.5.9: Simplified energy diagram of a metal/p-type organic interface forming (A) a so-called ohmic contact and (B) a Schottky barrier. The ohmic contact is essentially a low resistance contact. The width of the accumulation layer W depends on the intrinsic hole concentration of the organic semiconductor.

The term 'ohmic contact', however, is often loosely used to describe low resistance contacts when, in fact, the two cases are clearly distinguishable. Thus an ohmic contact is also said to be formed between a metal and semiconductor when the resistance associated with the contact is negligible compared to the series resistance of the semiconductor bulk [32]. Like Schottky barriers, the bending of the energy states in the semiconductor is mainly due to the work function difference between the metal and semiconductor. The energy bending attracts holes to accumulate at the interface thus giving rise to a much smaller contact resistance as shown in *figure 4.5.9 (A)*. So although the contact made between a high work function metal

and a p-type organic solid is essentially a low resistance contact, it is often termed as an ohmic contact.

The so-called ohmic contact made with p-type organic materials are known to allow the passage of holes in both directions. The energy bending shown in *figure 4.5.9 (A)* allows holes to be transferred into the metal with relative ease. In contrast, the movement of holes into the semiconductor is impeded by the presence of a potential barrier. Fortunately, the carriers only see a parabolic shaped potential barrier at the metal/organic interface. This barrier can be easily reduced with the application of an external voltage across it. With the application of an appropriate bias, the accumulation width reduces and a much smaller barrier is seen by the majority carriers in the metal. The width of the accumulation layer is largely dependent on the free carrier concentration of the organic film and it decreases with increasing hole density. Hence it can be said that the presence of excess carriers in the neighbourhood of the metal/organic interface tends to flatten any barrier that may be present.

In Schottky barriers, the presence of an almost vertical potential barrier makes it impossible to have an unrestricted flow of majority carriers from the metal as illustrated in *figure 4.5.9 (B)*. This contact barrier can only be overcome by applying an infinitely large electric field across the metal/organic interface and this is impossible to achieve in practice. Incidentally, Schottky barriers owe their rectifying behaviour almost entirely to this feature of the contact barrier. The transport of majority carriers is determined by the height of the barrier and therefore by the magnitude and polarity of the applied bias.

Due to difficulties in determining the doping level of polytriarylamine, the work function of the material remains unknown but its ionisation potential is said to be ~ 5.1 eV [33]. Therefore in order to significantly reduce the contact barrier, the Au and Cu electrodes are pre-treated with pentafluorobenzenethiol. PFBT is said to modify the metal work function by forming a self-assembled monolayer which acts as an electron acceptor. The increment in the metal work function could be over 1 eV.

From *figure 4.5.8*, the highest forward current and hence the highest rectification ratio is obtained for the PTAA diode with a modified Au electrode. The electrical characterisation of this diode is discussed in detail in *section 4.5*. Clearly, the saturation current of this diode rises more sharply than the rest of the devices. The steeper rise in current is thought to be associated with space charge effects dominating conduction in the neutral region of the organic material at higher applied voltages. Space charge limited currents typically show a larger voltage dependence which is found to be even greater in the case of disordered

materials. The current density voltage relationship for disordered semiconductors is given by $J \propto V^{m+2}$.

The forward currents are significantly lower for diodes made with Cu as the back contact which suggests that a potential barrier exist at the metal/organic interface. This is consistent with the idea that the contact barrier for the injection of holes decreases with increasing metal work function. The forward saturation current of the PTAA diodes with a pure and modified Cu electrode differs by over 2 orders of magnitude. It is highly unlikely that the difference in forward currents is caused by variation in film thicknesses since all the samples were prepared as identically as possible. The extremely poor rectifying behaviour exhibited by the unmodified Cu diode is attributed to the formation of a relatively large contact barrier. The diode only gives a rectification ratio of ~ 10^2 as the forward current is limited by the reverse biased Schottky barrier.

The relatively small rectification ratio obtained for the modified Cu diode is attributed to the ineffectiveness of the deposited PFBT monolayer in increasing the work function of Cu. If not, with a possible increment of greater than 1 eV, the modified Cu electrode should form an ohmic contact with PTAA. Clearly this is not the case since the forward saturation current through the modified Cu diode is only slightly higher than the pristine Au sample.

Besides the PFBT-modified Au diode, the rest of the devices are essentially pairs of back-to-back diodes where the forward current is limited by the reverse biased back Schottky contact. Unlike the forward currents, the current in the reverse direction is unaffected by the back metal contact since it is forward biased when the main Schottky barrier is reversed biased.

At low negative voltages, the reverse biased back contact seems to have no influence on the exponential rise in current. The Schottky barrier continues to dominate current as almost all the potential is dropped across the barrier and the space charge region adjacent to it. With increase in applied voltage, however, the back contact barrier height increases and the space charge region associated with the contact widens. This causes a higher fraction of the potential to fall across the back metal/organic interface and the neutral region. Consequently, the current is no longer dictated by the exponential distribution of carriers given by the Maxwell Boltzmann statistics but instead it is limited by the properties of the metal/organic interface.

The conduction mechanism in the neutral region of PTAA can be determined by plotting a double logarithmic plot of current density against bulk voltage. As discussed in the previous section, for the PTAA diode with a modified Au contact, current through the neutral region obeys Ohm's law at low applied voltages and becomes space charge limited with further increase in bias. The close agreement of the experimental plot with both the theories suggests that the modified Au electrode makes a good ohmic contact with PTAA. For the rest of the devices, however, the experimental plot of J against V_{bulk} does not yield slopes which are close to the theoretical values predicted by either mechanism. The lack of agreement is attributed to the fact that the back metal/organic contacts in these devices are essentially Schottky barriers. Hence it is no longer possible to analyse the J-V characteristics of these diodes in terms of a regional model since a fraction of the bulk voltage is in fact dropped across the reverse biased Schottky barrier.

Since the organic films are solution cast, it is unlikely that the width of the space charge region at both contacts will be comparable to the film thickness. Hence, it is assumed that there is no overlap of depletion regions and a neutral region unaffected by the contacts still exists in the semiconductor. An energy diagram for a device consisting of two non-interacting back-to-back diodes is shown in *figure 4.5.10.*

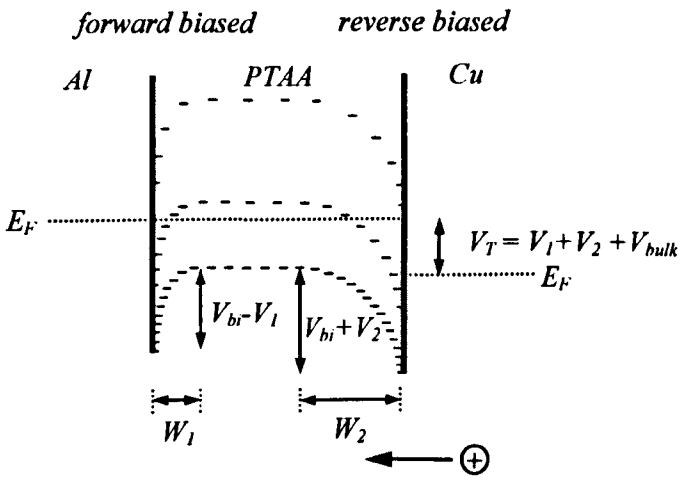

Figure 4.5.10: Simplified energy diagram for a pair of non-interacting back-to-back Schottky diodes with the Al/PTAA contact forward biased. W_1 and W_2 represent the width of the space charge region at the Al/PTAA and Cu/PTAA interface respectively. The two space charge regions are not expected to overlap since PTAA is a solution-cast film. V_T corresponds to the total voltage applied across the device.

4.5.2 EFFECT OF DOPING WITH DDQ

The introduction of dopant molecules into organic semiconductors generally enhances the overall conductivity of the intrinsic material. *Figure 4.5.11* shows the current density voltage characteristics for polytriarylamine Schottky diodes doped with 0.5% DDQ by weight with pristine and modified Au and Cu back electrodes. The *J-V* curves indicate that the addition of DDQ molecules leads to higher current levels even when the devices are essentially pairs of back-to-back diodes. The much higher reverse currents observed in all the diodes are clear evidence of the higher doping densities.

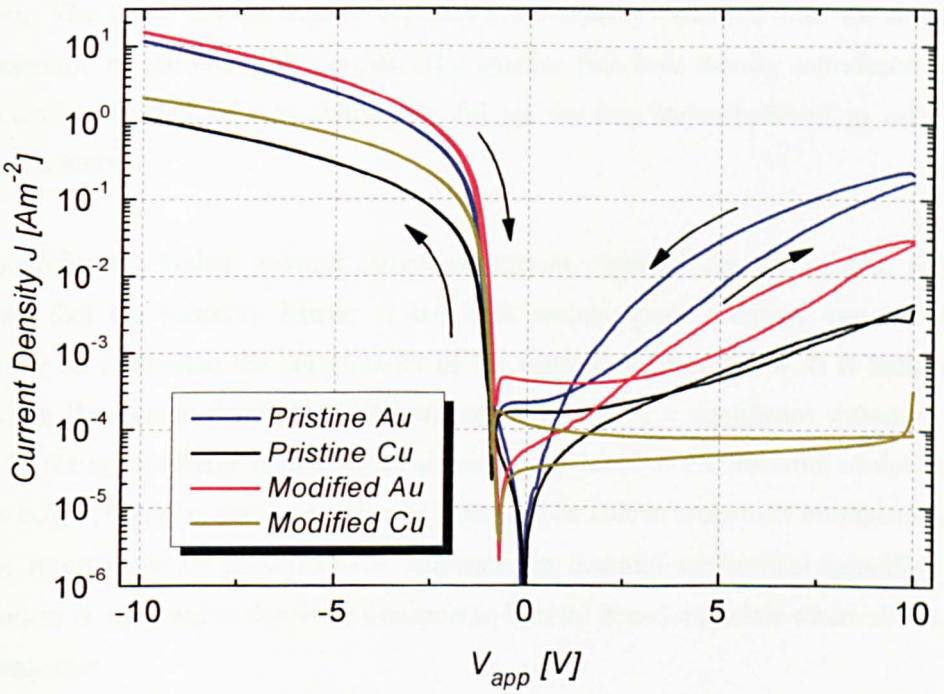

Figure 4.5.11: Current density against V_{app} for 0.5% doped Al-PTAA Schottky diodes with different metal electrodes and surface conditions. The much higher reverse currents are indicative of the increased dopant densities expected from the incorporation of DDQ molecules. The voltage was applied on the top aluminium electrode.

In the pristine Cu diode for example, the forward saturation current increased by almost 3 orders of magnitude thus leading to a rectification ratio of ~ 10^2. This is almost an order of magnitude larger than its undoped counterpart. The significant improvement in rectifying behaviour is caused in particular by the much larger gain in forward current compared to the reverse current. Increase in current flow through doped p-type organic diodes is expected as additional carriers from the dopant molecules obey Pauli Exclusion Principle and rapidly fill

up lower energy states with increasing doping. At lower energies, the localised states are much larger in number and therefore are less far apart. This makes it easier for carrier hopping to take place and hence support a much larger current through the semiconductor. The higher dopant density also prevents the occurrence of space charge effects in the semiconductor bulk as there are sufficient acceptor ions to screen the positive charge of the increasing hole concentration.

In general, much lower rectification ratios are obtained for the doped samples due to the reduced bulk resistance of the organic film. The modified Cu diode, however, manages to retain its rectification ratio of ~ 10^4 due to the significantly lower reverse current. This is believed to be associated with the fact that a large proportion of the dopants added remain inactive. The lower dopant density explains the similarity observed with the reverse *J-V* characteristic of the undoped samples. The smaller free hole density introduced into the polytriarylamine film fails to completely fill up the trap states believed to exist in the intrinsic material.

The significantly higher forward saturation current obtained for the pristine Cu diode suggests that the Schottky barrier at the back metal/organic interface can be partially overcome by increasing the conductivity of the organic semiconductor. It is believed that increasing the dopant density in the semiconductor causes a significant reduction in the width of the space charge region which consequently leads to the lowering of the effective barrier height. So an increasing number of holes will be able to cross over into the metal. The current, however, is not expected to be influenced by quantum mechanical tunnelling as this mechanism is only said to dominate transport in heavily doped materials where the barrier is extremely thin.

A value for the energetic distribution of localised states may be determined directly from the slope of the exponential current regime. For doped PTAA diodes, the value of T_c is found to lie in the range of 500 - 600K which is slightly smaller compared to the pure PTAA Schottky diode. The higher than expected T_c value obtained suggests that the density of states consist of a combination of intrinsic and extrinsic states.

The non-saturation of the reverse current seen in most of the diodes results from the filling up of trap states by the additional free carriers contributed by the dopant molecules. The quasi Fermi level is thus no longer pinned and the Schottky barrier is effectively lowered by a space charge region which expands with increasing positive bias being applied on the Al electrode. For analysis, consider the experimental plot of reverse current density against $V^{0.25}$

of the modified Au diode as in *figure 4.5.12*. Interestingly, the diode is found to quite accurately obey the ¼ power law with the incorporation of DDQ. At applied voltages above 1V, the dopant density for the doped PTAA film is calculated to be ~ 9.3×10^{17} cm^{-3}.

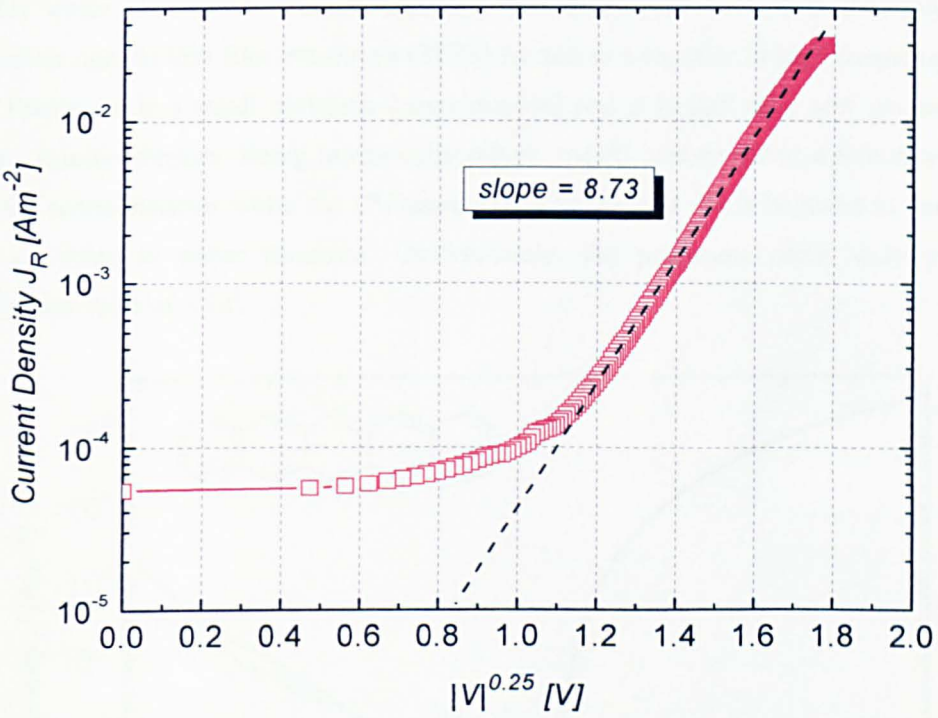

Figure 4.5.12: J_R against $|V|^{0.25}$ for the 0.5% doped Al-PTAA Schottky diode with PFBT modified Au electrode. The deviation observed at low voltages is believed to be due to the $(V_{bi} - V_{app} - kT_c/q)$ term. The slope yields a dopant density of ~9.3×10^{17} cm^{-3}.

4.6 ELECTRICAL CONDUCTION IN VACUUM-DEPOSITED PENTACENE

Figure 4.6.1 shows the semi-logarithmic current density voltage characteristic for a vertical Schottky diode with a layer of pentacene sandwiched between an Al and Au electrode on a Si/SiO_2 wafer. The vertical diode approach was employed since it is the only likely competitor against thin film transistors (TFTs) for use as a rectifier in high frequency RFID tags. Pentacene is a small molecule based material and it is part of a new generation of organic semiconductors. Being intrinsically p-type, the Al contact forms a Schottky barrier with the semiconductor while the UV/ozone (UV/O_3) cleaned Au is believed to permit the flow of holes in either direction. Unfortunately, the pentacene diode only yields a rectification ratio of ~ 10^2.

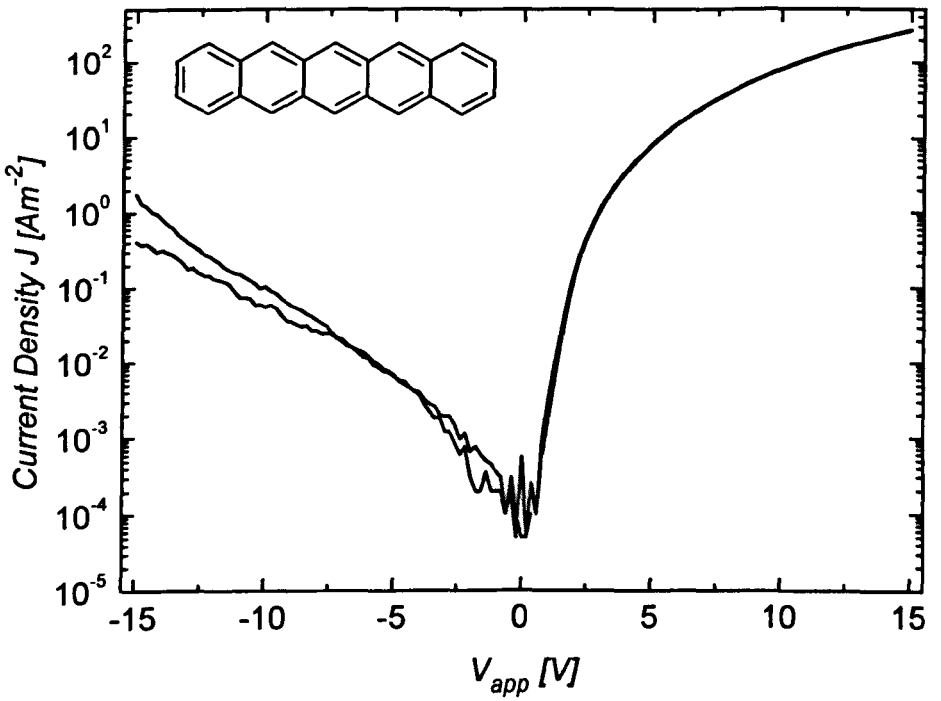

Figure 4.6.1: Current density voltage characteristic of UV/ozone cleaned Au-pentacene-Al vertical diode. The voltage was applied on the bottom gold electrode. The effective thickness of the pentacene film was calculated to be ~ 160 nm. Inset is a schematic illustration of the chemical structure of pentacene. The experimental data was provided by S. Steudel [5].

Despite its high work function, Au is widely reported to form a large hole injection barrier upon contact with most conjugated organic molecular materials including pentacene [34-36]. Hole injection from even a highly conductive polymer like poly(3,4-ethylenedioxythiophene)/poly(sytrenesulfonate) (PEDOT/PSS) has been found to be substantially more efficient than Au albeit both electrodes have similar work functions (~ 5

eV). The inefficiency of Au has been attributed to the adsorption of contaminants mainly hydrocarbon on the metal surface upon exposure to ambient atmosphere. The electron density tailing from the free surface into vacuum is pushed back into the solid upon adsorption thus reducing the surface dipole and effectively lowering the metal work function [37]. The extension of the electron density beyond a metal surface originates from the fact that an abrupt edge will require the application of an infinitely large electric field and this is impossible to achieve in practice. Hence the vacuum level outside the metal free surface is higher than its value at infinity representing the smaller but finite probability of finding an electron. It has been reported that the reduced work function of contaminated Au is more beneficial for hole injection in organic diodes than atomically clean Au [38]. Pristine Au is said to have a larger interface dipole and as a consequence, a larger hole injection barrier.

The oxidisation of the Au surface by UV/ozone treatment, however, has been reported to increase the metal work function. The higher work function is caused by Au oxide formation and surface-adsorbed carbon and oxygen species [39]. Through ultraviolet photoelectron spectroscopy (UPS) measurements, the AuO_x surface is reported to exhibit an air stable high work function ranging from about 5.25 - 5.5 eV [39, 40]. But more importantly, the hole injection barrier formed at the AuO_x/pentacene interface is reduced to ~ 0.25 eV from ~ 0.85 eV. The barrier at AuO_x/pentacene interface matches that of a conducting polymer/pentacene interface. The substantial reduction in hole injection barrier (~ 0.6 eV) suggests that the AuO_x/organic interface is in the Fermi level pinning regime. The contact made between a modified Au electrode and pentacene can therefore be considered as being essentially ohmic.

The pentacene layer was deposited at an extremely high deposition rate (~ $3 Å s^{-1}$) to achieve very small dense grains. At high deposition rates, the diffusion length of the organic molecules is very short which results in the formation of relatively small crystals. This prevents the occurrence of microscopic pinholes and inhomogeneities in the organic film.

In disordered organic semiconductors, the amorphous nature of the material results in a Gaussian shaped distribution of localised states which can be rather accurately approximated by an exponential function for small carrier concentrations. Small molecule organic semiconductors are however slightly different as they consist of individual arrays of small crystals which are separated from each other by narrow regions of amorphous material. The amorphous region is referred to as grain boundaries. The analysis of current flow in the pentacene Schottky diode is largely based on the analytical model developed by Eccleston for polycrystalline semiconductors [6].

Grain boundaries in small molecule based organic semiconductors are assumed to have a density of states (DOS) typical of disordered organic materials and it is thus given by

$$N(E)=\frac{N_0}{kT_c}\exp\left(\frac{E}{kT_c}\right) \qquad 4.6.1$$

where N_0 is the density of traps per unit volume, k is the Boltzmann constant, E is the energy and T_c is the characteristic temperature representing the energy distribution of traps. The appropriateness of using this model will become more apparent from comparison with experiments.

Like disordered materials, the trap levels below the Fermi level must be donor-like and acceptor-like in the top half of the energy gap. For convenience, the possibility of the traps being amphoteric is ignored. This configuration is believed to pin the Fermi level close to the centre of the gap thus preserving the intrinsic properties of the material at the grain boundaries. In the grain centre, however, the movement of the Fermi level is unrestricted. Hence, the Fermi level moves closer to the HOMO level reflecting the increasing hole density as shown in *figure 4.6.2*. A HOMO level is defined in the grain as it is expected to have electronic properties similar to that of single crystals.

The requirement that the material have the same ionisation potential leads to the assumption that a transport level with an abrupt edge must exist in the grain boundaries. The transport level is simply an arbitrary energy level capable of supporting a similar current to that of an exponential DOS under thermal equilibrium conditions. The HOMO and transport level at adjacent edges of the grain and grain boundary must be continuous. It is worth noting that the use of a transport level limits the model to small carrier concentrations. The concentration of holes at the edge of each grain is dictated by the position of the Fermi level. The extent of the dip of the HOMO level is dependent on the relative size of the effective Debye length and the grain. The effective Debye length in the grain is given by

$$L_{De}=\left[\frac{kT\varepsilon_0\varepsilon_g}{q^2p(x)}\right] \qquad 4.6.2$$

where k is the Boltzmann constant, T is the absolute temperature, q is the electronic charge, ε_0 is the permittivity of free space, ε_g is the dielectric constant of the grain and $p(x)$ is the hole density at the grain centre. The shape of the HOMO level for a semi-infinite grain is also shown in *figure 4.6.2*. The HOMO level will coincide with that of single crystals at infinity. Large potential barriers exist at the grain boundaries. The size of the grain boundaries

relative to the grain is slightly exaggerated in *figure 4.6.2*. In the model, the uniform columnar grain boundaries are assumed to be much smaller in size compared to the grains and therefore the potential drop across the grain boundaries is negligible. In practice the size of the grains will vary but in this model, it is assumed to be of equal sizes of *2a*.

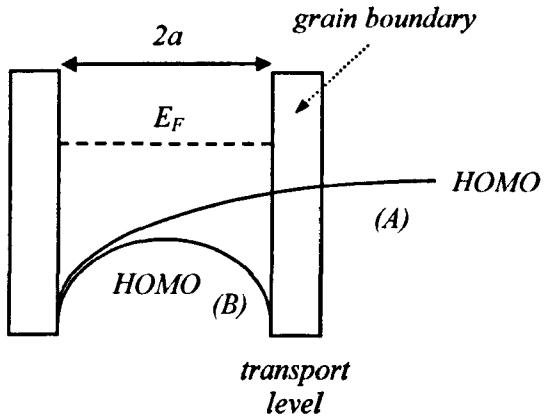

Figure 4.6.2: The variation of the HOMO level for (A) a semi infinite grain and (B) a small grain between two grain boundaries with no applied field. The HOMO level for (A) will reach that of a single crystal material at infinity. In (B), the HOMO level reaches a maximum midway between the two grain boundaries where the density of holes is the highest. A flat quasi Fermi level is assumed indicating that the carriers in the grain are in thermal equilibrium.

The motion of carriers in any given semiconductor may be described through drift and diffusion. *Figure 4.6.3* shows the energy diagram for a quasi-diffusion model. At low voltages, the energy difference between the HOMO level maximum and the Fermi level changes between adjacent grains but there is no net potential drop between adjacent grain boundaries. The carrier density at the centre of the grain reduces progressively with increasing distance due to the potential barrier at the grain boundaries. The decreasing hole density at grain centres is reflected by the increasing distance of the Fermi level relative to the HOMO level maximum. The resulting concentration gradient closely resembles that of classic diffusion but the mechanism is not termed the same since the carriers do not vary linearly with distance.

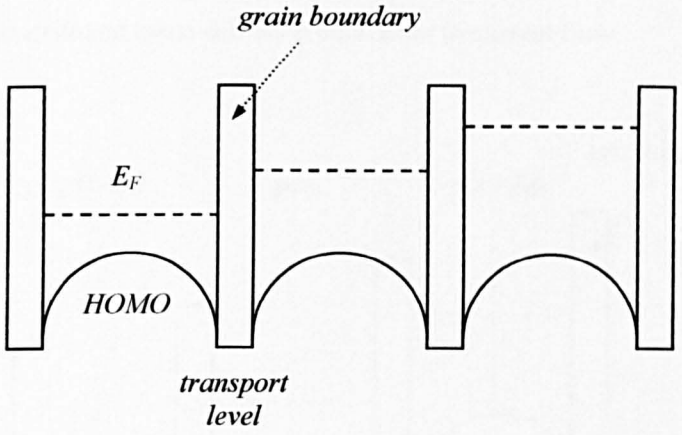

Figure 4.6.3: In the quasi-diffusion model, the HOMO level remains the same but the Fermi level changes between adjacent grains relative to the HOMO level. The hole concentration at the grain centres thus fall with increasing distance.

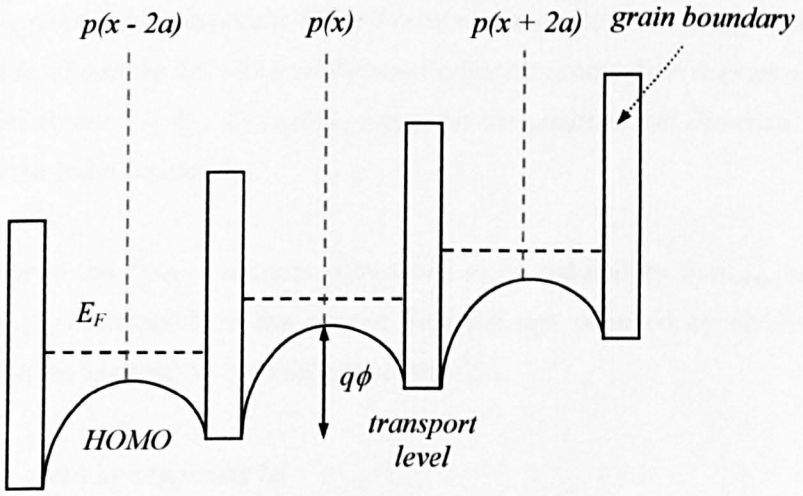

Figure 4.6.4: Energy band diagram for the quasi-drift model. The potential barrier at the grain boundary is progressively lowered thus causing the hole concentration at the grain centres to remain the same.

At increasing applied voltages, there will be a net potential drop between adjacent grains but the Fermi level remains the same with respect to the HOMO level maximum. This is akin to drift as illustrated in *figure 4.6.4*. Again this is termed as quasi-drift as charge transport occurs across a series of grain boundaries. The hole density at the grain centres is constant as the potential barrier at the grain boundary is progressively lowered by the externally applied

field *i.e.* $p(x-2a) = p(x) = p(x+2a)$. *Figure 4.6.5* shows the energy diagram for the general case where both quasi-drift and quasi-diffusion contribute to current flow.

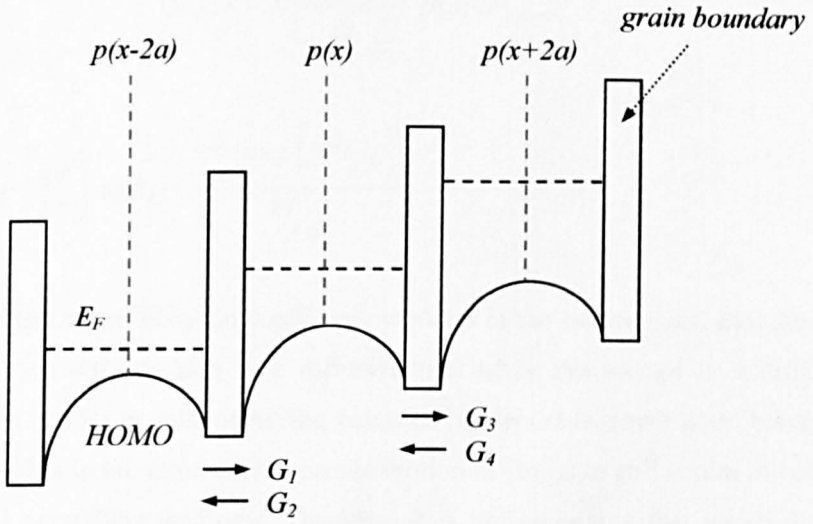

Figure 4.6.5: Energy diagram when both quasi-diffusion and quasi-drift contribute to current flow. The applied field reduces the HOMO level maxima while the energy difference between the Fermi level and the HOMO level between adjacent grains decreases as a result of the diffusion component. G_1, G_2, G_3 and G_4 represent the position and direction of the carrier flux across the grain boundaries.

The potential barrier to the flow of carriers is assumed to be reduced by $2aF_{xmean}$ at each grain boundary. F_{xmean} corresponds to the electric field strength obtained by dividing the voltage falling across the material by the thickness of the film.

The flux at x is thus given by *(Appendix H)*

$$G(x) = 8av\,p(x)\exp-\frac{q\phi}{kT}\left[\sinh\frac{qaF_{xmean}}{kT}\right]-8a^2v\frac{\partial p}{\partial x}\exp-\frac{q\phi}{kT}\left[\cosh\frac{qaF_{xmean}}{kT}\right] \quad 4.6.3$$

where v is the frequency of holes crossing a grain boundary, $p(x)$ is the density of holes at the grain centre and ϕ corresponds to the potential barrier at the grain boundary relative to the centre of the grain in the absence of an applied field. The flux of holes across a particular grain boundary is assumed to be proportional to the hole density in the grain adjacent to the barrier.

When the electric field is small or the grain size is large such that $F_{xmean} \leq kT/qa$, *equation 4.6.3* may be simplified to

$$G(x) = -D\left[\frac{dp(x)}{dx}\right] + p(x)\mu F_{xmean} \qquad 4.6.4$$

where $D = a^2 v \exp\left(\frac{q\phi}{kT}\right)$ and $\mu = \frac{a^2 v \exp\left(q\phi/kT\right)}{kT/q}$.

Here D represents the quasi-diffusion coefficient whilst μ is the carrier quasi-mobility. The first term in *equation 4.6.4* is akin to a diffusive flux while the second to a drift flux. *Equation 4.6.4* tells us that in spite of having potential barriers at adjacent grain boundaries limiting the carrier flux in the grain centre, carrier motion in the grain still comes out closely resembling that of crystalline materials. Therefore it is not surprising that combining the relationships obtained for D and μ leads to the Einstein Relationship.

$$D = \frac{\mu kT}{q} \qquad 4.6.5$$

Being able to derive *equation 4.6.5* suggests that the concepts of quasi-drift and quasi-diffusion are appropriate for describing carrier motion within the grains. It should be noted, however, that both D and μ show an exponential dependence on the potential barrier at the grain boundary.

The hole flux $G(x)$ is related to the hole concentration and the gradient of the Fermi level and is thus given by

$$G(x) \propto p(x)\frac{d\xi}{dx} \qquad 4.6.6$$

where $d\xi/dx$ is the gradient of the Fermi level. For a given flux, the gradient of the Fermi level should increase as the hole concentration falls at the grain boundary. This effect is considered to be negligible and therefore ignored in the analysis. But it may contribute to the effective lowering of the barrier at the edge of the grains.

In disordered materials, charge transport occurs via thermally assisted tunnelling (*i.e.* hopping) between localised energy states. Transport in small molecule organic solids, however, is significantly different since the material consists of crystalline-like regions called grains and grain boundaries which are amorphous in nature. In the above analysis,

carrier flux in the grain centres is demonstrated to resemble that of crystalline materials but with different temperature dependencies. This property is unique to the grain and cannot be extended to the adjacent grain boundaries where large densities of traps are assumed to exist. For algebraic convenience, the wide energetic distribution of traps in the grain boundaries is described by an exponential function.

When an external field is applied, the potential variation at the grain boundary will determine the effective barrier seen by carriers in the adjacent grain. Hence, the concentration of carriers able to participate in current flow will depend on the position of the Fermi level relative to the edge of the grain. Carrier motion is therefore essentially controlled by the energetic distribution of traps in the grain boundaries and so is the current through the diode.

In crystalline semiconductors, the motion of carriers is traditionally described by a unique mobility term. This practice is widely accepted since charge carriers generally occupy the high density of states available at the conduction/valence band edge and as a result have a similar effective mass. In disordered organic semiconductors, however, carriers are distributed across a wide range of energies which makes the concept of mobility a poor one. Due to the non-uniform distribution of energy states, carriers at different energies are expected to experience different hopping rates. In *chapter 2*, it was demonstrated that for an exponential density of states, the so-called effective mobility is related to the carrier concentration via a power law similar to that given by the Universal Mobility Law (UML). The concept of carrier mobility can therefore be completely excluded in materials with an exponential DOS by incorporating the UML into the drift current equation as follows:

$$J = Kqp^{m+1}F \qquad 4.6.7$$

Here J is the current density, p is the density of holes, m is the temperature and material dependent exponent and F is the electric field. *Equation 4.6.7* essentially says that an increment in carrier density will result in a significant enhancement in current transport. It is worth noting is that no account was taken of the carrier transport mechanism when developing the UML. The generalised treatment of the problem allows the concept to be used on a wide range of materials and under various conditions.

In Schottky diodes, when a metal is contacted with a semiconductor, the energy levels close to the interface will bend due to the work function difference between the two materials. For a small molecule organic semiconductor, the plane corresponding to the potential barrier may lie anywhere within the grain or the grain boundary. But having said that, it will most

likely be located within the grain since the grain is much wider compared to the grain boundary. Fortunately, irrespective of the position of the potential barrier within the material, the barrier is believed to be controlled by the density of traps in the grain boundary. So despite the crystalline-like charge transport predicted in the grains, the current voltage characteristic of Schottky diodes will be typical of disordered organic semiconductors. Nevertheless, carriers attracted towards the Schottky interface by the external field are believed to move along the grain centres rather than over the grain boundaries. Recognising that *equation 4.6.7* is applicable for any material with an exponential DOS, it is used to analyse current flow through the pentacene diode.

From *figure 4.6.1*, a sharp rise in current with applied bias is observed in the reverse direction. The reverse current increases by over 4 orders of magnitude which is even larger than that observed in the as-synthesised P3HT diode. Hence a much higher dopant density is predicted for the pentacene film. The rise in current is believed to result from the lowering of the Schottky barrier by a combination of the electric field in the space charge region and the image force effect. The reverse current density must thus obey the simplified Schottky theory given by

$$J_R = J_0 \exp\left[\frac{q}{kT}\left(\frac{q^3 N_A\left(V_{app} - V_{bi} - kT/q\right)}{8\pi^2 \varepsilon_0^{\,3} \varepsilon_s \varepsilon_\infty^{\,2}}\right)^{1/4}\right] \qquad 4.6.8$$

where J_0 is a constant, k is the Boltzmann constant and T is the absolute temperature. *Figure 4.6.6* shows the experimental plot of reverse current density against $V^{0.25}$ for the vacuum-deposited pentacene Schottky diode.

The straight line fit obtained at voltages above 1V suggests a close agreement with *equation 4.6.8*. The theory assumes a uniform distribution of dopant ions in the space charge region. From *figure 4.6.6*, a slope of 6.95 corresponding to an acceptor ion concentration N_A of $3.75\times10^{17}\,cm^{-3}$ is obtained. As predicted, this dopant density value is about an order of magnitude larger compared to as-synthesised P3HT. The high dopant density determined in P3HT was attributed to the presence of residual dopants from the synthesis process. With pentacene, the material purchased from Fluka was further purified by gradient sublimation at 100 mTorr under forming gas (96% N_2, 4% H_2). In addition, the *I-V* measurement was carried out in a nitrogen glovebox. Hence, the unintentional doping of the pentacene film could have only occurred during the thermal evaporation process.

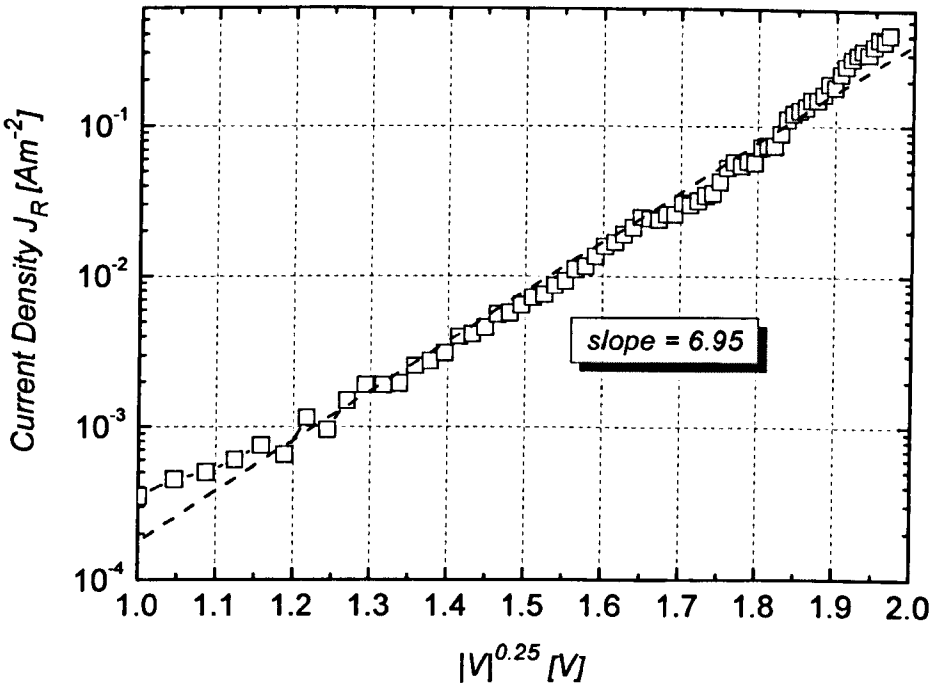

Figure 4.6.6: Semi-logarithmic J_R against $|V|^{0.25}$ plot for the modified Au-Pentacene-Al vertical diode. The dopant density calculated from the slope is 3.75×10^{17} cm^{-3}.

When a positive voltage is applied on the gold electrode, the potential barrier for holes is significantly reduced. The exponential rise in current is attributed to the exponential decline in carrier occupancy given by the Maxwell Boltzmann approximation of the Fermi Dirac statistics. In small molecule organic semiconductors, an exponential distribution of traps is assumed to exist in the grain boundaries. Hence, most of the injected carriers are expected to become trapped in the grain boundaries as a result of the large density of traps. The amount of trapping taking place in the grain boundary will control the hole concentration in the neighbouring grain. The density of holes getting across the top of the Schottky barrier is therefore essentially limited by trapping effects at the grain boundary. With an increasing density of trapped holes, the energy difference between the Fermi level and the grain edge will become smaller. Like in disordered materials, a transport level is defined in the grain boundaries to represent the exponential density of trapped carriers which is believed to control the current across the barrier.

Hence, integrating from the top of the barrier (*i.e. transport level)* to infinity gives the following current density.

$$J \alpha \frac{N_0 T_0}{T_c} \exp\left(\frac{E_F}{kT}\right) \exp - \left(\frac{E_B}{kT_0}\right) \exp\left(\frac{qV_{app}}{kT_0}\right) \qquad 4.6.9$$

Here E_F is the Fermi level, E_B is the energy at the top of the barrier, V_{app} is the applied voltage and T_0 is the characteristic temperature defining the exponential distribution of trapped holes.

Equation 4.6.9 can be simplified to

$$J \alpha \exp\left(\frac{qV_{app}}{kT_0}\right) \qquad 4.6.10$$

Figure 4.6.7 shows the forward *J-V* characteristic for the vacuum-deposited pentacene diode. Interestingly, the exponential part of the experimental plot accurately obeys *equation 4.6.10* with the slope giving a value of T_0 equal to ~ 2206 K. This is believed to describe the intrinsic carrier distribution since dopant states are too high in energy to contribute to current flow. It must be said that this value of T_0 is relatively large compared to those calculated for as-synthesised P3HT and PTAA. This suggests that the trapped holes supporting the exponential current come from ~ $7kT$ of the transport level. The corresponding value of T_c is estimated to be ~ 347 K. This subsequently gives a Meyer Neldel energy and m of 30 meV and 0.16 respectively. The ideality factor η for the Al-pentacene diode is ~ 7.4. The large value of η is believed to be associated with the structural inhomogeneties inherent to small molecule organic semiconductors.

As the voltage across the diode is increased, a higher fraction of the potential falls across the semiconductor bulk and the current starts to strongly deviate from *equation 4.6.10*. The current is hence no longer limited by the concentration of holes getting across the Schottky barrier but rather by the series resistance of the semiconductor bulk as the modified Au/organic interface is deemed to be essentially ohmic. The potential falling across the neutral region is determined by measuring the voltage deviation along the x-axis for each of the measured forward currents as illustrated in *figure 4.6.7*.

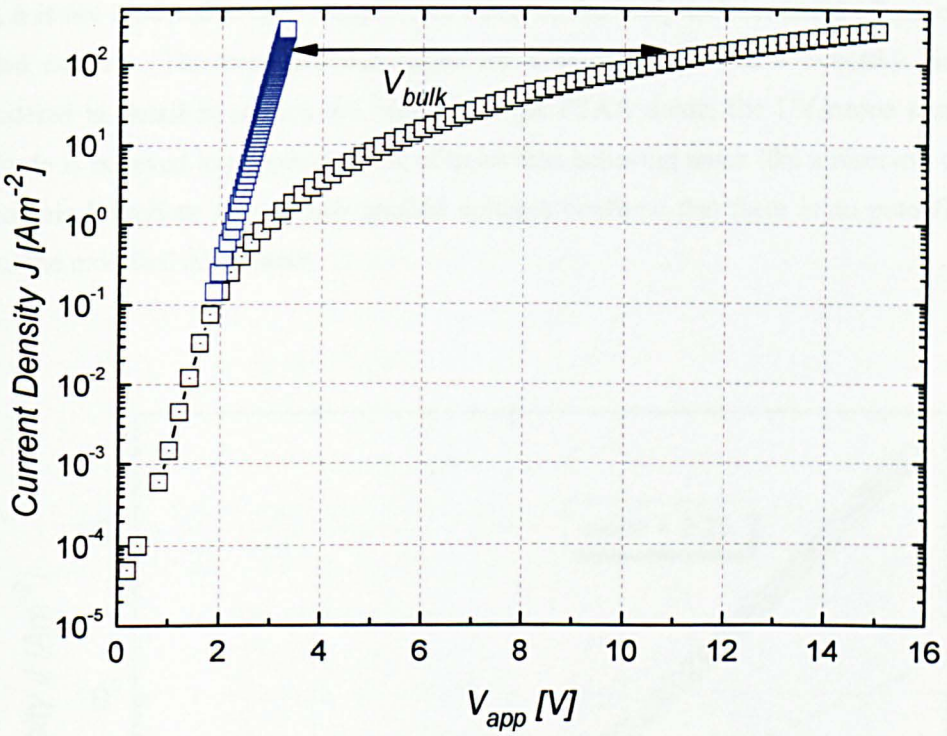

Figure 4.6.7: Forward J-V characteristic for the modified Au-Pentacene-Al diode. At higher applied voltages, only a small fraction of the potential falls across the barrier and the space charge region. The potential drop for each of the measured current level can be determined from the straight line fit of the exponential region.

Figure 4.6.8 shows the experimental plot of the forward current density against bulk voltage for the vertical Al-pentacene diode. Provided there is no potential drop across the Au electrode, the neutral region is expected to exhibit either ohmic or space charge limited behaviour. At low applied voltages, the double logarithmic plot gives a slope of ~ 1.01. This is in close agreement with the theoretical value of 1 expected for materials obeying Ohm's law. The ohmic region, however, is only accurately obeyed for a small voltage range and thereafter the current begins to rise sharply with further increase in applied voltage. The slope at higher applied voltages is estimated to be ~ 2.25, which corresponds to space charge limited conduction. Despite having a much larger dopant density than even as-synthesised P3HT, space charge effects appear to dominate conduction in pentacene at high applied fields. The departure from Ohm's law is attributed to the trapping of a large concentration of carriers at the grain boundaries. The constant positive space charge created by holes trapped in the grain boundaries is believed to be only partially screened by the fixed ionised dopant ions and consequently leads to a non-linearly varying electric field.

Although the boundary conditions in a Schottky diode differ slightly from the conventional case, it is not expected to have a significant effect on the analytical treatment of space charge limited currents. The boundary conditions for a neutral region of a Schottky diode are considered in detail in *section 4.5*. Similar to the PTAA diode, the UV/ozone treated Au electrode is believed to permit the flow of holes thus behaving much like a reservoir contact. The ohmic behaviour seen at low applied voltages confirms that there is no potential drop across the modified Au contact.

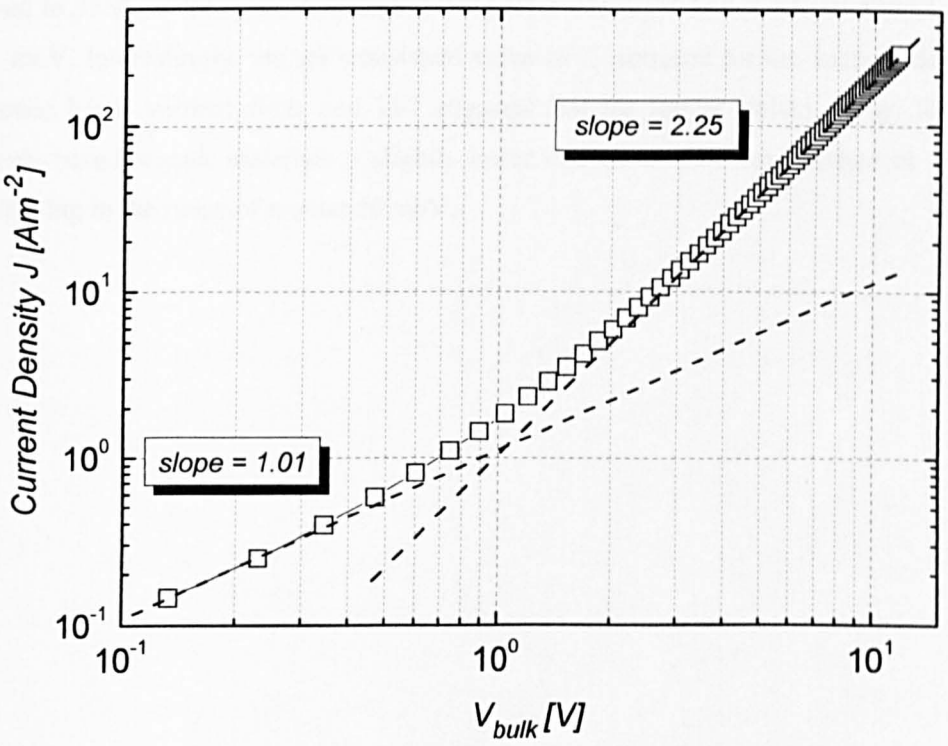

Figure 4.6.8: Current density against bulk voltage for UV/ozone cleaned Au-Pentacene-Al diode. Slopes of ~ 1.01 and 2.25 are obtained at low and high applied voltages respectively. The space charge effects are believed to be caused by the high density of holes trapped in the grain boundaries of the pentacene film.

In this model, the grain boundaries are assumed to control current flow through the diode and since the boundaries are amorphous in nature, the current voltage relation is expected to obey the newly developed SCL current equation. As discussed earlier, the UML used to develop the SCL current equation is not confined to only disordered semiconductors. In fact the concept is more universal as it is applicable to any material having an exponential density of states. Hence the space charge limited transport observed in the pentacene film is best

described by the modified current voltage dependence. According to the new SCLC model, a slope of ~ 2.25 corresponds to a value of m equal to ~ 0.25. This gives a T_c value of ~ 375 K and a Meyer Neldel energy of 32 meV. This means that the trap levels at higher energies are also part of the intrinsic distribution of states. The dopant states must therefore lie within the grains.

The self-consistent values of T_c and T_0 obtained from the exponential and saturation part of the forward *J-V* characteristic gives confidence in the validity of the analytical model used. Previously, the analytical modelling of a vacuum-deposited pentacene TFT gave a value of T_c equal to 365K in the quasi-drift regime [41]. This corresponds to a Meyer Neldel energy of 31 meV. Interestingly, the self-consistent value of T_c obtained for the vacuum-deposited pentacene based vertical diode and TFT suggests that the Meyer Neldel energy for small molecule based organic materials is slightly lower than disordered semiconductors with the former lying in the range of around 30 meV.

4.7 CONCLUSIONS

Organic semiconductors are promising candidates for producing low cost, large area electronic circuits. Recently, small molecule organic materials particularly TIPS-pentacene demonstrated field effect mobilities greater than 1 $cm^2V^{-1}s^{-1}$ thereby increasing the likelihood of making high frequency organic RFID tags [42]. The study of Schottky diodes is deemed important since it is one of the competing approaches for making organic rectifiers in RFID circuits. Special attention is given to the saturation region of diodes since high currents are needed to satisfy the demands of the circuit.

Schottky diodes made with high purity polytriarylamine (PTAA) as the active material are studied. A layer of pentafluorobenzenethiol (PFBT) is deposited onto the Au electrode to reduce the potential barrier for the injection of holes. The self-assembled monolayer (SAM) of PFBT is reported to increase the work function of the metal by over 1 eV. The modified Au electrode is thus believed to make an ohmic contact with PTAA. The modified Au-PTAA-Al diodes give a rectification ratio of ~ 10^8 and 10^6 when processed from xylene and dichlorobenzene (DCB) respectively. The extremely low off currents obtained makes the diodes ideal for low current circuit operations.

The reverse current of the PTAA diode processed from dichlorobenzene saturates with increasing applied bias and therefore does not obey the $V^{0.25}$ law. This anomaly is attributed to the presence of traps in the semiconductor which is believed to pin the Fermi level and consequently restrict the space charge region from extending further with increasing bias. In addition, the exponential current in the forward characteristic does not give the expected T_0 and T_c values. The values of T_0 and T_c were estimated to be ~ 481K and 799K respectively. It is believed that an exponential distribution of extrinsic states exists at lower energies which when combined with the intrinsic DOS yields a significantly larger T_c value. The extrinsic states probably result from the formation of a non-ideal Schottky metal/organic interface.

With further increase in applied voltage, the forward current saturates as only a small fraction of the potential falls across the barrier and the space charge region. From a double logarithmic plot of J against V_{bulk}, a slope of ~ 0.98 and 2.56 was obtained at low and high voltages respectively. A value close to 1 obtained at low applied fields suggests that the current voltage relationship obeys Ohm's law. The current, however, changes from being ohmic to space charge limited with increasing bias. Space charge effects are observed in PTAA as the material is believed to contain far less quantities of dopant. The amount of dopant ions present is insufficient to compensate the increasing hole concentration in the

semiconductor bulk. The boundary conditions for space charge limited current in the neutral region of a diode are slightly different to those stated in the classical treatment of the theory. In the PTAA diode for instance, the neutral region is sandwiched between a space charge region and a modified Au electrode. The potential falling across the space charge region is thought to be sufficient to get holes exiting the neutral region across the barrier and therefore support the SCL current. By comparing with a p-n junction, it is believed that a flat quasi Fermi level can also be assumed in the space charge region of a Schottky diode.

A new space charge limited current (SCLC) expression is developed for disordered organic material as the practice of assigning a unique mobility term to carriers which are widely distributed in energy is deemed inappropriate. Applying the new SCLC to the PTAA diode gave a value for m equal to ~ 0.56. Hence a T_c corresponding to ~ 468K and a Meyer Neldel energy of ~ 40 meV was obtained. This result suggests that the localised states at higher energies are also part of the intrinsic density of states. The absence of dopant states in polytriarylamine is in agreement with the notion that PTAA is a much purer semiconductor than its predecessor poly(3-hexylthiophene).

The effect of changing the back metal/organic interface on the saturation current region is also studied. Although the metal work function is expected to increase by over 1 eV upon treatment with PFBT, the modified Cu electrode incidentally forms a Schottky barrier with PTAA. Besides the modified Au-PTAA-Al diode, the rest of the samples are essentially pairs of back-to-back diodes. This configuration however has negligible effect on the reverse J-V characteristics of the diodes because the back metal/organic interface is then forward biased. Due to the potential drop across the back metal/organic interface, the J-V characteristics can no longer be analysed in terms of a regional model. The experimental J against V_{bulk} plot of these diodes do not yield slopes which are consistent with either purely ohmic or space charge limited conduction. In general, doping polytriarylamine with DDQ results in higher current levels. The improvement in conductivity is, however, accompanied by a significant reduction in the rectifying property of the diodes. The significant rise in reverse currents reflects the increased dopant density in the organic films. The additional carriers contributed by the dopants are expected to obey Pauli Exclusion Principle and rapidly fill up lower energy states. In contrast to the undoped samples, these diodes have reverse currents which do not saturate with increasing bias. This suggests that the devices are no longer affected by Fermi level pinning as the trap states are filled by additional free carriers contributed by the dopant molecules. In addition, the experimental J-V_{bulk} curves at higher applied voltages yield slopes of less than 2 which suggest that the neutral region is no longer dominated by space charge effects.

Interestingly, the *J-V* characteristic of a vacuum-deposited pentacene diode sandwiched between an Al and UV/ozone cleaned Au electrode fits the analytical model developed for disordered organic semiconductors. The oxidation of pristine Au surfaces by UV/O_3 treatment is said to increase the metal work function to ~ 5.5 eV thereby reducing the barrier at the AuO_x/pentacene interface to only ~ 0.25 eV. Pentacene is a small molecule organic solid akin to inorganic polycrystalline material. Analysis of current flow in the pentacene diode is extensively based on the model developed by Eccleston [6]. The boundary regions separating the individual arrays of small molecules are considered to be highly amorphous and are consequently described by an exponentially rising density of traps. The traps pin the Fermi level close to the centre of the energy gap thus causing potential barriers to form at the grain edges.

An arbitrary energy level with an abrupt edge capable of supporting a current equal to the exponential DOS under thermal equilibrium conditions is defined in the grain boundary. It is called the transport level. The transport level has to be continuous with the HOMO level so that carriers in the grain and grain boundary have similar ionisation potentials. Despite the potential barrier at the grain boundaries, transport through the grains is found to closely resemble that of crystalline solids. The diffusion coefficient D and the mobility μ of carriers in the grain were found to be strongly dependent on the potential barrier at the edge of the grain. The parameters also demonstrate distinctly different temperature dependencies. Nevertheless, due to the high density of trapping in the grain boundaries, current through the diode is believed to be controlled by the exponential distribution of traps similar to disordered organic solids. Fortunately, the generalised treatment used in developing the Universal Mobility Law (UML) makes the concept applicable to any exponential density of states. The model merely states that in a system where the carriers are distributed in energy, the so-called effective mobility will demonstrate a strong dependence on carrier density.

The Al-pentacene vertical diode only gives a rectification ratio of $\sim 10^2$. The reverse current of the Al-pentacene diode obeys the simplified Schottky theory and hence yields a dopant density of ~ 3.75×10^{17} cm^{-3}. In the forward direction, a value of T_0 equal to ~ 2206K was calculated directly from the slope of the exponential current region. This gave a value of T_c equal to ~ 347K and a corresponding Meyer Neldel energy of ~ 30 meV. This result suggests that the trap levels at lower energies belong to the intrinsic DOS. With further increase in positive bias on the Al electrode, the current saturates as most of the potential is dropped across the semiconductor bulk. Like the PTAA diode, the experimental plot of J against V_{bulk} yields a slope of ~ 1.01 and 2.25 at low and high voltages respectively. Again, a build up of

positive charges in the neutral region of the diode results in space charge effects dominating current flow. The slope of about 2.25 gave a value of m equal to ~ 0.25 and hence a T_c of ~ 375K. The Meyer Neldel energy was calculated to be ~ 32 meV. The values of T_c determined from the exponential and saturation current regimes only differ by about 10%. The self-consistent value of T_c suggests that the analytical model is also applicable to small molecule organic semiconductors.

Although the doping density estimated for the pentacene film is over an order of magnitude larger than that of as-synthesised P3HT, the intrinsic value of T_c determined from the saturation regime suggests the absence of dopant states. The dopant states are therefore speculated to lie within the grains since the *J-V* curve only allows the density of states in the grain boundaries to be analysed. But despite this high doping density, the vacuum-deposited pentacene still demonstrates space charge effects. This is attributed to the trapping of large numbers of free carriers in the grain boundaries. The trapped carriers produce a constant positive charge which in turn creates a non-linearly varying electric field in the semiconductor bulk.

Previously, the modelling of a vacuum-deposited pentacene TFT gave a value of T_c equal to ~ 365K in the quasi-drift regime [41]. This is consistent with a Meyer Neldel energy of ~ 31 meV. The self-consistent Meyer Neldel energy obtained for vacuum-deposited pentacene based diode and TFT suggests that small molecule based organic semiconductors may be characterised by an energy close to 30 meV. Meanwhile, the corresponding energy characteristic of crystalline and disordered semiconductors are 26 meV and around 33 - 40 meV respectively.

4.8 REFERENCES

[1] K. Finkenzeller, *"RFID Handbook"* Vol. 1, Wiley, New York, 2002.

[2] S. F. Nelson, Y. –Y Lin, D. J. Gundlach and T. N. Jackson, *App. Phys. Lett.* **72**, 1854, 1998.

[3] D. J. Gundlach, Y. –Y. Lin, T. N. Jackson and D. G. Schlom, *Appl. Phys. Lett.***71**, 3853, 1997.

[4] S. K. Park, C. –C. Kuo, J. E. Anthony and T. N. Jackson, *IEDM Tech. Dig.* 113-116, 2005.

[5] S. Steudel, K. Myny, V. Arkhipov, C. Steibel, S. De Vusser, J. Genoe and P. Heremans, *Nature Mater.* **4**, 597, 2005.

[6] W. Eccleston, *IEEE Trans. Electron Devices* **53**, 474, 2006.

[7] A. Rose, *Phys. Rev.* **97**, 1538, 1955.

[8] M. A. Lampert and P. Mark, *Phys. Rev.* **103**, 1648, 1956.

[9] M. A. Lampert and P. Mark, *"Current Injection in Solids"*, Academic Press, New York, 1970.

[10] N. F. Mott and R. W. Gurney, *"Electronic Processes in Ionic Crystals"*, Clarendon Press, Oxford, 1940.

[11] M. C. J. M. Vissenberg and M. Matters, *Phys. Rev. B* **57**, 12964, 1998.

[12] A.R. Brown, C. P. Jarrett, D. M. de Leeuw and M. Matters, *Synth. Met.* **88**, 37, 1997.

[13] P. Mark and W. Helfrich, *J. Appl. Phys.* **33**, 205, 1962.

[14] D. J. Gundlach, L. Jia and T. N. Jackson, *IEEE Electron Devices Lett.* **22**, 571, 2001.

[15] J. F. Chang, B. Sun, D. W. Breiby, M. N. Nielsen, T. I. Sölling, M. Giles, I. McCulloch and H. Sirringhaus, *Chem. Mater.* **16**, 4772, 2004.

[16] D. M. Taylor and H. L. Gomes, *J. Phys. D: Appl. Phys.* **28**, 2554, 1995.

[17] M. Raja, G. C. R. Lloyd, N. Sedghi, W. Eccleston, R. Di Lucrezia and S. J. Higgins, *J. Appl. Phys.* **92**, 1441, 2002.

[18] J. Nowaczyk, W. Czerwiński and E. Olewnik, *Polymer Degradation and Stability* **91**, 2022, 2006.

[19] A. Vollmer, H. Weiss, S. Rentenberger, I. Salzmann, J. P. Rabe and N. Koch, *Surface Sci.* **600**, 4004, 2006.

[20] M. L. Chabinyc, R. A. Street and J. E. Northrup, *App. Phys. Lett.* **90**, 123508, 2007.

[21] M. Raja, *Phd Thesis*, University of Liverpool, 2004.

[22] H. L. Gomez, G. W. Jones and D. M. Taylor, *Synth. Met.* **85**, 1351, 1997.

[23] M. Raja, N. Sedghi, S. Badriya, S. J. Higgins, G. C. R. Lloyd and W. Eccleston, *ESSDERC Proc.*, 253-256, 2005.

[24] I. Musa, S. J. Higgins and W. Eccleston, *J. Appl. Phys.* **83**, 5558, 1998.

[25] I. Musa, S. J. Higgins and W. Eccleston, *J. Appl. Phys.* **81**, 2288, 1997.

[26] V. R. Nikitenko, H. Heil and H. von Senggem, *J. Appl. Phys.* **94**, 2480, 2003.

[27] G. C. R. Lloyd *(private communication).*

[28] A. K. Jonscher, "*Principles of Semiconductor Device Operation*", G. Bell & Sons Ltd., 1960.

[29] H. C. F. Martens, P. W. M. Blom and H. F. M. Schoo, *Phys. Rev. B* **61**, 7489, 2000.

[30] M. Raja, D. Donaghy, G. C. R. Lloyd, S. Badriya, S. J. Higgins and W. Eccleston, *Proc. SPIE* **5464**, 382, 2004.

[31] W. F. Pasveer, J. Cottaar, C. Tanase, R. Coehoorn, P. A. Bobbert, P. W. M. Blom, D. M. de Leeuw and M. A. J. Michels, *Phys. Rev. Lett.* **94**, 206601, 2005.

[32] K. C. Kao and W. Hwang, *"Electrical Transport in Solids"*, International Series in the Science of the Solid State, Vol. 14, Pergamon Press, 1981.

[33] G. C. R. Lloyd *(private communication).*

[34] N. Koch, A. Kahn, J. Ghijsen, J.-J. Pireaux, J. Schwartz, R. L. Johnson and A. Elschner, *App. Phys. Lett.* **82**, 70, 2003.

[35] N. Koch, A. Elschner, J. Schwartz and A. Kahn, *App. Phys. Lett.* **82**, 2281, 2003.

[36] L. Diao. D. C. Frisbie, D. D. Schroepfer and P. Paul Ruden, *J. Appl. Phys.* **101**, 014510, 2007.

[37] H. Ishii, K. Sugiyama, E. Ito and K. Seki, *Adv. Mat.* **11**, 605, 1999.

[38] A. Wan, J. Hwang, F. Amy and A. Kahn, *Org. Electron.* **6**, 47, 2005.

[39] S. Rentenberger, A. Vollmer, E. Zojer, R. Schennach and N. Koch, *J. Appl. Phys.* **100**, 053701, 2006.

[40] N. Koch and A. Vollmer, *App. Phys. Lett.* **89**, 162107, 2006.

[41] D. Donaghy and W. Eccleston *(private communication).*

[42] S. K. Park, T. N. Jackson, J. E. Anthony and D. A. Mourey, *App. Phys. Lett.* **91**, 063514, 2007.

CHAPTER 5

TEMPERATURE DEPENDENCE OF SCHOTTKY DIODES BASED ON ORGANIC SEMICONDUCTORS

This chapter is primarily concerned with studying the temperature variation of the current density voltage characteristics of as-synthesised poly(3-hexylthiophene) (P3HT) and polytriarylamine (PTAA) Schottky diodes. The notion of a self-consistent T_c with changing temperature is explored through the quantitative modelling of the forward exponential current slope of both diodes and the saturation current region of the PTAA Schottky diode. This chapter also presents the activation energy for P3HT and PTAA determined experimentally from the Arrhenius plot of the reverse current density at relatively high temperatures.

5.1 INTRODUCTION

Research into solution-processed organic semiconductors has intensified over recent years due to a growing interest in the charge transport mechanism of these materials. The continued focus in this particular area of the subject reflects the sheer complexity of the problem of hopping mobility. Numerous transport models have been proposed so far in an attempt to elucidate the hopping mechanism governing carrier transport and hence conduction in disordered solids. However, an agreement is yet to be reached as some researchers propose analytical models which are based on a Gaussian density of states [1-3] while others consider an exponential DOS to be a sufficiently accurate approximation [4-6].

In our analytical model, we have chosen to approximate the tail of the Gaussian distribution of localised states by an exponential function as it provides considerable insight into the operation of organic devices. Hence, the most important material dependent parameter is the characteristic temperature T_c representing the exponential DOS. Further study into the widely observed carrier density dependence of mobility confirms that the energetic distribution of carriers also follows an exponential function. It is, however, described by a different characteristic temperature called T_0. This finding has led us to believe that T_0 will vary with temperature whilst T_c remains a constant. This is because there is no mechanism, classically, by which the distribution of localised states may vary with sample temperature. Experimentally, the self-consistency of the value of T_c with varying sample temperature has been confirmed by high frequency capacitance voltage *(C-V)* measurements performed on an as-synthesised P3HT metal-insulator-semiconductor (MIS) diode [7].

In this chapter, the temperature dependence of *J-V* measurements performed on a highly regioregular poly(3-hexylthiophene) (P3HT) and polytriarylamine (PTAA) based Schottky diodes are discussed in detail. The exponential current regions of both the diodes are analysed with the aid of the conventional and newly derived current density expression for organic Schottky diodes. For the PTAA diode, the quantitative modelling of the forward saturation current with the newly developed space charge limited current (SCLC) expression provides an additional means of determining the magnitude of T_c. The chapter also discusses factors which may limit the applicability of the analytical model with decreasing temperature.

In organic semiconductors, it is suggested that the hopping transition of carriers in an exponential DOS can be effectively described in terms of activation from the Fermi level to a specific transport energy. This thermally activated behaviour of carriers consequently leads

to the commonly observed Arrhenius-like temperature dependence. The activation energy for both P3HT and PTAA is determined experimentally from an Arrhenius plot of the reverse current density at relatively high temperatures. Interestingly, for the P3HT Schottky diode, the Arrhenius plot of conductivity measured over a similar temperature yields a comparable value of E_a.

5.2 TEMPERATURE DEPENDENCE OF AN AS-SYNTHESISED POLY(3-HEXYLTHIOPHENE) (P3HT) SCHOTTKY DIODE

The current density voltage characteristic of a highly regioregular P3HT Schottky diode at room temperature was studied in detail in *chapter 3*. Fortunately, the analytical relationships developed gave satisfactory agreement with the experimental result. In particular, the exponential rise in forward current at low applied voltages provided a means of determining the individual characteristic temperatures representing the energetic distribution of intrinsic carriers and localised states.

In disordered organic semiconductors, charge transport takes place via thermally assisted tunnelling (*i.e.* hopping) between localised states thus resulting in carrier motion being strongly dependent on sample temperature. The temperature dependence is further enhanced by the empirical relationship between mobility and carrier density. At low temperatures, the reduced carrier concentration is expected to yield a much lower effective mobility. Thus, to gain a more comprehensive understanding of the operation of a P3HT based Schottky diode, a detailed study concerning the temperature variation of its *J-V* characteristic is undertaken.

The variable temperature measurement was performed in ~ 10^{-1} mbar vacuum to diminish any reaction between the organic film and the atmosphere and also to facilitate the varying of the temperature. The diode was fabricated on a polyethylene terephthalate (PET) flexible substrate instead of a glass slide to minimise the discrepancy between the measured temperature and the sample temperature. However, there might still be a small difference between the two temperatures since plastic substrates possess poor thermal conductivity. A liquid nitrogen cryostat was used to cool the sample down and the DC characterisation was performed using a PC controlled Keithley voltage source and electrometer. *Figure 5.2.1* shows the current density voltage characteristics for an as-synthesised P3HT Schottky diode measured at different temperatures ranging from 126K to 290K.

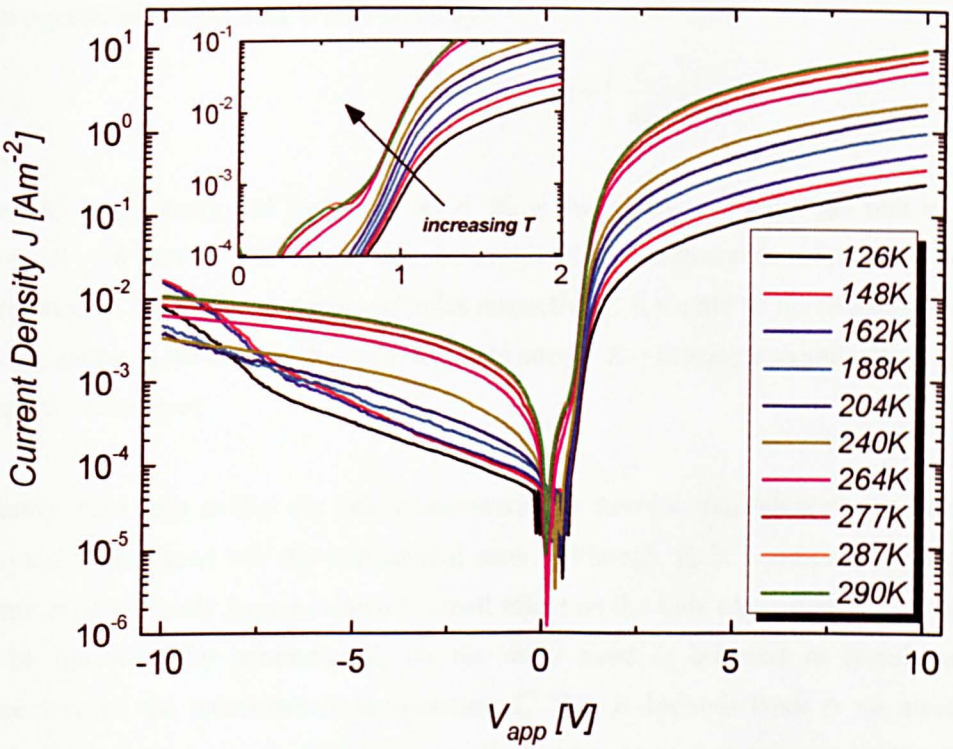

Figure 5.2.1: Semi-logarithmic J-V characteristics for an Au-P3HT-Al Schottky diode measured at various different temperatures. The voltage was applied on the bottom gold electrode. The current through the diode decreases with temperature although a much smaller fall in current is observed in the exponential region (inset).

It is evident that the current through the Schottky diode falls with decreasing sample temperature with the forward saturation current falling by almost 2 orders of magnitude in the measured temperature range. By comparison, the drop in reverse current is less significant. From the inset in *figure 5.2.1*, the decrease in the exponential current seems to only become pronounced at relatively low temperatures. At room temperature, the diode gives a rectification ratio of ~ 10^3. At first sight, the most likely cause for the fall in current level is thought to be the strong dependence of carrier density on temperature. In the case of a p-type semiconductor for instance, the quasi Fermi level is predicted to shift to lower energies as the drop in the average hole thermal energy leads to a larger number of holes occupying higher energy states. Also the temperature dependence of the Fermi Dirac statistics means that a sharper exponential drop in free hole density at energies below the quasi Fermi level may be expected. In disordered organic semiconductors, only holes occupying states lower than the Fermi level are believed to contribute to current flow since at

lower lying energies, the localised states are located less far apart. The hole concentration p in an organic semiconductor is thus given by

$$p = \frac{N_0 T_0}{T_c} \exp - \left(\frac{E_F}{kT_c} \right) \qquad 5.2.1$$

where E_F is the energy of the Fermi level, N_0 is the number of states per unit volume at energy $E = 0$ and T_c and T_0 are the characteristic temperatures describing the energetic distribution of the localised states and holes respectively. It should be noted that the negative sign appearing in the exponential term is due to energy $E = 0$ being energetically higher than the quasi Fermi level.

Equation 5.2.1 tells us that the hole concentration is strongly dependent on the position of the quasi Fermi level via the exponential term. Although T_0 is a temperature dependent parameter, it will only have a relatively small effect on the hole concentration and therefore can be ignored. The parameter T_c on the other hand is believed to remain constant irrespective of the measurement temperature T. This is because there is no mechanism, classically, by which the distribution of localised states may vary with sample temperature. And so far there is no evidence that suggests the possibility of such a phenomenon.

In extrinsic semiconductors, the dopant states introduced at energies much further away from the quasi Fermi level are assumed to be almost entirely ionised at room temperature. The holes contributed by these shallow dopant states will obey Pauli Exclusion Principle and rapidly fill up intrinsic states lying at lower energies. For convenience, this phenomenon is referred to as 'carrier inversion' and is illustrated in *figure 5.2.2*. The density of holes contributed by dopants is generally much higher than the intrinsic hole density and is thus said to dominate conduction in extrinsic semiconductors. Decreasing the sample temperature, however, will promote the recombination of the ionised dopant states with their charge carriers. The energetic shift of the quasi Fermi level towards the dopant states with decreasing temperature means that an increasing fraction of dopant states will become occupied. Nevertheless, in conventional semiconductors like silicon, it has been found that the recombination process is only of importance at particularly low temperatures (< 100K). This region is known as the freeze-out range [8]. In the temperature range between 100K and 300K, the carrier density continues to retain its extrinsic value as most of the dopant states remain ionised. This region is thus appropriately called the saturation range.

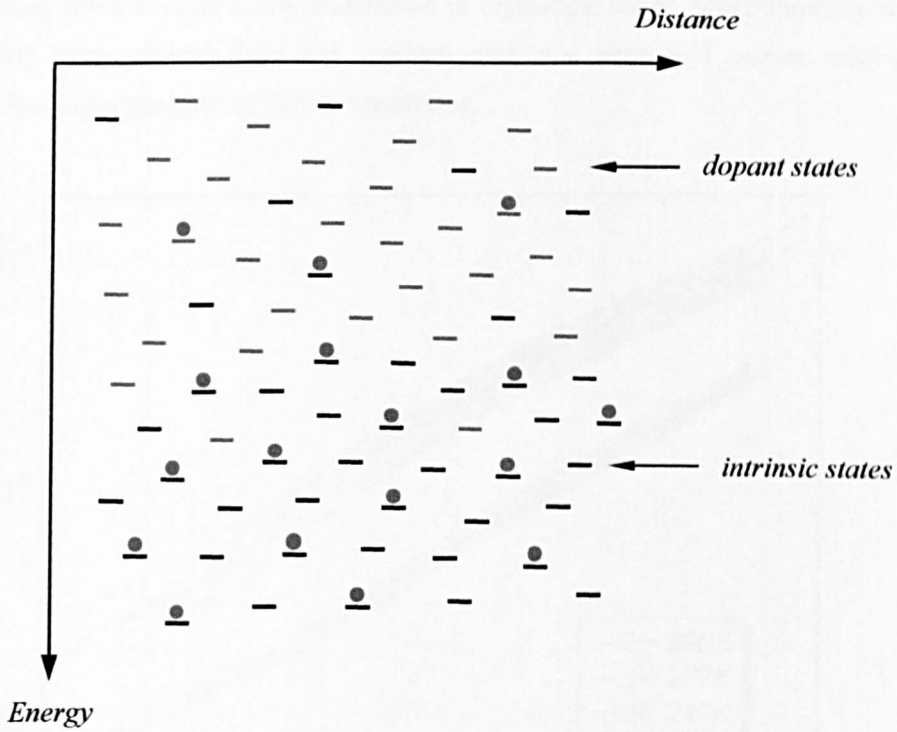

Figure 5.2.2: Schematic representation of the phenomenon called 'carrier inversion' where holes (filled circles) contributed by the dopant states obey Pauli Exclusion Principle and rapidly fill up the lower lying intrinsic states. The holes are, however, expected to recombine with the dopant ions as the quasi Fermi level shifts to lower energies with decreasing temperature.

In the reverse direction, the small increment in current observed with increasing negative voltage suggests that the Schottky barrier is being effectively lowered by both the image force effect and the field in the space charge region. At temperatures between 240K and 290K, the experimental plot of $ln\ J_R$ against $V^{0.25}$ gives a straight line fit with a nearly constant dopant density of ~ 10^{16} cm^{-3} in spite of the current falling by almost an order of magnitude. The dopant density calculated at temperatures of 240K, 277K and 290K are approximately $1.05\times10^{16}\,cm^{-3}$, $1.17\times10^{16}\,cm^{-3}$ and $1.42\times10^{16}\,cm^{-3}$ respectively. Below 240K, however, the anomalous rise in reverse current at higher applied voltages leads to a lack of agreement with the basic Schottky theory. Consequently, it is not possible to determine the dopant density at temperatures below 240K. The almost constant slope obtained in *figure 5.2.3* suggests that like silicon, the shift in quasi Fermi level in the narrow temperature range fails to lead to a significant deionisation of dopant ions and as a result the free hole density stays almost constant. Hence, current transport in P3HT will be dominated by the extrinsic carrier density contributed by the dopants. The concept of 'carrier inversion'

and its resulting effect is more easily understood in crystalline solids where impurity states can be clearly distinguished from the conduction/valence band and carrier motion is governed by band like transport at high temperatures.

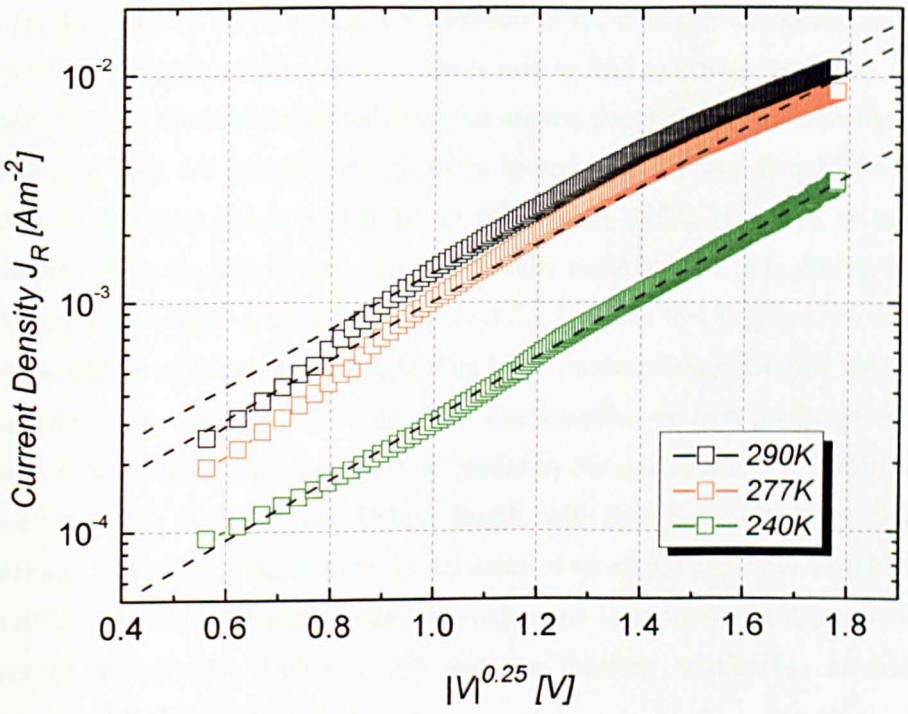

Figure 5.2.3: Plots of ln J_R against $|V|^{0.25}$ for the Au-P3HT-Al Schottky diode at temperatures between 240K and 290K. The virtually constant dopant densities estimated from each of the slopes suggest that the free hole density in as-synthesised P3HT is dominated by a phenomenon referred to as 'carrier inversion'. This effect was first observed in extrinsic inorganic semiconductors.

In the basic Schottky theory, the space charge region is assumed to have an abrupt edge. In practice, however, the majority carrier concentration gradually increases to its bulk value over a distance known as the effective Debye length L_{De}. It is impossible to have a step-like rise in carrier density as it requires the application of an infinitely large electric field. The effective Debye length at the edge of the space charge region is thus given by

$$L_{De} = \sqrt{\frac{\varepsilon_0 \varepsilon_s k T_c}{q^2 N_A}} \qquad 5.2.2$$

where ε_0 is the permittivity of free space, ε_s is the static dielectric constant of the semiconductor, T_c is the characteristic temperature of the exponential density of states and N_A is the acceptor ion concentration.

Classically, L_{De} shows a dependence on the absolute temperature T but in the case of organic semiconductors, the parameter surprisingly depends on the characteristic temperature of the exponential DOS T_c. This undoubtedly comes from approximating the Gaussian band tail by an exponential function and subsequently integrating the free carrier density from the quasi Fermi level to infinity. Nevertheless, the variation in L_{De} is largely dependent on the carrier density where a higher carrier concentration is said to lead to smaller screening lengths. At room temperature, the equilibrium hole concentration is generally equal to the dopant density as the dopant ions are mostly ionised. From experiments, it was found that this effect continues to dominate the hole density up till at least 240K. However, at much lower temperatures when the dopant states are almost fully occupied, the hole density is expected to vary with temperature according to *equation 5.2.1*. When that happens, N_A in the above expression will be replaced by the equilibrium hole concentration p. Despite the presence of the constant T_c in *equation 5.2.1*, the hole concentration is still predicted to fall with temperature due to the shifts in energy experienced by the quasi Fermi level. Thus, according to *equation 5.2.2*, the effective Debye length will increase with decreasing sample temperature. This raises concern over the accuracy of an abrupt depletion edge at fairly low temperatures. The abrupt depletion edge approximation is important as it helps validate the concepts of an effective Debye length and the Einstein relationship as well as the applicability of the Fermi Dirac statistics.

The fall in current flow through the P3HT Schottky diode is believed to be associated with the increasing Schottky barrier height and also the temperature dependence of the Fermi Dirac statistics which causes the redistribution of holes to higher energies. As carrier motion in disordered solids is governed by hopping distances, an exponential DOS means that a steep increase in hopping transitions are to be expected with decreasing energy. So although the free hole concentration is essentially preserved, the hopping rate may still be affected by the smaller number of localised states located at higher energies.

In organic semiconductors, the carrier density is widely known to have a considerable effect on the so-called effective mobility. According to the Universal Mobility Law (UML), the effective mobility in materials characterised by an exponential DOS varies superlinearly with carrier density. In *chapter 2*, it was demonstrated that an expression for the experimentally determined effective mobility can be obtained through a simple comparison with conventional inorganic solids. But the drawback with this method is that it leads to a prefactor which consist mainly of parameters associated with crystalline solids. So, in an attempt to relieve the expression of such variables, an organic semiconductor characterised

by a single transport energy E_T with an abrupt edge and an effective density of states N_T is used for comparison.

So, alternatively, the effective hole mobility in disordered organic solids with an exponential DOS can be expressed as

$$\mu_{eff} = \mu_T N_T \exp -\left(\frac{E_T}{kT}\right)\left[\frac{T_c}{N_0 T_0}\right]^{\frac{T_c}{T}} p^{\left(\frac{Tc}{T}\right)-1} \qquad 5.2.3$$

where N_T corresponds to the effective density of states at the hypothetical transport energy E_T, μ_T is simply an arbitrary constant which has the same units as the effective mobility and $m = {}^{T_c}/_{T} - 1$.

The exponential temperature dependence observed in *equation 5.2.3* suggests that the prefactor will fall appreciably with decreasing temperature. More interesting, however, is the fact that m is inversely proportional to temperature. This implies that lowering the sample temperature will lead to an enhanced dependence of effective mobility on hole concentration. The only other instance where a larger value of m is observed is when the intrinsic organic semiconductor is intentionally doped with DDQ [9]. Then, the increase in m is attributed to the much larger value of T_c describing the combined energetic distribution of intrinsic and extrinsic dopant states. Physically, it is hard to see why a decreasing temperature should lead to a higher m value. But it means that the drop in hole density and mobility prefactor will have to be sufficiently large not only to offset the increase in the exponent term but also to yield an effective mobility which falls with temperature.

It should also be noted that the empirical relationship between mobility and carrier density described in *equation 5.2.3* takes no account of the hopping rate of carriers between localised states. So although the free carrier density in extrinsic semiconductors is dominated by 'carrier inversion', variation in the energetic distribution of carriers with temperature means that the effective carrier mobility may no longer be governed by *equation 5.2.3*.

In general, the strong temperature dependence of the effective mobility is believed to be associated with the thermally activated behaviour of carriers in disordered semiconductors. At lower temperatures, the lower energy states will become scarcely populated and the holes will experience much smaller hopping rates as the thermal energy of carriers is significantly reduced. Experimentally, the effective mobility has been found to fall with forward current in spite of the dopant density and hence the free hole density staying virtually constant till ~

240K. Following the practice of Brown *et al.* in plotting mobility against conductivity fails to yield a reasonable value for the exponent m as the free hole density is essentially independent of temperature. 'Carrier inversion' therefore appears to severely affect the applicability of *equation 5.2.3.*

At very high temperatures, the intrinsic hole concentration p_i is expected to exceed the dopant density and hence dominates conduction. The material is said to resemble an intrinsic semiconductor as the quasi Fermi level approaches and eventually coincides with its intrinsic level E_i. The rise in intrinsic carrier density is caused by the significantly higher thermal generation of electron-hole pairs. An expression for the intrinsic carrier density in disordered organic materials can be obtained by simply following the same stages as in crystalline solids. Previously, the majority carrier concentration in disordered material is determined by assuming that only carriers lying at the quasi Fermi energy and above are free and therefore contribute to current transport. The Fermi level was set as the lower integration limit although it was noted that this introduced an error of 2 which was deemed to be negligible. Further confidence in the approximation was gained when the universal relationship between the so-called effective mobility and carrier density was proven using *equation 5.2.1.* Nonetheless, it is common practice in semiconductor device physics to avoid integrating from the quasi Fermi level. The importance of this practice becomes increasingly apparent when developing the expression for the intrinsic carrier density p_i. The use of the Fermi level as a common integration limit to derive the individual expressions for the equilibrium electron and hole concentration leads to erroneous results. The carrier densities are therefore determined by integrating from their respective transport energies instead of the quasi Fermi level. The intrinsic carrier density in disordered organic solids is thus given by *(Appendix I)*

$$p_i = \sqrt{N_{0n} N_{0p}} \left(\frac{T_0}{T_c}\right) \exp - \left(\frac{E_g}{2kT_0}\right) \qquad 5.2.4$$

where N_{0n} and N_{0p} are the number of states per unit volume at energy $E = 0$ for the electron and hole density of states respectively, T_0 is the characteristic temperature describing the energetic distribution of carriers, k is the Boltzmann constant and E_g is the so-called energy gap which corresponds to the energy difference between the electron and hole transport energies.

Equation 5.2.4 appears to closely resemble the expression obtained for inorganic semiconductors. The exponential temperature dependence will certainly dominate p_i but the increase with temperature will be less steep as the denominator contains the slightly larger T_0 term. At low temperatures, p_i is substantially smaller compared to the extrinsic carrier

density contributed by the dopant states. Hence, the relative contribution of the intrinsic carriers to the total current is considered to be negligible.

In inorganic semiconductors, free carriers mostly reside in energy levels close to the conduction/valence band edge. This makes it easier to identify the energy barrier that all carriers must climb to in order to cross into the metal. To enable us to apply the same concept to disordered organic materials, a hypothetical transport energy is defined beyond which carriers can hop between localised states with relative ease due to the smaller site spacing. So far the use of a transport energy has allowed the successful interpretation of experimental results obtained for Schottky diodes at room temperature. The determination of T_0 directly from the exponential current region suggests that most of the carriers supporting the current come from within an energy kT_0 wide which is equal to ~ $4kT$. This result gives us reason to believe that organic solids may after all behave in much the same way as their crystalline counterpart.

The energetic position of the transport energy in organic solids is believed to be strongly dependent on carrier density. Consequently, it is quite probable that the transport energy will experience a shift to lower energies at relatively low temperatures and vice versa. However, the reduced thermally activated behaviour of carriers at lower temperatures makes it hard to establish if the transport energy is in fact temperature dependent. It may even be that the concept of a transport energy is only valid for a specific temperature range. Between 240K and 290K, the transport energy is thought to remain the same since the free carrier density does not appear to differ much. Although the model assumes a hypothetical transport energy, more work is needed to verify the validity of this approximation.

In conventional semiconductors, the free carrier density is determined by integrating across the entire energy range starting from the edge of the conduction/valence band to infinity. In doing so, the effective density of states is found to be given by

$$N = 2\left(\frac{2\pi m^* kT}{h^2}\right)^{3/2} \qquad 5.2.5$$

where m^* is the effective mass of the carriers, k is the Boltzmann constant, T is the absolute temperature and h is the Planck constant. According to *equation 5.2.5*, N shows a temperature dependency proportional to $T^{3/2}$. This temperature dependence indicates that a wider energy range is needed to support the increasing carrier concentration at higher temperatures.

Interestingly, it can be demonstrated that the expression for N given in *equation 5.2.5* essentially represents the density of states in an energy kT wide from the band edge. The density of states in 3-D systems, in general, can be expressed as [10]

$$N(E)\,dE = \frac{\sqrt{2}}{\pi^2}\left(\frac{m^*}{\hbar^2}\right)^{3/2} E^{1/2}\,dE \qquad 5.2.6$$

Here $\hbar$ corresponds to the reduced Planck constant and is equal to $h/2\pi$.

Integrating *equation 5.2.6* from the band edge where $E = 0$ to $E = kT$ yields the resulting expression for the density of states.

$$N(E) \approx 1.5\left(\frac{2\pi m^* kT}{h^2}\right)^{3/2} \qquad 5.2.7$$

Equation 5.2.7 is considered to be essentially the same as *equation 5.2.5.* This implies that the effective density of states defined in crystalline solids mainly represents the energy levels lying within an energy kT from the band edge. Although the energy kT will vary with temperature, it will not affect the effective mass of carriers as the latter is inversely proportional to the curvature of the parabolic shaped conduction/valence band which is a constant. Hence an effective density of states which is weakly temperature dependent is obtained. *Equation 5.2.7* proves that the abrupt edge approximation works well in these materials largely due to the fact that the Fermi Dirac distribution function becomes negligibly small at larger energies. This approximation is enhanced further by the gradual rise in the density of states.

Unfortunately, a similar analysis cannot be performed for disordered materials since it lacks an expression akin to the effective density of states in conventional semiconductors. But provided that $T_c > T$, the Fermi Dirac statistics will also dominate the energetic distribution of carriers in organic solids. However, the width of the energy range where most of the carriers reside is expected to be larger than that of inorganic materials due to the exponentially rising DOS. In fact, kT_0 has been found experimentally to be approximately equal to $4kT$. Within an energy kT_0, the Fermi Dirac statistics will cause the carrier density to fall to almost $1/3$ its initial value. This explains why the expressions developed for disordered semiconductors by incorporating the Universal Mobility Law (UML) can easily be reduced to its conventional form by making m equal to zero.

Based on the simplified model, the forward current density for organic Schottky diodes is given by [11]

$$J \propto \exp\left(\frac{qV_{app}}{kT_0}\right) \qquad 5.2.8$$

At room temperature, the magnitude of T_0 determined directly from the slope of the exponential current regime is comparable with the values measured from other devices made with the same organic material. In fact, the accurate determination of T_0 suggests that trapping in extrinsic states is negligible. At 290K, the value of T_0 estimated from the forward *J-V* characteristic of the Al-P3HT diode is ~ 1048K. The corresponding value of T_c can be calculated using the following expression:

$$\frac{1}{T_0} = \frac{1}{T} - \frac{1}{T_c} \qquad 5.2.9$$

Equation 5.2.9 yields a value of T_c equal to ~ 401K. This relates to a Meyer Neldel energy of ~ 35 meV.

Traditionally, the current density for Schottky diodes is expressed as

$$J \propto \exp\left(\frac{qV_{app}}{\eta kT}\right) \qquad 5.2.10$$

Here η is known as the ideality factor. Comparing *equation 5.2.8* with *equation 5.2.10* gives $T_0 = \eta T$. In crystalline silicon diodes, the ideality factor is generally determined to be very close to unity. This is thought to indicate the almost ideal Schottky barrier formed at the metal/silicon interface. The interface is thus almost free of extrinsic trap states and carriers contributing to current transport come from within an energy ~ kT wide of the conduction/valence band edge. In addition, the ideality factor of these diodes also exhibits a distinct temperature dependence [12]. Most frequently, the η of silicon diodes increases when the sample temperature is lowered but other trends have also been observed [13-15]. The commonly reported negative temperature coefficient of η has been explained using models based either on a particular distribution of interface states, tunnelling or inhomogeneous barrier heights. Tung was the first to model imperfect Schottky barriers by assuming lateral variations in the barrier height. He reported that increasing the inhomogeneity of the Schottky barrier height effectively leads to larger ideality factors [16, 17].

As stated earlier, the exponential slope of the as-synthesised P3HT diode shows a distinct fall with temperature below ~ 204K. At higher temperatures, the almost parallel slopes seen in the inset of *figure 5.2.1* prevent large variations in η. *Figure 5.2.4* shows that the values of η determined from the forward *J-V* characteristics are a strong function of temperature.

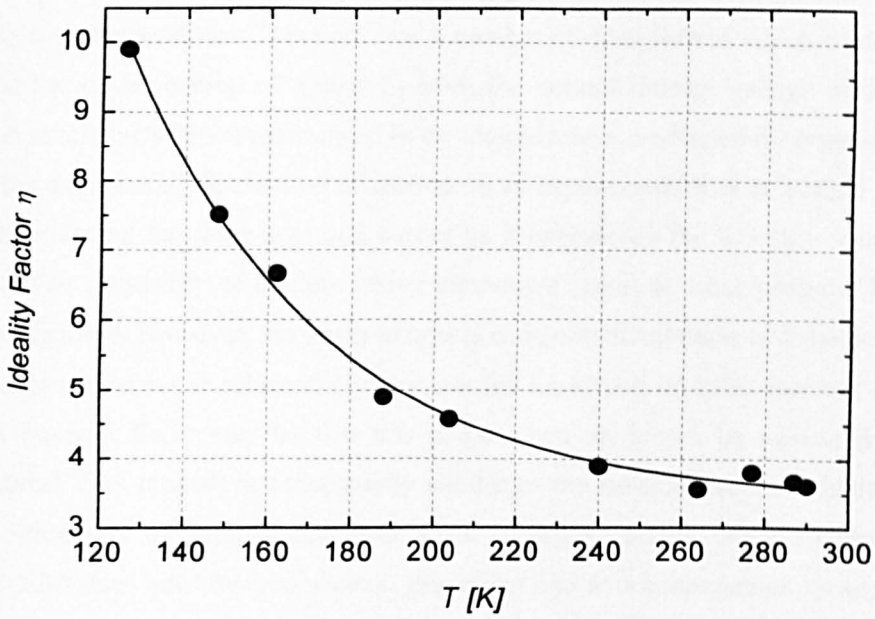

Figure 5.2.4: Variation in ideality factor η with temperature for the Au-P3HT-Al Schottky diode. The large increase in η with decreasing temperature is believed to be related to the anomalous behaviour of the Schottky barrier interface.

It is evident from *figure 5.2.4* that below ~ 240K, the ideality factor of the Al-P3HT diode increases drastically with decreasing temperature. At 126K, the value of η is estimated to be approximately 9.9 which is nearly 3 times the value measured at room temperature.

The significant rise in η for the Al-P3HT diode suggests that reducing the temperature adversely affects the Schottky metal/organic interface. At lower temperatures, determining the magnitude of T_0 directly from the exponential slope leads to erroneous results since the Schottky barrier interface can no longer be assumed to be free of extrinsic trapping states or other non-ideal behaviours. In fact, the value of T_0 was found to increase with decreasing temperature over most of the measured temperature range. This increase in T_0 is, however, deemed to be counter intuitive since it is known that the Fermi Dirac statistics which governs the carrier distribution falls more sharply with decreasing energy as the temperature is lowered. Consequently, a decreasing kT_0 with temperature is expected as the energetic distribution of holes becomes increasingly narrow.

In conventional semiconductors, a greater-than-unity ideality factor usually prompts the suggestion of interface states. In contrast, ideality factors in the range of between 3 - 5 observed for organic Schottky diodes at room temperature has been successfully associated with the exponential distribution of intrinsic states. Hence, it is hard to discern if the presence of extrinsic trapping states is the likely cause for the steep rise in η seen at relatively low temperatures. There are also a number of other factors which could possibly influence the determination of η and T_0 from the current density voltage characteristics measured at relatively low temperatures. In the simple model developed for organic Schottky diodes, the exponential distribution of carriers in an exponential DOS is thought to lead to each carrier seeing the same potential barrier as it approaches the Schottky metal/organic interface. The possibility of carriers taking alternative routes to other potential barriers is altogether ignored. However, the much narrower energetic distribution of holes predicted at lower temperatures could substantially increase the likelihood of holes crossing into other potential barriers. So it may be that this process can no longer be neglected at lower temperatures. This process is conceptually similar to the inhomogeneous Schottky barrier heights introduced by Tung which also leads to larger ideality factors. Unfortunately, *equation 5.2.8* does not take into account this effect and as a consequence its applicability may be limited.

Equation 5.2.8 also relies heavily on the tacit assumption of a flat quasi Fermi level across the whole length of the organic film under steady state conditions. This is deemed to be a reasonable approximation at room temperature largely based on the fact that the values of T_0 and hence T_c extracted from the *J-V* characteristic are in close agreement with the values obtained from other devices. For a flat quasi Fermi level to exist, the carriers injected from the back metal electrode will have to percolate down through the distribution of localised states until they finally reach a state of quasi equilibrium. This process, however, becomes increasingly difficult at fairly low temperatures as the thermal energy of carriers is significantly reduced. The much smaller hopping rates predicted suggest that the carriers may only be capable of accurately obeying the Fermi Dirac distribution function further into the organic film. Hence, the assumption of a flat quasi Fermi level may not work as well at lower temperatures.

According to the simplified Schottky theory, the barrier lowering as a function of applied voltage V_{app} is given by

$$\Delta\phi_B = \left[\frac{q^3 N_A}{8\pi^2 \varepsilon_0^{\,3} \varepsilon_s \varepsilon_\infty^{\,2}} \left(V_{bi} - V_{app}\right)\right]^{1/4} \qquad 5.2.11$$

where N_A is the acceptor ion concentration, ε_0 is the permittivity of free space, ε_s is the static dielectric constant of the semiconductor, ε_∞ is the high frequency permittivity of the semiconductor and V_{bi} is the built in potential. *Equation 5.2.11* tells us that the barrier lowering is strongly dependent on dopant density. Above 240K, the self-consistent value of dopant density obtained from the reverse *J-V* characteristics suggests that the width of the space charge region is likely to be independent of temperature and so will the image force induced barrier lowering. However, at significantly lower temperatures when the dopant states become mostly occupied, the carrier density in the semiconductor will fall. This will cause the space charge region to extend over a larger distance thereby leading to a reduction in $\Delta\phi_B$.

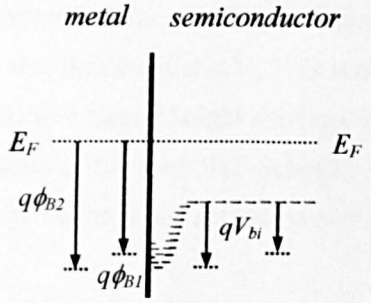

Figure 5.2.5: Simplified energy diagram for a metal/p-type disordered organic semiconductor at different temperatures and in the absence of an applied voltage. A fall in measurement temperature is expected to cause the quasi Fermi level to shift towards lower energies and consequently lead to an increase in barrier height. $q\phi_{B1}$ and $q\phi_{B2}$ correspond to the effective barrier height at higher and lower temperatures respectively.

The predicted shift in the quasi Fermi level with temperature is also likely to affect the effective barrier height ϕ_B at the Al/P3HT interface since the height of the potential barrier is largely dependent on the difference in work function between the metal and the semiconductor. The increase in barrier height as illustrated in *figure 5.2.5* means that a smaller number of holes will possess sufficient thermal energy to cross into the metal and consequently the current through the diode will fall with temperature in consistent with the experiment. A similar increase in barrier height is also expected at the back metal/organic interface. Hence, at relatively low temperatures, the device may behave like a pair of back-to-back Schottky diodes.

It is believed that hopping in an exponential DOS can be effectively described in terms of activation from the Fermi level to a single transport energy [4, 19, 20]. This explains the

commonly observed Arrhenius-like behaviour in organic solids. The activated jump of carriers is a direct result of having a larger number of localised states at higher energies. Experimentally, it is possible to extract the activation energy E_a of a disordered semiconductor from an Arrhenius plot of the reverse current density at relatively high temperatures [18]. The activation energy generally shows a weak dependence on temperature. *Figure 5.2.6 (a)* shows the experimental plot of J_R against *1000/T* for the Al-P3HT Schottky barrier at an applied voltage of -1V and in the temperature range of between 240K and 290K. At temperatures below 240K, the carriers are thought to no longer exhibit thermally activated behaviour. Consequently, the *J-V* characteristic measured at lower temperatures is believed to be dominated by tunnelling and leakage current. An activation energy of ~ 0.18 eV is estimated from the slope of the curve in *figure 5.2.6 (a)*. A similar graph is also plotted for the reverse voltage of -5V and interestingly, the activation energy was found to be comparable to that measured at -1V. This is consistent with the fact that the activation energy unlike the effective barrier height does not change with increasing reverse bias. The forward current densities of the Al-P3HT Schottky diode, however, seem to lend themselves less well to the determination of the activation energy.

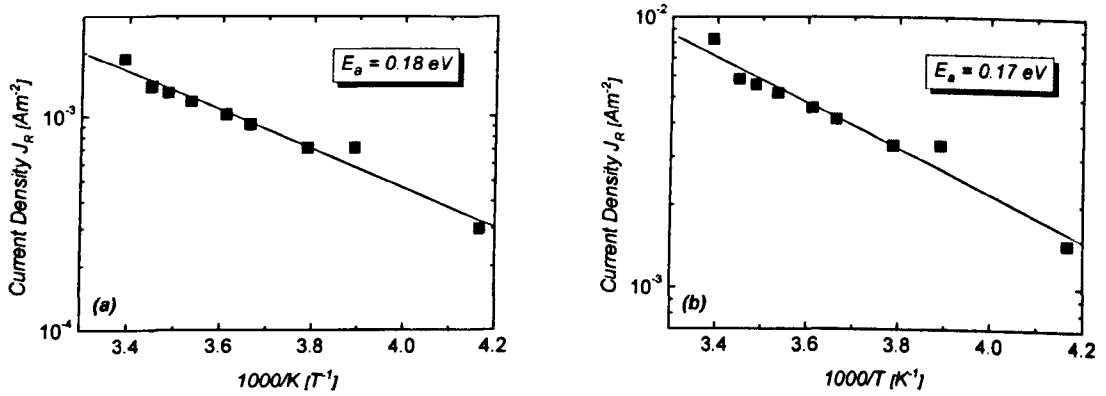

Figure 5.2.6: Arrhenius plots of reverse current density J_R in the thermally activated regime at a reverse voltage of (a) -1V and (b) -5V. The activation energy E_a remains almost independent of applied bias.

Besides the reverse current, the conductivity of organic solids is also predicted to exhibit Arrhenius-like temperature dependence *i.e.* $\sigma \sim \exp - [E_a/(kT)]$. For the Al-P3HT Schottky diode, the conductivity of the organic film can be determined by measuring the deviation along the voltage axis for each of the measured forward current levels.

The conductivity of the organic film is given by

$$\sigma = \frac{J x_p}{q \Delta V} \qquad 5.2.12$$

where J is the current density, x_p is the film thickness, q is the electronic charge and ΔV is the potential drop across the neutral region. The solution-cast film is assumed to have a thickness of 1μm.

Figure 5.2.7 shows the Arrhenius plot of conductivity over a similar temperature range. Interestingly, the activation energy is found to be equal to ~ 0.17 eV which is in close agreement with previous results. The conductivity values calculated at lower temperatures must, however, be treated with caution as small deviations in current were observed at higher applied voltages. This is believed to be caused by the temperature dependence of the back metal/organic barrier height. The self-consistent value of E_a obtained using different methods suggests that the energetic position of the transport energy remains virtually constant in the temperature range of between 240K and 290K.

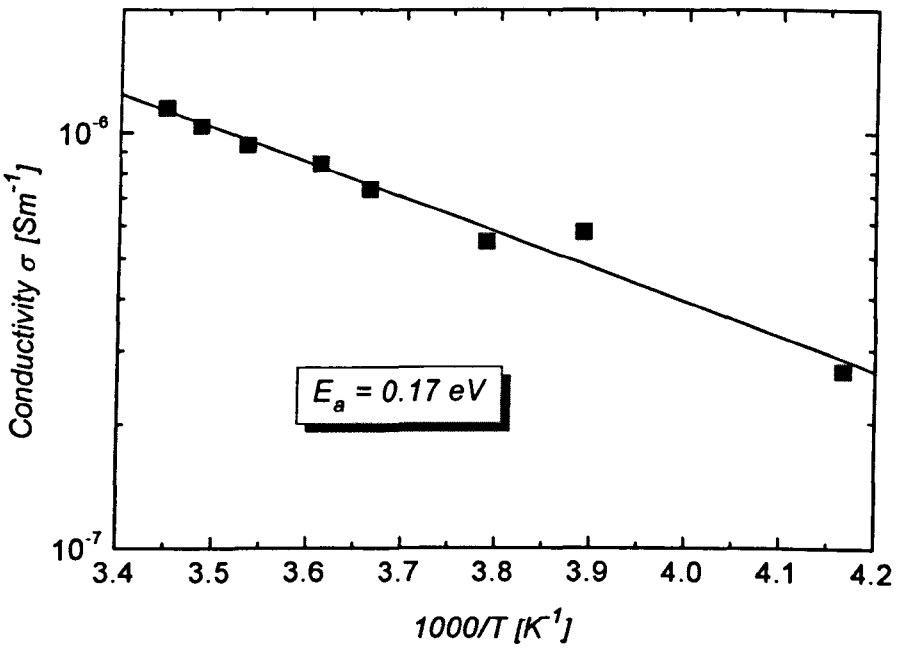

Figure 5.2.7: Arrhenius plot of conductivity for the as-synthesised P3HT film in the temperature range of between 240K and 290K. The conductivity is determined by measuring the potential drop across the neutral region. An activation energy of ~ 0.17 eV is estimated from the slope of the curve.

5.3 TEMPERATURE DEPENDENCE OF A POLYTRIARYLAMINE (PTAA) SCHOTTKY DIODE

Figure 5.3.1 shows the experimental current density voltage characteristics for a polytriarylamine Schottky diode measured at temperatures ranging between 101K and 295K. Similar to the P3HT diode, the measurements were performed in a vacuum of ~ 10^{-1} mbar and the device was cooled down using a liquid nitrogen cryostat.

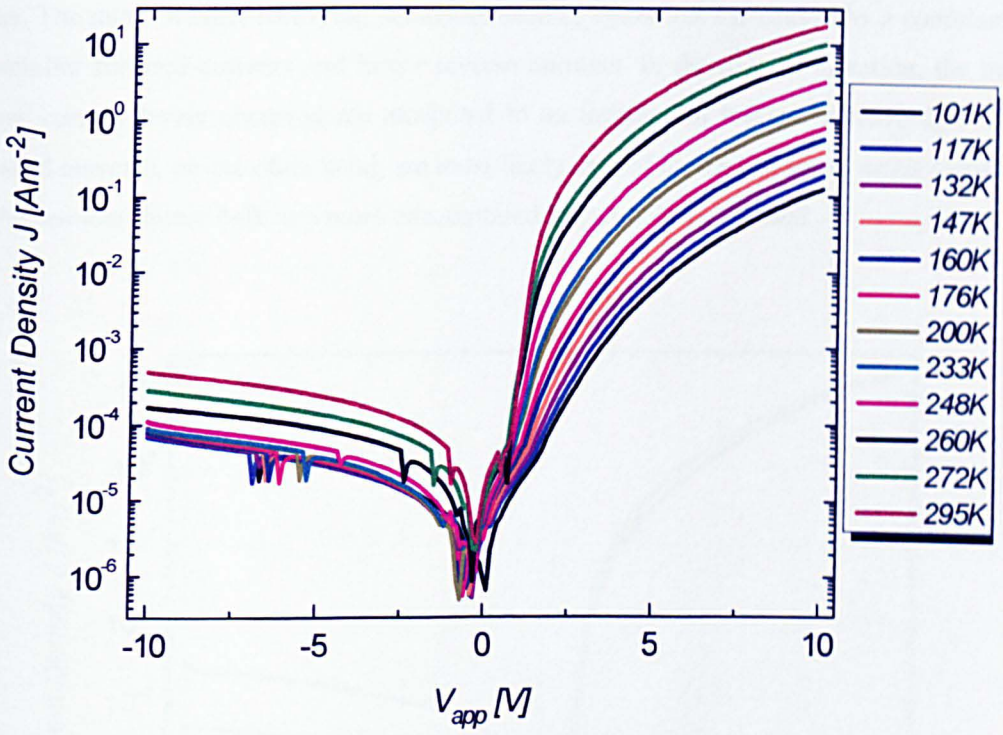

Figure 5.3.1: Current density voltage characteristics for a modified Au-PTAA-Al Schottky diode measured at different temperatures. The voltage was applied on the bottom Au electrode. Within the measured temperature range, the rectification ratio of the diode falls by about an order of magnitude i.e. from ~ 10^4 to ~ 10^3.

The diode was fabricated on a polyethylene terephthalate (PET) flexible substrate to diminish the difference between the measured temperature and the sample temperature. In addition, a highly concentrated solution of PTAA (S1105) was solution-cast onto the metal coated flexible substrate to avoid the occurrence of pinholes. The solution was made up by dissolving about 50 mg of PTAA, a proprietary semiconductor purchased from Merck Chemicals Ltd., in approximately 5 ml of xylene. The Au surface is treated with pentafluorobenzenethiol (PFBT) prior to the polymer deposition. This step is needed to ensure that the gold electrode makes an ohmic contact with polytriarylamine.

From *figure 5.3.1*, the current through the PTAA Schottky diode clearly drops with temperature and the fall is most pronounced in the forward direction. The forward saturation current decreases by almost two orders of magnitude whilst the change in reverse current is only around 10^1. The latter is undoubtedly related to the fact that the reverse current stays almost the same below 248K. The nearly constant reverse currents may be related to a higher contribution of leakage current. The rectification ratio obtained for this particular diode is fairly low in the region of about 10^4 at room temperature. Previously, rectification ratios as high as 10^8 have been obtained for diodes made with the same material but fabricated on glass. The much weaker rectifying behaviour seen in *figure 5.3.1* is caused by a combination of smaller forward currents and larger reverse currents. In the reverse direction, the much larger current levels observed are attributed to an increase in leakage current. The lower forward currents, on the other hand, are most likely caused by the enhanced series resistance of the semiconductor bulk as a more concentrated PTAA solution is used.

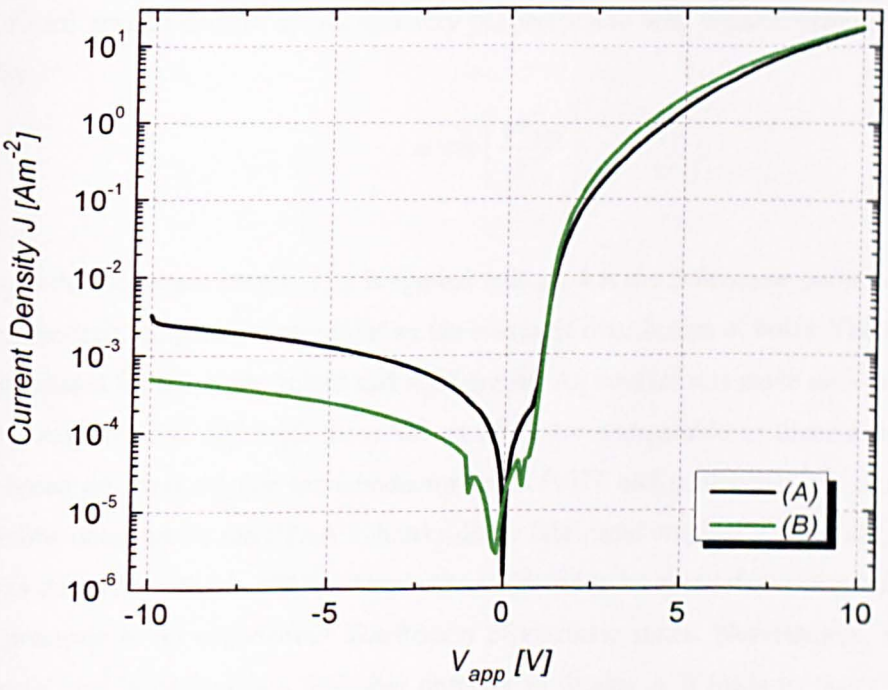

Figure 5.3.2: Semi-logarithmic current density voltage characteristics of the modified Au-PTAA-Al Schottky diode (A) prior to making the Au-Ag contact and (B) after the Au gold wire is secured using Ag paint. The voltage was applied on the bottom Au electrode. The reverse current is significantly lowered and the steepness of the forward saturation current is altered by the presence of the additional Au-Ag contact.

For temperature measurements, additional contacts are made to the metal electrodes by placing small lengths of gold wire on the metal surface and securing them using silver paint. It has been widely reported that Ag forms an ohmic contact with poly(3-hexylthiophene) [21]. For PTAA, it is suggested that modified Ag electrodes will make an ohmic contact with the semiconductor [22]. But interestingly, *figure 5.3.2* shows that the incorporation of the Au-Ag contact leads to a significant improvement in the rectifying property of the PTAA Schottky diode.

The reverse current of the PTAA Schottky diode appears to have dropped by almost an order of magnitude. But more importantly, the slope of the forward saturation current is significantly altered by the introduction of the Au-Ag contact which seems to enhance hole injection into the organic film at each of the applied voltages. The exponential rise in current, however, remains almost the same. The magnitude of T_0 can be determined directly from the slope of the exponential current regime.

The forward current density across Schottky barriers made with organic semiconductors is given by

$$J \alpha \exp\left(\frac{qV_{app}}{kT_0}\right) \qquad 5.3.1$$

where q is the electronic charge, V_{app} is applied voltage, k is the Boltzmann constant and T_0 is the characteristic temperature representing the energetic distribution of holes. The magnitude of T_0 calculated for the diode before and after the Au-Ag contact was made are ~ 1441K and ~ 1273K respectively. Although these values of T_0 are comparable to those measured for diodes based on other organic semiconductors such P3HT and pentacene, it is much higher than the one obtained for the PTAA Schottky diode fabricated on glass. Previously, the value of T_0 was determined to be ~ 481K. This was considered to be an artefact caused most likely by the presence of an exponential distribution of extrinsic states. Nevertheless, a stronger exponential rise in current is a desirable property in diodes as it leads to faster switching speeds. It is well known that the electrical characterisation of organic Schottky diodes can be strongly affected by fabrication conditions. Here the two most obvious differences between the devices are the substrate and the concentration of the PTAA solution used.

A value for T_c is subsequently calculated using the following relationship.

$$\frac{1}{T_0} = \frac{1}{T} - \frac{1}{T_c} \qquad 5.3.2$$

where T is the absolute temperature. The magnitude of T_c calculated for the PTAA Schottky diode with and without the additional contacts are ~ 384K and ~ 371K respectively. This relates to a Meyer Neldel energy of approximately 33 meV and 32 meV. Both these values of T_c are believed to correspond to the characteristic temperature of the intrinsic exponential density of states as dopant states are too high in energy to contribute to conduction at low applied voltages. In fact, PTAA is considered to be a relatively pure organic semiconductor as it shows a lack of dopant states even in the saturation current regime.

In *figure 5.3.2*, the diode without the additional Au-Ag contact shows another distinct exponential current regime at extremely low applied voltages. A similar non-ideal behaviour has previously been observed in Schottky diodes made with poly(3-hexylthiophene). The much steeper rise in current yields a T_0 value of approximately 362K. This is in close agreement with the result obtained for the PTAA diode fabricated on glass but the latter only shows a single exponential slope prior to the current being limited by the series resistance of the semiconductor bulk. The *J-V* characteristic for this particular diode is presented in *chapter 4*. The result suggests that the extrinsic trapping states must be distributed across a much wider energy range in the PTAA diode made on glass. The energy range containing the altered DOS is, however, significantly reduced when a more concentrated solution of PTAA is used. By gradually increasing the applied bias, an exponential region which is almost free of any extrinsic trapping states is obtained. According to *equation 5.3.2*, the lower exponential current region corresponds to a T_c value of ~ 1594K. This is significantly larger than any of the T_c values quoted so far. It relates to a Meyer Neldel energy of ~ 0.14 eV. More work is needed to gain an in depth understanding on the dependence of the exponential current region on fabrication conditions.

As stated earlier, it is evident that making the Au-Ag contact results in a small change in the forward saturation current. But the sharp rise in current with increasing bias in both cases suggests a transition from ohmic to space charge limited conduction. The region can therefore be modelled using the newly developed space charge limited current expression for disordered organic semiconductors which is given by

$$J = \frac{K}{q^m}\left(\frac{\varepsilon_0\varepsilon_s\theta\,(m+1)}{m+2}\right)^{m+1}\left(\frac{2m+3}{m+2}\right)^{m+2}\frac{V_{app}{}^{m+2}}{x^{2m+3}} \qquad 5.3.3$$

where K is the mobility prefactor, q is the electronic charge, ε_0 is the permittivity of free space, ε_s is the dielectric constant of the semiconductor, θ is the ratio of injected free carrier density at higher energy states to the total injected carrier density, m is the exponent in the

Universal Mobility Law (UML), V_{app} is the applied voltage and x is the organic film thickness.

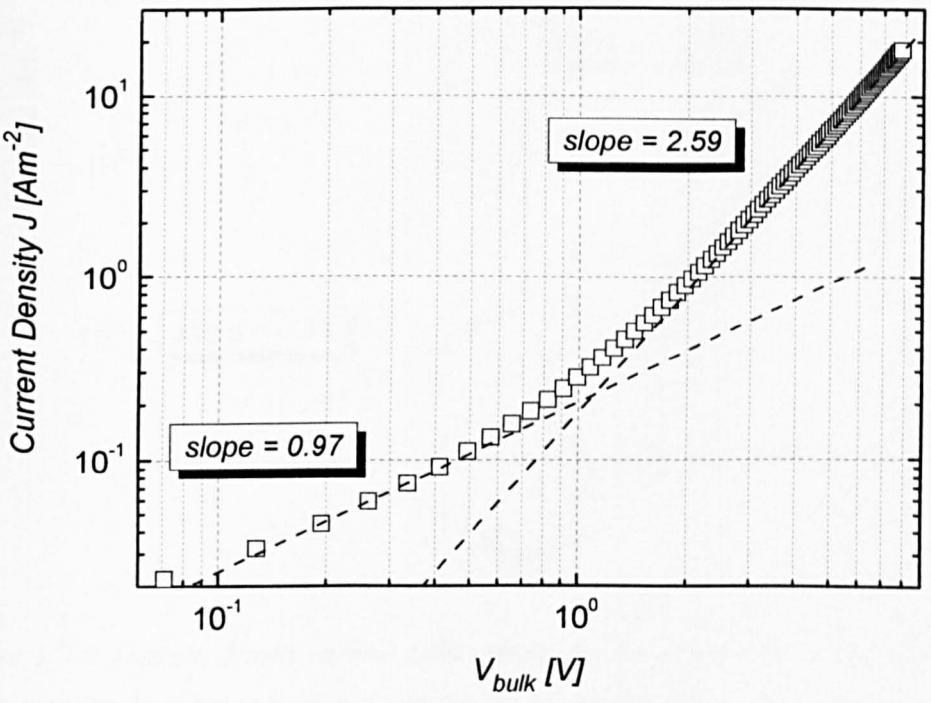

Figure 5.3.3: Current density against V_{bulk} for the modified Au-PTAA-Al diode before the Au wire-Ag contact is made on both the metal electrodes. Slopes of ~ 0.97 and ~ 2.59 are estimated at low and high fields respectively. The slope of greater than 2 at higher applied voltages suggests that the current must be space charge limited

A slope of ~ 2.59 is extracted from the double logarithmic plot of current density against V_{bulk} in *figure 5.3.3*. This yields a value of m equal to ~ 0.59. The corresponding value of T_c can be calculated using the following expression.

$$m = \frac{T_c}{T} - 1 \qquad 5.3.4$$

Equation 5.3.4 gives a T_c of ~ 478K and consequently a Meyer Neldel energy of ~ 41 meV. This result suggests that the localised states at higher energies are also part of the intrinsic distribution of states. Interestingly, the introduction of the Au-Ag contact enhances the saturation current to such an extent that it reduces the value of m to less than half its original value. A value of m equal to ~ 0.23 is obtained as illustrated in *figure 5.3.4*.

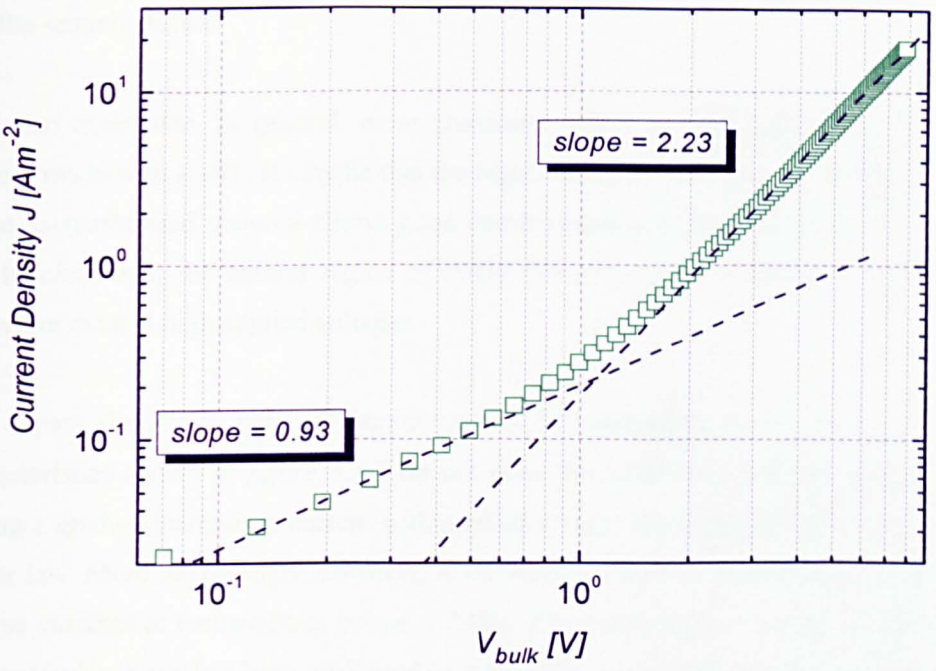

Figure 5.3.4: Current density against bulk voltage for the modified Au-PTAA-Al Schottky diode once the Au wires are secured onto the metal surfaces using silver paint. The slope at low voltages is ~ 0.93 which is in close agreement with the ideal value of 1 for ohmic conduction. But with further increase in applied field, the slope only rises to ~ 2.23 which is significantly lower compared to the result shown in figure 5.3.3.

The smaller value of m gives a T_c of approximately 363K and hence a Meyer Neldel energy of ~ 31 meV. The discrepancy in the measured value of m clearly demonstrates the sensitivity of organic based devices on the quality of the contact made between the back metal and the organic semiconductor. The probing method used for measuring the devices may also have an influence on the results.

From previous experiments involving a variety of organic semiconductors and devices, it was observed that there is a rather obvious spread in the Meyer Neldel (MN) energy corresponding to the exponential DOS. The most commonly quoted value for the MN energy is close to ~ 40 meV but based on our experiments, we find that the energy could range from anywhere between ~ 30 meV and 40 meV [23-25]. So what at first sight looked like a natural variation in the MN energy may in fact be a direct consequence of having differing qualities of ohmic metal contacts. Besides, gold is widely known to be a relatively difficult metal to probe. A similarly low value of m has previously been extracted from TFTs based on the same material [26]. So it may be that using the Au wire and silver paint contact to measure

the device when in vacuum improves the contact made between the modified Au electrode and the semiconductor.

It is also noted that, in general, more consistent values of MN energy are obtained for devices made with P3HT. It may be that the higher background doping levels observed even in the as-synthesised material allows good ohmic contacts to be made with metals such as Au. In *chapter 3*, the neutral region of P3HT Schottky diode is found to exhibit ohmic behaviour even at high applied voltages.

The dopant density in polytriarylamine cannot be established as the set of reverse *J-V* characteristics shown in *figure 5.3.1* do not obey the simplified Schottky theory. Despite having a gradual increase in current with applied voltage, the diode still fails to obey the ¼ power law. More interestingly, however, is the observed lack of temperature dependence of reverse currents at temperatures below ~ 248K. The much higher reverse current seen for this particular diode has been attributed to a possible rise in leakage current caused by the smaller film thickness. In general, leakage currents possess a relatively weak temperature dependence and become dominant at lower temperatures and higher doping densities. So, in the lower temperature regime, the relative contribution of the leakage current to the total current may be significantly higher. Consequently, the reverse current will appear to be independent of measurement temperature as the thermal energy of holes is reduced.

As for the forward *J-V* characteristics, there is a distinct fall in exponential current with temperature across the entire measured temperature range in contrast to the P3HT Schottky diode. The decrease in current through the diode as the temperature is lowered is attributed mainly to the shift in the quasi Fermi level to lower energies. This causes the effective barrier height at the Al/PTAA interface to increase as it is essentially determined by the difference in work function between the metal and the semiconductor. In addition, the current will also be affected by changes in the energetic distribution of holes with temperature. The free hole concentration in disordered organic semiconductors is given by

$$p = \frac{N_0 T_0}{T_c} \exp - \left(\frac{E_F}{kT_c} \right) \qquad 5.3.5$$

where E_F corresponds to the energy of the Fermi level and N_0 is the number of states per unit volume at energy $E = 0$.

The strong dependence of the hole density on the Fermi energy implies that the free hole density will reduce significantly with temperature. Hence, a smaller number of holes will have the energy needed to cross into the metal and contribute to conduction.

The classical expression for current density in Schottky diodes is given by

$$J \propto \exp\left(\frac{qV_{app}}{\eta kT}\right) \qquad 5.3.6$$

where η corresponds to the ideality factor. The accurate determination of T_0 from the exponential slope is largely dependent on the fact that the ideality factor is unaffected by trapping in extrinsic states and other non-ideal behaviours. However, it seems that this condition is less likely to be satisfied as the temperature is lowered. The non-linear variation of η with temperature determined for the Al-PTAA Schottky diode is shown in *figure 5.3.5*. The substantial fall in exponential current observed in *figure 5.3.1* leads to extremely large values of η. The ideality factor increases from ~ 4.32 at 295K to as high as ~ 59.3 at 101K. Similar reduction in exponential current levels has also been reported in Schottky diodes made with vacuum-deposited pentacene [18].

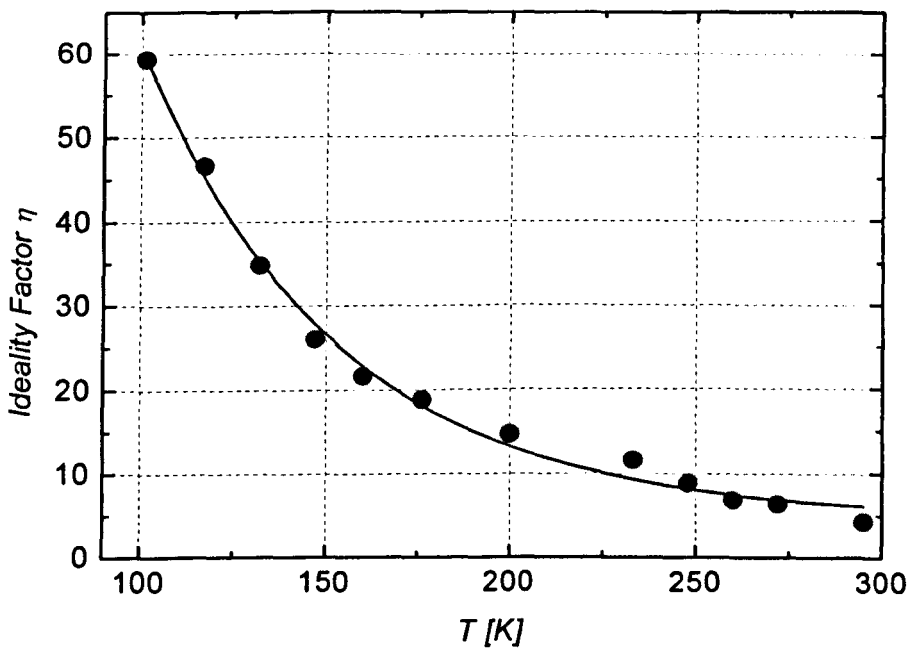

Figure 5.3.5: Temperature dependence of the ideality factor η for the Al-PTAA Schottky diode. The increase in ideality factor for this diode is more pronounced compared to the Al-P3HT diode consistent with the belief that polytriarylamine has a higher degree of disorder.

The large increase in η again results in an almost linear increase in the magnitude of T_0. This result is deemed to be erroneous since the predicted dominance of the Fermi Dirac statistic at $T < T_c$ suggests that the energetic distribution of holes should become increasingly narrow as the temperature is lowered. Based on this fact, a kT_0 that decreases with temperature is expected. Factors that could possibly affect the accurate determination of η and hence T_0 from the forward exponential slope at lower temperatures have been discussed in detail in *section 5.2.*

With further increase in applied voltage, the forward current starts to deviate from *equation 5.3.1* as it becomes limited by the resistivity of the semiconductor bulk. As shown in *figure 5.3.3* and *figure 5.3.4*, the diode clearly exhibits a transition from ohmic to space charge limited conduction in the saturation regime. The occurrence of space charge limited currents in PTAA Schottky diodes is attributed to the lack of dopant ions needed to compensate the build up of charge carriers in the neutral region of the organic film. This hypothesis has been confirmed by the extraction of T_c corresponding to the intrinsic density of states from the saturation current regime. In contrast, for as-synthesised P3HT diodes, a much larger value of T_c is obtained in the saturation region suggesting the presence of a large density of dopants.

Since a good agreement is obtained between the newly developed SCLC model and the *J-V* characteristic measured at room temperature, the forward saturation currents measured at lower temperatures is also modelled using *equation 5.3.3*. *Figure 5.3.6* shows the calculated Meyer Neldel energy for temperatures ranging between 117K and 295K. Interestingly, in the region between 248K and 295K, a constant MN energy of ~ 31 meV is obtained. Beyond 248K, however, a rather steep decline in the calculated MN energy is observed. The self-consistent MN energy obtained at relatively high temperatures reinforces the belief that the exponential distribution of states is independent of temperature.

The significantly smaller MN energies obtained at lower temperatures are mainly attributed to the formation of a potential barrier at the modified Au/PTAA interface. With the quasi Fermi level of the semiconductor predicted to shift to lower energies with decreasing temperature, a potential barrier is thought to form at the back metal/organic interface. The barrier will impede the injection of holes into the semiconductor and hence the forward saturation current through the diode. Furthermore, the bulk voltage determined by measuring the voltage deviation along the *x*-axis for each of the measured current levels will also include the potential drop across the reverse biased Schottky barrier. It is therefore no longer appropriate to use the regional model approach to analyse the *J-V* curves at fairly low

temperatures. Hence the erroneous values of the MN energy obtained at temperatures below ~ 248K should probably be ignored.

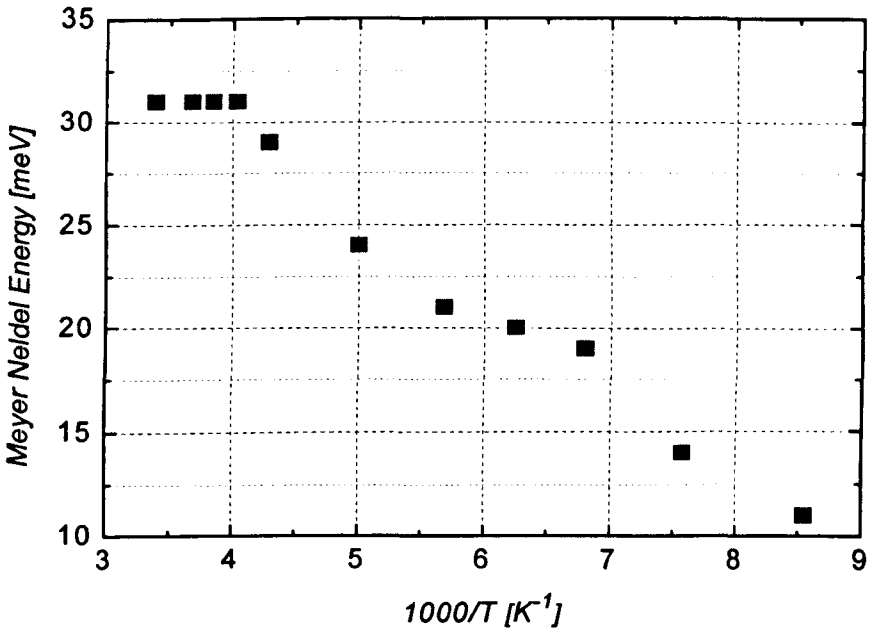

Figure 5.3.6: Variation of the Meyer Neldel energy measured from the saturation current region at higher applied fields with temperature. A slope of greater than 2 suggests that the region continues to be dominated by space charge effects even as the temperature is varied. A constant MN energy of ~ 31 meV is obtained till ~ 248K.

Other factors may also contribute to the inaccuracy of the quantitative modelling of the saturation current region using *equation 5.3.3* at lower temperatures. For instance, although PTAA is said to contain significantly smaller quantities of dopant ions, the carriers are more likely to recombine with the dopants as the temperature is reduced. Consequently, a larger decrease in the width of the space charge region is expected with increasing applied bias and the approximation that the neutral region has a nearly constant width will be less accurately obeyed at lower temperatures. Hence the dependence of the space charge limited current on x can no longer be ignored.

Another important assumption that is also likely to fail at lower temperatures is the flat quasi Fermi level. The approximation of a flat quasi Fermi level is extremely crucial to the modelling of semiconductor devices as it allows the use of the Fermi Dirac distribution function to account for the probability of occupancy of energy states under steady state conditions. The approximation of a flat quasi Fermi level in organic materials is, however, further complicated by the presence of an exponential distribution of states. It is believed that

carriers which are injected from the back metal electrode into the various energy states will have to percolate down through the distribution of states until it reaches quasi thermal equilibrium. But this condition may be harder to achieve at lower temperatures as the thermal energy of holes is significantly reduced. Hence the carriers may only be able to obey the Fermi Dirac statistics much deeper into the organic film. This makes the validity of a flat quasi Fermi level rather doubtful at relatively low temperatures. Similarly all the expressions developed including *equation 5.3.3* which are largely based on the notion of flat quasi Fermi level may no longer be applicable with decreasing temperature.

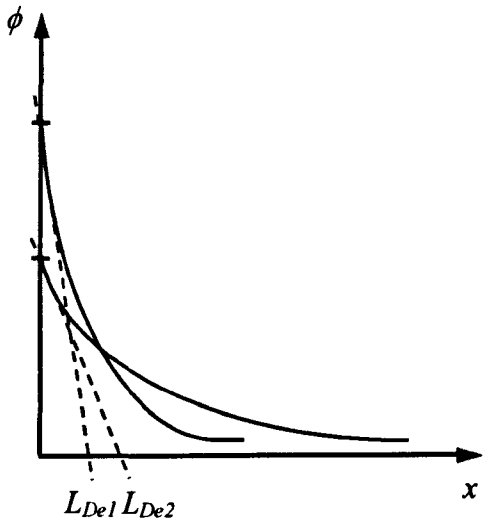

Figure 5.3.7: The effective Debye length at the edge of the space charge region is expected to increase with decreasing temperature and carrier density. The larger Debye length L_{De2} observed at lower temperatures suggests that holes exiting the neutral region will experience a smaller diffusion rate.

In general, the neutral region in a Schottky diode neighbours a region where the carrier density falls exponentially to a relatively low value as it approaches the space charge region. The distance over which this occurs is known as the effective Debye length and it may be expressed as

$$L_{De} = \sqrt{\frac{\varepsilon_0 \varepsilon_s k T_c}{q^2 p}} \qquad 5.3.7$$

where ε_0 is the permittivity of free space, ε_s is the static dielectric constant of the semiconductor, T_c is the characteristic temperature of the exponential density of states and p is the equilibrium bulk hole density. According to *equation 5.3.7*, the drop in free hole density with decreasing temperature will lead to larger screening lengths as illustrated in

figure 5.3.7. The wider L_{De} will cause the resulting field across the region to be smaller and as a consequence, the carriers will experience a smaller diffusion rate. This could affect the transport of holes exiting the neutral region at lower temperatures. In the conventional treatment of SCL current, the semiconductor is sandwiched between two metal electrodes of low resistivity. So, while the cathode serves as an infinite reservoir of electrons, the anode does not restrict the flow of carriers leaving the semiconductor. Because of this, contact effects are generally ignored in the model which greatly simplifies the analysis of SCL currents. However, a smaller rate of diffusion at the edge of neutral region may limit the flow of holes and the analysis of SCL currents in the diode may be adversely affected by the changing boundary conditions.

As stated in *section 5.2*, the Arrhenius-like temperature dependence commonly observed in organic semiconductors is thought to originate from the activated jump of carriers from the Fermi level to a single transport energy. The activation energy E_a of polytriarylamine is determined from the Arrhenius plot of the reverse current density at fairly high temperatures as the thermally activated behaviour of carriers is thought to be limited by significant reduction in measurement temperatures. *Figure 5.3.8* shows the experimental plot of J_R against *1000/T* for the Al-PTAA Schottky diode at a reverse bias of -2V and -5V and in the temperature range of between 233K and 295K. An activation energy of ~ 0.21 eV and ~ 0.19 eV is determined directly from the slope of the curve at -2V and -5V respectively. The E_a measured from the reverse *J-V* characteristics of the PTAA sample seems to demonstrate a small bias dependence. Although the concept of a single transport energy is a widely used in disordered semiconductors, further work is needed to verify the validity and possible limitations associated with it.

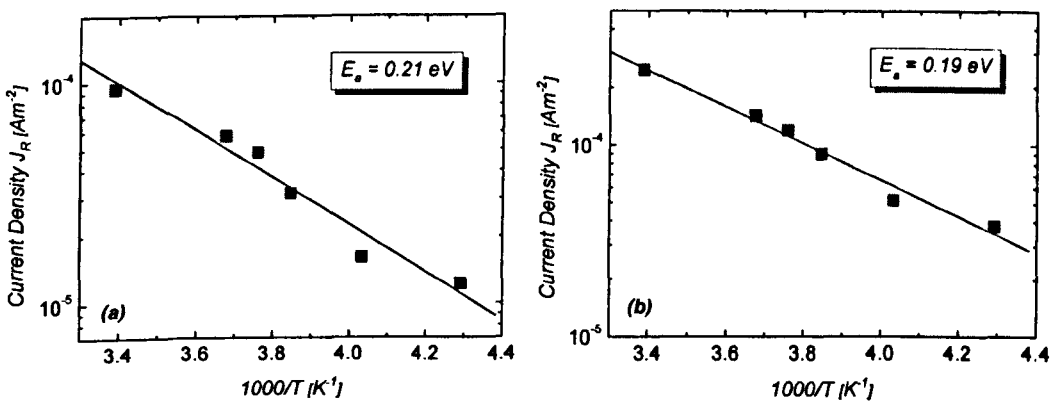

Figure 5.3.8: Arrhenius plots of reverse current density J_R in the temperature range of between 233K and 295K at an applied bias of (a) -2V and (b) -5V. The measured activation energy seems to exhibit a small dependence on applied voltage.

5.4 CONCLUSIONS

The chapter is primarily concerned with studying the temperature dependence of the current density voltage characteristics of as-synthesised poly(3-hexylthiophene) (P3HT) and polytriarylamine (PTAA) Schottky diodes. The diodes were fabricated on polyethylene terephthalate (PET) flexible substrate to minimise the discrepancy between the measured temperature and the sample temperature. The variable temperature measurements were performed in a vacuum of ~ 10^{-1} mbar and the samples were cooled down using a liquid nitrogen cryostat.

There is a distinct fall in current through the diodes as the temperature is reduced. In the Al-P3HT Schottky diode, the forward saturation current fell by almost 2 orders of magnitude whilst the drop in reverse current was slightly less significant. As for the exponential regime, the fall in current only becomes increasingly obvious at temperatures below ~ 204K. In the reverse direction, the semi-logarithmic plot of J_R against $V^{0.25}$ yields a nearly constant doping density in the temperature range of between 240K and 290K. The dopant densities estimated from the slopes at 240K, 277K and 290K were approximately 1.05×10^{16} cm^{-3}, 1.17×10^{16} cm^{-3} and 1.42×10^{16} cm^{-3} respectively. This result suggests that the dopant states remain ionised even as the temperature is reduced similar to the saturation region observed in crystalline silicon [8]. The holes contributed by the shallow dopant states are thus expected to obey Pauli Exclusion Principle and rapidly fill up the lower energy intrinsic states. This phenomenon is referred to as 'carrier inversion'. At much lower temperatures, however, the predicted shift of the quasi Fermi level to lower energies will promote the recombination of the dopant states with their carriers. Unfortunately, the anomalous rise in current at higher applied fields prevents the determination of the dopant density at lower temperatures.

At room temperature, it has been demonstrated that the magnitude of T_0 which represents the energetic distribution of carriers can be determined directly from the exponential current regime. This is made possible largely by the fact that the measured ideality factor η seems to be unaffected by trapping in extrinsic states or other non-ideal behaviours. With decreasing temperature, however, there is a significant increase in η which consequently leads to an almost linear rise in the magnitude of T_0. The much larger ideality factor obtained as the temperature is lowered is thought to be related to the anomalous behaviour of the Schottky barrier interface. The rise in T_0 with temperature is deemed to be erroneous since the distribution of carriers is governed by the Fermi Dirac distribution function. At lower temperatures, the Fermi Dirac statistics falls more sharply with decreasing energy.

Consequently, the energetic distribution of holes is expected to become increasingly narrow thus leading to smaller T_0 values.

A number of factors could influence the determination of η and hence T_0 from the forward *J-V* characteristics of the Schottky diode at lower temperatures. For one, the model relies heavily on the assumption of a flat quasi Fermi level existing throughout the organic film. But the smaller hopping rate experienced by holes with decreasing temperature means that the Fermi Dirac statistics may only be obeyed at increasing distances from the back metal/organic interface. In addition, the model also ignores the possibility of carriers taking alternative routes to other potential barriers. The probability of this occurring is thought to increase as carriers become distributed over a smaller energy range. This could considerably affect charge transport across the Schottky barrier interface. In fact, this process resembles the idea of inhomogeneous Schottky barrier height introduced by Tung which has already been proven to lead to larger ideality factors.

In an exponential DOS, there are suggestions that carrier hopping can be effectively described as an activated jump from the Fermi level to a single transport energy due to the larger number of states available at higher energies. This characteristic feature of organic materials is thought to result in the Arrhenius-like temperature dependence. For the Al-P3HT diode, the experimental plot of J_R against *1000/T* at high temperatures yield an activation energy of ~ 0.18 eV and ~ 0.17 eV at a reverse voltage of -1V and -5V respectively. This virtually constant value of E_a obtained suggests that it is independent of applied bias. Interestingly, the activation energy estimated from the slope of the Arrhenius plot of conductivity is also ~ 0.17 eV. The self-consistent value of E_a suggests that the energetic position of the transport energy remains nearly the same in the temperature range of between 240K and 290K.

Similar to the P3HT diode, the drop in the forward saturation current of the Al-PTAA diode is more pronounced compared to the reverse current. The nearly constant reverse currents observed at temperatures below ~ 248K are probably caused by a higher contribution of leakage current. Overall, the PTAA diode fabricated on the PET flexible substrate revealed a much weaker rectifying behaviour. Small changes in the *J-V* characteristic of the diode are observed when a small length of gold wire is placed onto the metal electrodes and secured using silver paint for the purpose of temperature measurements. The values of T_0 extracted from the exponential current regime of the diode before and after the Au-Ag contact was made were ~ 1441K and ~ 1273K respectively. Interestingly, these values of T_0 are comparable to those obtained for diodes made with other organic semiconductors. This

consequently gave values of T_c equal to ~ 384K and ~ 371K respectively. This is consistent with the belief that only the intrinsic distribution of localised states is involved in conduction at low applied voltages.

In contrast to the P3HT sample, the exponential region of the Al-PTAA diode shows a distinct fall in current with decreasing temperature. Consequently, the measured ideality factor rises from ~ 4.32 at room temperature to as high as 59.3 at 101K. This anomalous rise in η with decreasing temperature may be associated with the presence of extrinsic trapping states, carriers taking alternative routes to other potential barriers or even the lack of validity of the flat quasi Fermi level approximation.

With further increase in applied voltage, conduction in the neutral region of polytriarylamine changes from ohmic to space charge limited. Modelling the saturation region at high fields with the newly developed SCL current expression allows a value for m and hence T_c to be determined. The values of m obtained for the diode with and without the additional Au-Ag contact were ~ 0.59 and 0.23 respectively. This consequently yields to a Meyer Neldel energy of ~ 41 meV and 31 meV respectively. So what was previously thought to be a natural variation in the MN energy may in fact be directly related to having differing qualities of ohmic metal contacts. A value of m equal to ~ 0.27 has previously been extracted from TFTs made with PTAA [26]. Interestingly, more consistent values of MN energy are generally obtained for devices made with poly(3-hexylthiophene). This is thought to be associated with the much higher levels of background doping observed in as-synthesised P3HT.

A constant MN energy of ~ 31 meV was estimated from the saturation region of the PTAA diode in the temperature range of between 248K and 295K. Below 248K, however, the MN energy declines sharply with decreasing temperature. The erroneous value of MN energy measured at fairly low temperatures is mainly attributed to the formation of a potential barrier at the back metal/organic interface. Other factors which may also contribute to the inaccuracy of the measured MN energy are the breakdown in the assumption of a flat quasi Fermi level, a changing neutral region width and an increasing effective Debye length. The self-consistent MN energy obtained at relatively high temperatures gives us further confidence that the characteristic temperature of the exponential DOS is independent of temperature.

For the Al-PTAA diode, the activation energy of holes was determined experimentally from a plot of J_R against $1000/T$ in the temperature range of between 233K and 295K. The slope of

the curve gave an activation energy of ~ 0.21 eV and ~ 0.19 eV at applied voltages of -2V and -5V respectively. Surprisingly, the activation energy in PTAA seems to demonstrate a small dependence on applied bias.

5.5 REFERENCES

[1] H. Bässler, *Phys. Stat. Solidi B* **175**, 15, 1993.

[2] S. D. Baranovskii, H. Cordes, F. Hensel and G. Leising, *Phys. Rev. B* **62**, 7934, 2000.

[3] O. Rubel, S.D. Baranovskii, P. Thomas and S. Yamasaki, *Phys. Rev. B* **69**, 014206, 2004.

[4] M. C. J. M. Vissenberg and M. Matters, *Phys. Rev. B* **57**, 12964, 1998.

[5] G. Horowitz, R. Hajlaoui and P. Delannoy, *J. Phys. III France* **5**, 355, 1995.

[6] G. Horowitz, *J. Mater. Chem.* **9**, 2021, 1999.

[7] N. Sedghi, D. Donaghy, M. Raja, S. Badriya, S. J. Higgins and W. Eccleston, *J. Non-Cryst. Solids* **352**, 1641, 2006.

[8] S. M. Sze, *"Physics of Semiconductor Devices"*, J. Wiley and Sons, 1981.

[9] M. Raja, N. Sedghi, S. Badriya, S. J. Higgins, G. C. R. Lloyd and W. Eccleston, *ESSDERC Proc.*, 253-256, 2005.

[10] B. G. Streetman and S. K. Banerjee, *"Solid State Electronic Devices"* 6th Ed., Pearson Prentice Hall, New Jersey, 2006.

[11] W. Eccleston *(private communication)*.

[12] L. J. Brillson, *"Contacts to Semiconductors – Fundamentals and Technology"*, William Andrew Publishing/Noyes, 1993.

[13] M. O. Aboelfotoh, *J. Appl. Phys.* **64**, 4046,1988.

[14] M. O. Aboelfotoh, *J. Appl. Phys.* **66**, 262, 1989.

[15] I. Dökme, S. Altindal and M. M. Bülbül, *Appl. Surf. Sci.* **252**, 7749, 2006

[16] R. T. Tung, *Appl. Phys. Lett.* **58**, 2821, 1991.

[17] R. T. Tung, *Phys. Rev. B* **45**, 13509, 1992.

[18] L. Diao, D. C. Frisbie, D. D. Schroepfer and P. Paul Ruden, *J. Appl. Phys.* **101**, 014510, 2007.

[19] D. Monroe, *Phys. Rev. Lett.* **54**, 146, 1985.

[20] S. D. Baranovskii, T. Faber, F. Hensel and P. Thomas, *J. Phys.: Condensed Matter* **9**, 2699, 1997.

[21] L. Bürgi, T. J. Richards, R.H. Friend and H. Sirringhaus, *J. Appl. Phys.* **94**, 6129, 2003.

[22] G. C. R. Lloyd *(private communication)*.

[23] A.R. Brown, C. P. Jarrett, D. M. de Leeuw and M. Matters, *Synth. Met.* **88**, 37, 1997.

[24] E. J. Meijer, M. Matters, P.T. Herwig, D. M. de Leeuw and T. M. Klapwijk, *App. Phys. Lett.* **76**, 3433, 2000.

[25] J. C. Wang and Y. F. Chen, *Appl. Phys. Lett.* **73**, 948, 1998.

[26] M. Raja, D. Donaghy, G. C. R. Lloyd, S. Badriya, S. J. Higgins and W. Eccleston, *Proc. SPIE* **5464**, 382, 2004.

CHAPTER 6

CONCLUSIONS AND RECOMMENDATIONS FOR FURTHER WORK

The work undertaken along with the main conclusions of this thesis is presented in this chapter. Further work in areas relating to the charge transport mechanism in organic semiconductors, device stability and Schottky diodes are suggested in the future work section.

6.1 CONCLUSIONS

The main characteristic feature of disordered organic semiconductors is their Gaussian distribution of localised states. The electrical characteristics of organic based devices are thus strongly dependent on the nature of the localised states lying in the top and bottom half of the energy gap. There are three possible types of states namely acceptor-like, donor-like and amphoteric. An acceptor-like state is one that exists only in a negative or neutral condition, a donor-like state only in a positive or neutral condition and finally an amphoteric state is one that can exist in any of the three conditions. Ignoring amphoteric states, the only combination of states consistent with experiments was found to be acceptor-like in the top half of the energy gap and donor-like in the bottom half. Only under such conditions will a small gate voltage be sufficient to reach minimum channel current in a transistor.

In crystalline solids, carrier transport is traditionally described by a single mobility term as carriers mostly occupy energy levels close to the band edge. In contrast, carriers in disordered materials are distributed across a much wider energy range and thus experience different hopping rates. Hence it would seem rather inappropriate to assign a unique mobility term to carriers in disordered semiconductors. In our analytical model, the band tail of the Gaussian distribution is approximated by an exponential function. By making a direct comparison with crystalline semiconductors, it is demonstrated that the exponential density of states (DOS) can be represented by a single transport energy. In doing so, an effective mobility which is strongly dependent on carrier density was obtained for organic solids. This empirical relationship is formally known as the Universal Mobility Law (UML). The effective mobility also shows a dependence on the characteristic temperature representing the exponential density of states, T_c via the exponent term. The Universal Mobility Law is extremely important as it forms the basis of all the analytical models used throughout this thesis.

The current density voltage characteristic of the Al-P3HT-Au diode revealed a relatively weak rectifying behaviour with an on/off ratio of only ~ 10^3. A good straight line fit was obtained for the experimental plot of $ln\ J_R$ against $V^{0.25}$ which suggests that the organic film has a uniform doping profile. The dopant density for the as-synthesised P3HT was estimated to be ~ 1.73×10^{16} cm^{-3}. The relatively high dopant density measured in as-synthesised P3HT is attributed to the presence of residual dopants from the synthesis process. The validity of the abrupt depletion edge approximation in organic Schottky diodes was established by

comparing the width of the space charge region W to the effective Debye length L_{De}. For an applied voltage of 1V, the ratio of W/L_{De} was estimated to be ~ 8.

The simple analytical expression developed for organic Schottky diodes allows the characteristic temperature of the energetic distribution of carriers, T_0 to be determined directly from the exponential current regime of the forward J-V characteristic. The value of T_0 for the P3HT diode was found to be ~ 1301K. This is believed to correspond to carriers occupying the intrinsic DOS since dopant states are located too high in energy to contribute to conduction at low applied voltages. The ideality factor η calculated for the P3HT diode was ~ 4.3. The much larger η is thought to be directly related to the exponential DOS of organic materials. The characteristic temperature of the intrinsic DOS T_c was calculated to be ~ 390K and the corresponding Meyer Neldel (MN) energy was ~ 34 meV. The Al-P3HT diode also demonstrated non-ideal behaviour at much lower applied voltages which is believed to be associated with the presence of extrinsic trap states. The stronger exponential rise in current yields values of T_0 and T_c of ~ 621K and 580K respectively. A comparable value of T_c has previously been observed when dopant states are involved in conduction.

A slope of ~ 1.09 was obtained from the experimental plot of J against V_{bulk} which suggests that as-synthesised P3HT exhibits ohmic behaviour. This value of close to unity also implies that no potential is dropped across the Au electrode. In addition, the effective bulk mobility of holes determined from the saturation current region was ~ 2.7×10^{-5} $cm^2 V^{-1} s^{-1}$.

To improve the conductivity of P3HT, the material is deliberately doped with 0.5% of 2,3-dichloro-5,6-dicyano-1,4-benzoquinone (DDQ) by weight. The extrinsic carriers contributed by DDQ are expected to obey Pauli Exclusion Principle and rapidly fill up lower lying energy states. The plot of $ln\ J_R$ against $V^{0.25}$ exhibits two distinct slopes thus suggesting a non-uniform distribution of dopants across the space charge region. The dopant densities were estimated to be ~ 1.37×10^{15} cm^{-3} and 3.57×10^{16} cm^{-3} at low and high applied voltages respectively. The relatively small increase in dopant density compared to the undoped P3HT sample is believed to be associated with the fact that a large fraction of the DDQ molecules added remain inactive. These DDQ molecules are presumably not ideally located within the polymer matrix for charge transfer reactions to occur. The values of T_0 and T_c extracted from the exponential slope of the Al-0.5% doped P3HT Schottky diode were ~ 1239K and 396K respectively. This is consistent with the notion that the dopant states introduced by the DDQ molecules lie at higher energies. The double logarithmic plot of J against V_{bulk} gave a slope of

~ 1.29. The significantly larger slope value is believed to result from the formation of a potential barrier at the Au/organic interface.

For Schottky diodes made with polytriarylamine (PTAA) (S1105) as the active material, the Au electrode is pre-treated with pentafluorobenzenethiol (PFBT) in order to enhance the injection of holes. The modified Au-PTAA-Al diodes yield a rectification ratio of ~ 10^8 and 10^6 when processed from xylene and dichlorobenzene (DCB) respectively. The extremely low off currents obtained makes the diodes ideal for low current circuit operations.

The current density voltage characteristic of the Al-PTAA diode processed from dichlorobenzene was selected for further analysis. The diode was found not to obey the $V^{0.25}$ law as the reverse current continued to saturate with increasing applied bias. This anomaly is attributed to the presence of extrinsic traps which causes the Fermi level to be pinned and consequently restricts the space charge region from extending further with increasing bias. The values of T_0 and T_c estimated from the forward exponential current were ~ 481K and 799K respectively. The much larger value of T_c suggests the presence of an exponential distribution of extrinsic states at lower energies.

The experimental plot of J against V_{bulk} of the Al-PTAA diode gave a slope of ~ 0.98 and 2.56 at low and high applied fields respectively. This result suggests that the current through the neutral region changes from ohmic to space charge limited with increasing bias. The neutral region of the diode is thought to be affected by space charge effects due to the high purity of polytriarylamine. The amount of dopants ions present is insufficient to compensate the increasing density of holes in the semiconductor bulk. A new space charge limited current (SCLC) expression which incorporates the UML is developed for disordered organic semiconductors as the practice of assigning of specific mobility term to carriers which are widely distributed in energy is regarded as being inappropriate. A value of m equal to ~ 0.56 was obtained from the SCL region of the J-V_{bulk} curve. This corresponds to a T_c value of ~ 468K and a Meyer Neldel energy of ~ 40 meV. This confirms the absence of dopant states at higher energies in agreement with the notion that PTAA is a much purer semiconductor than its predecessor poly(3-hexylthiophene).

The effect of changing the back metal/organic interface on the forward saturation current of the Al-PTAA diodes was also studied. The much lower forward currents observed for devices made with pristine Au, pristine Cu and PFBT-modified Cu as the back metal electrode suggest that the devices are essentially pairs of back-to-back Schottky diodes. The experimental J against V_{bulk} plots of these diodes fail to yield slopes which are consistent

with either purely ohmic or space charge limited behaviour. Due to the potential drop across the back metal/organic interface, it is no longer possible to analyse the *J-V* characteristic of the diodes in terms of a regional model.

Although doping PTAA with DDQ yields higher current levels, it also significantly reduces the rectifying property of the diodes. The significant rise in reverse currents is caused by an increase in doping level. The non-saturation of the reverse currents suggest that the diodes are no longer affected by Fermi level pinning as the trap states are now filled by additional free carriers contributed by the DDQ molecules. Also, the double logarithmic plots of J against V_{bulk} at higher applied fields yield slopes of less than 2 which suggest that the neutral region of the diodes are less severely affected by space charge effects.

The *J-V* characteristic of the vacuum-deposited pentacene diode was found to lend itself rather well to the analytical model developed for disordered organic semiconductors. Pentacene belongs to a new generation of small molecule organic semiconductors that closely resembles inorganic polycrystalline semiconductors. Analysis of current transport in the pentacene diode was extensively based on the model developed by Eccleston. For convenience, the structure of the vacuum-deposited pentacene was assumed to consist of arrays of small molecules called grains which are separated by highly amorphous boundary regions. The highly disordered grain boundaries are believed to be characterised by an exponential distribution of traps. The traps pin the Fermi level close to the centre of the gap thus causing a potential barrier to be formed at the edge of the grains. A single transport level with an almost abrupt edge capable of supporting a current equal to the exponential DOS was defined. Despite the potential barrier at the grain boundaries, transport across the grain was found to be akin to crystalline solids. The charge carriers are therefore more likely to traverse through the organic film via the grains. But due to the high density of trapping in the grain boundaries, current through the diode is believed to be controlled by the exponential distribution of traps similar to disordered semiconductors.

The Al-pentacene diode yields a rectification ratio of ~ 10^2 which is comparable to as-synthesised P3HT Schottky diodes. The semi-logarithmic plot of J_R against $V^{0.25}$ gave a good straight line fit. A dopant density of ~ 3.75×10^{17} cm^{-3} was extracted from the slope of the curve. In the forward direction, a value of T_0 equal to ~ 2206K was calculated directly from the slope of the exponential current region. This yields a value of T_c equal to ~ 347K and a MN energy of ~ 30 meV. This suggests that the density of states at lower energies is free of dopant states. Similar to the PTAA diode, the experimental curve of J against V_{bulk} yields a

slope of ~ 1.01 and 2.25 at low and high voltages respectively. The slope of larger than 2 obtained at higher fields implies that the neutral region of the diode is dominated by space charge effects. A value of m equal to ~ 0.25 and hence a T_c of ~ 375K was obtained. The latter relates to a Meyer Neldel energy of ~ 32 meV. The intrinsic value of T_c obtained from the saturation current region indicates the absence of dopant states. But the relatively high dopant density measured for the pentacene film suggests that the dopant states are most probably located in the grains since the *J-V* measurement only allows the DOS in the grain boundaries to be analysed. The space charge effects observed in the diode is thus attributed to the constant positive charge produced by the high density of free carriers that become trapped in the grain boundaries.

The temperature dependence of the *J-V* characteristics of as-synthesised P3HT and PTAA Schottky diodes fabricated on polyethylene terephthalate (PET) flexible substrate was also studied. In the Al-P3HT diode, the forward saturation current fell by almost 2 orders of magnitude whilst the drop in reverse current was less significant. The plot of $ln\ J_R$ against $V^{0.25}$ gave a nearly constant dopant density in the temperature range of between 240K and 290K. This result suggests that the dopants will remain ionised at relatively high temperatures similar to crystalline silicon. The holes contributed by the shallow dopant states are expected to obey Pauli Exclusion Principle and fill up increasingly lower energy states. For convenience, this phenomenon is referred to as 'carrier inversion'. The dopant density at temperatures below 240K, however, cannot be determined due to the anomalous rise in reverse current at higher applied voltages.

Below room temperature, the ideality factor η of the Al-P3HT diode was found to increase drastically with decreasing temperature. At lower temperatures, the large increase in ideality factor led to an almost linear rise in T_0. This result, however, was deemed as being erroneous since the energetic distribution of holes is governed by the Fermi Dirac statistics which at lower temperatures, falls more sharply with decreasing energy. Hence, the value of T_0 is expected to fall with temperature. The anomalous rise in η with decreasing temperature may be associated with a number of factors such as the presence of extrinsic trap states, carriers taking alternative routes to other potential barriers or even the lack of validity of the flat quasi Fermi level approximation. An activation energy of ~ 0.18 eV and 0.17 eV were measured for the highly regioregular P3HT from an Arrhenius plot of J_R at a reverse voltage of -1V and -5V respectively. Interestingly, an activation energy of ~ 0.17 eV was obtained from the plot of conductivity versus *1000/T*. The self-consistent value of E_a suggests that the energetic position of transport energy stays almost the same in the temperature range of between 240K and 290K.

Surprisingly, the Al-PTAA diode fabricated on PET substrate produced a much weaker rectifying behaviour. There was a more distinct fall in the exponential current of the Al-PTAA Schottky diode compared to the P3HT diode which resulted in even larger values of ideality factor at lower temperatures. In the reverse direction, the current stayed virtually constant at temperatures below 248K which is thought to be due to a higher contribution of leakage current. Small changes in the *J-V* characteristic were observed when a small length of Au wire was placed onto the metal electrodes and secured using silver paint for the purpose of temperature measurements. The values of T_0 estimated from the exponential slope of the diode before and after the Ag-Au contact was made were ~ 1441K and ~ 1273K respectively. This gave values of T_c equal to ~ 384K and ~ 371K.

Modelling the saturation current region with the newly developed SCLC equation gave values of m equal to approximately 0.59 and 0.23 respectively. The discrepancy in the estimated value of m suggests that the supposedly natural variation in MN energies might actually be a result of having differing qualities of ohmic metal electrodes. More consistent MN energies are obtained for devices made with as-synthesised P3HT as the active material which is thought to be related to the higher doping densities observed in the semiconductor. Between 248K and 295K, a self-consistent MN energy of ~ 31 meV was measured from modelling the saturation region of the Al-PTAA diode with the newly developed SCLC equation. At lower temperatures, however, the MN energy falls sharply with decreasing temperature. This is mainly attributed to the formation of potential barrier at the back metal/organic interface caused presumably by the energetic shift in Fermi level with temperature. Other factors such as the breakdown in the assumption of a flat quasi Fermi level, a changing neutral region width and an increasing effective Debye length may also adversely affect the analysis at lower temperatures. The constant MN energy obtained at fairly high temperatures gives us further confidence that the exponential distribution of states does not change with temperature. The experimental plot of J_R versus *1000/T* at relatively high temperatures yields an activation energy of ~ 0.21 eV and ~ 0.19 eV at an applied voltage of -2V and -5V respectively.

6.2 FUTURE WORK

Numerous charge transport models have been proposed so far to describe carrier motion in disordered organic solids. Some of the models are based on a Gaussian density of states whilst others favour the exponential approximation. We have chosen to adopt the latter mainly because it allows conventional device physics to be employed. Interestingly, we find that our model demonstrates the Universal Mobility Law (UML) without taking into account the hopping mechanism which is believed to govern charge transport in organic solids. In the Variable Range Hopping (VRH) model, for instance, it relies heavily on percolation theory to develop an analytical expression for conductivity. This necessitates the existence of an infinite percolation path across the localised states for carrier transport to occur. Further work is needed to understand the reason why the universal dependence between mobility and carrier density can be established without having to use the percolation approach. At present it is unclear if there is an underlying correlation between applying the percolation theory and assuming an exponential density of states.

Instability is one of the main concerns involving organic based devices. It is an aspect of organic solids which needs to be resolved to guarantee commercial viability of electronic applications based on these materials. A common manifestation of instability in organic devices is the observation of hysteresis in the electrical characteristics. In the past, hysteresis has been attributed to the drifting of mobile ions and also photo-oxidation of the organic solids upon exposure to air. More recently, however, adsorption of ozone has been singled out as the main cause of performance degradation in organic based devices. This finding means that encapsulation of devices may be critical for the production of more stable organic devices. Hence, a simple yet effective method of encapsulating organic devices needs to be developed.

The simplified Schottky theory was originally developed for inorganic semiconductors but has since been adopted for diodes made with disordered materials. This theory is commonly used to determine the dopant densities in organic Schottky diodes. The drawback with this method is that it takes no account of the conduction process in semiconductors. We know that charge transport in crystalline solids is governed by band-like transport whereas in disordered materials, carrier motion is limited by hopping transitions between localised states. So, despite the organic diodes showing good fits for the experimental plots of $ln\ J_R$ against $V^{0.25}$, the impact of an exponential distribution of states on the Schottky theory needs to be explored. Special attention needs to be given to understanding the injection of majority carriers into localised states which are widely distributed in energy.

The concept of a single transport energy is often used in disordered materials to explain the thermally activated behaviour of carriers. However, there is yet to be any compelling evidence that proves the existence of a transport energy. In our model, we suggest that under thermal equilibrium conditions, the current supported by an exponential distribution of states may be represented by a single hypothetical transport energy with an abrupt edge akin to crystalline solids. By doing so, the so-called effective mobility of carriers demonstrates a strong dependence on carrier density. In the analysis involving Schottky diodes, the minimum energy beyond which carriers are able to hop between states with relative ease is referred to as the transport energy. This definition allows an expression for the forward exponential current density to be developed but it neither proves nor disproves the notion of a transport energy. It is quite likely for disordered semiconductors to have a transport energy since the energetic distribution of carriers in this materials is dominated by the Fermi Dirac statistics as it is in the case of crystalline solids. But more experimental and analytical work is needed to verify the validity of a transport energy in organic semiconductors.

Finally, more conclusive experimental evidence is needed to establish if the characteristic temperature of the exponential density of states T_c is in fact independent of temperature. Further work is also needed to verify if the magnitude of T_c depends on the temperature at which the organic semiconductor is deposited. It is widely known that the morphology of organic films can be modified through a simple annealing step. It will therefore be interesting to know if varying the deposition temperature of solution-processed organic materials has any effect on the intrinsic distribution of states.

APPENDICES

APPENDIX A: Definition of Commonly Used Symbols

A	*area* (m^2)
D_n, D_p	*diffusion coefficient for electrons, holes* (m^2s^{-1})
E	*energy (J, eV)*
E_B	*energy of the top of the barrier (J, eV)*
E_c, E_v	*energy of the conduction band, valence band edge (J, eV)*
E_F	*extrinsic Fermi level (J, eV)*
E_{Fe}, E_{Fh}	*quasi Fermi level for electrons, holes (J, eV)*
E_i	*intrinsic Fermi level (J, eV)*
E_g	*energy gap (J, eV)*
E_T	*transport energy (J, eV)*
F	*electric field strength* (Vm^{-1})
$f(E)$	*Fermi Dirac distribution function*
G	*carrier flux* ($m^{-2}s^{-1}$)
$g(E)$, $N(E)$	*density of states at energy E*
h	*Planck constant (Js)*
$\hbar$	*reduced Planck constant (Js)*
I	*current (A)*
J	*current density* (Am^{-2})
J_0	*saturation current density* (Am^{-2})
k	*Boltzmann constant (J/K, eV/K)*
K	*prefactor in the Universal Mobility Law* ($cm^{-2}V^{-1}s^{-1}$)
L_D	*Debye length (m)*
L_{De}	*effective Debye length (m)*
m^*	*effective mass of carrier in crystalline semiconductors (kg)*
m	*exponent in the Universal Mobility Law*
kT/q	*thermal voltage at 300K (eV)*
kT_c	*Meyer Neldel energy (eV)*
n, n_f	*electron concentration* (cm^{-3})
n_i	*intrinsic electron concentration* (cm^{-3})
n_0	*equilibrium electron concentration* (cm^{-3})
N_A	*acceptor ion concentration* (cm^{-3})
N_D	*donor ion concentration* (cm^{-3})
N_c, N_v	*effective density of states at the conduction band, valence band edge* (cm^{-3})
N_T	*density of states at the transport energy* (cm^{-3})
N_t	*density of trap states* (cm^{-3})

N_0	density of states at energy E = 0 (cm^{-3})
p	hole concentration (cm^{-3})
p_i	intrinsic hole concentration (= n_i) (cm^{-3})
p_0	equilibrium hole concentration (cm^{-3})
q	electronic charge (C)
R	resistance (Ω)
T	absolute temperature (K)
T_0	characteristic temperature describing the exponential energetic distribution of carriers (K)
T_c	characteristic temperature describing the exponential density of states (K)
t	time (s)
V	voltage (V)
V_{bi}	built in voltage (V)
V_{bulk}	voltage across the semiconductor bulk (V)
W	width of the space charge region (m)
x , x_p	semiconductor thickness (m)
x_m	distance from the metal/semiconductor interface at $\Delta\phi_B$
ε_0	permittivity of free space
ε	relative dielectric constant
ε_g	dielectric constant of the grain
ε_s	static dielectric constant of the semiconductor
ε_∞	high frequency permittivity of the semiconductor
$d\xi/dx$	gradient of the Fermi level
θ	ratio of free carriers to the total carriers in the space charge limited current (SCLC) theory
η	ideality factor
μ	mobility ($m^2V^{-1}s^{-1}$)
μ_{eff}	effective mobility ($m^2V^{-1}s^{-1}$)
μ_0	mobility prefactor ($m^2V^{-1}s^{-1}$)
ρ	resistivity (Ωm)
σ	conductivity ($\Omega^{-1}m^{-1}$)
ν	carrier frequency (s^{-1})
ϕ	electrostatic potential (V)
ϕ_B	metal-semiconductor barrier height (V)
$\Delta\phi_B$	metal-semiconductor barrier lowering (V)
ϕ_m	metal work function (V)

ϕ_s	*semiconductor work function (V)*
ϕ_{ms}	*difference in work function between metal and semiconductor (V)*

APPENDIX B: Expression for the Free Carrier Density in Disordered Organic Semiconductors

In disordered semiconductors, the density of states at the Gaussian band tail may be quite accurately approximated by an exponential function given by

$$N(E) = \frac{N_0}{kT_c} \exp\left(\frac{E}{kT_c}\right) \qquad B.1$$

where N_0 is the number of states per unit volume at energy $E = 0$, k is the Boltzmann constant and T_c corresponds to the characteristic temperature describing the exponential DOS.

At energies above the Fermi level E_F, the probability of carrier occupancy may be given by the Maxwell Boltzmann approximation of the Fermi Dirac statistics.

$$f(E) = \exp -\left(\frac{E - E_F}{kT}\right) \qquad B.2$$

Assuming that only hopping events taking place above the Fermi level contribute to conduction, the electron density in an n-type disordered organic solid is thus given by

$$n(E) = \int_{E_F}^{\infty} \frac{N_0}{kT_c} \exp\left(\frac{E}{kT_c}\right) \exp -\left(\frac{E - E_F}{kT}\right) dE$$

$$n(E) = \int_{E_F}^{\infty} \frac{N_0}{kT_c} \exp\left(\frac{E_F}{kT}\right) \exp - E\left(\frac{1}{kT} - \frac{1}{kT_c}\right) dE$$

Assigning $\frac{1}{T_0} = \frac{1}{T} - \frac{1}{T_c}$ simplifies the expression to

$$n(E) = \int_{E_F}^{\infty} \frac{N_0}{kT_c} \exp\left(\frac{E_F}{kT}\right) \exp - \frac{E}{kT_0} dE$$

$$n(E) = \frac{N_0 T_0}{T_c} \exp\left(\frac{E_F}{kT}\right) \exp -\left(\frac{E_F}{kT_0}\right)$$

$$n(E) = \frac{N_0 T_0}{T_c} \exp\left(\frac{E_F}{kT_c}\right) \qquad B.3$$

The term T_0 is thought to represent the energetic distribution of carriers which also follows an exponential function. The electron concentration dependence on T_c is believed to be associated with the fact that E_F lies in the band tail of the Gaussian distribution.

APPENDIX C: Derivation of the Effective Debye Length L_{De}

The effective Debye length L_{De} is an important material dependent parameter in semiconductors. In general, it refers to the characteristic length over which a charge imbalance is neutralised by majority carriers under steady state or equilibrium conditions.

Assuming a uniform distribution of holes in a p-type disordered semiconductor, the hole concentration is given by the one-dimensional Poisson's equation.

$$\frac{dF}{dx} = \frac{qp_s}{\varepsilon_0 \varepsilon_s} \qquad C.1$$

where F is the electric field strength, p_s is the surface hole concentration, ε_0 is the permittivity of free space and ε_s is the static dielectric constant of the semiconductor.

The surface hole density can be expressed in terms of its intrinsic hole concentration p_0 and is given by

$$p_s = p_0 \exp -\left(\frac{q\phi_s}{kT_c}\right) \qquad C.2$$

where ϕ_s represents the potential at the semiconductor surface. Substituting the expression for p_s into *equation C.1* and integrating from the semiconductor surface to the edge of hole accumulation layer gives

$$\int_0^F F\,dF = -\frac{qp_0}{\varepsilon_0 \varepsilon_s} \int_0^{\phi_s} \exp -\left(\frac{q\phi_s}{kT_c}\right) d\phi$$

Taking into account $\exp -\left(q\phi_s / kT_c\right) >> 1$ simplifies the expression to

$$F = \left[\frac{2p_0 kT_c}{\varepsilon_0 \varepsilon_s} \exp -\left(\frac{q\phi_s}{kT_c}\right)\right]^{1/2} \qquad C.3$$

Due to a combination of drift and diffusion, carriers within an accumulation layer will see an exponential fall in carrier density with distance. The potential ϕ will also demonstrate a similar spatial variation since it is closely related to carrier density. The extrinsic Debye length L_D corresponds to the distance over which the potential reduces to ϕ_s/e which is ⅓ its surface value. Hence, L_D accounts for almost 70% of the total concentration of accumulated carriers.

Substituting $F = -d\phi/dx$ into *equation C.3* and integrating from $\phi = \phi_s$, $x = 0$ to $\phi = \phi_s/e$, $x = L_D$ yields

$$-\int_{\phi_s}^{\phi_s/e} \frac{1}{\left[\frac{2p_0kT_c}{\varepsilon_0\varepsilon_s}\exp-\left(\frac{q\phi_s}{kT_c}\right)\right]^{1/2}} d\phi = \int_0^{L_D} dx$$

$$L_D = \left(\frac{2\varepsilon_0\varepsilon_s kT_c}{q^2 p_0}\right)^{1/2} \exp\left(\frac{q\phi_s}{2kT_c}\right)\left(1-\exp\left(\frac{q\phi_s}{2kT_c}\right)^{1/e-1}\right) \qquad C.4$$

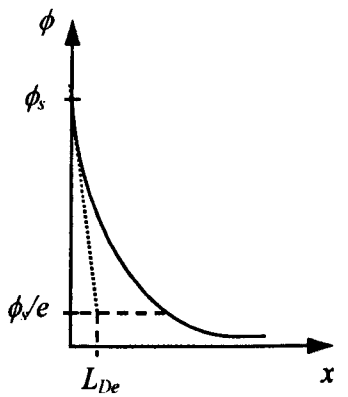

Assuming that term $\exp\left(\frac{q\phi_s}{2kT_c}\right)^{1/e-1} \approx 0$ allows *equation C.4* to be simplified to

$$L_D = \left[\frac{2\varepsilon_0\varepsilon_s kT_c}{q^2 p_0 \exp-\left(\frac{q\phi_s}{kT_c}\right)}\right]^{\frac{1}{2}} \qquad C.5$$

By substituting *equation C.2* into *equation C.5*, the Debye length is thus given as

$$L_D = \left(\frac{2\varepsilon_0\varepsilon_s kT_c}{q^2 p_s}\right)^{\frac{1}{2}} \qquad C.6$$

And as tradition would have it, an effective Debye length is defined.

$$L_{De} = \frac{L_D}{\sqrt{2}} = \left(\frac{\varepsilon_0\varepsilon_s kT_c}{q^2 p_s}\right)^{\frac{1}{2}} \qquad C.7$$

APPENDIX D: Expression for the Forward Current Density in Organic Schottky Diodes

In forward bias, the exponential rise in current observed at low applied voltages is associated with the exponential fall in carrier occupancy with energy as dictated by the Maxwell Boltzmann approximation of the Fermi Dirac statistics.

Hence the total hole concentration contributing to current flow in the forward direction of a Schottky diode is given by

$$\int N(E) f(E)\, dE = \int \frac{N_0}{kT_c} \exp -\left(\frac{E_F - E}{kT}\right) \exp -\left(\frac{E}{kT_c}\right) dE \qquad D.1$$

where N_0 is the number of localised states per unit volume, k is the Boltzmann constant, E_F is the Fermi level and T_c is the characteristic temperature representing the exponential distribution of states.

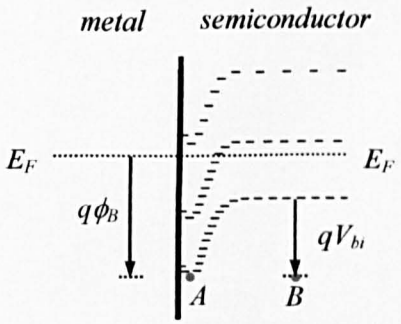

Since a flat quasi Fermi level is assumed throughout the semiconductor material even under steady state conditions, the hole concentration at point A must be the same as the hole concentration at B. Hence, the current density is determined by integrating from the top of the barrier to infinity and is given by

$$J \propto \int_{-\infty}^{E_B + qV_{app}} \frac{N_0}{kT_c} \exp -\left(\frac{E}{kT_c}\right) \exp -\left(\frac{E_F - E}{kT}\right) dE$$

$$J \propto \frac{N_0}{kT_c} \exp -\left(\frac{E_F}{kT}\right) \int_{-\infty}^{E_B + qV_{app}} \exp\left(\frac{E}{kT_0}\right) dE$$

$$J \propto \frac{N_0 T_0}{T_c} \exp -\left(\frac{E_F}{kT}\right) \exp -\left(\frac{E_B}{kT_0}\right) \exp\left(\frac{qV_{app}}{kT_0}\right) \qquad D.2$$

where E_B is the energy corresponding to the top of the barrier and T_0 is the characteristic temperature describing the exponential distribution of holes. This is a generalised treatment as no account is taken of the charge transport mechanism across the potential barrier.

APPENDIX E: Expression for θ in the New Space Charge Limited Current (SCLC) Equation

In disordered semiconductors, the localised states containing both trapped and free charge carriers are believed to belong to the intrinsic exponential density of states. In the simplified model, carriers lying below the Fermi level are regarded as trapped whilst carriers located at higher energies are deemed as free owing to the much larger density of scarcely populated states. For convenience, the probability of occupancy of the energy states are approximated by the Maxwell Boltzmann statistics which is given by

$$f(E)=\begin{cases}\exp-\left(\dfrac{E-E_F}{kT}\right) & \text{if } E>E_F \\ 1 & \text{if } E\le E_F\end{cases} \qquad E.1$$

where E is the energy of the localised states, E_F is the Fermi level, k is the Boltzmann constant and T is the absolute temperature.

The trapped carrier density is determined by integrating from $E = 0$ to the Fermi level and is thus given by

$$n_t = N_0 \exp\left(\frac{E_F}{kT_c}\right) \qquad E.2$$

where N_0 is the number of states per unit volume at $E = 0$ and T_c is the characteristic temperature representing the intrinsic distribution of states.

Similarly, the free carrier density in the organic solid is given as

$$n_f = \frac{N_0 T_0}{T_c} \exp\left(\frac{E_F}{kT_c}\right) \qquad E.3$$

where T_0 is the characteristic temperature of the energetic distribution of carriers which also follows an exponential function.

Consequently, the factor θ which is essentially the ratio of injected free carrier density to the total injected carrier density in disordered materials is given by

$$\theta = \frac{n_f}{n_f + n_t}$$

$$\theta = \frac{\frac{N_0 T_0}{T_c}\exp\left(\frac{E_F}{kT_c}\right)}{\frac{N_0 T_0}{T_c}\exp\left(\frac{E_F}{kT_c}\right) + N_0 \exp\left(\frac{E_F}{kT_c}\right)}$$

$$\theta = \frac{T_0}{T_0 + T_c} \qquad E.4$$

By using the expression $\frac{1}{T_0} = \frac{1}{T} - \frac{1}{T_c}$, *equation E.4* can be further simplified to

$$\theta = \frac{T}{T_c} \qquad E.5$$

Equation E.5 clearly shows that θ is a temperature dependent parameter. Also, the value of θ is limited to being less than 1 as the analytical model is only valid for $T_c > T$ and small carrier densities. When T becomes larger than T_c, it is no longer possible to have a closed form solution as the carrier density ceases to fall with increasing energy.

APPENDIX F: Expression for the Reverse Current Density in the Absence of an Expanding Space Charge Region

Suppose the dopant density in the semiconductor is relatively low. The space charge region is then more likely to reach the back of the film with increasing reverse bias. When this happens, the enhanced field dependence leads to a much lower effective barrier height and hence higher reverse currents. As a result, the current no longer obeys the $V^{0.25}$ law but instead varies as a function of $V^{0.5}$.

In general, the reverse current density may be expressed as

$$J_R = J_0 \exp\left(\frac{q\Delta\phi_B}{kT}\right) \qquad F.1$$

where J_0 is the saturation current density, k is the Boltzmann constant, T is the absolute temperature and $q\Delta\phi_B$ is the barrier lowering.

The total potential energy of carriers in the space charge region of a semiconductor depends on both the image force effect and the external electric field and is thus given as

$$E = \frac{q^2}{16\pi\varepsilon_0\varepsilon_s x} + qFx \qquad F.2$$

Here q is the electronic charge, ε_0 is permittivity of free space, ε_s is the static dielectric constant, x is the distance measured from the metal semiconductor interface and F is the applied field.

The peak of the Schottky barrier refers to the point of maximum energy and at this point, $dE/dx = 0$. Using this relationship, the distance of the peak from the metal semiconductor interface x_m is determined as

$$\frac{d}{dx}\left(\frac{q^2}{16\pi\varepsilon_0\varepsilon_s x_m} + qFx_m\right) = 0$$

$$x_m = \sqrt{\frac{q}{16\pi\varepsilon_0\varepsilon_s F}} \qquad F.3$$

The expression for the barrier lowering is given as

$$\Delta\phi_B = \frac{q}{16\pi\varepsilon_0\varepsilon_s x_m} + Fx_m \qquad F.4$$

Equation F.4 can be rewritten in the following form after substituting for x_m from *equation F.3*.

$$\Delta\phi_B = \frac{q}{16\pi\varepsilon_0\varepsilon_s\left(\frac{q}{16\pi\varepsilon_0\varepsilon_s F}\right)^{1/2}} + F\left(\frac{q}{16\pi\varepsilon_0\varepsilon_s F}\right)^{1/2}$$

$$\Delta\phi_B = 2\left(\frac{qF}{16\pi\varepsilon_0\varepsilon_s}\right)^{1/2} \qquad F.5$$

The semiconductor will resemble an insulator when the space charge region extends to the back of the film. So, for an insulator sandwiched between two metal electrodes, the applied field is simply given by

$$F = \frac{V_R - V_{bi}}{x_p} \qquad F.6$$

where V_R is the reverse voltage, V_{bi} is the built in potential and x_p is the film thickness.

Equation F.5 can be rewritten as follows after substituting for the electric field F using *equation F.6*

$$\Delta\phi_B = \left[\frac{q(V_R - V_{bi})}{4\pi\varepsilon_0\varepsilon_s x_p}\right]^{1/2} \qquad F.7$$

Hence, when the width of the space charge region coincides with the film thickness, the reverse current density is given by

$$J_R = J_0 \exp\left(\frac{q}{kT}\left[\frac{q(V_R - V_{bi})}{4\pi\varepsilon_0\varepsilon_s x_p}\right]^{1/2}\right) \qquad F.8$$

APPENDIX G: Current Continuity Equation

In most cases, charge transport in semiconductors occurs under the combined influence of drift and diffusion. Carrier motion under the influence of an external field is termed drift whilst diffusion refers to charge transport caused by the existence of a concentration gradient. The current density is thus given by

$$J = -qD\frac{dp}{dx} + qp\mu F \qquad G.1$$

where q is the electronic charge, D is the diffusion coefficient, dp/dx is the change in hole density with distance, p is the hole density, μ is the hole mobility and F is the applied field.

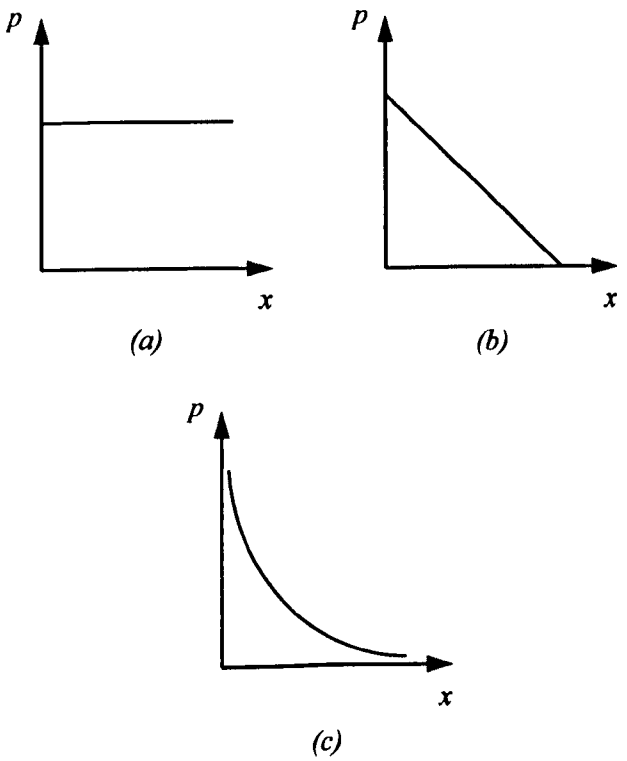

Spatial variation of the hole concentration under (a) pure drift (b) pure diffusion and (c) drift and diffusion combined.

Einstein Relationship

At equilibrium, both the drift and diffusion components of the current are equal and can thus be expressed as

$$qD\frac{dp}{dx} = qp\mu F \qquad G.2$$

Substituting $F = -d\phi/dx$ into *equation G.2* gives

$$qD\frac{dp}{d\phi}\left(\frac{d\phi}{dx}\right) = -qp\mu\left(\frac{d\phi}{dx}\right) \qquad G.3$$

Then differentiating $p = p_i \exp -\left(\frac{q\phi}{kT_c}\right)$ and substituting the result into *equation G.3* gives

$$D\left(\frac{qp}{kT_c}\right) = p\mu$$

$$D = \left(\frac{kT_c}{q}\right)\mu \qquad G.4$$

Interestingly, *equation G.4* demonstrates that the Einstein relationship developed for organic solids is dependent on the constant T_c and not the absolute temperature as it is in the case of crystalline solids. Nevertheless, the mobility term in *equation G.4* is known to have a temperature dependence associated with it.

Now substituting $F = -d\phi_F/dx$ and *equation G.4* into *equation G.1* gives

$$J = -\mu kT_c\frac{dp}{d\phi_D}\left(\frac{d\phi_D}{dx}\right) - qp\mu\frac{d\phi_F}{dx} \qquad G.5$$

where $d\phi_D/dx$ and $d\phi_F/dx$ correspond to the change in potential with distance associated with the diffusive and drift process respectively.

Again substituting the first derivative of $p = p_i \exp -\left(\frac{q\phi}{kT_c}\right)$ into *equation G.5* gives

$$J = -\mu kT_c\left(\frac{qp}{kT_c}\right)\frac{d\phi_D}{dx} - qp\mu\frac{d\phi_F}{dx}$$

$$J = -\mu qp\left(\frac{d\phi_D}{dx} + \frac{d\phi_F}{dx}\right)$$

$$J = -\mu qp\left(\frac{d\xi}{dx}\right) \qquad G.6$$

where $d\xi/dx$ is the gradient of the Fermi level. The most obvious consequence of *equation G.6* is that the Fermi level will be flat in the absence of current flow. Under steady state

conditions, however, *equation G.6* predicts that a particular current level can be supported either by a large variation in carrier density or a negligibly small slope in the Fermi level. This simple relationship is crucial to understanding the flat quasi Fermi level approximation widely used in semiconductor devices under steady state conditions.

APPENDIX H: Expression for Carrier Flux in the Grains of Small Molecule Organic Semiconductors

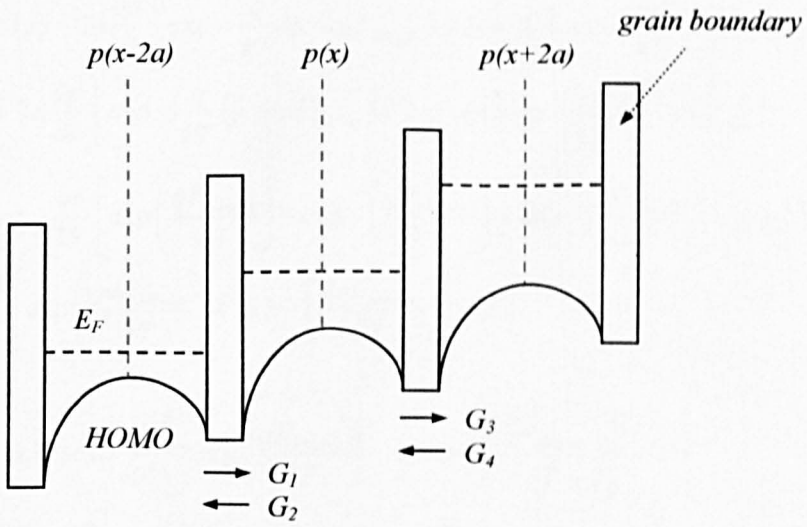

Flux for any charged species corresponds to the rate of carriers passing through per unit area. The carrier flux G_1 across the grain boundary is given by

$$G_1 = 2av\left[p(x) - 2a\frac{\partial p}{\partial x}\right]\exp -\frac{q}{kT}\left(\phi - aF_{xmean}\right) \qquad H.1$$

where ϕ is the potential barrier at the grain boundary in the absence of an applied field, $p(x)$ is the hole density at the grain centre and v is the frequency of attempted jumps. The potential barrier ϕ is lowered by the application of an external field and F_{xmean} represents the electric field strength obtained by dividing the voltage drop across the organic film by its thickness. The concentration of holes in the adjacent grain centre $(x-2a)$ is approximated by $\left[p(x) - 2a\,{}^{\partial p}/_{\partial x}\right]$.

The carrier flux G_2 on the other hand is given by

$$G_2 = 2avp(x)\exp -\frac{q}{kT}\left(\phi + aF_{xmean}\right) \qquad H.2$$

Similar expressions can be written for G_3 and G_4.

When all the individual fluxes are combined, the following expression is obtained for the carrier flux at the plane corresponding to x.

$$G(x)=2av\left[p(x)-2a\frac{\partial p}{\partial x}\right]\exp-\frac{q}{kT}(\phi-aF_{xmean})-2avp(x)\exp-\frac{q}{kT}(\phi+aF_{xmean})$$
$$-2av\left[p(x)+2a\frac{\partial p}{\partial x}\right]\exp-\frac{q}{kT}(\phi+aF_{xmean})+2avp(x)\exp-\frac{q}{kT}(\phi-aF_{xmean})$$

$$G(x)=2avp(x)\exp-\frac{q\phi}{kT}\left[\exp\left(\frac{qF_{xmean}}{kT}\right)-\exp-\left(\frac{qF_{xmean}}{kT}\right)-\exp-\left(\frac{qF_{xmean}}{kT}\right)+\exp\left(\frac{qF_{xmean}}{kT}\right)\right]$$
$$-4a^2v\frac{\partial p}{\partial x}\exp\frac{q\phi}{kT}\left[\exp\left(\frac{qaF_{xmean}}{kT}\right)+\exp-\left(\frac{qaF_{xmean}}{kT}\right)\right]$$

$$G(x)=2avp(x)\exp\frac{q\phi}{kT}\left[2\exp\left(\frac{qF_{xmean}}{kT}\right)-2\exp-\left(\frac{qF_{xmean}}{kT}\right)\right]$$
$$-4a^2v\frac{\partial p}{\partial x}\exp\frac{q\phi}{kT}\left[\exp\left(\frac{qaF_{xmean}}{kT}\right)+\exp-\left(\frac{qaF_{xmean}}{kT}\right)\right] \qquad II.3$$

Using the hyperbolic functions $\sinh(x)=\frac{1}{2}(e^{x}-e^{-x})$ and $\cosh(x)=\frac{1}{2}(e^{x}+e^{-x})$ allows *equation H.3* to be simplified to

$$G(x)=2avp(x)\exp\frac{q\phi}{kT}\left[4\sinh\frac{qaF_{xmean}}{kT}\right]-4a^2v\frac{\partial p}{\partial x}\exp\frac{q\phi}{kT}\left[2\cosh\frac{qaF_{xmean}}{kT}\right]$$
$$G(x)=8avp(x)\exp\frac{q\phi}{kT}\left[\sinh\frac{qaF_{xmean}}{kT}\right]-8a^2v\frac{\partial p}{\partial x}\exp\frac{q\phi}{kT}\left[\cosh\frac{qaF_{xmean}}{kT}\right] \qquad II.4$$

Equation H.4 takes account of both the current transport mechanisms; the first term corresponds to quasi-drift whilst the second to quasi-diffusion. When the field in the grain is small or the grain size is large *i.e.* $F_{xmean}\leq kT/qa$, both the hyperbolic functions in *equation H.4* is considered to be negligible.

APPENDIX I: Expression for the Intrinsic Carrier Density in Disordered Organic Semiconductors

In general, intrinsic carriers are expected to dominate current transport at relatively high temperatures and in undoped semiconductors. The latter is, however, not applicable to most organic semiconductors since the materials normally contain some level of doping even in their intrinsic form.

In disordered semiconductors where the density of states is approximated by an exponential function, the equilibrium concentration of electrons can be expressed as

$$n = \frac{N_{0n}T_0}{T_c}\exp\left(\frac{E_F}{kT}\right)\exp-\left(\frac{E_{Tn}}{kT_0}\right) \qquad I.1$$

where N_{0n} is the number of states per unit volume at energy $E = 0$, E_F is the Fermi level, E_{Tn} is the electron transport energy, k is the Boltzmann constant, T is the absolute temperature and T_0 and T_c are the characteristic temperature corresponding to the energetic distribution of carriers and states respectively.

A similar expression can also be derived for the equilibrium hole concentration.

$$p = \frac{N_{0p}T_0}{T_c}\exp-\left(\frac{E_F}{kT}\right)\exp\left(\frac{E_{Tp}}{kT_0}\right) \qquad I.2$$

Here N_{0p} is the number of states per unit volume at energy $E = 0$ of the density of states for holes and E_{Tp} is the hole transport energy. In both cases, the carrier density is determined by integrating from the transport energy instead of the Fermi level since using the latter as a common integration limit leads to erroneous results.

The intrinsic carrier concentration in organic solids is determined using the individual electron and hole concentrations given by *equations I.1* and *I.2* respectively. It is thus given by

$$p_i^2 = np$$

$$p_i^2 = N_{0n}N_{0p}\left(\frac{T_0}{T_c}\right)^2\exp\left(\frac{E_F}{kT}\right)\exp-\left(\frac{E_{Tn}}{kT_0}\right)\exp-\left(\frac{E_F}{kT}\right)\exp\left(\frac{E_{Tn}}{kT_0}\right)$$

$$p_i^2 = N_{0n}N_{0p}\left(\frac{T_0}{T_c}\right)^2\exp-\left(\frac{E_{Tn}-E_{Tp}}{kT_0}\right)$$

$$p_i = \sqrt{N_{0n}N_{0p}}\,\frac{T_0}{T_c}\exp-\left(\frac{E_g}{2kT_0}\right) \qquad I.3$$

where E_g is the so-called energy gap which corresponds to the energy difference between the electron and hole transport energies. *Equation I.3* clearly demonstrates that the intrinsic carrier density is independent of the Fermi level and consequently it must be independent of the type of semiconductor. In addition, *equation I.3* also indicates that p_i has an exponential dependence on temperature since T_0 is predicted to vary with temperature. However, the actual temperature dependence will be stronger due to the additional T_0 term in the expression.